

Progress in Deep Geologic Disposal Safety Assessment in the U.S. since 2010

Spent Fuel and Waste Disposition

*Prepared for
U.S. Department of Energy
Spent Fuel and Waste Science Technology*

*P.E. Mariner, L.A. Connolly,
L.J. Cunningham, B.J. Debusschere,
D.C. Dobson, J.M. Frederick, G.E. Hammond,
S.H. Jordan, T.C. LaForce, M.A. Nole,
H.D. Park, F.V. Perry, R.D. Rogers, D.T. Seidl,
S.D. Sevougian, E.R. Stein, P.N. Swift,
L.P. Swiler, J. Vo, M.G. Wallace*

Sandia National Laboratories

September 16, 2019

M2SF-19SN010304041

SAND2019-12001 R



DISCLAIMER

This information was prepared as an account of work sponsored by an agency of the U.S. Government. Neither the U.S. Government nor any agency thereof, nor any of their employees, makes any warranty, expressed or implied, or assumes any legal liability or responsibility for the accuracy, completeness, or usefulness, of any information, apparatus, product, or process disclosed, or represents that its use would not infringe privately owned rights. References herein to any specific commercial product, process, or service by trade name, trade mark, manufacturer, or otherwise, does not necessarily constitute or imply its endorsement, recommendation, or favoring by the U.S. Government or any agency thereof. The views and opinions of authors expressed herein do not necessarily state or reflect those of the U.S. Government or any agency thereof.



Sandia National Laboratories

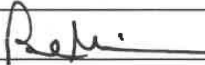
Sandia National Laboratories is a multi-mission laboratory managed and operated by National Technology & Engineering Solutions of Sandia, LLC., a wholly owned subsidiary of Honeywell International, Inc., for the U.S. Department of Energy's National Nuclear Security Administration under contract DE-NA0003525.

APPENDIX E NTRD DOCUMENT COVER SHEET¹

Name/Title of Deliverable/Milestone/Revision No. Progress in Deep Geologic Disposal Safety Assessment in the U.S. since 2010, M2SF-19SN010304041

Work Package Title and Number GDSA - Framework Development – SNL, SF-19SN01030404

Work Package WBS Number 1.08.01.03.04

Responsible Work Package Manager Paul E. Mariner 
(Name/Signature)

Date Submitted September 16, 2019

Quality Rigor Level for Deliverable/Milestone ²	<input type="checkbox"/> QRL-1 <input type="checkbox"/> Nuclear Data	<input type="checkbox"/> QRL-2	<input checked="" type="checkbox"/> QRL-3	<input type="checkbox"/> QRL-4 Lab QA Program ³
--	---	--------------------------------	---	---

This deliverable was prepared in accordance with Sandia National Laboratories
(Participant/National Laboratory Name)

QA program which meets the requirements of
 DOE Order 414.1 NQA-1 Other

This Deliverable was subjected to:

Technical Review

Peer Review

Technical Review (TR)

Peer Review (PR)

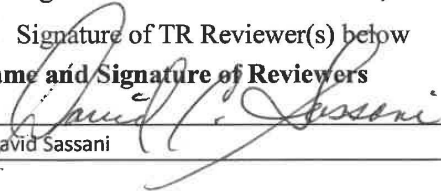
Review Documentation Provided

Review Documentation Provided

- Signed TR Report or,
- Signed TR Concurrence Sheet or,
- Signature of TR Reviewer(s) below

- Signed PR Report or,
- Signed PR Concurrence Sheet or,
- Signature of PR Reviewer(s) below

Name and Signature of Reviewers

David Sassani 
David Sassani

NOTE 1: Appendix E should be filled out and submitted with the deliverable. Or, if the PICS:NE system permits, completely enter all applicable information in the PICS:NE Deliverable Form. The requirement is to ensure that all applicable information is entered either in the PICS:NE system or by using the NTRD Document Cover Sheet.

- In some cases there may be a milestone where an item is being fabricated, maintenance is being performed on a facility, or a document is being issued through a formal document control process where it specifically calls out a formal review of the document. In these cases, documentation (e.g., inspection report, maintenance request, work planning package documentation or the documented review of the issued document through the document control process) of the completion of the activity, along with the Document Cover Sheet, is sufficient to demonstrate achieving the milestone.

NOTE 2: If QRL 1, 2, or 3 is not assigned, then the QRL 4 box must be checked, and the work is understood to be performed using laboratory QA requirements. This includes any deliverable developed in conformance with the respective National Laboratory / Participant, DOE or NNSA-approved QA Program.

NOTE 3: If the lab has an NQA-1 program and the work to be conducted requires an NQA-1 program, then the QRL-1 box must be checked in the work Package and on the Appendix E cover sheet and the work must be performed in accordance with the Lab's NQA-1 program. The QRL-4 box should not be checked.

ACKNOWLEDGEMENTS

The authors greatly appreciate the formal technical review of this report by David Sassani and the informal reviews of various sections and appendices by Carlos Jove-Colon, Ed Matteo, Yifeng Wang, Kris Kuhlman, Tom Lowry, and Peter Swift. Also, many thanks to Mohamed Ebeida for helping initiate the VoroCrust/PFLOTRAN collaboration and to Jeralyn Prouty for developing several illustrations in this report.

EXECUTIVE SUMMARY

The Spent Fuel and Waste Science and Technology (SFWST) Campaign of the U.S. Department of Energy (DOE) Office of Nuclear Energy (NE), Office of Spent Fuel & Waste Disposition (SFWD) is conducting research and development (R&D) on geologic disposal of spent nuclear fuel (SNF) and high-level nuclear waste (HLW). Two high priorities for SFWST disposal R&D are design concept development and disposal system modeling (DOE 2011, Table 6). These priorities are directly addressed in the SFWST Geologic Disposal Safety Assessment (GDSA) work package, which is charged with developing a disposal system modeling and analysis capability for evaluating disposal system performance for nuclear waste in geologic media.

This report documents progress made in Geologic Disposal Safety Assessment (GDSA) R&D in FY 2019 and provides an overview of GDSA development since 2010. In 2010, DOE initiated the Used Fuel Disposition (UFD) Campaign. The purpose of the UFD Campaign was, in part, to focus GDSA R&D on new repository concepts and new potential host rocks. This report summarizes the evolution of GDSA performance assessment (PA), how PA priorities were initially determined and have been recently updated, and how GDSA PA capabilities have advanced under the UFD Campaign through FY 2017 and under the SFWST Campaign thereafter.

In the early years of the UFD Campaign, GoldSim was used to develop simplified PA models for generic disposal environments. Other disposal R&D activities at the time focused on process model simulations, repository design, and updating the features, events, and processes (FEPs) database. In 2011, a major effort was made to assess and prioritize disposal R&D priorities (DOE 2012), and work packages were established to support these priorities. Work package activities included experimental studies on various host rocks and engineered materials, process model development, international collaboration, and probabilistic GDSA. A recap of the early years is provided in Section 1.

In 2013, after a review of available codes and methodologies (Freeze and Vaughn 2012), a new GDSA computational framework was established. This framework today is known as GDSA Framework. The primary codes of this framework are PFLOTRAN and Dakota. PFLOTRAN is a multiphase flow and reactive transport code designed for simulating flow and reactive transport in the subsurface. Dakota is an uncertainty quantification and sensitivity analysis code. These codes are open source, freely available, and built for high performance computing. The full set of codes and tools in GDSA Framework is used to probabilistically simulate the various possible mechanisms and pathways for release and migration of radionuclides from waste packages in a deep geologic repository to the biosphere.

Since 2013, many new capabilities have either been added to PFLOTRAN or are in the process of being added. They include:

- Radionuclide processes (decay and ingrowth in all phases, isotope partitioning between phases, solubility limits, mineral-specific linear sorption, species-specific diffusion, colloids);
- Source term processes (waste form process models, waste package degradation, waste form dissolution, instantaneous release fractions, decay and ingrowth within the waste form, criticality);
- Geophysical properties (discrete fracture networks, density-driven flow, permeability scaling, buffer evolution);
- Biosphere processes (well water ingestion dose model, dose effects of sorption enhancement of unsupported radionuclides);
- Uncertainty quantification and sensitivity analysis (uncertainty sampling, stepwise linear regression, partial correlation coefficients, rank transformations, sensitivity indices); and

- Coupled surrogate models (polynomial chaos, neural network, nearest neighbors).

These features and improvements are summarized in Section 2.

Computational improvements to PFLOTRAN and GDSA Framework are also summarized in Section 2. Computational improvements include:

- A process model coupling framework added to PFLOTRAN;
- Improved analytical derivatives for PFLOTRAN;
- New and improved nonlinear solvers for PFLOTRAN;
- A tool for calculating physically consistent boundary conditions for cells in which a new phase appears or an initial phase disappears;
- Enhanced restart capability; and
- New mesh generation tools.

In FY 2019, code development primarily focused on four activities. One involved the development of a reduced-order criticality model, which is being added to PFLOTRAN to investigate potential impacts to repository performance of criticalities that may occur in dual purpose canisters (DPCs) in an underground repository. This new capability effectively simulates the changes in radionuclide inventories and heat output resulting from a critical event. Another code development activity involved optimizing the Newton-Raphson nonlinear solvers for the unsaturated alluvium reference case and developing a new trust region nonlinear solver. Development of these solvers is needed to improve convergence in unsaturated reference cases with high heat loads. Surrogate models to simulate the fuel matrix degradation (FMD) model is the third code development activity in FY 2019. The new FMD surrogate models are highly accurate relative to the FMD process model with faster execution and, when coupled to PFLOTRAN, will allow PA simulations to account for the effects of radiolysis and growth of an alteration layer when calculating spent fuel dissolution rates. The fourth code development activity in FY 2019 involves the testing and development of an open source meshing generator, VoroCrust, which may become a standard mesh generator for GDSA Framework. These code development activities are discussed in Section 2.3.1 and Appendix A.

In addition to code development, the GDSA team increased its efforts in FY 2019 regarding PFLOTRAN quality assurance (QA). Major progress was made in developing QA documentation for PFLOTRAN, including drafts of a software quality assurance plan, a requirements document, and a verification and validation document. Such documentation will be needed when PFLOTRAN is applied in a regulatory environment. In addition, a QA test harness was developed for the verification test suite, and several new 1D and 2D verification tests were successfully performed and added to the test suite. Information on these QA developments are in Section 2.3.3 and Appendix B.

An important responsibility of the GDSA team is to integrate with disposal R&D activities across the SFWST Campaign to ensure that R&D activities support the safety cases being developed. In FY 2019, the GDSA team conducted a special multi-day, campaign-wide meeting to assess progress in disposal R&D since the 2012 roadmap and to update roadmap priorities going forward. This work produced the 2019 roadmap update (Sevougian et al. 2019b), a report that will be highly useful for planning and prioritizing disposal R&D activities over the next several years.

A comparison of the 2019 R&D Activity state-of-the-art level (SAL) values in the 2019 roadmap update (Sevougian et al. 2019b) with the “primary” FEP state-of-the-art values from 2012 indicates that significant progress has been made because many SAL scores have improved. The 2019 R&D Roadmap Update reflects the need for continuing R&D on many of the 2012 R&D Issues, plus some obvious new priorities,

such as R&D on disposal of DPCs (dual purpose canisters), which now contain a significant fraction of the Nation's spent fuel. The 2019 R&D prioritization effort is now closely integrated with the development of the SFWST Campaign's generic performance assessment model/software framework (the GDSA Framework), so that much of the ongoing R&D work is designed to directly support the development of improved process models that feed the PA model and software. Given the importance of post-closure performance assessment in building confidence in the safety case, this is believed to be appropriate and essential. Integration will be essential for enhancing understanding and confidence in a safety case for a repository in any geologic media, and in support of future decisions regarding site screening, selection and characterization. The FY 2019 roadmap update work is recapped in Section 5. An overview of the various disposal R&D activities across the SFWST Campaign contributing to GDSA development is provided in Section 4. To further enhance integration, the GDSA team built a SharePoint library for all the major disposal R&D reports, storage and transportation R&D reports, and integrated waste management R&D reports generated since 2010 (Section 4.7).

In FY 2019, members of the GDSA team also worked on advancing generic disposal system reference case simulation and uncertainty quantification and sensitivity analysis (UQ/SA). These activities fall primarily under the GDSA Repository Systems Analysis work package and the GDSA Uncertainty and Sensitivity Analysis Methods work package. Progress in those areas is documented in the milestones of those work packages (Sevougian et al. 2019d, in progress; Swiler et al. 2019, in progress). This report highlights the general scope of those activities. Reference cases that have been developed to date (argillite, crystalline, salt, and unsaturated alluvium) are summarized in Section 3, and UQ/SA scope and activities are summarized in Section 2.3.2.

Each year, our GDSA Framework improves as additional modelers and programmers from around the world use, apply, and contribute to its development (Section 2.3.4). GDSA Framework is accessible to everyone because the primary codes, PFLOTRAN and Dakota, are open source, available for free download, and have supporting documentation online. The GDSA team has worked to increase the number of users and participants by

- Maintaining a collaborative web site (pa.sandia.gov);
- Expanding online documentation of verification testing, generic reference cases, and code features;
- Developing quality assurance documentation and a user manual;
- Conducting PFLOTRAN short courses (in FY 2019 in New Mexico, Australia, and Switzerland); and
- Presenting multiple papers and posters on GDSA Framework capabilities at international forums.

Outreach like this supports a primary objective of the GDSA work package by facilitating testing of, and feedback on, PFLOTRAN and GDSA Framework and by increasing the likelihood outside users will contribute directly to code development in the future. Collaboration with outside users is made possible by online version control systems (e.g., Bitbucket.org) and open source access. By encouraging and facilitating use in the outside community, the GDSA team expects to accelerate development of GDSA Framework and to establish GDSA Framework as a leading geologic repository safety assessment tool.

The ability to simulate increasingly complex repository reference cases continues to affirm that HPC-capable codes can be used to simulate important multi-physics couplings directly in a total system safety assessment. The generic repository systems modeled to date indicate that PFLOTRAN and its coupled codes can simulate complex coupled processes in a multi-kilometer domain while simultaneously simulating sub-meter-scale coupled behavior in the repository. Continued development is needed to ensure GDSA Framework is ready for application to potential sites that may be selected in the future. The challenge

is to address the remaining needs using available resources. Meeting this challenge will require close integration with technical teams across the SFWST Campaign.

This report fulfills the GDSA Framework Development Work Package Level 2 Milestone – *Progress in Deep Geologic Disposal Safety Assessment in the U.S. since 2010*, M2SF-19SN010304041.

CONTENTS

	Page
Acknowledgements.....	iv
Executive Summary.....	v
Nomenclature.....	xvi
1. Introduction.....	1
1.1 UFD and SFWST Campaigns.....	1
1.2 Early R&D in Disposal Research.....	1
1.3 GDSA Objectives.....	2
1.4 Report Objectives.....	3
2. GDSA Framework.....	5
2.1 Conceptual Framework.....	5
2.2 Computational Framework.....	6
2.2.1 PFLOTRAN.....	8
2.2.2 Dakota.....	8
2.3 GDSA Framework Capabilities and Development.....	9
2.3.1 Code Development.....	9
2.3.2 Uncertainty Quantification and Sensitivity Analysis.....	27
2.3.3 Quality Assurance.....	33
2.3.4 User Group.....	37
3. Repository Reference Cases.....	40
3.1 Reference Case Development.....	40
3.1.1 Repository Concepts.....	40
3.1.2 Geologic Framework Model.....	41
3.2 Reference Cases.....	44
3.2.1 Argillite.....	44
3.2.2 Crystalline.....	52
3.2.3 Salt.....	61
3.2.4 Alluvium.....	68
4. Supporting Disposal R&D.....	72
4.1 Argillite R&D Activities.....	72
4.2 Crystalline R&D Activities.....	76
4.3 Salt R&D Activities.....	81
4.4 International R&D Activities.....	86
4.5 Engineered Barrier System.....	90
4.6 Dual Purpose Canisters.....	99
4.6.1 Criticality Module.....	99
4.6.2 Results.....	100
4.6.3 Future Work.....	102

4.7	SDA Legacy Document Archive	102
5.	Disposal R&D Roadmap	105
5.1	2012 Roadmap	105
5.2	2019 Roadmap Update.....	108
5.2.1	Methods.....	109
5.2.2	Analysis and Results	111
6.	Summary and Path Forward	122
7.	References	125
Appendix A.	Surrogate Modeling of the Fuel Matrix Degradation (FMD) Model	A-1
Appendix B.	PFLOTRAN QA Test Suite	B-1

FIGURES

	Page
Figure 2-1. Schematic diagram of the conceptual model framework of a generic geologic disposal system.....	6
Figure 2-2. GDSA Framework structure.....	7
Figure 2-3. Flow diagram for the Isotope Partitioning Model.	10
Figure 2-4. Source term features and processes.	12
Figure 2-5. Example results from the Waste Form Process Model.....	15
Figure 2-6. Example DFN representation for a crystalline host rock.	16
Figure 2-7. Schematic illustration of affinity of ²²² Rn for the aqueous phase, relative to ²²⁶ Ra.	18
Figure 2-8. An example hierarchy of process model couplers embedded within the module workflow.	19
Figure 2-9. The local minimum of Branin function is found after 18 outer iterations and 1 inner iteration using the trust region method. Red and grey numbers illustrate the solution location and the trust region size, respectively, after each of the first 7 iterations. The region shrinks from iteration 3 to 4.	21
Figure 2-10. Newton's method (NT) has very fast convergence; however, it could lead to wrong solutions as in Branin and Bohavhechevsky functions. The steepest descent (SD) is the simplest to implement but requires most iterations. The trust region and line search are both robust, but trust region converges in fewer iterations in average.	22
Figure 2-11. Three of the exemplar models used to benchmark VoroCrust mesh simulations.	24
Figure 2-12. Neural network surrogate model predictions versus FMD calculations.....	26
Figure 2-13. k-Nearest Neighbors regressor (kNNr) surrogate model relative pointwise absolute error (RPWAE) compared to the true UO ₂ flux values for the case with 15169 training runs.....	26
Figure 2-14. Uncertainty quantification and sensitivity analysis is an iterative process.....	27
Figure 2-15. Dakota interface with computational model.....	29
Figure 2-16. Complementary cumulative distribution functions (CCDFs) comparing predicted normalized release (R) to containment criteria expressed as a piece-wise uniform CCDF (dashed line). For each of 100 realizations, the CCDF comprises 10,000 futures (left). Mean, median, and bounding CCDFs (right). Example from Swiler et al. (2019, Chapter 4, in progress).	31
Figure 2-17. Example flowchart of PFLOTRAN configuration management processes from the Configuration Management Document.	35
Figure 2-18. Example of PFLOTRAN's QA test suite work flow.	36
Figure 2-19. Hits on PFLOTRAN website by users around the world. Larger circles indicate larger numbers of visits.	38
Figure 3-1. Location of the Shale GFM showing thickness contours of the Pierre Shale (Perry et al. 2014) and locations of boreholes used to define the stratigraphy of the GFM.....	42

Figure 3-2. Block diagram of the Shale GFM viewed from the northeast with a 10x vertical exaggeration. The shaded top surface is a DEM of the region..... 43

Figure 3-3. Surfaces (formation tops) used as the basis for meshing the features of the GFM. 44

Figure 3-4. Schematic drawing of a generic deep geologic repository in argillite or shale, and the engineered barrier system designed to isolate waste. 45

Figure 3-5. Sketch of generic disposal in emplacement boreholes showing elements of the engineered barriers (Jové Colón et al. 2014). 47

Figure 3-6. Stratigraphic section used for generic argillite/shale reference case. 49

Figure 3-7. ¹²⁹I concentration versus time at three observation points in the limestone aquifer: 30 m (a), 2500 m (b), and 5,000 m (c) downgradient of the repository. 51

Figure 3-8. Schematic illustration of the Crystalline Reference Case..... 53

Figure 3-9. Cutaway of a DFN realization mapped to the porous medium grid, showing the far half of the model host rock domain and the full repository. The overlying alluvial sediments are not shown. Fractures of the DFN realization are shown in orange. Unconnected fractures are removed. Five deterministic fracture zones, three sub-vertical (gray) and two with a dip of approximately 30 degrees (red), are common to each DFN realization. Observation points are located above the midline of the repository where the deterministic fracture zones intersect the top boundary. 56

Figure 3-10. ¹²⁹I concentration contours for DFN 1 at 300 years, showing the full repository and a section of the plume..... 58

Figure 3-11. XZ cross section at the Y midpoint of the domain showing the locations of observation points (small teal spheres) (Mariner et al. 2016). 58

Figure 3-12. Predicted concentration of ¹²⁹I versus time for 15 fracture realizations at three observation points at the top of the model. The heavy orange line is Domain6, the fracture realization used in probabilistic simulations. 60

Figure 3-13. Schematic illustration of the Salt Reference Case (Based on Sevougian et al. (2019d, in progress)). The “Stratigraphic Unit Sequence” is the conceptualized stratigraphic section that is included in the reference case model. Note that the “Backfill Layer” is granular salt. The enlarged view, showing the EBS represents the central portion of the drift. The first waste package is set back 25 m from the entrance of the drift. The bottom portion of the model volume is empty, because the thickness of the rock units included in the Salt Reference Case model is less than the other reference case models. The extra volume is included in this figure to facilitate comparisons between the reference cases..... 61

Figure 3-14. Generic stratigraphic column for salt reference case. The repository horizon is centered between the two thin beds of anhydrite at z = 661 m (Sevougian et al. 2016, Figure 4-3). 65

Figure 3-15. Transparent view of the model domain. The 3D structure inside the half-symmetry domain is the repository, including 8 disposal panels and 2 shafts (Sevougian et al. 2016, Figure 4-4). 67

Figure 3-16. ¹²⁹I concentration at 100,000 years in the deterministic simulation (Sevougian et al. 2016, Figure 4-13). 68

Figure 3-17. Schematic of potential unsaturated zone geologic repository. The lithologic heterogeneity that is expected in basin-fill valleys is depicted. Alluvial fans, fluvial systems, spring discharge areas, and playas are common features..... 69

Figure 3-18. The simulation model for the configuration of the repository and natural barrier system. Upper basin fill is shown in light blue and grey, lower basin fill is in dark blue, repository and damage zone are pink and red. 71

Figure 4-1. Schematic drawing of the Mont Terri URL (from Mont Terri website at <https://www.mont-terri.ch/en/experiments/the-most-important-experiments.html>)..... 73

Figure 4-2. Schematic drawing of the FEBEX "In-Situ" Test at the Grimsel Switzerland URL..... 74

Figure 4-3. dfnWorks Workflow. The input for dfnWorks is a fractured site characterization that provides distributions of fracture orientations, radius, and spatial locations. DFNGEN: 1) FRAM - Create DFN: Using the fractured site characterization networks are constructed using the feature rejection algorithm for meshing. 2) LaGriT - Mesh DFN: The LaGriT meshing toolbox is used to create a conforming Delaunay triangulation of the network. 3) DFNFLOW PFLOTRAN- Compute Pressure Solution: The steady-state pressure solution in the DFN is obtained using PFLOTRAN. DFNTRANS: 4) Lagrangian Transport Simulation. A Lagrangian particle tracking method is used to determine pathlines through the network and simulate transport. (Wang et al. 2017) 77

Figure 4-4. Summary figure showing the context of the FMDM within the source term calculation information flow (adapted from Jerden et al. 2017). (Wang et al. 2018b)..... 80

Figure 4-5. Mass ratios of WIPP brines. Blue ellipse: WIPP fluid inclusions; yellow ellipse: near MB-139; green ellipse: near MB-140; red dashed ellipse: E-140 boreholes. (Kuhlman et al. 2018, Figure 7) 82

Figure 4-6. Schematic drift view of satellite observation boreholes and central borehole (Mills et al. 2019, Figure 2)..... 83

Figure 4-7. FE Heater Test at Mont Terri URL: experiment setup and borehole layout (from Zheng et al. 2015). (Birkholzer et al. 2018, Figure 3.1-5)..... 87

Figure 4-8. Schematic cross section of the FEBEX Test at Grimsel Test Site (NAGRA 2014). (Birkholzer et al. 2018, Figure 3.3-6)..... 88

Figure 4-9. Schematic showing GREET tunnel design in a cross-section and photos taken during construction (Iwatsuki 2016). (Birkholzer et al. 2018, Figure 3.2-5) 89

Figure 4-10. 2D cross-sectional mesh for the THMC model..... 94

Figure 4-11. Temperature profiles at the center of the waste package (Cell 27), in the buffer (Cell 149), and in the DRZ (cell 342)..... 100

Figure 4-12. 3D rendering of the simulation domain at 2 times where temperature near the waste package spikes..... 101

Figure 4-13. Screenshot of the SFWD Document Archive SharePoint site..... 104

Figure 5-1. Priority scores for UFDC R&D issues. 106

Figure 5-2. Typical elements of the safety case for geologic disposal..... 112

Figure 5-3. Histogram of priority scores for each host-rock breakout session (including gaps). 113

Figure 5-4. Fraction CDF of priority scores for each host-rock breakout session (including gaps). 113

Figure 5-5. Histogram of priority scores for each R&D activity grouping (including gaps). 114

Figure 5-6. Fraction CDF of priority scores for each R&D activity grouping (including gaps)..... 114

TABLES

	Page
Table 2-1. Performance of the Trust Region Method and Newton’s Method.	23
Table 2-2. Summary of PFLOTRAN software quality assurance primary documents, status and schedule.	34
Table 2-3. PFLOTRAN short courses conducted during FY 2019.....	39
Table 3-1. Repository concepts and generic cases implemented with PFLOTRAN and GDSA Framework.....	40
Table 3-2. Comparison of repository characteristics for generic configurations using 12-, 24- and 37-PWR assembly waste packages, compiled from Mariner et al. (2017b) and Sevougian et al. (2019c).	46
Table 3-3. Key characteristics and processes included in the reference case PA.	50
Table 3-4. Dimensions for the crystalline reference case repository (modified from Wang et al. 2014).	54
Table 3-5. Conceptual representation of the engineered and natural barriers in PA.	56
Table 3-6. Dimensions and counts for the DOE-managed waste bedded Salt Reference Case (Sevougian et al. 2016, Table 4-1).	62
Table 3-7. Dimensions and counts for the commercial SNF bedded Salt Reference Case (Sevougian et al. 2019c, Table 5-1).	64
Table 3-8. Conceptual representation of the engineered and natural barriers in PA (Sevougian et al. 2016, Table 4-6).	66
Table 4-1. NE 81 Disposal Research (DR) documents.....	103
Table 4-2. NE 81 Storage and Transportation (S&T) documents.....	103
Table 4-3. NE 82 Integrated Waste Management (IWM) documents.	103
Table 5-1. Relative priority of groups of R&D issues sorted by processes and geologic media.	107
Table 5-2. Priority ranking of cross cutting technical issues.	108
Table 5-3. High priority R&D activities.	115
Table 5-4. Medium-high priority R&D activities.	116
Table 5-5. High impact R&D topics.	118
Table 5-6. Comparison of 2012 “State-of-the-Art” with 2019 SAL values for R&D activities.....	120
Table 5-7. 2019 SAL (State-of-the-Art Level) metric values and definitions.	121

NOMENCLATURE

1D, 2D, 3D, 4D	one-, two-, three-, and four-dimensional
ANDRA	French national radioactive waste management agency
ANL	Argonne National Laboratory
BATS	Brine Availability Test in Salt
C(A)SH	calcium (aluminum) silicate hydrate
CCDF	complementary cumulative distribution function
CDF	cumulative distribution function
CMD	Configuration Management Document
CSNF	commercial SNF
CTD	closure test drift
d	day
DECOVALEX	Development of COupled models and their VALidation against Experiments
DEM	digital elevation model
DFN	discrete fracture network
DGR	deep geologic repository
DID	Design, Theory, User's Manual, and Implementation Documents
DMS	Document Management System
DOE	U.S. Department of Energy
DPC	dual-purpose canister
DR	disposal research
DRZ	disturbed rock zone
DSNF	DOE-managed SNF
EBS	engineered barrier system
ECPM	equivalent continuous porous medium
EDZ	excavation disturbed zone
EoS	equation of state
Eq.	equation
FEBEX	Full-scale Engineered Barriers Experiment
FEP	feature, event, and process
FMD	Fuel Matrix Degradation
FMDM	FMD model
ft	feet
FY	fiscal year
g	gram
GDSA	Geologic Disposal Safety Assessment
GREET	Groundwater REcovery Experiment in Tunnel
GWd	gigawatt day
HDF5	hierarchical data format, version 5
HF	higher fidelity
HLW	high-level radioactive waste
HotBENT	High temperature effects on BENTonite buffers
HPC	high-performance computing
IAEA	International Atomic Energy Agency
ISC	importance to safety case

IWM	Integrated Waste Management
J	Joule
JAEA	Japan Atomic Energy Agency
K	Kelvin
km	kilometer
kNNr	k Nearest-Neighbors regressor
KOSINA	Konzeptentwicklung für ein generisches Endlager für wärmeentwickelnde Abfälle in flach lagernden Salzschieben in Deutschland sowie Entwicklung und Überprüfung eines Sicherheits- und Nachweiskonzeptes (Concept development for a generic final repository for heat-generating wastes in flat-bedded salt layers in Germany as well as development and examination of a safety and verification concept)
L	liter
LANL	Los Alamos National Laboratory
LBNL	Lawrence Berkeley National Laboratory
LF	lower fidelity
LHS	Latin hypercube sampling
LOE	level of effort
LTDE	Long Term Sorption Diffusion Experiment
m	meter
MD	Munson-Dawson
mm	millimeter
mol	mole
MPa	megapascal
MTHM	metric tons of heavy metal
MWd	megawatt day
NA	not applicable
NBS	natural barrier system
NE	Office of Nuclear Energy
NEA	Nuclear Energy Agency
NM	New Mexico
NQA	Nuclear Quality Assurance
NT	Newton's method
OECD	Organization for Economic Co-operation and Development
OFCT	Office of Fuel Cycle Technology
OoR	out of reactor
ORNL	Oak Ridge National Laboratory
PA	performance assessment
PCC	partial correlation coefficient
PDE	partial differential equation
PETSc	Portable Extensible Toolkit for Scientific Computation
PFLOTRAN	massively parallel reactive flow and transport model for describing subsurface processes (pflotran.org)
pH	negative logarithm of hydrogen ion activity
PICS:NE	Program Information Collection System: NE
PL	practice level
PMC	process model coupler
PNNL	Pacific Northwest National Laboratory

PRCC	partial rank correlation coefficient
PWR	pressurized water reactor
QA	quality assurance
R&D	research and development
RBI	Reference Biosphere 1
RBSN	Rigid-Body-Spring-Network
RD	Requirements Document
RPWAE	relative pointwise absolute error
S&T	Storage and Transportation
SA	sensitivity analysis
SAL	state-of-the-art level
SCC	simple correlation coefficient
SCM	surface complexation model
SDA	SFWD Document Archive
SFWD	Spent Fuel and Waste Disposition
SFWST	Spent Fuel and Waste Science and Technology
SIAM	Society for Industrial and Applied Mathematics
SKB	Swedish Nuclear Fuel and Waste Management Company
SNF	spent nuclear fuel
SNL	Sandia National Laboratories
SQAP	Software Quality Assurance Plan
SRC	standardized regression coefficient
SRCC	Spearman rank correlation coefficient
SSQAP	Sandia SQAP
Sv	sievert
TBD	to be determined
TH	thermal-hydrologic
THC	thermal-hydrologic-chemical
THM	thermal-hydrologic-mechanical
THMC	thermal-hydrologic-mechanical-chemical
TR	trust region
TSPA	total system performance assessment
UFD	Used Fuel Disposition
UFDC	UFD Campaign
ULR	unclassified limited release
UNF	used nuclear fuel
UO ₂	uranium dioxide
UQ	uncertainty quantification
URL	underground research laboratory
U.S.	United States of America
USA	United States of America
UUR	unclassified unlimited release
V&V	verification and validation
VEVAD	Verification and Validation Document
W	watt

WEIMOS	Weiterentwicklung und Qualifizierung der bergbaumechanischen Modellierung für die HAW-Endlagerung im Steinsalz (Further Development and Qualification of the Rock Mechanical Modeling for the Final HLW Disposal in Rock Salt)
WF	waste form
WFPM	Waste Form Process Model
WIPP	Waste Isolation Pilot Plant
WP	waste package
yr	year

1. INTRODUCTION

The Spent Fuel and Waste Science and Technology (SFWST) Campaign of the U.S. Department of Energy (DOE) Office of Nuclear Energy (NE), Office of Spent Fuel & Waste Disposition (SFWD) is conducting research and development (R&D) on geologic disposal of spent nuclear fuel (SNF) and high-level nuclear waste (HLW). Two of the highest priorities for SFWST disposal R&D are design concept development and disposal system modeling (DOE 2011, Table 6). These priorities are directly addressed in the SFWST Geologic Disposal Safety Assessment (GDSA) Framework work package, charged with developing a disposal system modeling and analysis capability for evaluating disposal system performance for nuclear waste in geologic media.

The capability being developed is a software package referred to as GDSA Framework. The primary codes used by GDSA Framework are PFLOTRAN and Dakota (Section 2.2). Each code is designed for massively-parallel processing in a high-performance computing (HPC) environment.

1.1 UFD and SFWST Campaigns

The DOE Office of Nuclear Energy, Office of Fuel Cycle Technology (OFCT) began planning for a R&D program investigating options for permanent disposal of used nuclear fuel and high-level radioactive waste from existing and future fuel cycles in the summer of 2009, with formal funding beginning in the first quarter of FY 2010 for what became the Used Fuel Disposition (UFD) Campaign. Consistent with programmatic changes within the DOE, the name of the campaign changed to Spent Fuel and Waste Science and Technology R&D Campaign in the first quarter of FY 2017 within SFWD. The mission of the campaign and the broad outline of its scope remain largely unchanged.

In the first year of the campaign work focused on research related to generic options for disposal in mined repositories, emphasizing concepts in salt, granitic crystalline rocks, and clay/shale rocks. Generic disposal research has continued to the present, as described in subsequent sections of this report. In addition, the campaign expanded in FY 2011 to include R&D related to the extended storage and subsequent transportation of used fuel, consistent with the growing recognition that fuel would be in storage decades longer than originally intended. This storage- and transportation-related R&D identified knowledge gaps (Hanson et al. 2012) potentially relevant to extended storage, and focused resources on experimental and modeling studies to provide supporting data in three primary areas: evaluating the physical properties of used fuel (and specifically high-burnup fuel and its cladding) during and following extended storage; evaluating the integrity of dry storage canisters during extended use; and evaluating the transportability of used fuels, and in particular high-burnup fuels, following extended storage.

1.2 Early R&D in Disposal Research

In the early years of the UFD Campaign, GoldSim was used to develop simplified PA models for generic disposal environments (Wang and Lee 2010; Clayton et al. 2011). These models provided probabilistic scoping calculations for salt, clay, and deep borehole environments. Other disposal R&D activities at this time focused on process model simulations, repository design, and developing the FEPs database.

In 2011, to help prioritize future disposal R&D activities, the leads of the various disposal research efforts worked together to identify and rank FEPs based on importance to the safety case. This work is documented in the Used Fuel Disposition Campaign Disposal Research and Development Roadmap (DOE 2012). FEPs were identified that were expected to be highly or moderately important in argillite, crystalline, or salt host rocks. The FEPs were also graded based on the level of understanding and readiness for implementation in PA models. Because of this work, funds and plans were adjusted across the UFD Campaign work packages to place more attention on R&D that addressed FEPs of high and moderate importance and low understanding. (In 2019, the Roadmap was revisited and a new set of rankings and priorities (Sevougian et al. 2019b). This work is addressed in Section 5.)

By 2012, it was clear that continued development of PA modeling capabilities required a more advanced modeling framework than GoldSim. A search was conducted for codes that could be used for repository PA simulations. Of the six research codes and five commercial codes evaluated, PFLOTRAN, ASCEM, and Albany were found to be the most suitable (Freeze and Vaughn 2012).

In 2013, PFLOTRAN was chosen as the multi-physics code for PA, and Dakota was chosen for probabilistic implementation. PFLOTRAN is a multiphase flow and reactive transport model for describing surface and subsurface processes (Hammond et al. 2011a; Lichtner and Hammond 2012), and Dakota is an uncertainty quantification and sensitivity analysis code (Adams et al. 2012; Adams et al. 2013). These codes were chosen because they are open source, massively parallel, and together have the potential to simulate a total integrated geologic repository system and its surroundings probabilistically and in three dimensions. These two codes continue to provide the primary framework for GDSA Framework.

Since its adoption as part of GDSA Framework, PFLOTRAN has gained many new features and capabilities for simulating repository performance. New features since 2013 are highlighted in Section 2. In addition, the reference case models have transformed from simple 1D models to fully-coupled 3D thermal, hydrologic, and solute transport models, and grid sizes have grown to millions of cells. The current states of the reference case models are summarized in Section 3.

UFD and SFWST disposal research conducted outside of the PA group since 2010 has supported the PA effort by continuing to improve understanding of near-field processes, coupled phenomena, and radionuclide behavior. Such research has been carried out in the laboratory, in international underground research facilities, and on the computer. The data and models resulting from this R&D add to the technical bases. Involved work packages include those addressing argillite host rock, crystalline host rock, salt host rock, engineered barrier systems, dual-purpose canisters, and international collaboration studies (e.g., DECOVALEX). Section 4 provides summaries of work performed in these areas and discusses how the R&D helps support safety assessment.

1.3 GDSA Objectives

The purpose of the GDSA Framework Development work package is to develop a GDSA capability that:

- Integrates updated conceptual models of subsystem processes and couplings developed under this and other disposal research work packages,
- Is used to evaluate disposal research R&D priorities,
- Leverages existing computational capabilities (e.g., meshing, visualization, high-performance computing (HPC)) where appropriate, and
- Is developed and distributed in an open-source environment.

The long-term goal for the GDSA team is to develop a safety assessment capability that can simulate all potentially important FEPs for a given repository environment. Such a capability is years away, but a DOE timeline suggests that a PA model for a potential candidate site will likely not be needed for a license application until at least 2037 (DOE 2013b). Although the specific timing is more uncertain, with additional time, continued advances in computing speed, and continued code development, it is expected that much progress will be made toward the long-term goal by the time the capability is applied for its ultimate purpose.

For the near term, GDSA objectives are focused on adding FEPs to the PA model and on developing a suite of probabilistic repository reference case applications. (Prioritization of these FEPs are discussed in Section 5.) These objectives are in line with the long-term goal. In addition, the products of these near-term

objectives are useful for evaluating the effects of FEPs and input parameters on repository performance, which is useful for R&D planning.

For FY 2019, five tasks were addressed:

- Identify additional capabilities needed to advance the GDSA Framework to a robust PA model (e.g., multiphase processes, temperature dependencies, colloids, EBS degradation processes, control variate method, code efficiency, convergence, grid refinement). The GDSA work package will work closely with other work packages as applicable in identifying these needs, determining what is required to sufficiently address them, and working to fulfill them.
- Integrate subsystem models developed under this and other work packages into the GDSA-PA system model architecture (e.g., waste form degradation, waste package degradation, colloid stability and transport, EBS chemistry, EBS flow and transport, fracture representation, thermal-hydrological-mechanical processes, natural system flow and transport).
- Develop, perform, and document verification and validation analyses of relevant GDSA model processes and expand regression testing to demonstrate and assure continued quality.
- Demonstrate the freely-available PFLOTRAN GDSA Framework and modeling capability at national and international forums and conduct one or more workshops to promote accelerated use of the capability worldwide. Expanding the user base is expected to provide additional testing of the code and opportunities for additional development by outside contributors.
- Plan and conduct R&D integration and prioritization workshops to evaluate and summarize the status of SFWST R&D conducted to date (from 2010 to 2019) on generic deep geologic repositories (DGRs), and to prioritize R&D still desirable to enhance confidence in the generic safety case for DGRs in various host rocks. These workshops will be conducted jointly with the Crystalline, Argillite, and Salt work packages.

As documented in this report, good progress was made on each of these tasks.

1.4 Report Objectives

This report documents progress and accomplishments on each of the FY 2019 tasks listed in the previous section. In addition, it describes the development of GDSA under the UFD and SFWST Campaigns over the past ten years. The specific objectives of this report are:

- To provide an overview of the GDSA effort since the UFD Campaign was initiated in 2010,
- To highlight progress in GDSA code development and reference case simulations since 2010, and
- To identify priorities for additional GDSA capability development going forward.

Accomplishments prior to this year are summarized and cited so that the reader may refer to the primary documents for more details.

Section 2 describes the conceptual model framework and the PFLOTRAN-based computational framework for GDSA. That framework and the codes that comprise it are collectively referred to as GDSA Framework. In addition, Section 2 summarizes the major capabilities added and developed during the UFD and SFWST Campaigns for PFLOTRAN and Dakota as well as development of an international PFLOTRAN user group. Section 3 addresses the application of GDSA Framework to repository system modeling and summarizes the status of the reference case models developed in four different host geologies. Section 4 highlights work performed in other UFD and SFWST work packages that support technical bases and safety assessment of the various potential host rocks and repository concepts. That work contributes significantly

to GDSA Framework development. Section 5 revisits the disposal R&D roadmap activities performed earlier this year and provides additional analysis of priorities for future GDSA Framework development. Conclusions are summarized in Section 6.

This report fulfills the GDSA work package (SF-19SN01030404) Level 2 Milestone M2SF-19SN010304041, *Progress in Deep Geologic Disposal Safety Assessment in the U.S. since 2010*. In addition to reporting FY 2019 accomplishments for this work package, it reports in Section 2.3.1 and Appendices A and B progress in FY 2019 on the GDSA Modeling work package (SF-19SN01030406). Further, this report provides a summary of important accomplishments in GDSA performance assessment over the past ten years and identifies priorities for future GDSA PA capability development. Therefore, this report incorporates information from the following supporting milestones: Wang and Lee (2010); Clayton et al. (2011); Freeze and Vaughn (2012); Freeze et al. (2013a); Sevougian et al. (2013); Vaughn et al. (2013); Sevougian et al. (2014); Mariner et al. (2015); Mariner et al. (2016); Mariner et al. (2017b); Mariner et al. (2018b); Sevougian et al. (2019b); Sevougian et al. (2019c).

2. GDSA FRAMEWORK

A performance assessment (PA) for underground disposal of nuclear waste utilizes a comprehensive analysis of features, events, and processes (FEPs) potentially affecting the release and transport of radionuclides to the biosphere. In a comprehensive PA, plausible scenarios and processes that may affect repository performance are addressed. FEPs and scenarios are evaluated and screened. Potentially pertinent FEPs are identified for simulation in a quantitative PA model. Probabilistic simulations are performed, and results are evaluated against performance metrics. Uncertainty and sensitivity analyses may also be performed to inform prioritization of additional research and model development.

The PA framework consists of a conceptual model framework (Section 2.1) and a computational framework (Section 2.2). An overview of PA methodology and terminology is presented in Sevougian et al. (2014, Section 2.2), Meacham et al. (2011, Section 1) and elsewhere (Rechard 2002).

2.1 Conceptual Framework

A safety case for a deep geologic disposal facility is a comprehensive analysis designed to assess regulatory compliance with safety standards. More specifically, it is a widely accepted approach for documenting the basis for the understanding of the disposal system, describing the key justifications for its safety, and acknowledging the unresolved uncertainties and their safety significance (OECD 2004; IAEA 2006; Freeze et al. 2013b). In general, building such a safety case requires three primary components (as shown in Figure 5-2 in Section 5.2.2): a safety strategy, technical bases, and a safety assessment.

- The safety strategy provides direction and boundaries for the safety case. It guides the safety case by identifying requirements for site location, repository design, and safety objectives.
- Technical bases are the laws of nature and the physical and chemical barriers that govern the system. They address each feature, event, and process (FEP) that could potentially facilitate or inhibit the transport of radionuclides from the repository to the biosphere. Development of the technical bases involves site characterization, FEPs identification, waste inventory, barriers to radionuclide release and migration, radionuclide behavior, natural analogs, model validation, code verification, and uncertainty quantification.
- Safety assessment involves the analysis of technical bases to evaluate whether the objectives of the safety strategy are met. In safety assessment, each FEP included in the technical bases is either incorporated into the probabilistic PA model or is addressed in separate analyses or process model simulations. In the PA model, probabilistic predictions of regulatory metrics (e.g., annual dose rate) are calculated to compare to regulatory limits.

The goals and objectives of the GDSA team focus on safety assessment and, more specifically, on the development of the PA model. Conceptually, the long-term vision for the GDSA effort is to ensure that the GDSA modeling capability can adapt to, and take advantage of, future advances in computational software and hardware and future advances in process modeling. In line with this vision, the near-term mission is to develop a robust suite of fully functional generic repository reference case applications (1) for application to candidate sites by the time they are selected and (2) for evaluation of the effects of FEPs and input parameters on repository performance to inform R&D planning.

Consistent with the long-term vision, two open-source, HPC codes serve as the core of the GDSA Framework: PFLOTRAN and Dakota. PFLOTRAN is a thermal-hydrologic-chemical (THC) flow and transport code, and Dakota is a versatile probabilistic code (Section 2.2). The PFLOTRAN code is being developed by the GDSA team to accommodate new geologic disposal process models and capabilities through additional code development and coupling with external process models. The HPC capabilities of

PFLOTRAN and Dakota allow for ever higher fidelity in total system performance assessment modeling as more powerful HPC resources become available.

As the GDSA modeling capability evolves, the GDSA team will continue to generate and refine three-dimensional models of disposal repository concepts complete with surrounding geospheres and connected biospheres. Sensitivity analyses will be performed on these models to distinguish the importance of features, processes, and parameters on model results. These analyses are expected to assist prioritization of future disposal R&D.

A conceptual model framework requires a coherent representation of pertinent FEPs. Figure 2-1 schematically illustrates the conceptual model framework for a repository system. To calculate a dose to a receptor in the biosphere, radionuclides released from the waste form must pass through the repository engineered barrier system (EBS) and the surrounding natural barrier system (NBS).

A FEPs database like the one developed and described in Freeze et al. (2011) can be used to help identify a full set of potentially important FEPs for a specific conceptual repository model. Many of the FEPs in a FEPs database may be directly simulated in the PA model. In a comprehensive PA, excluded FEPs (i.e., FEPs not simulated in the PA model) must be addressed in separate analyses and arguments.

Important processes and events in the conceptual model are those that could significantly affect the movement of radionuclides in the EBS and NBS. Such processes and events include waste package corrosion, waste form dissolution, radionuclide release, radioactive decay, heat transfer, aqueous transport, advection, diffusion, sorption, aqueous chemical reactions, precipitation, buffer chemical reactions, gas generation, colloidal transport, earthquakes, and inadvertent human intrusion of the repository.

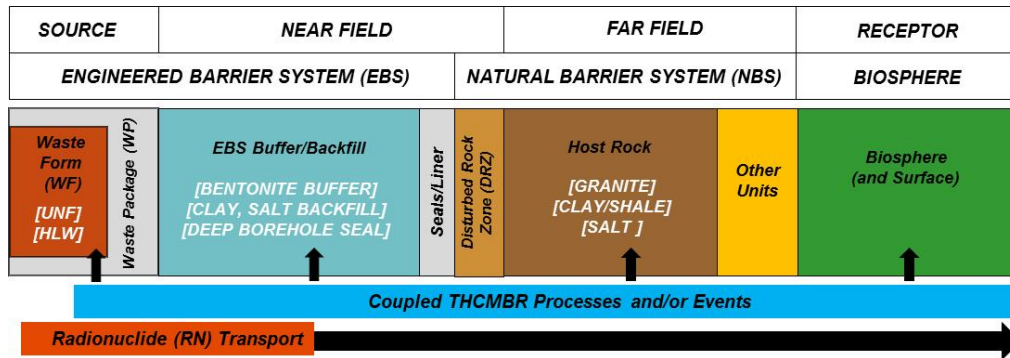


Figure 2-1. Schematic diagram of the conceptual model framework of a generic geologic disposal system.

2.2 Computational Framework

Performance assessment of a geologic repository is enhanced by directly modeling the important coupled processes in the system and by executing multiple probabilistic realizations. The approach of using detailed models directly in a PA is a continuation of the successful modeling approach adopted for the Waste Isolation Pilot Plant (WIPP) PAs (Rechard 1995; Rechard 2002; Rechard and Tierney 2005) and differs from the modeling approach adopted for past PAs for disposal of spent nuclear fuel (SNF) and high-level radioactive waste (HLW) in volcanic tuff (Rechard and Stockman 2014). For this reason, GDSA Framework is designed for massively-parallel processing in a HPC environment.

GDSA Framework consists of the following components:

- Input parameter database
- Software for sampling, sensitivity analysis, and uncertainty quantification (Dakota)

- Petascale multiphase flow and reactive transport code (PFLOTRAN), working in concert with coupled process model codes (e.g., Fuel Matrix Degradation (FMD) Model)
- Computational support software and scripts for meshing, processing, and visualizing results (e.g., CUBIT, Python, ParaView, VisIt).

The two primary components of this computational framework are PFLOTRAN and Dakota. PFLOTRAN is a thermal-hydrologic-chemical multi-physics code (Hammond et al. 2011a; Lichtner and Hammond 2012) that is used to simulate coupled multi-physics processes affecting waste isolation in a repository system and transport of released radionuclides to the biosphere over time. Simulated processes include heat flow, fluid flow, waste dissolution, radionuclide release, radionuclide decay and ingrowth, precipitation and dissolution of secondary phases, and radionuclide transport. Dakota is an uncertainty sampling and propagation code (Adams et al. 2012; Adams et al. 2013). Dakota is used to propagate uncertainty in PFLOTRAN simulations and to analyze PFLOTRAN results to assess sensitivities of model processes and inputs. These two codes are described in more detail in Sections 2.2.1 and 2.2.2.

The flow of data and calculations through the components of GDSA Framework is illustrated in Figure 2-2. In a probabilistic simulation, Dakota generates stochastic input for each PA realization based on parameter uncertainty distributions and input parameter correlations. The sampled inputs are used by PFLOTRAN and its coupled process models to simulate source term release, EBS evolution, flow and transport through the EBS and NBS, and uptake in the biosphere. After the simulation, various software may be used to reduce and illustrate the output results of parameters and performance metrics. Dakota may also be used to evaluate the effects of parameter uncertainty on specific outputs.

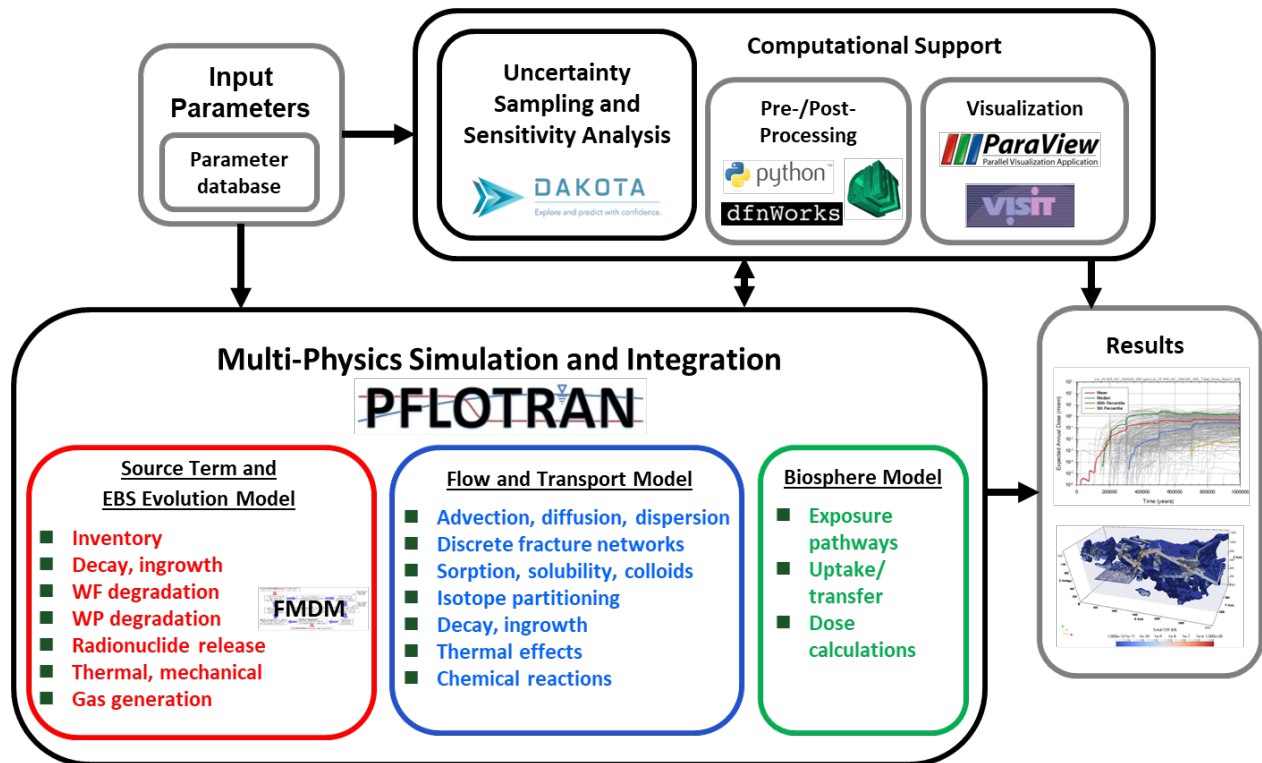


Figure 2-2. GDSA Framework structure.

2.2.1 PFLOTRAN

PFLOTRAN (Hammond et al. 2011a; Lichtner and Hammond 2012) is an open source, reactive multi-phase flow and transport simulator designed to leverage massively-parallel high-performance computing to simulate subsurface earth system processes. PFLOTRAN has been employed on petascale leadership-class DOE computing resources (e.g., Jaguar [at Oak Ridge National Laboratory (ORNL)] and Franklin/Hopper [at Lawrence Berkeley National Laboratory (LBNL)]) to simulate THC processes at the Nevada Test Site (Mills et al. 2007), multi-phase CO₂-H₂O for carbon sequestration (Lu and Lichtner 2007), CO₂ leakage within shallow aquifers (Navarre-Sitchler et al. 2013), and uranium fate and transport at the Hanford 300 Area (Hammond et al. 2007; Hammond et al. 2008; Hammond and Lichtner 2010; Hammond et al. 2011b; Chen et al. 2012; Chen et al. 2013). PFLOTRAN is also under development for use in PA at the Waste Isolation Pilot Plant (WIPP).

PFLOTRAN solves the non-linear partial differential equations describing non-isothermal multi-phase flow, reactive transport, and geomechanics in porous media. Parallelization is achieved through domain decomposition using the Portable Extensible Toolkit for Scientific Computation (PETSc) (Balay et al. 2013). PETSc provides a flexible interface to data structures and solvers that facilitate the use of parallel computing. PFLOTRAN is written in Fortran 2003/2008 and leverages state of the art Fortran programming (i.e. Fortran classes, pointers to procedures, etc.) to support its object-oriented design. The code provides “factories” within which the developer can integrate a custom set of process models and time integrators for simulating surface and subsurface multi-physics processes. PFLOTRAN employs a single, unified framework for simulating multi-physics processes on both structured and unstructured grid discretizations (i.e. there is no duplication of the code that calculates multi-physics process model functions in support of structured and unstructured discretizations). The code requires a small, select set of third-party libraries (e.g., MPI, PETSc, BLAS/LAPACK, HDF5, Metis/Parmetis). Both the unified structured/unstructured framework and the limited number of third-party libraries greatly facilitate usability for the end user.

Specific PFLOTRAN capabilities for the simulation of generic disposal systems include:

- Multi-physics
 - Multi-phase flow
 - Multi-component transport
 - Biogeochemical processes
 - Thermal and heat transfer processes
- High-Performance Computing (HPC)
 - Built on PETSc – parallel solver library
 - Massively parallel
 - Structured and unstructured grids
 - Scalable from laptop to supercomputer
- Modular design based on object-oriented Fortran 2003/2008 for easy integration of new capabilities

2.2.2 Dakota

The Dakota software toolkit is open source software developed and supported at Sandia National Laboratories (Adams et al. 2012; Adams et al. 2013). Dakota provides deterministic codes an extensible interface for propagating uncertainty into a set of realizations and for performing sensitivity analysis and

optimization. GDSA Framework uses Dakota's sampling schemes, principally Latin Hypercube Sampling (LHS), to propagate input value uncertainty into probabilistic PFLOTRAN simulations. Dakota is also used in sensitivity analyses to analyze the effects of input value uncertainty on probabilistic GDSA Framework results. Dakota is discussed in more detail in Section 2.3.2.2.

2.3 GDSA Framework Capabilities and Development

Incorporating process models and probabilistic tools into repository PA simulations greatly facilitates evaluation of the importance of FEPs and their interactions in PA applications. Developing these capabilities has been a major goal of the GDSA team for many years. Collaboration with other work packages of the UFD and SFWST Campaigns and interactions with the international community have aided in this development. Many examples of these collaborations are highlighted in Section 4.

This section describes GDSA Framework development since its inception in 2013. Section 2.3.1 summarizes the capabilities developed and added to PFLOTRAN and the tools developed for generating and visualizing meshes. Section 2.3.2 summarizes the scripts and visual tools developed for uncertainty quantification and sensitivity analysis using Dakota. Section 2.3.3 addresses the quality assurance (QA) documentation and QA verification testing that have been developed. Section 2.3.4 discusses the growing PFLOTRAN community and the benefits of open source coding and collaboration with PFLOTRAN users and developers external to the GDSA team.

2.3.1 Code Development

By the time PFLOTRAN was adopted as the main code for GDSA PA modeling, it was already well-established as a thermal-hydrologic-chemical code for groundwater flow and reactive transport. However, to apply it to a nuclear waste repository, many new capabilities were needed. The following subsections summarize important capabilities added to PFLOTRAN for radionuclide processes (Section 2.3.1.1), source term processes (Section 2.3.1.2), representation of geophysical properties (Section 2.3.1.3), and biosphere processes (Section 2.3.1.4). In addition, there have been important improvements in PFLOTRAN's computational capabilities (Section 2.3.1.5) and in the development and coupling of surrogate models (Section 2.3.1.6).

2.3.1.1 Radionuclide Processes

To improve PA simulation of radionuclide behavior in geologic media, several radionuclide processes and features have been added to PFLOTRAN over the past few years. They include decay and ingrowth in all phases, isotope partitioning among phases, aqueous solubility limits for isotopes, and linear sorption to specific minerals. Other capabilities, such as colloidal partitioning, are in the process of being added or improved.

Decay and Ingrowth: Previously, PFLOTRAN could only simulate decay and ingrowth using the chemistry process model of PFLOTRAN via the reactive transport solver. That approach is insufficient for repository system modeling because it cannot be applied to precipitated isotopes. A new approach was needed to perform decay and ingrowth outside the chemistry process model, one that would perform decay and ingrowth in all phases.

To do this, an algorithm was developed that uses Newton's method to solve the Bateman equation for any length and combination of decay chains. The Bateman equation solves the conservation equation that describes the abundance of a radionuclide in a decay chain as a function of time. A description of this model is provided in (Mariner et al. 2017b).

Isotope Partitioning: The Isotope Partitioning Model was added to PFLOTRAN to provide a reduced-order alternative to the PFLOTRAN chemistry process model. Though the PFLOTRAN chemistry process model is well-established (Lichtner et al. 2015), it has important limitations – it requires significant effort

to ensure that all desired reactions are included and correct and significant computer time on large meshes. Further, the chemistry process model and its database were developed for elemental and molecular species, not isotopes.

The Isotope Partitioning Model is an equilibrium model that distributes isotopes and elements among aqueous, adsorbed, and precipitate phases based on element-specific adsorption coefficients (e.g., K_d values) and element-specific solubility limits. For solubility, instead of identifying and simulating specific minerals and chemical reactions, the user defines redox-specific elemental solubility limits or their probability distributions. The model distributes isotopes of the same element across the phases such that the isotope mole fractions for a given element are the same in each phase (i.e., no fractionation). Distributing isotopes in this way maximizes entropy (i.e., equilibrium partitioning) and ensures that important isotopes are not disproportionately trapped within a precipitate phase. A flow diagram of the Isotope Partitioning Model is shown in Figure 2-3. All calculations within the Isotope Partitioning Model are exact and require no iteration.

To simulate solubility limits accurately, the model requires that all isotopes that could potentially have a significant contribution to the aqueous elemental concentration be included in the simulation. An additional limitation is that the model is highly conditional. It requires the user to predetermine redox-specific elemental solubility limits and equilibrium adsorption coefficients. Additional information about this partitioning model can be found in Mariner et al. (2016).

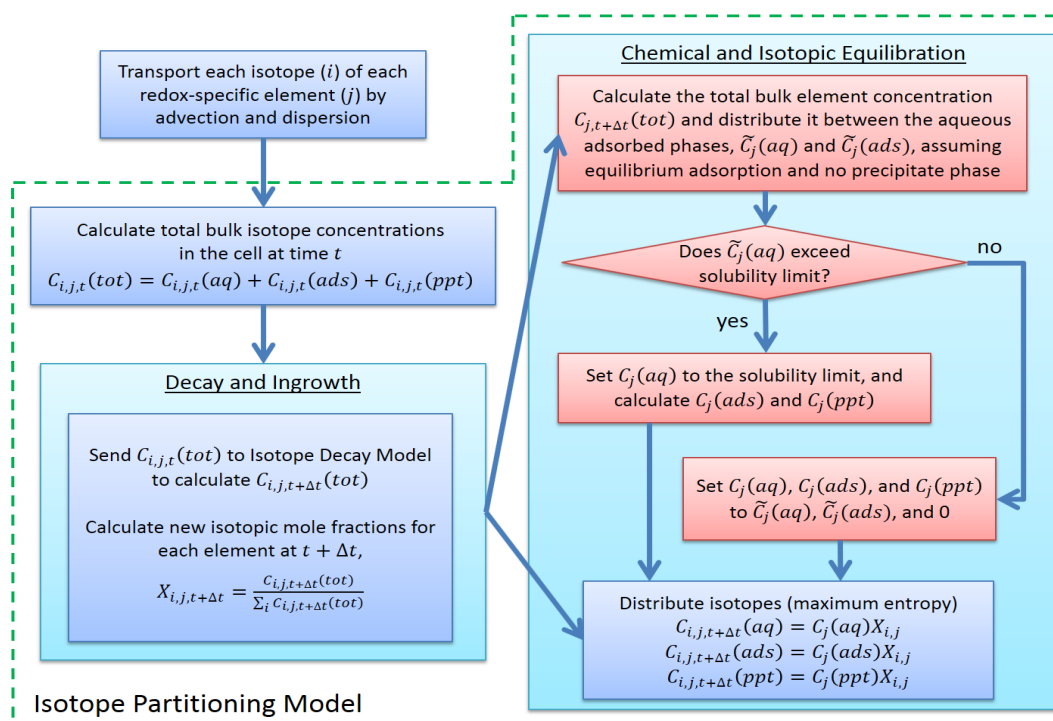


Figure 2-3. Flow diagram for the Isotope Partitioning Model.

Solubility: In the Isotope Partitioning Model, each isotope of an element is assumed to have identical solubility in isolation. This is a reasonable assumption because the differences in solubility between isotopes of the same element are expected to be small compared to the uncertainty in environmental conditions that affect solubility (e.g., temperature, pH).

The solubility of a radionuclide in the Isotope Partitioning Model is calculated to be the product of the solubility of the isotope's element and the isotope's elemental mole fraction. Thus, the model requires that all isotopes with significant elemental mole fractions (e.g., >1%) be included in the simulation if the element's aqueous concentration could be limited by solubility. Contributing isotopes may be stable, naturally occurring, and/or introduced by EBS materials. Excluding potentially significant isotopes from the simulation effectively inflates the elemental solubility causing increased mobility for the included isotopes.

Elemental solubility is entered as a constant in the PFLOTRAN input file. Future plans are to include functional relationships for elemental solubility so that its value can depend on important environmental variables like temperature and pH.

Sorption: Although PFLOTRAN can perform surface complexation modeling (SCM), SCM is complex, data intensive, and requires the PFLOTRAN chemistry process model. For repository PA simulations, a simpler and faster model, such as a linear K_d model, is expected to be suitable in most cases and does not require running the chemistry process model.

For GDSA Framework, the linear K_d model of PFLOTRAN was upgraded to be mineral specific. Future plans are to add new adsorption relationships, such as Langmuir and Freundlich isotherms, and to include functional relationships so that adsorption constants can depend on environmental conditions.

Colloids: A kinetic radionuclide-colloid partitioning model developed by Reimus et al. (2016) for GDSA Framework is ready for implementation. The mathematical basis for the model equations is provided in Reimus (2017) along with test cases. This model when implemented will be a significant enhancement to the current PFLOTRAN colloid model. Because this is a kinetic model, it cannot be incorporated directly within the Isotope Partitioning Model. Instead, an operator-splitting approach is proposed for accommodating isotope partitioning (Mariner et al. 2017a).

2.3.1.2 Source Term Processes

The source term in a repository PA simulation is a combination of emplaced inventory (the source) and the rate of release of this source over time. The emplaced inventory consists of the volumes and locations of emplaced waste forms in the repository and the concentrations of radionuclides within these waste forms. An additional source term for radionuclides in repository simulations is neutron activation of isotopes in waste package materials, e.g., ^{59}Ni from ^{58}Ni (SKB 2006, Section 3.2); this process is not yet simulated by GDSA Framework.

The various features and processes developed for the source term in GDSA Framework are summarized in Figure 2-4. Defining the source inventory and its packaging is relatively routine compared to predicting the release rates. Predicting the release rates of radionuclides over time requires predicting the performance of waste package barriers over time and thereafter the rates of waste form dissolution and radionuclide release from the waste.

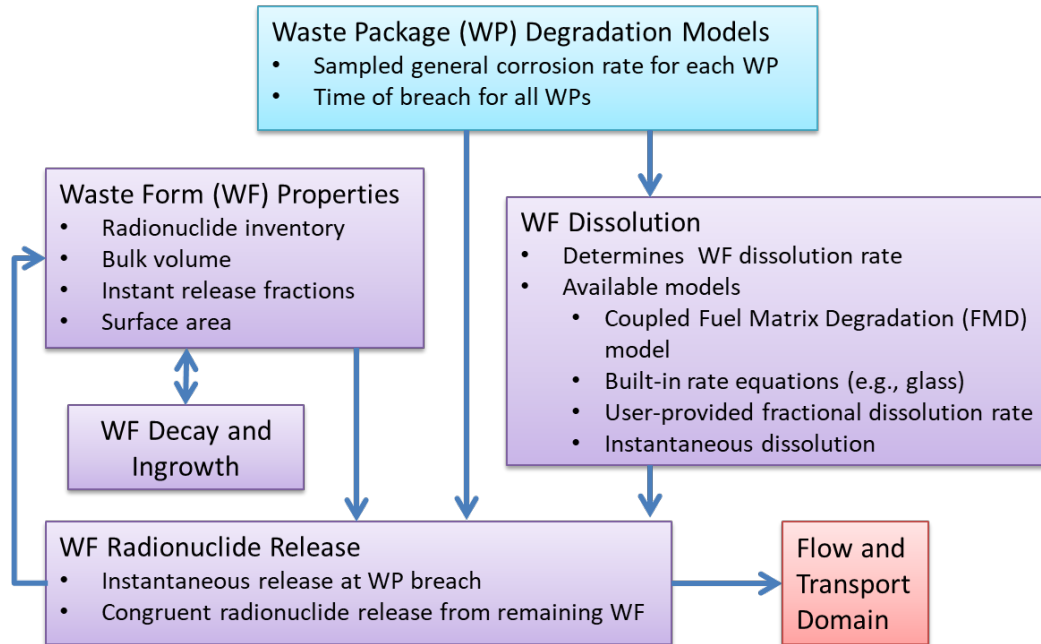


Figure 2-4. Source term features and processes.

Waste Form Process Model: The Waste Form Process Model (WFPM) was developed as a PFLOTRAN module for GDSA Framework to calculate and track the source term for each waste package over time, all while maintaining mass balance. The WFPM effects important degradation processes over time and releases radionuclides as waste forms dissolve. Multiple waste forms may be included in each waste package, each with its own waste form dissolution process. All the while, decay and ingrowth of radionuclides within the waste are simulated and tracked to improve radionuclide release rate calculations.

The WFPM has three main components: (i) a waste package degradation model, (ii) a waste form object, and (iii) a waste form dissolution mechanism. The waste package degradation model determines waste package breach. Once the waste package has breached, the waste form object begins dissolving according to its assigned dissolution mechanism, and the radionuclide source term is calculated. See Section 3.2.1 and Section 3.2.2 in Mariner et al. (2016) for an in depth description of the WFPM. Each waste package can be defined as a waste form region object so that it can include multiple cells in a mesh (Mariner et al. 2017b).

Waste Package Degradation: The first component of the WFPM is the waste package degradation model. The user can specify either a time of breach for all waste packages or a waste package degradation rate coefficient for a general corrosion mechanism. For the latter approach, the degradation rate is coupled to the evolving local temperature at each time step using the Arrhenius equation. Further, entering the degradation rate coefficient as a distribution will increase the variation in breach times among waste packages across the repository. The waste package degradation model tracks the remaining vitality of the waste package (e.g., the waste package wall thickness), and once it drops to zero, a Boolean flag will turn on the waste package's waste form object.

Waste Form Object: The second component of the WFPM is the waste form object. This object is generic and contains only the information that is common between any waste form types. The user defines each waste form object's location in the domain, as well as its initial volume, and exposure factor (a surface area multiplying factor to the waste form's effective dissolution rate). Within the waste form object, the value of its effective dissolution rate is stored. Each waste form object has a pointer to the waste form mechanism (the third component of the process model) that describes waste form type-specific information. The dissolution equation that defines the effective dissolution rate is obtained from the waste form mechanism.

The waste form object also stores the concentrations of the set of radionuclides it contains. The initial set of radionuclides is obtained from the waste form mechanism.

Radionuclide decay and ingrowth is internally calculated for the set of radionuclides in each waste form according to a 3-generation analytical solution derived for multiple parents and grandparents and non-zero initial daughter concentrations (Mariner et al. 2016). The solution is obtained explicitly in time. Internal calculation of radionuclide decay and ingrowth allows the ability to account for instantaneous release fractions for certain radionuclides upon canister breach.

Waste Form Dissolution: Upon canister breach, the waste form object begins to dissolve according to the dissolution model that is defined by the third component of the WFPM, the waste form dissolution mechanism. Waste form volume decreases accordingly. This component is specific to the type of waste form being simulated and contains information which defines the behavior of each waste form type. The mechanism contains the value of the waste form bulk density, the set of initial radionuclides (initial mass fractions, molecular weights, decay rates, daughter species, and instantaneous release fractions), and a pointer to the waste form dissolution model. In some cases, it also stores the waste form specific surface area.

Because a performance analysis simulation typically contains hundreds or thousands of waste form objects but only a few waste form “types,” separating the waste form type-specific information into the waste form mechanism improves modularity and numerical efficiency. An additional benefit of the modularity is that new waste form types can easily be created in PFLOTRAN by simply creating new waste form mechanisms.

Currently, four types of waste form mechanisms have been implemented. Details of each mechanism may be found in Mariner et al. (2016) and Mariner et al. (2017b). They include:

- Instantaneous dissolution (e.g., for metallic spent fuel)
- Dissolution rate
- Fractional dissolution rate
- Transition state theory dissolution rate equation
- Kienzler dissolution rate for HLW glass
- Fuel Matrix Degradation (FMD) Model (Jerden et al. 2015)

In addition, an instantaneous release fraction model is implemented in the WFPM to allow user-defined fractions of waste form inventories of certain radionuclides to be released to the surroundings immediately upon waste package breach.

Spent Fuel Dissolution Example: Figure 2-5 shows an example of what the WFPM calculates and tracks over time. In this example, a waste package containing spent nuclear fuel (300W – 500W bin) breaches at approximately 1,000 years (Mariner et al. 2016). After breach, the waste form dissolves by the FMD mechanism. The initial inventory assumes a 30-year decay time, commercial pressurized water reactor (PWR) assemblies, 60,000 MWd/MTHM burn-up, and 4.73% enrichment. The larger PFLOTRAN simulation portrays the evolution of a single waste form inside a cube of 27 (3×3×3) 1-m³ grid cells. It assumes no fluid flow, no diffusive flux across the domain boundaries, and a constant temperature of 25°C. The figure shows the values of the following parameters over time:

- Normalized waste package wall thickness, labeled “canister vitality”
- Waste form volume
- Waste form dissolution rate

- Radionuclide mass fractions in the waste form
- Radionuclide release rates from the waste form
- Aqueous radionuclide concentrations in groundwater

Note that several radionuclides experience increases in mass fraction or concentration due to decay and ingrowth. Note also that solubility limits control the aqueous concentrations of several of the released radionuclides, and in conjunction with the Isotope Partitioning Model (Section 2.3.1.1), prevents the groundwater from being supersaturated with any of the isotopes relative to the solubility limiting constraint.

Criticality: A criticality event in an emplaced waste package would markedly change the source term for both radionuclides and heat. Such an event is being incorporated in PA simulations involving the direct disposal of dual-purpose canisters (DPCs). A reduced-order model is being developed for PFLOTRAN to approximate the effects on radionuclide inventories and heat generation as observed in complex process modeling of a criticality. This work is described in more detail in Section 4.6.

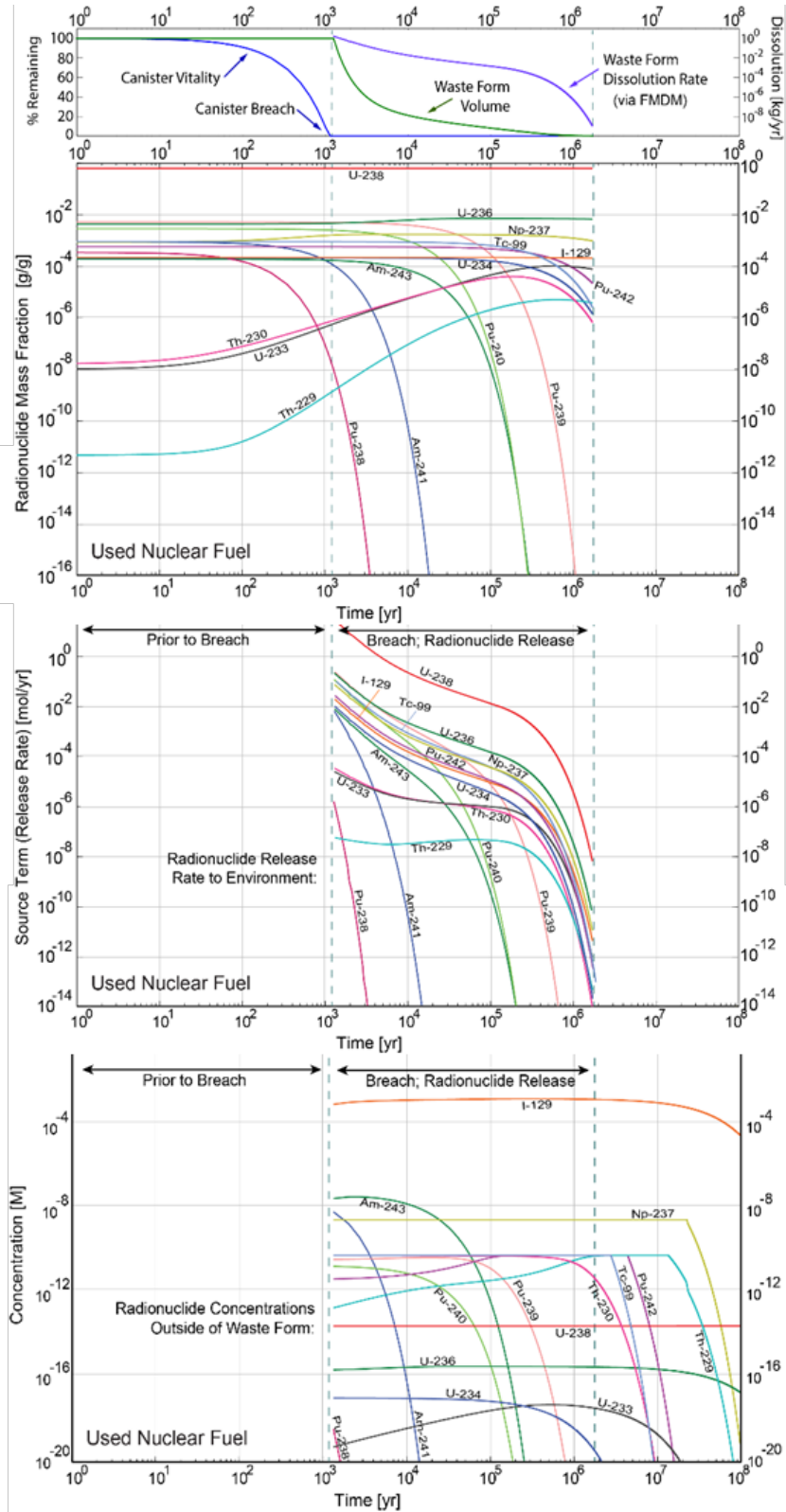


Figure 2-5. Example results from the Waste Form Process Model.

2.3.1.3 Geophysical Properties

The need to model discrete fracture networks (DFNs), unsaturated conditions, and buffer/backfill evolution has required development within and outside of PFLOTRAN. Several of these developments are described below.

Discrete Fracture Networks: Fracture networks are key to radionuclide transport in crystalline rock. Beginning in 2015, the crystalline host rock reference case was implemented in GDSA Framework. (Mariner et al. 2016). DFNs were generated with dfnWorks (Hyman et al. 2015a; Hyman et al. 2015b) assuming fracture sets and fracture domains similar to those at Forsmark, Sweden. At Forsmark, large-scale mappable features of concentrated brittle and/or ductile deformation (termed “deformation zones”) bound volumes of relatively undeformed rock (Follin et al. 2014; Joyce et al. 2014). Each volume of relatively undeformed rock (termed a “fracture domain”) is sparsely fractured, and the fractures within each were described in terms of a number of “fracture sets,” distinguished from each other on the basis of fracture orientation.

Because PFLOTRAN uses a finite volume grid, which is advantageous for predicting heat flow, a mapping tool was developed for GDSA Framework to map the DFNs generated with dfnWorks into the equivalent continuous porous medium (ECPM) domain simulated by PFLOTRAN. This tool was coded in Python and was named mapDFN (Mariner et al. 2016). mapDFN takes as input the output from dfnWorks and parameters describing the desired ECPM model domain and discretization, including the origin and extent of the domain and the size (length) of the grid cells, which are constrained to be cubic. It determines which fractures intersect which grid cells and calculates grid cell permeability and porosity on the basis of fracture permeability and aperture. Anisotropic grid cell permeability is calculated by summing the contributions of all the fractures intersecting the cell.

Figure 2-6 shows an example of an ECPM after a DFN was mapped to it. Fractures of the DFN realization are shown in orange. Unconnected fractures are removed prior to mapping. Five deterministic fracture zones, three sub-vertical (gray) and two with a dip of approximately 30 degrees (red), are also shown. Observation points 2, 4, 6, and 8 are located above the midline of the repository where the deterministic fracture zones intersect the top boundary.

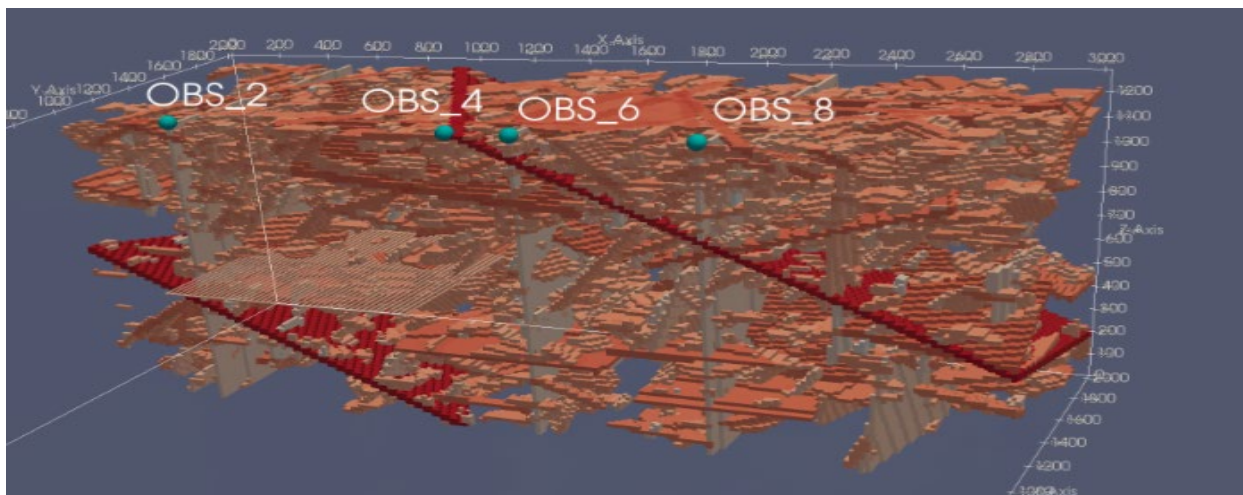


Figure 2-6. Example DFN representation for a crystalline host rock.

Density-Driven Flow: For certain repository concepts, such as deep borehole disposal or a repository near the ocean, density-driven flow may be important. PFLOTRAN was equipped with an equation that

calculates fluid density as a function of salinity, temperature, and pressure, where salinity is determined from the concentration of a conservative tracer with the molecular weight of NaCl. This capability was used to evaluate density stratification and the potential for deep advection of fresh water (Freeze et al. 2019).

Permeability Scaling: Rather than using full-tensor permeability, PFLOTRAN employs a scalar permeability along each principal axis of the simulation coordinate system. When grid block faces are misaligned with the principal axes of permeability and permeability is anisotropic (e.g., dipped bedding that is not aligned with the grid), obtaining the effective permeability across a cell face by simple multiplication of permeability in each principal direction by the unit normal vector across the face can yield non-physical results. Therefore, PFLOTRAN offers the option to compute scalar permeability either in the direction of flow and scalar permeability in the direction of the potential gradient and apply this permeability to the grid cell face. If cell faces are mainly aligned with the predominant direction of the potential gradient, then the former option would be appropriate. If cell faces are aligned with the predominant flow direction (e.g. aligned with bedding), the latter should be used.

Buffer Evolution: Field tests and process models predict that buffer materials surrounding waste packages will likely evolve over time. Changes may be to porosity, permeability, water saturation, adsorption capacity, etc. Work is underway to capture important changes in a surrogate model that could be coupled with PFLOTRAN or built into the PFLOTRAN code.

2.3.1.4 Biosphere Processes

An important metric in repository safety assessment is the annual dose rate to a human from radionuclides escaping the repository. In FY 2017, a well water ingestion dose model, called Reference Biosphere 1 (RB1), was built into the GDSA Framework PFLOTRAN code (Mariner et al. 2017b).

The core of RB1 is the dose equation of the IAEA Example Reference Biosphere Model 1 (IAEA 2003). RB1 calculates the ingestion dose rate (Sv yr^{-1}) for a person regularly consuming contaminated well water. RB1 does not include dose due to inhalation of volatile radionuclides degassing from the well water, which is an additional process that may be added at a later date.

The RB1 model was enhanced for GDSA Framework by including dose due to “unsupported” radionuclides, as in the model of Olszewska-Wasiolek and Arnold (2011). Unsupported radionuclides are daughter products in a decay chain that are not explicitly modelled in the transport calculations due to short half-lives, e.g., ^{222}Rn . While total concentrations of unsupported radionuclides in the aquifer are considered to be in secular equilibrium with supporting ancestors, aqueous concentrations further depend on emanation efficiency and relative adsorption. Emanation efficiency is a measure of the fraction of the daughter radionuclide concentration released to the mobile (e.g., aqueous) phase from immobile solid particles (e.g., adsorbed phase) upon generation. Figure 2-7 illustrates the effect of relative adsorption on well water concentrations. Accounting for these differences in the case of ^{222}Rn results in largely enhanced well water concentrations of ^{222}Rn relative to ^{226}Ra and an increased dose rate. If these effects are not considered, dose rates can potentially be considerably underestimated (Mariner et al. 2017b).

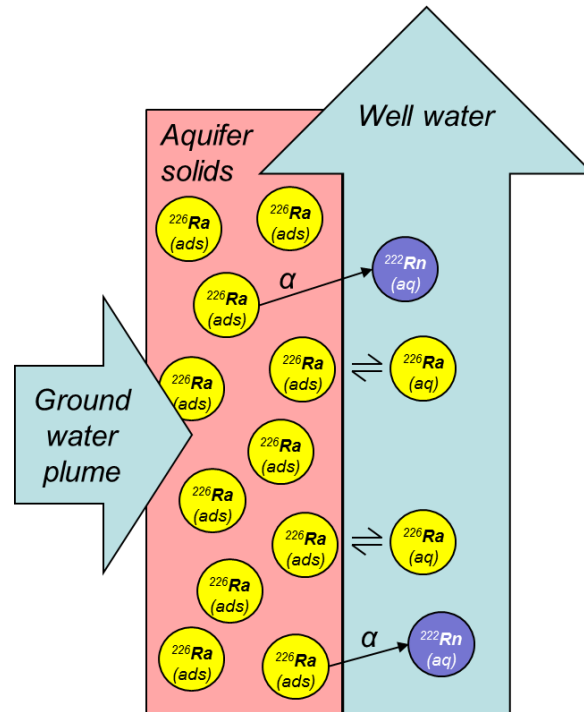


Figure 2-7. Schematic illustration of affinity of ^{222}Rn for the aqueous phase, relative to ^{226}Ra .

2.3.1.5 Computational Improvements

In addition to development of the physical and chemical mechanisms mentioned above, PFLOTRAN and GDSA Framework have undergone important computational enhancements. These enhancements improve coupling with process or surrogate models, meshing, initialization, debugging, solution convergence, simulation speed, and analysis of results.

Process Model Coupling: In 2013, PFLOTRAN was refactored into a more modular simulation framework with the use of modern Fortran (i.e. Fortran 2003/2008 capability). Modern Fortran classes provide encapsulation, inheritance and polymorphism through classes common to other object-oriented programming languages (e.g. C++, Java, etc.). They afford the programmer increased flexibility in developing an extensible simulation framework.

Within the execution step, any number of process models can be coupled and run at identical or dissimilar time scales. The “Process Model Coupler” or PMC class enables this flexibility. The PMC is a Fortran class that encapsulates a process model, providing numerical methods (time integrators and solvers) for solution, and establishes connectivity between process models. PFLOTRAN’s PMCs can be nested in sophisticated trees or graphs to accommodate any number of processes coupled across varying time scales.

The refactoring in 2013 allows a custom workflow such as the one shown in Figure 2-8. Note that a single time stepping loop does not apply to all process models. Instead, each process model coupler has its own time stepping loop that steps until a synchronization point (time) is reached. A custom factory is built for this simulation that creates the respective PMCs (including underlying data structures, process models, solvers, time integrators, etc.), establishes the hierarchical connectivity, and initializes the PMCs prior to execution and destroys them at shutdown. Often, the developer can create a custom factory as an extension of an existing factory through well-planned code reuse. For a more detailed explanation of this enhancement, the reader is referred to Mariner et al. (2015).

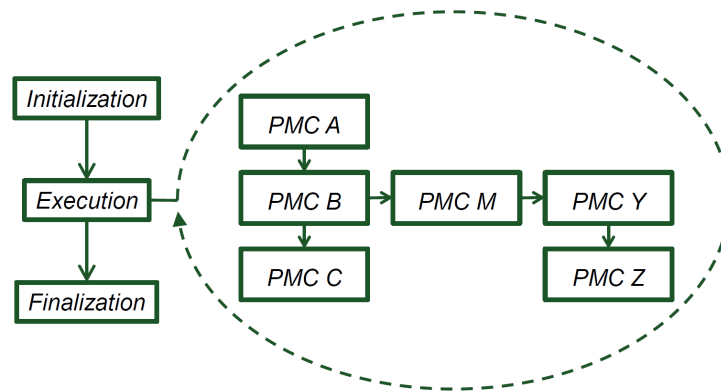


Figure 2-8. An example hierarchy of process model couplers embedded within the module workflow.

Analytical Derivatives. To simulate multiphase flow, PFLOTRAN solves a set of nonlinear equations governing energy and mass conservation over the entire problem domain using Newton’s method. Newton’s method requires the calculation of analytical or numerical derivatives. A detailed description of analytical and numerical derivatives and their derivation, accuracy, and relative speed in PFLOTRAN simulations is presented elsewhere (Mariner et al. 2017b). Here, a basic summary is provided along with discussion of how the implementation in 2017 of analytical derivatives in PFLOTRAN have improved multiphase flow simulations.

Consider the functional relationship

$$f(x) = x^2 \tag{2.1}$$

Using basic calculus, the analytical derivative is calculated as

$$f'(x)_{analytical} = 2x \tag{2.2}$$

To calculate the same derivative numerically, one may use perturbation theory, which for this equation simplifies to the fundamental theorem for calculus,

$$f'(x)_{numerical} = \frac{f(x + \Delta x) - f(x)}{\Delta x} \tag{2.3}$$

which for this example is

$$f'(x)_{numerical} = \frac{(x + \Delta x)^2 - x^2}{\Delta x} \tag{2.4}$$

Calculation of numerical derivatives can be problematic because accuracy is highly dependent upon the size of Δx . If Δx is too large or too small, the derivative may lose accuracy. Take for instance $x = 0.5$ and $\Delta x = 0.25$, the resulting numerical derivative is 1.25 whereas the analytical derivative is 1.0.

Calculation of analytical derivatives can also be problematic. For functions with discontinuities, the derivative is undefined at the discontinuity, and without smoothing (e.g. a polynomial fit through the discontinuity with matching derivatives on either side) the nonlinear solver can oscillate around the discontinuity should the solution be close to it. Analytical derivatives are also more challenging to implement within the simulation code. With numerical derivatives, only the function $f(x)$ needs to be encoded as the same function is evaluated with a perturbed input for the derivative calculation, while all

variants of the analytical derivative must be implemented. For complex nonlinear equations, where many variables within the equation are nonlinear functions of the primary variables and/or variables are inter-coupled, accounting for all variants of the derivatives can be challenging.

To improve the speed and convergence of PFLOTRAN's Newton iterations, a new set of analytical derivatives were determined and implemented in the code in 2017. As an indication of the scope of this work, there are now over 38 pages of derivatives in the LaTeX formatted PFLOTRAN design document for multiphase analytical derivatives.

The result of this work is that PFLOTRAN simulations converge more rapidly and frequently while maintaining accuracy similar to that of simulations using numerical derivatives, as shown in several different verification tests (Mariner et al. 2017b). For example, for a large nuclear waste repository composed of thousands of waste packages, 10.8 million grid cells (32.7 million unknowns altogether) and executed on 1024 processes, PFLOTRAN's analytical derivative implementation outperforms the numerical by a factor of three, taking 1.37 hours to the numerical's 4.05.

New Trust Region Nonlinear Solver: A trust region solver has been added to GDSA Framework in FY 2019 to improve convergence for unsaturated alluvium applications. GDSA simulations have lots of primary variable switching due to changes of state among liquid phase, two-phase, and gas phase. When variable switching occurs in one or more grid cells, Newton iterations fail due to several reasons, but mainly due to reaching a maximum iteration number while showing oscillations in the 2-norm and infinity-norm of the residuals. Currently, this problem is causing unacceptably large computational time due to lack of growth in time step sizes which is governed by a few factors, one of them being the number of Newton iterations to converge.

Using PETSc's trust region implementation, PFLOTRAN needed a modification in order to accommodate primary variable switching, in fact, the modification was needed for any iterative step-size search method such as the line search backtracking method. The update of PFLOTRAN non-isothermal miscible flow now has a feature where it forces an extra Newton iteration to get a solution vector in new states if the newly calculated residual vector states are changed. This implementation, however, is not the most optimized and accurate version yet. We, PFLOTRAN developers, have made a proposal to make some changes to PETSc so that it can be more flexible in accommodating the primary variable switching method.

The advantage of the trust region (TR) method that it is very robust compared to the Newton's method (NT) as it determines the appropriate step size first and then a step direction. The trust region Δ is a subset of the region of the objective function that is approximated using a model function. If this model function is adequate for the objective function, then the trust region is expanded, and if the approximation is poor, then it is contracted (Figure 2-9). Expansion or contraction can be controlled by the ratio ρ between the expected improvement of approximation and the actual improvement. Figure 2-10 illustrates the behavior and performance of the steepest descent, Newton's method, trust region, and line search on different functions. Newton's method exhibits very fast convergence but finds incorrect minima in Branin and Bohachevsky optimization test functions. The trust region method is slower than Newton's method, but it finds the minimum correctly on all test functions and requires the least number of iterations compared to steepest descent or line search methods.

The common behavioral difference between the two methods is that Newton's method tends to cut many more time steps in the simulation, because either the solution diverges or oscillates when the initial guess is far from the solution or there are multiple solutions. Table 2-1 shows the difference in performance of the two methods. In all cases, TR performed 2 to 3 times better than NT except the 1D case because TR is not completely integrated and optimized for primary variable switching and is arithmetically more complicated than NT. Also, the trust region method implemented in PETSc is simplistic in that it does not solve the trust region sub-problem but just stops the Krylov method once it is outside the trust region and backtracks to get to the trust region boundary, very similar to line search backtracking. Therefore, the proposed research has the potential for significant improvement in the near future.

On another note, a 37-PWR repository simulation is 2 to 4 times more computationally intensive than a 24-PWR repository simulation even though the number of unknowns are the same because it goes beyond the boiling point of water and completely dries out to a gas state. The 24-PWR simulation has state changes between liquid and two-phase. The 37-PWR simulation has state changes among liquid phase, two-phase, and gas phase.

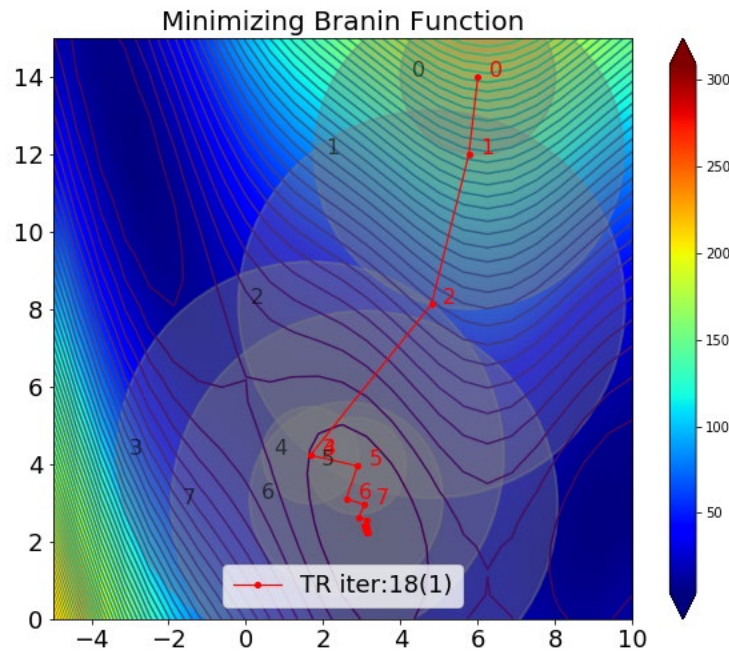


Figure 2-9. The local minimum of Branin function is found after 18 outer iterations and 1 inner iteration using the trust region method. Red and grey numbers illustrate the solution location and the trust region size, respectively, after each of the first 7 iterations. The region shrinks from iteration 3 to 4.

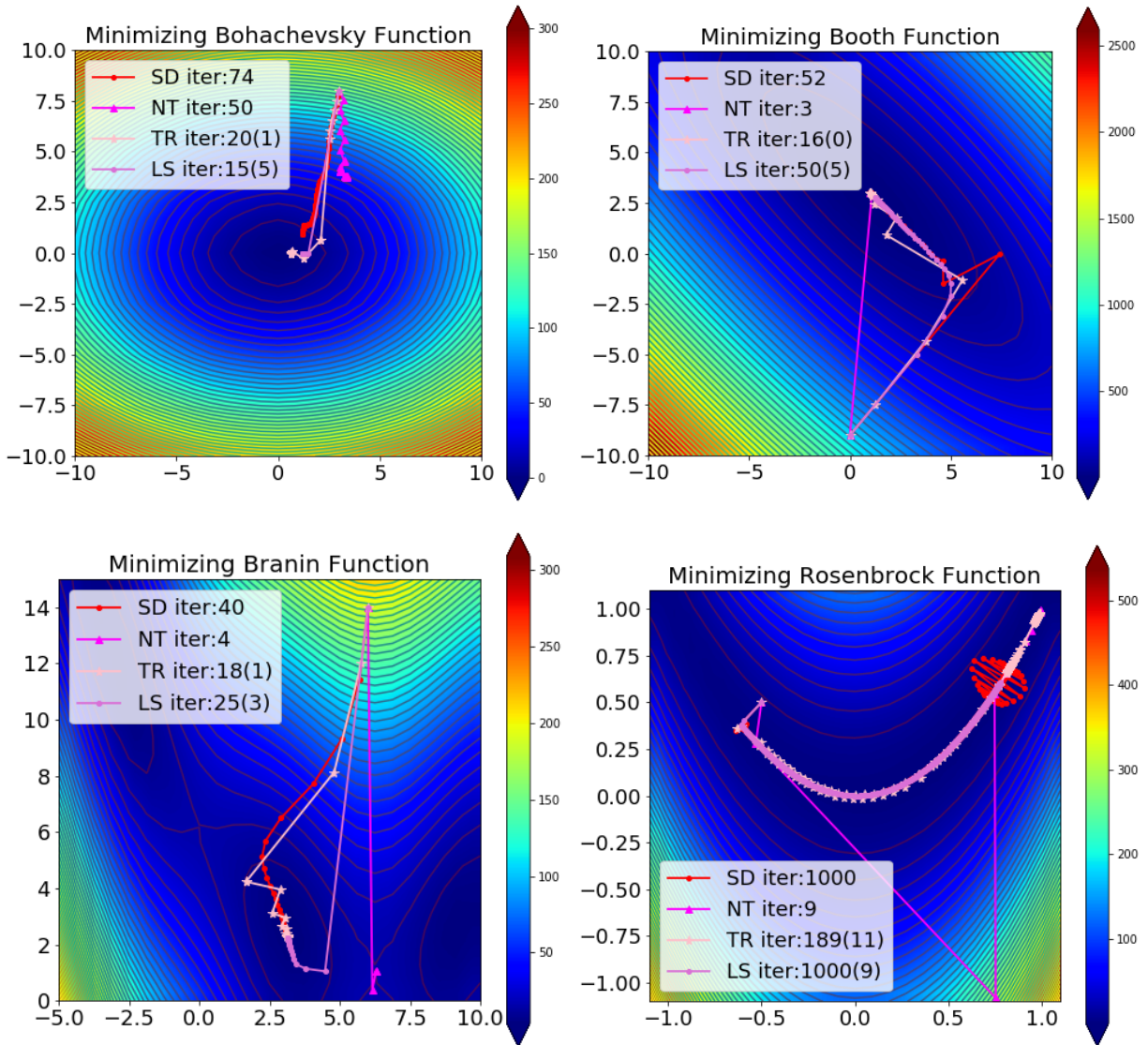


Figure 2-10. Newton's method (NT) has very fast convergence; however, it could lead to wrong solutions as in Branin and Bohachevsky functions. The steepest descent (SD) is the simplest to implement but requires most iterations. The trust region and line search are both robust, but trust region converges in fewer iterations in average.

Table 2-1. Performance of the Trust Region Method and Newton’s Method.

Nonlinear Solver	Time Steps	Nonlinear Iter.	Linear Iteration	Wall Clock
3D Coarse Unsaturated Zone 24-PWR Repository (190k unknowns, 8 cores)				
Newton’s Method (NT)	1,300	1,500	420,000	48 min
Trust Region (TR)	2,800	3,400	3,600	29 min
3D Coarse Unsaturated Zone 37-PWR Repository (190k unknowns, 8 cores)				
NT	2,300	19,000	1,200,000	180 min
TR	830	3,400	310,000	52 min
3D Fine 4-by-4 Array 37-PWR Waste Packages (120k unknowns, 16 cores)				
NT	8,500	9,400	220,000	34 min
TR	2,600	2,600	68,000	11 min

All results are rounded to 2-digit accuracy for readability.

Boundary Condition Mapping: When setting up a PFLOTRAN simulation, the user must define initial conditions and boundary conditions that specify the values of certain primary dependent variables (called a Dirichlet condition) or gradients of these variables (called a Neumann condition). Initial conditions for saturated reference cases define the pressure as hydrostatic, or the temperature field according to a simple geothermal gradient. Common boundary conditions include no fluid flow or no heat flow or apply a specific regional pressure gradient across the domain, for example.

The unsaturated reference case requires more complex initial and boundary conditions to set up the PFLOTRAN simulation. For an unsaturated reference case scenario, the initial condition must define the initial saturation field, initial liquid and gas pressure, and initial temperature. The set of initial variable values at each grid cell cannot simply be guessed. Rather, a spin-up simulation is required to create and define a physically consistent set of initial variable values. If the combination of initial variable values are not physically consistent, the problem becomes numerically difficult or even impossible to solve.

In 2018, the work flow required to set up the spin-up simulation was established, and the ability for PFLOTRAN to read in a gridded dataset of physically self-consistent variable values for the initial and boundary conditions was generalized. More information can be found on this capability in Mariner et al. (2018b).

Restart Capability: PFLOTRAN allows for restarting suspended simulations at any pre-specified simulation time from checkpoint files that are written as the simulator is running. Checkpoint files contain the minimum amount of information about the simulated system that is necessary to re-run from a specified point in time and produce exactly the same answer as if the simulation had been run once from start to finish. This functionality now covers the waste form process model.

The restart capability is flexible to allow for users to specify which process models they are interested in restarting: for example, the flow solution could be “restarted,” or read from a checkpoint file, while the reactive transport is reinitialized to conditions specified in the PFLOTRAN input deck. Simulation time can either be reset to 0 or set to the time at which the checkpoint file was written. This functionality is useful if, for instance, a user wanted to apply different reactive transport scenarios to a steady-state flow field on a given grid. In this instance the flow solution could be run until steady state is reached, and the

corresponding checkpoint file could be read to restart the flow solution while changing reactive transport IC/BC/source/sink constraints.

Stepwise Linear Regression: GDSA Framework uses the software package Dakota (Adams et al. 2018a) for sampling uncertain inputs and applying various methods of sensitivity analysis to the results. However, stepwise linear regression, a mainstay of traditional performance assessment sensitivity analyses, is not implemented in Dakota. In 2018, the GDSA team implemented a stepwise linear regression routine that takes as input the tabulated input and output parameter values returned by Dakota.

The stepwise linear regression routine, `stepwise.py`, is implemented in Python. It relies upon several freely available libraries for statistical analysis and array manipulation. These are `pandas` (<https://pandas.pydata.org>), `statsmodels` (<http://www.statsmodels.org>), `patsy` (<https://pypi.org/project/patsy/>), and `numpy` (<http://www.numpy.org>). It can be run with either Python 2 or Python 3. The theory and implementation of this capability is described in detail in Mariner et al. (2018b) along with a demonstration involving the shale reference case.

Meshing (VoroCrust): In the near future GDSA reference case models will incorporate more realistic geology. PFLOTRAN simulations on meshes of Voronoi cells will be more accurate than simulations on hexahedral meshes that are distorted to map to geological structures. Figure 2-11 shows examples of the models that VoroCrust can mesh.

In 2019 the GDSA team initiated a collaborative effort with the developers of the Sandia in-house Voronoi meshing software VoroCrust and Los Alamos to develop the capability to mesh geological features accurately. This FY the goal is to develop the software and I/O routines to mesh and run PFLOTRAN simulations on a series of 4 exemplar models, each representing a common geological structure. PFLOTRAN simulations will be run on each model using a Voronoi mesh and traditional hexahedral mesh. More information on this effort is available in a separate report (Sevougian et al. 2019d, in progress).

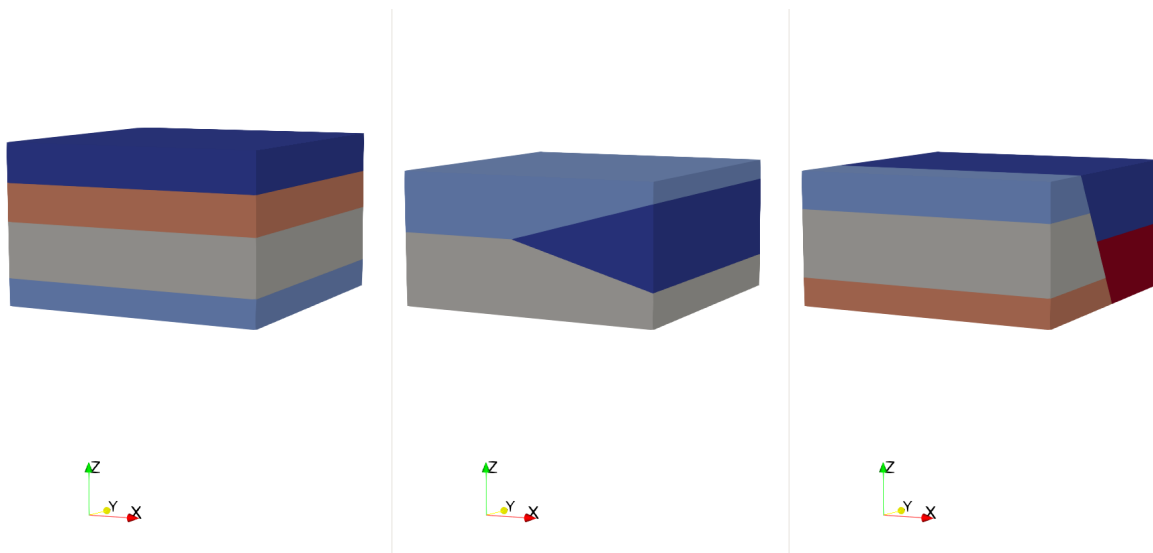


Figure 2-11. Three of the exemplar models used to benchmark VoroCrust mesh simulations.

2.3.1.6 Surrogate Models and Reduced-Order Models

Surrogate models and reduced-order models are being developed and tested for simulating the Fuel Matrix Degradation (FMD) process model (this section), buffer evolution (Section 2.3.1.3), and the effects of criticality on radionuclide inventory and heat source (Section 4.6). Such models are needed to speed up PA calculations. For example, in the case of the FMD model, each time step requires significant computational

time to simulate the coupled thermal-hydrological-chemical (THC) processes. With thousands of waste packages, PA simulations involving a directly coupled FMD process model are prohibitively expensive.

For the FMD process model, three types of surrogate models are under development – a polynomial regression surrogate, a neural network surrogate, and a k-Nearest Neighbors regressor (kNNr) surrogate (Mariner et al. 2019). Appendix A of this report provides a detailed report of the development and testing of these surrogates. Here, only a brief overview of that work is provided.

Each of the FMD surrogates (polynomial, neural network, and kNNr) are operational and are undergoing optimization. The training data (lookup table data in the case of kNNr) are generated from thousands of probabilistic FMD process model simulations.

So far, of the two active learners (polynomial and neural network), the neural network surrogate is more accurate. Results of a single layer feed-forward neural network model are shown in Figure 2-12. In this model, information from the previous time step, such as the corrosion layer thickness and concentrations of aqueous species within the corrosion layer, are not used. This model is currently being coupled with PFLOTRAN and is expected to run rapidly.

The kNNr lookup table surrogate has shown exceptionally high and reliable accuracy. It currently uses seven nearest neighbors and many times more FMD model data points in the lookup table than were used to train the active learner surrogates. Figure 2-13 plots the relative pointwise absolute error (RPWAE) versus the FMD model target output. These results are for the same set of predictors as used in the neural network surrogate, i.e., no information from the previous time step. The next important step for the kNNr surrogate is to couple it with PFLOTRAN and measure its speed.

The accuracy of each of these surrogates can be further improved by adding predictors such as the corrosion layer thickness. This is shown by an additional kNNr surrogate in Appendix A. However, for this to work with PFLOTRAN, the corrosion layer thickness would need to be calculated and tracked, and the surrogate model would have to predict changes in the corrosion layer thickness in addition to the target output. This can be done, but the overall improved accuracy may not be worth the cost of implementation.

Overall, the results of this work indicate that each of the surrogate models will enable GDSA Framework to rapidly and accurately simulate spent fuel dissolution for each individual breached spent fuel waste package in a probabilistic repository simulation.

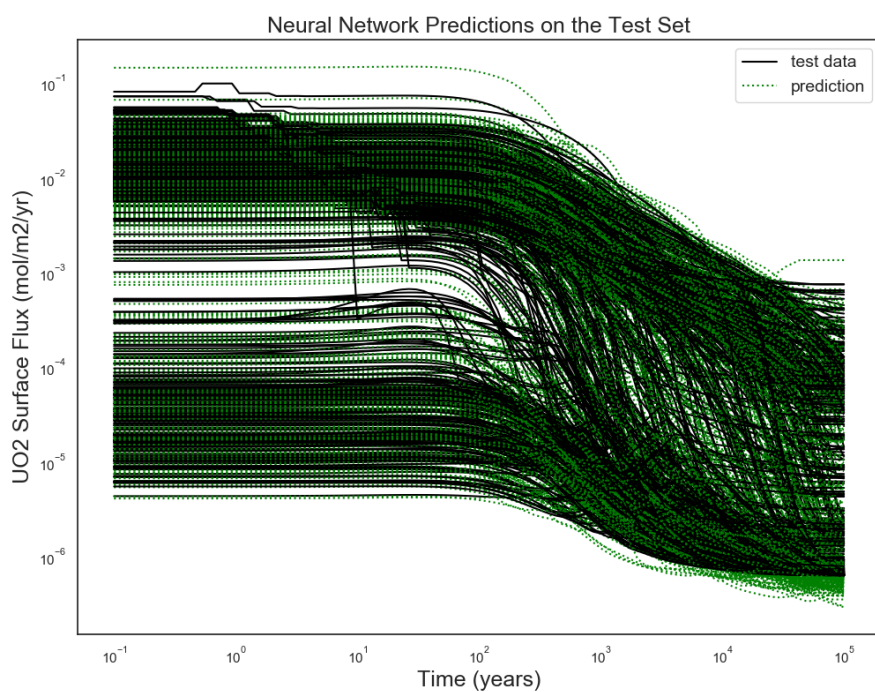


Figure 2-12. Neural network surrogate model predictions versus FMD calculations.

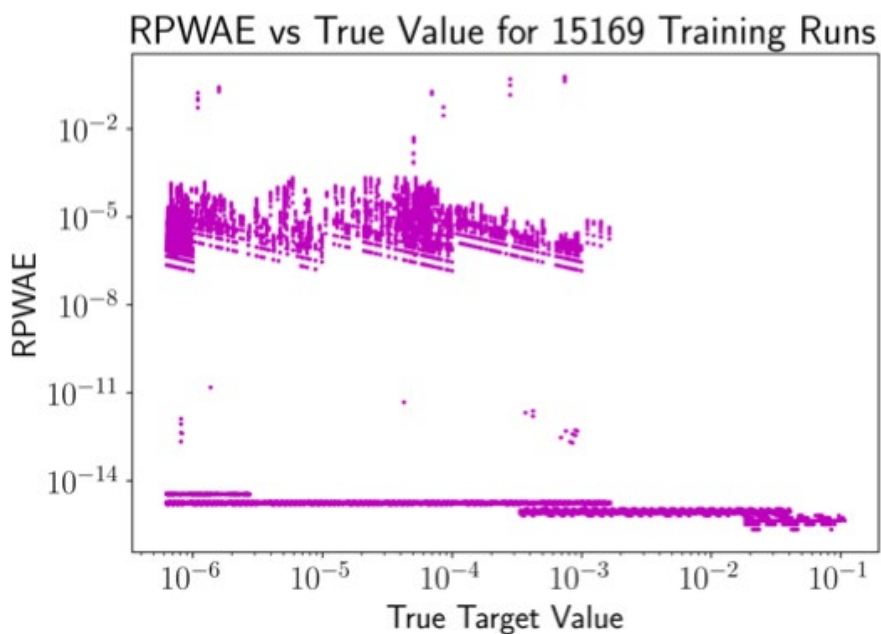


Figure 2-13. k-Nearest Neighbors regressor (kNNr) surrogate model relative pointwise absolute error (RPWAE) compared to the true UO₂ flux values for the case with 15169 training runs.

2.3.2 Uncertainty Quantification and Sensitivity Analysis

Tools for uncertainty quantification (UQ) and sensitivity analysis (SA) are essential components of GDSA Framework. Probabilistic performance assessment (PA) relies on propagating uncertainties in model inputs through a predictive model (or models) to quantify expected outcomes (e.g., mean dose to an individual, groundwater concentration, or cumulative radionuclide release) and associated probability distributions for comparison to regulatory limits. Probabilistic, sampling-based methods of sensitivity analysis are used to understand both qualitatively and quantitatively the contributions of uncertain inputs to uncertainty in model outputs and to enhance confidence in predictive models by providing a check that model behavior is reasonable and expected. UQ/SA is an iterative process. Results may guide further collection of data to reduce uncertainty in model predictions, identify processes for inclusion or exclusion in PA models, help debug numerical models, and enable design of a parsimonious final (regulatory) uncertainty analysis (Figure 2-14).

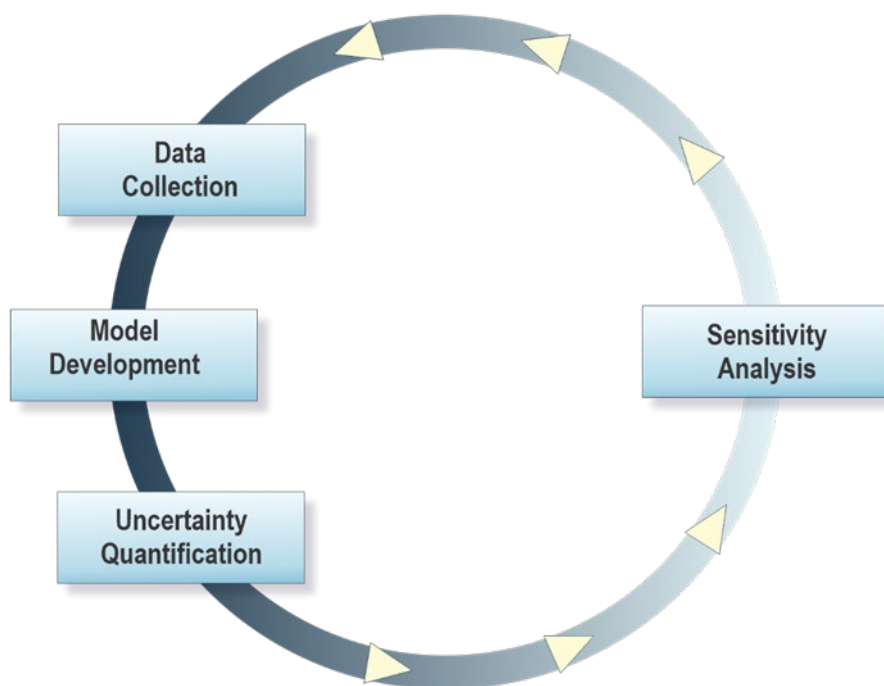


Figure 2-14. Uncertainty quantification and sensitivity analysis is an iterative process.

2.3.2.1 Development Objectives

Development of UQ/SA tools within GDSA Framework is driven by the overarching objectives of GDSA Framework development including:

- Enabling increasingly coupled, mechanistic multi-physics modeling;
- Leveraging existing high-performance computing capabilities;
- Remaining flexible enough to take advantage of future advances in hardware, software, and simulation and analysis methods; and
- Developing in an open-source environment so that implementations are transparent, and software is freely available to stakeholders.

Objectives specific to UQ/SA development include:

- Making available standard sampling-based methods of uncertainty propagation, sensitivity analysis, and uncertainty quantification typically used within U.S. nuclear waste disposal programs (e.g., DOE 2008; DOE 2014);
- Enabling adoption of new methods consistent with the current standard of practice in the UQ/SA community and appropriate for high-dimensional, highly coupled, nonlinear problems resulting from the implementation of mechanistic multi-physics simulations; and
- Creating a consistent, common framework that enables a user to perform a range of uncertainty and sensitivity analyses for a particular problem or set of simulations.

These are important goals for performance assessments now and in the future.

2.3.2.2 Tools

GDSA Framework uses Dakota for uncertainty propagation, quantification of uncertainty in the outputs, and sensitivity analysis, and it uses Python scripting language for data manipulation, visualization of results, and some methods of sensitivity analysis.

Dakota: Dakota, available at: <https://dakota.sandia.gov>, is an open-source toolkit of algorithms for optimization, uncertainty quantification, and sensitivity analysis. It has a rich set of parametric analysis methods that enable design exploration, model calibration, risk analysis, and quantification of margins and uncertainty with computational models (Adams et al. 2018b). Dakota provides a flexible, extensible interface between simulation codes and analysis methods (Figure 2-15), which include:

- Optimization with gradient and nongradient-based methods;
- Uncertainty quantification with sampling, reliability, stochastic expansion, and epistemic methods;
- Parameter estimation using nonlinear least squares (deterministic) or Bayesian inference (stochastic); and
- Sensitivity/variance analysis with design of experiments and parameter study methods.

These capabilities may be used on their own or as components within advanced strategies such as hybrid optimization, surrogate-based optimization, mixed-integer nonlinear programming, or optimization under uncertainty.

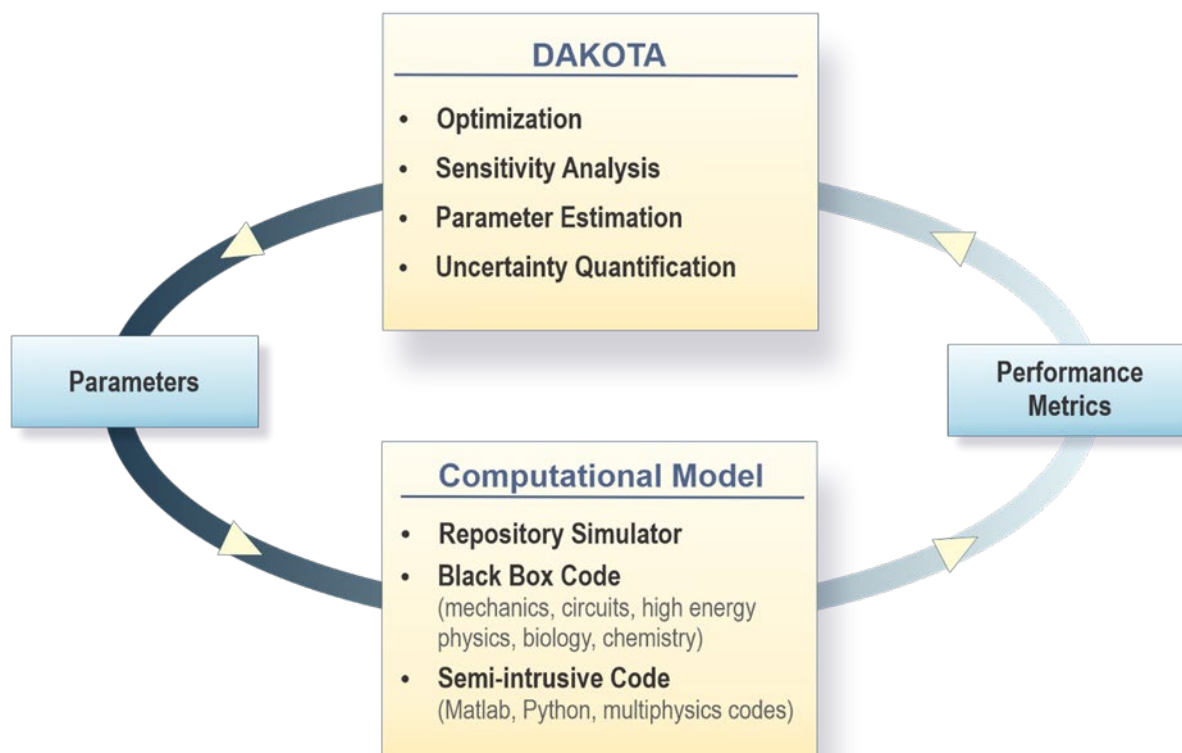


Figure 2-15. Dakota interface with computational model.

Dakota is a C++ code that has been under development at Sandia since 1994, primarily sponsored by DOE’s Advanced Simulation and Computing (ASC) program. As such, it has a focus on interfacing to and running simulations which are computationally expensive, require high performance computing and parallel execution, and exhibit nonlinearities, non-monotonic and/or discontinuous responses, and often involve noisy responses and high-dimensional inputs. Thus, a focus of the algorithm development in Dakota has been on methods that are as efficient as possible and minimize the number of runs required of a high-fidelity simulation model. Such algorithms include surrogate or emulator models, adaptive sampling approaches, and multi-fidelity UQ methods which augment a small number of high fidelity runs with many low fidelity runs to obtain comparable accuracy in statistical estimators.

Dakota contains the uncertainty quantification and sensitivity analysis methods typically used in the U.S. repository program. Dakota implements Latin Hypercube Sampling (LHS) with correlation control on input parameters. It calculates moments on responses of interest as well as correlation matrices (simple, partial, and rank correlations) between inputs and outputs. Dakota also contains an algorithm for performing incremental LHS which allows one to double an initial LHS study such that the second LHS study is a Latin design and the combined initial and second LHS studies together form a Latin hypercube design. Dakota allows nested studies to perform an “outer loop” epistemic sampling and an “inner loop” aleatory sampling to generate ensembles of distributions. Dakota returns a table of sampled inputs and resulting outputs amenable to further processing and visualization with additional tools developed within GDSA Framework or by an individual user. Additional methods that have been implemented in Python for use in GDSA Framework include calculation of standardized regression coefficients via stepwise linear regression and calculation of partial correlation coefficients via iterative loop.

The UQ/SA methods in Dakota have evolved as the standard of practice evolves. Over the past ten years, the Dakota team has invested in methods which calculate the Sobol' variance-based sensitivity indices in an efficient manner. Currently, a Dakota user can calculate these by extensive sampling of the simulation code, by using surrogate methods such as regression or Gaussian process models, and by the use of polynomial chaos expansions. These advanced methods are presented in more detail by Swiler et al. (2019, in progress), and we expect them to be very useful to the next generation of performance assessment.

Dakota is an actively maintained and developed code with formal releases issued twice per year. Dakota uses formal software quality development processes including advanced version control, unit and regression testing, agile programming practices, and software quality assessment.

Python: Python is an interpreted, object-oriented programming language whose built-in high-level data structures and dynamic typing and binding make it well-suited for rapid application development and for use as a glue language to connect existing components together (<https://www.python.org/doc/essays/blurb>). The Python interpreter and an extensive standard library are available as source or binary without charge and can be freely distributed. Python supports the use of modules and packages, and many well-maintained open-source libraries are available. UQ/SA tools developed in Python for GDSA Framework take advantage of several of these including matplotlib (<https://matplotlib.org>), numpy (<https://numpy.org>), pandas (<https://pandas.pydata.org>), and statsmodels (<https://www.statsmodels.org/stable/index.html>).

2.3.2.3 UQ/SA Applications

To date, UQ/SA development for GDSA Framework has focused on two primary applications. The first application is uncertainty quantification for use in a future regulatory environment, which GDSA assumes will require probabilistic uncertainty quantification to demonstrate compliance with post-closure safety criteria. The second application is sensitivity analysis methods for computationally expensive multi-physics models, i.e., GDSA performance assessment simulations of repository reference cases.

Uncertainty Quantification: The ultimate structure of a given post-closure performance assessment depends on the regulatory context in which it is performed. In the U.S., safety standards and implementing regulations are promulgated by the U.S. Environmental Protection Agency and the U.S. Nuclear Regulatory Commission. Safety standards and guidance are also available from national programs in other countries (Swiler et al. 2019, Chapter 10, in progress) and from international organizations (IAEA 2011; IAEA 2012). Regulations govern the criteria against which the performance of a geologic disposal system is to be judged (e.g., radionuclide releases to the accessible environment, groundwater concentrations, doses to members of the public, acceptable levels of risk), the time frame for which compliance must be demonstrated, how to quantify and present PA model outputs for comparison to regulatory limits, selection of future scenarios, and treatment of uncertainties (e.g., Howard et al. 2000; Rechard et al. 2014).

The UQ capability in GDSA Framework is intended for use in a future regulatory environment in which post-closure safety standards may be influenced by existing criteria and standards, either general or repository-specific, and the dose and/or risk metrics recognized internationally to be important to establishing repository safety (Freeze et al. 2017, Chapter 2; Swiler et al. 2019, Chapter 2, in progress).

In the U.S., post-closure repository PAs have been performed for the Waste Isolation Pilot Plant (DOE 2014) and Yucca Mountain (DOE 2008). The Waste Isolation Pilot Plant PA addresses the probability of radionuclide releases exceeding specified fractions of the inventory. Regulation requires that the results are presented in the form of complementary cumulative distribution functions (Howard et al. 2000), which provide a clear visualization of the probability of a release exceeding the regulatory limit (Figure 2-16 for example). The Yucca Mountain PA addresses the expected dose to a reasonably maximally exposed individual. In this PA, the mean predicted dose is compared to a regulatory limit (Rechard et al. 2014). In both PAs, Latin hypercube sampling (LHS) is employed to propagate uncertainty through the predictive model(s) to generate the desired outputs. In GDSA Framework, LHS is implemented in Dakota,

complementary cumulative distribution function (CCDFs) are created using Python, and calculation of means (as well as other statistical moments and percentiles) may be done with either Dakota or Python.

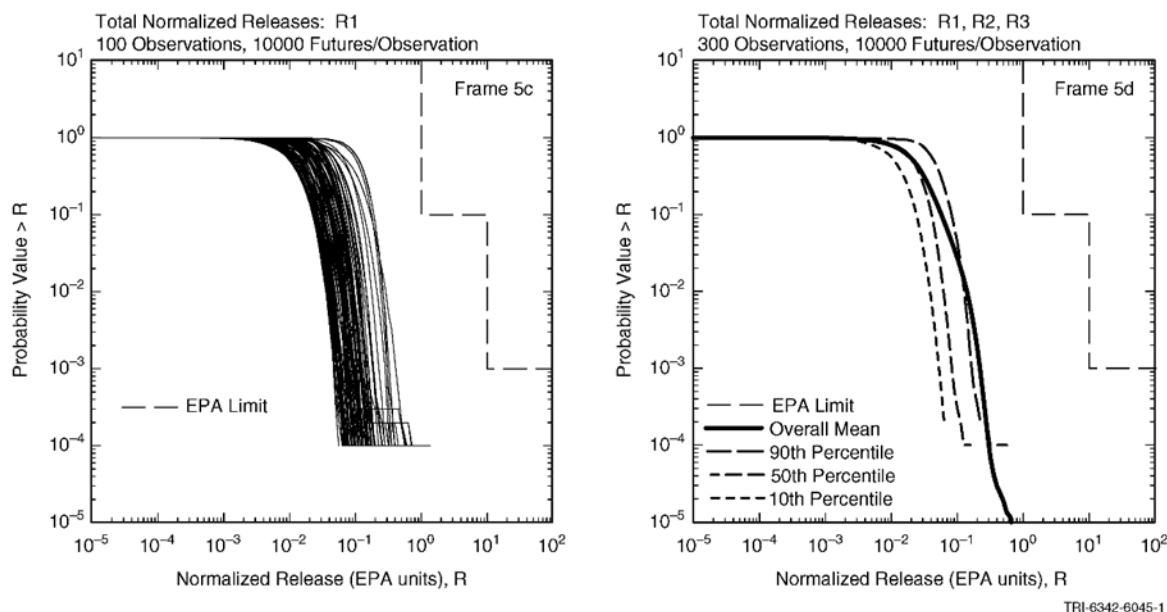


Figure 2-16. Complementary cumulative distribution functions (CCDFs) comparing predicted normalized release (R) to containment criteria expressed as a piece-wise uniform CCDF (dashed line). For each of 100 realizations, the CCDF comprises 10,000 futures (left). Mean, median, and bounding CCDFs (right). Example from Swiler et al. (2019, Chapter 4, in progress).

Latin hypercube sampling: Latin hypercube sampling is a stratified sampling method in which the range of each input variable is divided into segments of equal probability, and a value is randomly selected from each segment (Helton and Davis 2003; Adams et al. 2018b). Values thus chosen for each input variable are randomly combined to create vectors of inputs. LHS generally produces more stable estimates and results in faster convergence of statistics than Monte Carlo sampling (Helton and Davis 2003; Adams et al. 2018b). Dakota’s incremental LHS method incorporates the existing LHS sample into a subsequent sample of twice the size (Sallaberry et al. 2008). For instance, with an initial sample size of 50, 200 realizations provide three LHS samples of size 50, 100, and 200 for analysis. Latin hypercube sampling is a flexible method of propagating uncertainty because it allows a variety of sampling-based methods of sensitivity analysis to be applied to the results. For more about LHS, see Swiler et al. (2019, Chapter 4, in progress).

Sensitivity Analysis: Sensitivity analysis (SA) is useful in modeling studies for a variety of purposes including 1) to identify the model inputs in which a reduction of uncertainty would most reduce the uncertainty in the model output (factor prioritization); and 2) to identify model inputs that could be fixed or simplified without affecting model output (factor fixing) (Saltelli et al. 2008). It also provides a check that model behavior is realistic and robust and contributes to understanding the interactions between coupled processes. SA can be used in an iterative fashion throughout the processes of site selection, site characterization, analysis of features, events, and processes (FEPs analysis), and PA model development to inform data collection, discriminate between options, and design the PA. In these contexts, factor prioritization may be used to prioritize research that will reduce uncertainties in prediction of post-closure performance, and factor fixing may be used to create a parsimonious, computationally efficient, and transparent PA.

Both the WIPP and YM PAs rely on stepwise linear regression and calculation of partial correlation coefficients, with and without rank transformations, to identify the uncertain inputs that contribute the most to uncertainty in outputs (e.g., refs from reliability engineering). Standardized regression coefficients (SRCs) resulting from stepwise linear regression and partial correlation coefficients (PCCs) are numbers between -1 and 1 that indicate the strength and direction of the relationship between an input variable and an output variable. Both methods assume linear or monotonic (when rank transformation is used) relationships between uncertain inputs and model outputs. Within GDSA Framework, partial correlation coefficients and partial rank correlation coefficients (PRCCs) are returned by Dakota, and the stepwise linear regression capability is scripted in Python (Mariner et al. 2018b).

Because the processes affecting evolution of a deep geologic nuclear waste repository and radionuclide transport in the subsurface are highly coupled and nonlinear, methods of sensitivity analysis that do not assume linearity or monotonicity and that can quantify interactions between input parameters may be desirable as mechanistic process models are coupled into PA simulations. Additionally, methods of sensitivity analysis that are effective given a limited number of realizations are desirable, due to the computational expense of each simulation of the physical system. Since 2018, GDSA Framework development has focused on applying Sobol' variance decomposition using Gaussian process surrogate models and polynomial chaos expansions (implemented in Dakota) to generic repository PAs (Mariner et al. 2018b; Stein et al. 2019; Swiler et al. 2019, in progress).

(Mariner et al. 2018b, Chapter 4) provide brief explanations of how to perform stepwise linear regression, calculate partial correlation coefficients, use rank transformations, and find sensitivity indices. For more detailed explanations of each of these methods see Swiler et al. (2019, Chapters 4, 5, and 6, in progress) and references therein.

Partial Correlation: A partial correlation coefficient (PCC) is a measure of the linear relationship between two variables (x and y) after the effects of other variables have been removed. It is defined as the correlation between the residuals resulting from the linear regression of x_j with $x_{\sim j}$ and y with $x_{\sim j}$, respectively, where the notation $x_{\sim j}$ means all x except x_j .

Stepwise Linear Regression: In stepwise linear regression, input variables are added to a multiple linear regression one at a time. At each step, the variable added to the regression is chosen to maximize R^2 , the coefficient of multiple determination. Stepwise linear regression results in standardized regression coefficients (SRCs), the absolute magnitudes of which provide an indication of variable importance. Stepwise linear regression is, like the variance-based sensitivity indices described below, a method of variance decomposition, i.e., the fraction of variance in the output variable due to each input variable can be determined. When the input variables are uncorrelated, the difference between R^2 at the current step and the previous step of the regression is the fraction of the variance in the output accounted for by the latest addition to the regression model (Helton and Davis 2000).

Rank Transformation: Rank transformation improves regression and correlation analyses when the relationship between variables is nonlinear but monotonic or when there are differences in scale between variables (Helton and Davis 2000). In rank transformation, the raw values of x and y are replaced with rank values. The smallest value of each variable is assigned a rank of 1, the next largest value is assigned a rank of 2, etc. up to the largest value. If equal values of the variable occur, they are assigned an average rank. This method lessens the effect of outliers and differences in scale. Partial correlation coefficients and standardized regression coefficients can be calculated using rank transformed values.

Variance Decomposition: Through variance decomposition, first-order, higher-order, and total sensitivity indices, expressing the fraction of variance in an output variable due to the variance in an input variable or a combination of input variables, may be calculated (e.g., Saltelli et al. 2008). A first-order sensitivity index is a number between 0 and 1 that measures the fraction of the variance in the output variable due to a single input variable without including possible parameter interactions. A higher-order sensitivity index is a

measure of the effect of the interactions between two or more input variables on the variance in the output variable; and a total sensitivity index is a measure of the total effect (alone and through interactions with other variables) of an input variable on the variance in an output variable.

Variance decomposition can be performed independent of any assumptions about the form of the relationship (e.g., linear) between model inputs and outputs. However, the computational expense can be large given that at least $m(d+2)$ evaluations of the model (where m is the sample size and d is the number of uncertain inputs) are required to estimate the main and total effects of the input variables when using a sampling method to calculate the indices (Saltelli et al. 2010). Various authors have demonstrated that surrogate models such as Gaussian processes and polynomial chaos expansions built from a limited number of evaluations of the original computational model can be used to reliably estimate sensitivity indices for a variety of simple models with relatively few uncertain inputs (Sudret 2008; Weirs et al. 2012; Le Gratiet et al. 2017). Given the large number of coupled processes and large number of epistemic uncertain inputs typically associated with repository PA, construction of appropriate surrogate models for calculation of sensitivity indices has been a focus of recent work (e.g., Swiler et al. 2019, Chapter 7, in progress) and will continue to be of interest in the future.

2.3.3 Quality Assurance

To enhance confidence in PFLOTRAN calculations, a quality assurance (QA) program has been established to prepare standard QA requirements, QA plans, QA verification and validation testing, and software management procedures. Section 2.3.3.1 summarizes the development of QA program documents, and Section 2.3.3.2 addresses QA verification testing.

2.3.3.1 QA Documentation

Within the GDSA Framework, PFLOTRAN is the primary computational engine for repository performance assessment simulations of subsurface multiphase flow, energy, solute and colloidal transport through porous and fractured media. The code follows the GDSA goals of accessible open source software while maintaining compliance with nuclear software quality assurance guidelines as codified by the NQA-1 process (ASME 2015) as well as the complementary Sandia Software Quality Assurance Plan (SSQAP) (SNL 2018).

The structure and components of the software accordingly must also be developed according to a Practice Level (PL), which stems from DOE Order (O) 414.1-D Quality Assurance (DOE 2013a), and which is described in detail within the SSQAP. The selection of the appropriate PL determines the subsequent actions and documentation that are necessary to meet all relevant quality assurance objectives.

As documented in the draft PFLOTRAN Software Quality Assurance Plan (SQAP, Sandia August 2019), the GDSA team has established a PL of 2. Accordingly, a set of 5 PFLOTRAN software quality assurance documents are in stages of preparation. Table 2-2 summarizes the documents and supporting context, including the status of each component.

These documents will demonstrate compliance with the PFLOTRAN SQAP (Sandia August 2019) and are intended to cover the documentation needs outlined in ASME (2015). The PFLOTRAN quality assurance documentation suite also recognizes the dynamic nature of the open – source community paradigm. This adoption of publicly licensed resources and development platforms, including PETSc (numerical solvers tailored for a multiprocessor environment) and Bitbucket (for real - time configuration maintenance), has accelerated the emergence of PFLOTRAN as the premier hydrogeological/geochemical simulation package for high performance computing (HPC) environments.

The dynamic flavor of PFLOTRAN development is illustrated in the flowchart of Figure 2-17, which addresses the integration of the master branch of the code with separate limbs of ongoing development and of bug corrections. The chart also happens to illustrate that no single PFLOTRAN quality assurance product

is fully a static document. Rather, each is anticipated to be subject to revision as needed to reflect the constantly developing computational and software configuration.

Table 2-2. Summary of PFLOTRAN software quality assurance primary documents, status and schedule.

Document Title and Identifier	Description	Status	Schedule for Revision 1
PFLOTRAN Software Quality Assurance Plan (SQAP)	This document provides the regulatory basis and the operational plan, including a schedule to develop and maintain compliance with software quality assurance guidelines throughout PFLOTRAN’s software lifecycle. The primary topics of this plan are the remaining documents within this table.	A draft is undergoing internal technical and quality assurance review	Q1 2020 (fiscal year)
PFLOTRAN Requirements Document (RD)	This document defines the functional, performance, and attribute requirements for PFLOTRAN. These specifications are complemented by a Requirements Traceability Matrix (RTM). The RTM maps all of the requirements to the associated design features and test cases described in the DID and VEVAD documents that follow.	A draft is in development and will undergo review following the SQAP review.	Q2 2020
PFLOTRAN Design, Theory, User’s Manual and Implementation Documents (DID)	This four-volume document details the software design, the underlying theoretical foundations, the implementation of both, and the instructions for code execution and general use.	A draft is in development. The draft is primarily based on existing content, much of which is available online.	Q3 2020
PFLOTRAN Verification and Validation Document (VEVAD)	This three-volume document includes a Test Plan for establishing compliance of the code to the RD. The second volume documents and analyzes the results of each test. The final volume documents a full technical review of the first two volumes and requires a third party or parties not affiliated with the original testing.	Test cases are continuing to advance, and the VEVAD draft documentation is concurrently under development.	Q4 2020
PFLOTRAN Configuration Management Document (CMD)	The CMD provides management structure and operational flow charts in support of the software lifecycle. The CMD also documents the designated and ongoing maintenance and routine updates to the code. The CMD additionally defines the processes by which the software is acquired (and de-acquired) by a user, as well as the integration and testing of new features. Finally, the CMD identifies training and resources for the above tasks, including for any software problem reporting and corrections.	A draft is in development. The draft includes detailed flowcharts, descriptions of the configuration management processes, and forms for new features and software problem reports.	Q4 2020

The software quality assurance documentation and practices associated with the PFLOTRAN code are being developed in coordination with the GDSA Team, including PFLOTRAN developers, users and testers. As Table 2-2 summarizes, we anticipate that by the close of fiscal year 2020, PFLOTRAN will be further along for higher levels of quality assurance, which is also in alignment with the related publicly licensed features.

Appendix B benchmark both advection and dispersion in the solute transport module and also tests both structured and unstructured meshes. A test is considered passing if the maximum relative error is $< 2\%$ for a sufficient level of grid refinement.

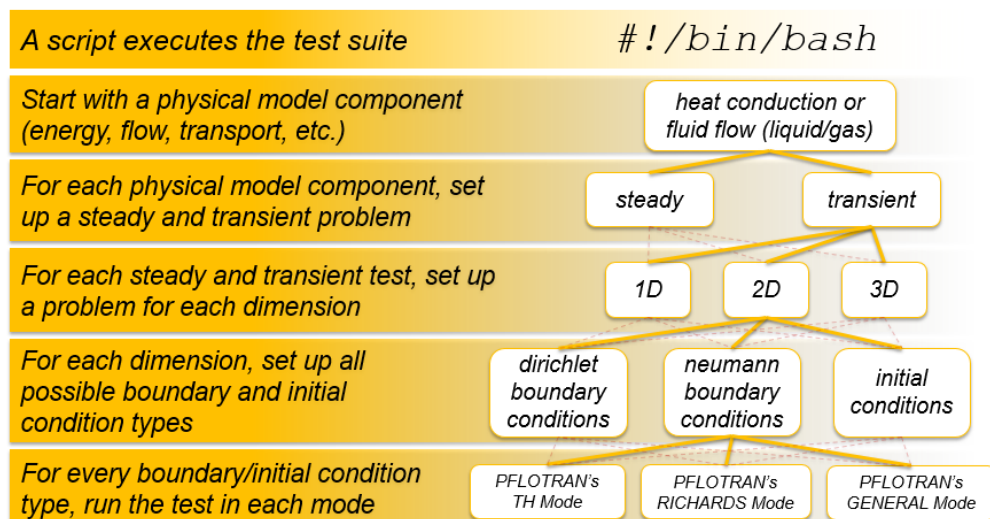


Figure 2-18. Example of PFLOTRAN's QA test suite work flow.

Each test is formally documented using the documentation program Sphinx (<http://www.sphinx-doc.org>). Documentation contains a mathematical description of the benchmark problem, the error comparison plot generated when executing the testing suite, the latest snapshot of the input deck required to run the problem, and the python script required to analyze the simulation results against the analytical solution. The current test suite documentation is available at <http://www.documentation.pflotran.org/index.html#qa-test-suite>.

The initial test suite (Mariner et al. 2017b) used analytical solutions to benchmark problems as a comparison metric, however this was limiting as the benchmark problems had to be relatively simple. There are few analytical models for complex coupled processes in three-dimensions.

Complex models can be benchmarked by extending the PFLOTRAN QA test suite. The extension of the test suite allows a user to compare a code to another code or to an analytical solution. For example, the QA test suite compares PFLOTRAN to CrunchTope for a 1D transport simulation and PFLOTRAN to TOUGH for a 1D flow simulation. A user can now easily implement new QA tests by following the template of other QA tests whereas before it was only able to create QA test between PFLOTRAN and a Python analytical solution. The use of a template also enables entering variables instead of hard-coded numbers. For example, PFLOTRAN can be tested on different sets of discretization of the domain to the analytical solution or it can be tested against other flow codes using different sets of permeability parameters. The QA test suite now compares the output in a unified 4D (x,y,z,t) NumPy array format so that a single absolute and relative error checking Python function can verify whether the test is within the expected error margins. The ultimate goal of the extension is to allow other code developers to use the same suite to easily embody QA capabilities with some flexibilities.

2.3.4 User Group

Although GDSA Framework is being development for DOE and its subcontractors, many of its software components are open source and utilized by a community of users from around the world for research beyond nuclear waste repository performance assessment. For instance, the PFLOTRAN simulator is open source and has been applied to simulate the fate of radionuclides and nuclear waste performance assessment by researchers from around the world (e.g., de Vries et al. 2013; Avasarala et al. 2017; Trincherro et al. 2017). Researchers within the DOE Office of Science have also employed PFLOTRAN to simulate contaminant fate and transport (e.g., Hammond and Lichtner 2010; Chen et al. 2013; Zachara et al. 2016) and Earth system modeling for years (e.g., Karra et al. 2014; Gardner et al. 2015; Kumar et al. 2016; Shuai et al. 2019). This section describes the open source strategy, the PFLOTRAN user community, and how investment in GDSA Framework development is benefitting not only nuclear waste repository performance assessment, but the entire field of subsurface simulation. This broader PFLOTRAN user community reciprocates by sharing conceptual models, incorporating novel physicochemical algorithms, optimizing code performance, debugging problematic issues, and generating grass-roots publicity, all of which benefit DOE in return.

2.3.4.1 Open Source

Open source software licensing governs the free distribution of source code and/or binaries among a group of software developers and users. PFLOTRAN utilizes the GNU LGPL (lesser general public license) which states that the code may be distributed and modified as desired, but any changes to the original source code must be free and publicly available. On the other hand, LGPL allows anyone to link a proprietary third-party library to the code or develop a graphical user interface on top of the code for profit.

It should be noted that open source licensing does not mandate that the code be available. One can license a code as open source and not distribute the code. From 2006 to 2012, PFLOTRAN was distributed on a password-protected server at Los Alamos National Laboratory. In 2012, the PFLOTRAN code base was migrated to a public repository at Bitbucket.org and has remained public ever since.

There are many benefits to open source collaboration, especially when tax payer funds support much of the code development. First, it encourages collaboration among a diverse team of developers. This collaboration pushes the code to the masses who can help test and debug the code while providing feedback regarding user interaction. Open source provides transparency that exposes implementation details that are often critical for scientific reproducibility and quality assurance. These details are often deliberately or unintentionally omitted from user documentation, journal publications and reports. From a financial standpoint, open source allows developers to pool funds across a diverse set of projects funded in academia, government laboratories or the private sector. In addition, funding that would be spent on licensing fees can be redirected towards development. Finally, although the most fit codes can survive under any licensing option, open source may provide a more level playing field for natural selection to run its course.

PFLOTRAN development is currently supported by a number of developer groups from around the world. The U.S. Department of Energy is perhaps the largest proponent of PFLOTRAN development through its national laboratories funded by the Offices of Environmental Management, Nuclear Energy and Science. In addition, private sector companies such as OpenGoSim (opengosim.com) have invested development in support of oil and gas and carbon sequestration efforts, while Amphos21 has developed PFLOTRAN capability for nuclear waste disposal (e.g., de Vries et al. 2013; Iraola et al. 2019).

2.3.4.2 International User Community

PFLOTRAN's open source licensing and accessible, online distribution facilitates collaboration amongst an international community. The PFLOTRAN website at www.pflogtran.org directs interested parties to the online documentation and the Bitbucket repository (including source code and documentation build status and code coverage). Developer and user mailing lists are managed through Google Groups.

Estimating the size and extent of the PFLOTRAN user community is relatively difficult due to the inability to track downloads on Bitbucket. However, through Google Analytics, the hits on the PFLOTRAN website are tracked providing a qualitative estimate. Figure 2-19 illustrates the hits on the PFLOTRAN website around the world between August 1, 2018 to August 1, 2019. This figure demonstrates that the PFLOTRAN users base is multi-national.

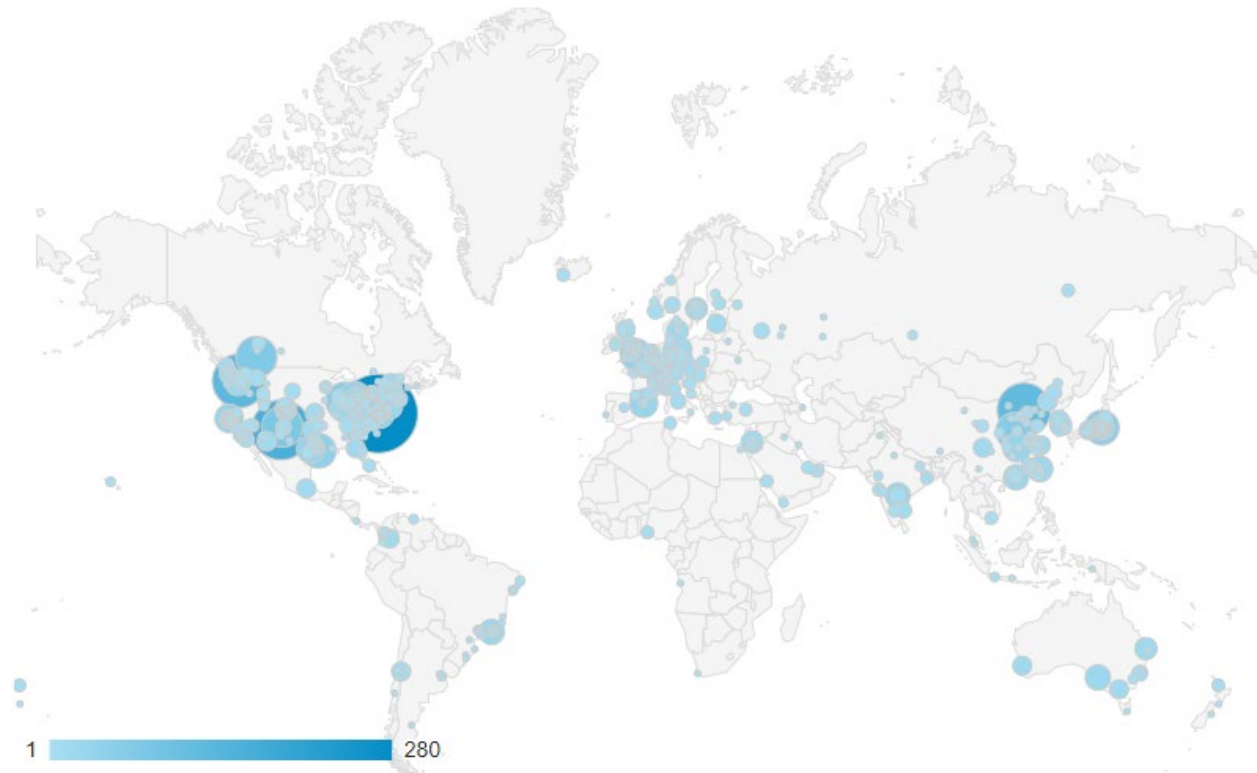


Figure 2-19. Hits on PFLOTRAN website by users around the world. Larger circles indicate larger numbers of visits.

2.3.4.3 PFLOTRAN Short Courses

Another indicator of the international userbase is the attendance to PFLOTRAN short courses. These short courses are conducted by PFLOTRAN developers with planning and scheduling coordinated through the hosting institution. Over the past year, three short courses were presented in Albuquerque, New Mexico; Adelaide, Australia and Bern, Switzerland. Table 2-3 lists these short courses, the short course sponsors and attendees.

Each short course is tailored to the sponsoring institution and the expected attendees. For example, the short course at the University of Bern was organized by Peter Alt-Epping, a senior assistant in the Institute of Geological Sciences, with assistance from Marek Pekala. Peter develops reactive transport models to research the effects of coupled physical and chemical processes in geologic systems. Much of his funding originates from the Swiss nuclear waste repository research program. Peter has been a member of the PFLOTRAN community for nearly a decade and is considered an expert user. The diverse group of nationalities listed in Table 2-3 demonstrates the positive impact of GDSA-funded researcher and development on a worldwide audience.

Table 2-3. PFLOTRAN short courses conducted during FY 2019.

Location	Sponsors	Number of Attendees	Nationality of Attendee Research Institutions
Albuquerque, NM	DOE NE, Vanderbilt Univ. (Kevin Brown)	3	U.S.
Adelaide, Australia	Sandia, CSIRO (Dirk Mallants)	13	Australia
Bern, Switzerland	DOE NE, Univ. Bern (Peter Alt-Epping, Marek Pekala)	35	Canada, Czech Republic, Germany, Israel, Italy, Japan, S. Korea, Spain, Sweden, Switzerland, UK

3. REPOSITORY REFERENCE CASES

The SFWST Campaign is working on generic geologic disposal systems in a number of host lithologies. Potential host rocks include argillite (e.g., shale), crystalline (e.g., granite), salt, and alluvium. In preparation for site characterization and evaluation of a potential future site, the GDSA framework is being developed for application to any of these host rocks.

3.1 Reference Case Development

A reference case for a nuclear waste repository depends on the host rock and the waste inventory. Section 3.1.1 cites the various reference cases developed for combinations of host rock and waste inventory. These reference cases are addressed in more detail in Section 3.2. Section 3.1.2 provides a summary of the geologic database tool being developed and used to prepare realistic representations of host rocks and overlying and underlying geology and hydrology.

3.1.1 Repository Concepts

Reference cases have been developed and simulated using PFLOTRAN and GDSA Framework for different combinations of host rocks and waste inventories. Table 3-1 identifies the core reference cases developed and their associated documentation.

Section 3.2 summarizes the reference cases implemented in GDSA Framework. They include reference cases in argillite, crystalline, salt, and alluvium.

Table 3-1. Repository concepts and generic cases implemented with PFLOTRAN and GDSA Framework.

Repository Type(s)	Conceptual Models	Computational Models
Argillite/shale repository (Section 3.2.1)		
SNF ranging from 4-PWR waste packages to 37-PWR DPCs	Jové Colón et al. (2014) Zheng et al. (2014)	Mariner et al. (2017b) Sevougian et al. (2019c)
Crystalline repository (Section 3.2.2)		
Commercial SNF DOE managed waste (cancelled by DOE in 2017)	Wang et al. (2014)	Mariner et al. (2016) Sevougian et al. (2016)
Salt repository (Section 3.2.3)		
Commercial SNF DOE managed waste (cancelled by DOE in 2017)	Sevougian et al. (2012) Freeze et al. (2013a)	Sevougian et al. (2016) Sevougian et al. (2019d, in progress)
Alluvium repository, unsaturated conditions (Section 3.2.4)		
SNF ranging from 12-PWR waste packages to 37-PWR DPCs	Mariner et al. (2018b)	Mariner et al. (2018b) Sevougian et al. (2019c) Sevougian et al. (2019d, in progress)
Deep borehole disposal (cancelled by DOE in 2017)		
Various waste types, including Cs/Sr capsules	Brady et al. (2009)	Freeze et al. (2016) Freeze et al. (2019)

3.1.2 Geologic Framework Model

3.1.2.1 Overview of Geologic Frameworks Models

A geologic framework model (GFM) is a representation of the geologic and hydrologic features of a site or region. By defining the geometric relationships between the geologic features in a volume of rock, a GFM provides a basis for meshing of geologic features for numerical modeling of coupled processes. With advances in software, GFMs have been increasingly used in the past twenty years to document the geologic environment (natural barrier system) of repository sites in different geologic media (e.g., Aaltonen et al. 2016; Pollok et al. 2018; Wang et al. 2018a). Development of GFMs support repository site evaluation and site characterization activities and are an important component of a safety case that demonstrates a robust understanding of the geologic environment.

GFMs are being developed for the reference cases to support disposal system modeling of more realistic geologic systems that are representative of host rock environments found in the U.S. Regions chosen for representation in GFMs are intended to be typical of host rock environments that might be considered for a repository based on international siting guidance (e.g., stable tectonic setting, simple geology, lack of competing natural resources). An argillite (shale) GFM has been developed to support the argillite reference case and to demonstrate a workflow that consists of constructing the GFM, exporting the relevant geologic features of the GFM for meshing, and using the mesh for flow and transport modeling in PFLOTRAN (Sevougian et al. 2019c). In addition, a GFM of an arid alluvial basin is being developed at LANL to support GDSA modeling of an unsaturated system.

Development of a GFM also provides an opportunity to determine how currently available geologic information can be integrated to formulate a reasonable representation of the subsurface in different geologic environments. The primary data for constructing a GFM are borehole data and geologic mapping, supplemented by published geology/hydrology studies and geophysical data where available. In the case of a GFM developed during repository site characterization activities, data gathered during the characterization phase would be used to continuously update and refine a GFM as part of an increased understanding of a site.

3.1.2.2 Development of the Shale GFM for the Argillite Reference Case

Perry and Kelley (2017) presented a conceptual model of a generic natural barrier system for the argillite reference case. The generic model used as a reference the stratigraphy and geologic setting of the Pierre Shale in the Northern Great Plains Province of the north-central U.S. Based on information from the conceptual model, the generic shale GFM was developed to be consistent with the geology and hydrology of a specific region of the Pierre Shale. The methodology used to build the shale GFM is described in detail in Sevougian et al. (2019c).

The region chosen to use as a conceptual model for the generic shale GFM is to the northeast of the Black Hills Uplift where the Pierre Shale is near or at the surface and has a thickness of between 450 and 550 meters (Figure 3-1). The extent of the GFM provides a relatively large regional representation of the geology (approximately 70x80 km; Figure 3-1). The size of the region allows for down-selection to smaller model domains within this area if needed for flow and transport modeling. The region meets the following criteria that are applicable to a shale environment:

- The top of the shale unit is at or near the surface so that it is reasonably accessible for site characterization and repository construction.
- Thickness of the shale unit is in the range of 400-550 meters to accommodate a repository at a depth of ~300-500 meters while still allowing some thickness of shale beneath the repository (also note that shale formations immediately below the host shale have a combined thickness of several hundred meters).

- A reasonable number of boreholes lie within the region, i.e., enough to provide data on the basic subsurface characteristics of the sedimentary stratigraphy, but not as many as would be found in a major oil and gas producing region.

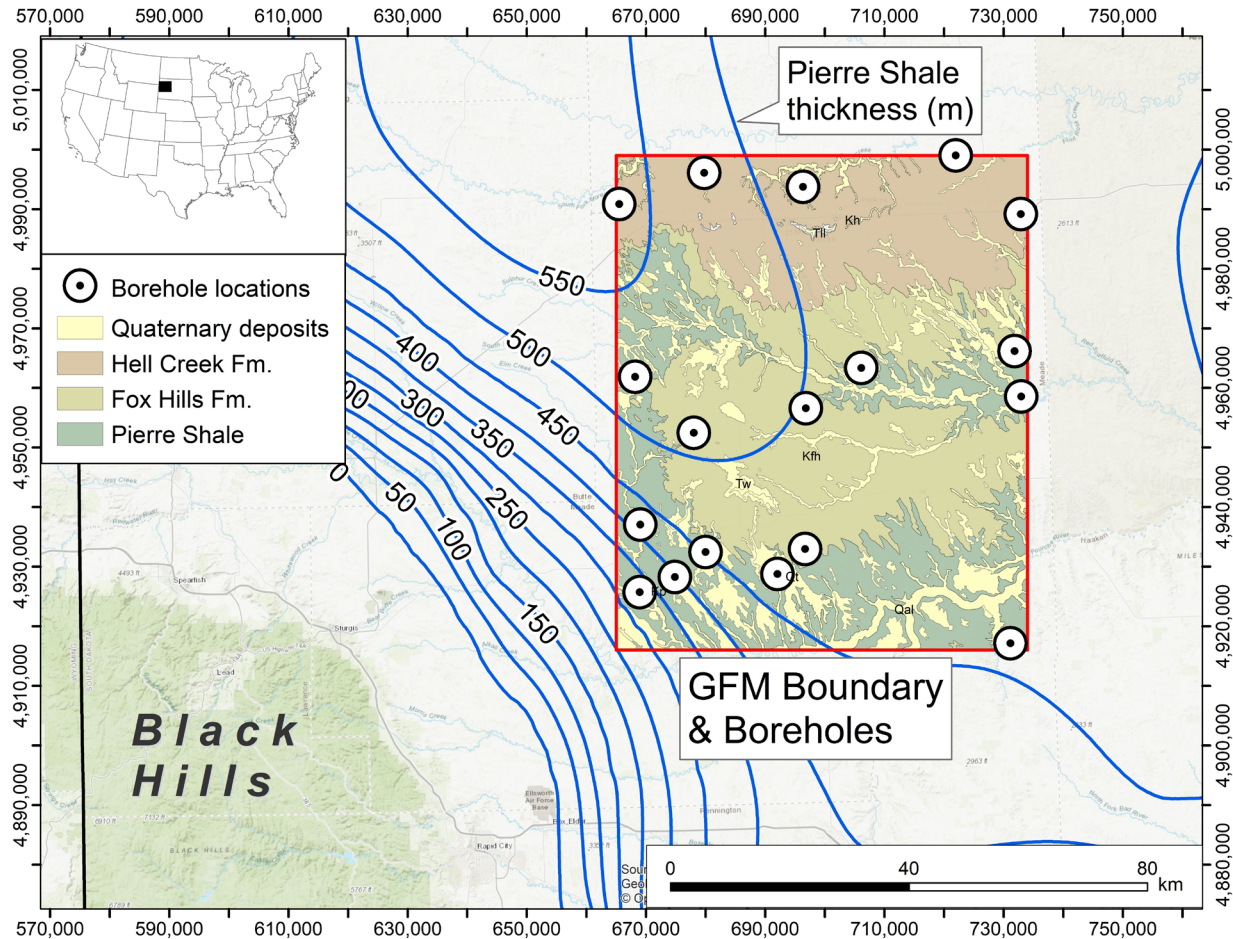


Figure 3-1. Location of the Shale GFM showing thickness contours of the Pierre Shale (Perry et al. 2014) and locations of boreholes used to define the stratigraphy of the GFM.

The Black Hills uplift is a source of groundwater recharge in the region and dominates the hydrology of the region with regional groundwater flow directions that are generally to the northeast (Driscoll et al. 2002). Paleozoic and Mesozoic sedimentary rocks thin towards the Black Hills and dip generally to the north away from the Black Hills (Driscoll et al. 2002). The stratigraphy of the Black Hills region is well established from geologic mapping and borehole data (e.g., Fahrenback et al. 2010).

Borehole logs (from the South Dakota Geological Survey) record elevation data for the top of each formation encountered in the boreholes located within the boundary of the GFM region (Figure 3-1). The elevation data for the formation tops were interpolated using a polynomial fit to create the 3D surfaces that define the geometry of the GFM (Figure 3-2). The modeled shapes of the surfaces also define the dip of strata and the variations in thickness of formations within the GFM. The upper surface of the GFM is defined by a digital elevation model (DEM) for the region.

The GFM represents a geologic environment with approximately 1000 meters of shale (the host rock) in the upper part of the stratigraphic column (Figure 3-2). The deeper stratigraphy of the GFM is comprised of sandstones, shales and limestones with a combined thickness of approximately 800 meters (Figure 3-2).

The sandstones (Inyan Kara and Minnelusa Formations) and limestones (Minnekahta and Madison Formations) in the deeper part of the GFM are the major aquifers of the region. The deepest formation represented in GFM is the Madison Group limestone. Below the depth of the Madison Group, borehole data is not sufficient to define the stratigraphy over the entire extent of the GFM. The Precambrian crystalline surface (McCormick 2010) lies a few hundred meters below the Madison Group and is shown for reference but is not included as part of the GFM. Further details of the GFM stratigraphy are described in Sevougian et al. (2019c).

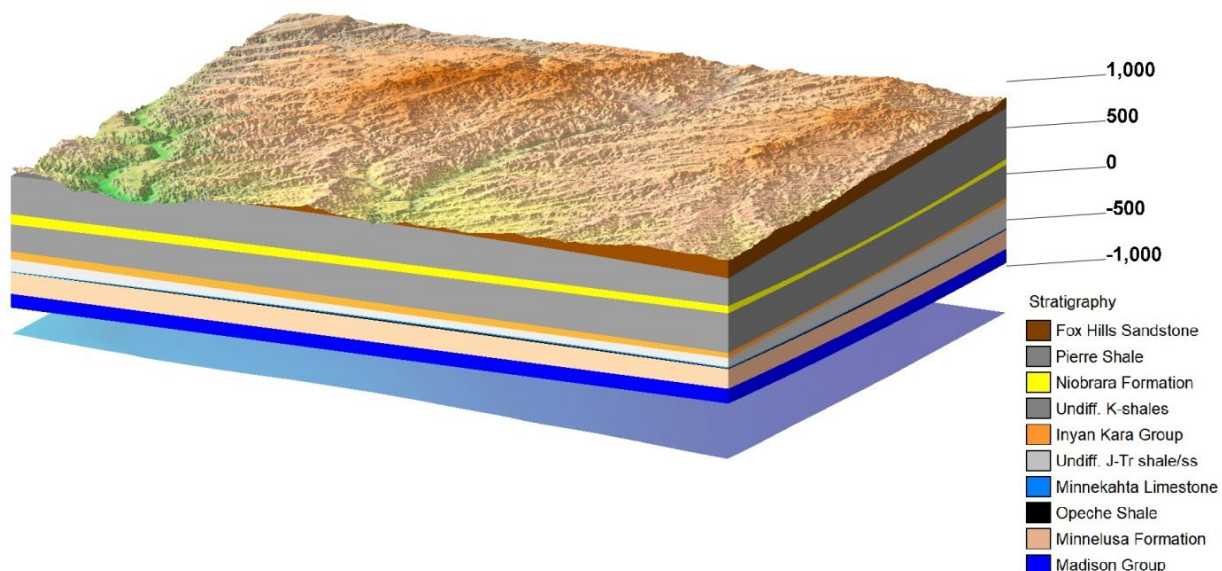


Figure 3-2. Block diagram of the Shale GFM viewed from the northeast with a 10x vertical exaggeration. The shaded top surface is a DEM of the region.

Several hydrologic features of the GFM area bear on flow and transport processes in the subsurface. The system is saturated with a shallow water table at a depth of a few meters to a few tens of meters below the surface. The shales represented in the GFM have extremely low permeability with values on the order of 10^{-19} m^2 (Perry and Kelley 2017). Except for the deep Minnelusa and Madison aquifers, the major regional aquifers are separated by shale confining units that limit groundwater transfer between aquifers (Figure 3-2). Assuming a reference repository depth of 300 to 500 meters, at least 300 meters of shale is present above and below the repository horizon. The exception is the Niobrara Formation (consisting of shale and chalky limestone), which is typically 50 meters thick and lies immediately below the Pierre Shale. While not considered an aquifer in this region, it has an estimated permeability of 10^{-14} m^2 (Perry and Kelley 2017).

A key step of the GFM workflow is to export appropriate elements of the GFM in a format that can be read into meshing software. In the case of the shale GFM, this is accomplished by exporting the geologic surfaces (formation tops) shown in Figure 3-3. These surfaces have been successfully meshed using CUBIT. GFM for other host rock environments will include more complex geometry (e.g., faulting, intrusions of crystalline rock) than is represented in the shale GFM.

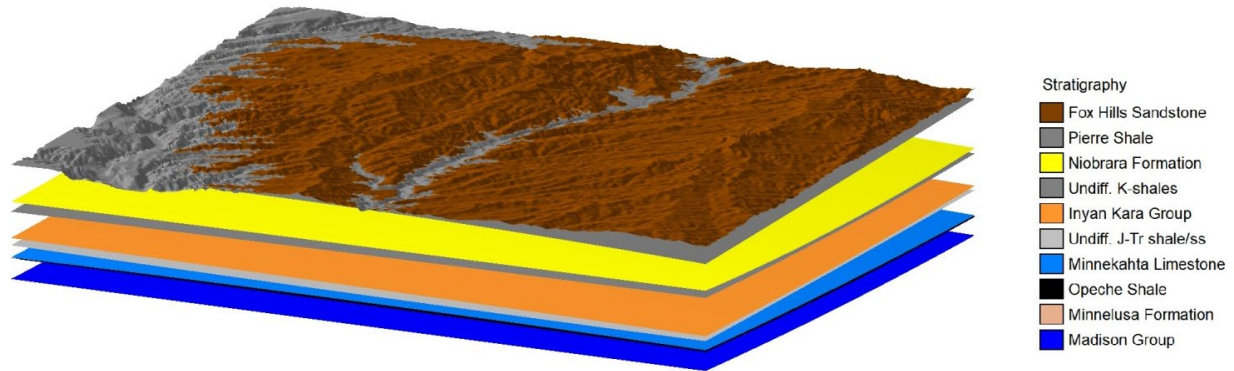


Figure 3-3. Surfaces (formation tops) used as the basis for meshing the features of the GFM.

3.2 Reference Cases

3.2.1 Argillite

The performance of a generic geologic repository in clay/argillite/shale host rock was first described and analyzed in Jové Colón et al. (2014), supplemented by Zheng et al. (2014). The initial analyses and reports were updated in part by Mariner et al. (2015). Mariner et al. (2017b) then published a thoroughly revised description of the reference case that included numerous model modifications and major advances in the capabilities and testing of the GDSA Framework. Sevougian et al. (2019c) described several additional modifications to the reference case including improvements to the Geologic Framework Model, and analyses of EBS configurations based on large DPC waste packages.

The GDSA reference cases include analyses of both the engineered and natural barrier systems associated with a mined geologic repository in argillite, clay or shale. Preliminary results are presented and briefly discussed. Ongoing work related to the development of improved process models and future enhancement of the performance assessment models incorporated in PFLOTRAN is also described.

3.2.1.1 Repository Characteristics

Figure 3-4 is a simplified sketch showing the elements of a generic deep geologic repository in argillite or shale host rock. The stratigraphic relationships are based on a Geologic Framework Model developed to realistically simulate the geologic environment. Access to the repository would be via shafts which connect to underground drifts or tunnels used to support repository operations, including mining, ventilation, and the transport of waste packages from the surface to emplacement drifts for disposal. In most disposal scenarios, waste packages (and any canister overpacks used for transportation and/or disposal) would be emplaced directly in drifts designed to isolate the waste for thousands of years.

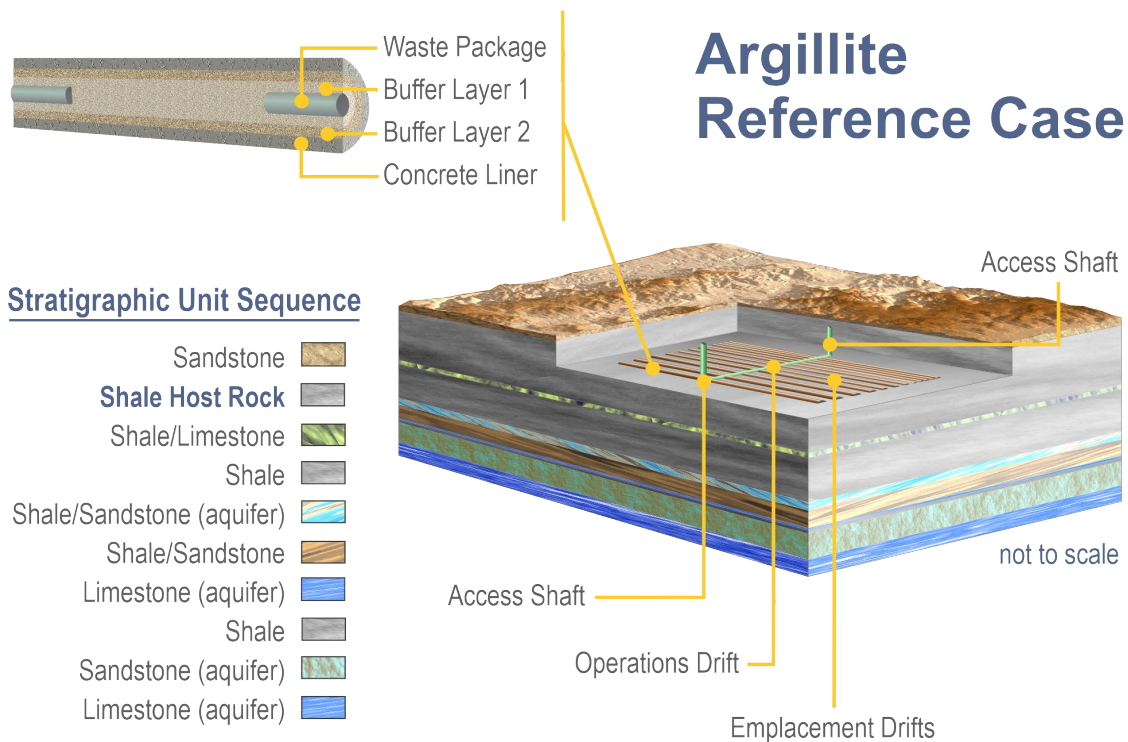


Figure 3-4. Schematic drawing of a generic deep geologic repository in argillite or shale, and the engineered barrier system designed to isolate waste.

The argillite/shale reference case assumes a mined repository located approximately 500 m below land surface, accessed by vertical shafts, and containing 70,000 MTHM of commercial SNF and/or HLW, the maximum amount allowed by the Nuclear Waste Policy Act, as amended in 1987. As noted in Section 3.1.2, the use of the stratigraphy in the region of the Pierre Shale is not intended to imply an intent to characterize the area for suitability as a repository site, but rather to ensure that simulations of generic repository performance are based on realistic and reasonable assumptions.

3.2.1.2 Engineered Barrier System

The assumptions related to the configuration and characteristics of the repository and the design of the engineered barriers have evolved over the past few years. The primary components of the EBS include:

- The configuration and characteristics of repository excavations (emplacement drifts or boreholes, access and operational drifts, shafts and other underground openings)
- The inventory and physical and thermal characteristics of the SNF and HLW waste form(s)
- The materials and characteristics of the waste package, and any overpack used for disposal
- The configuration and characteristics of the liner, buffer(s), and other EBS materials

Figure 3-4 also shows a simplified expanded generic cross section of an emplacement drift, with a waste canister and overpack surrounded by one or more buffer layers and/or a concrete liner. The size and spacing of emplacement drifts in the repository, and the spacing of waste canisters in the drifts, would depend on the size of the waste packages, the thermal output of the waste, and the thermal characteristics of the engineered materials and the host rock. All access drifts and emplacement drifts would be supported with

shotcrete or concrete liners (Jové Colón et al. 2014). Seals of compacted bentonite supported by concrete plugs would be placed at ends of disposal drifts, within shafts, and possibly at intervals within disposal and/or access drifts. Access drifts and shafts (except where sealed) are likely to be filled with backfill rather than compacted bentonite, for instance crushed rock, or a mixture of crushed rock and swelling clay.

The 2017 reference case analyzed repositories with relatively small waste packages (4-PWR and 12-PWR SNF assemblies), consistent with previous U.S. and international repository program precedent. In 2019, recognizing the increasingly common practice in the U.S. of storing SNF in large DPCs, the reference case analyzed disposal configurations with much larger waste packages (24-PWR and 37-PWR). Except for the 4-PWR waste package scenario, all generic reference cases were based on disposal within emplacement drifts, although the details of specific configurations vary based on the size and capacity of waste packages, and the thermal characteristics of the waste and engineered barriers. Table 3-2 presents a summary of key repository characteristics for the generic reference design concepts analyzed, including the dimensions and numbers of waste packages, the waste package spacing within drifts, the size, number and spacing of emplacement drifts, and the total emplacement footprint. As the table shows, there are significant differences in the number of waste packages required, as well as the number and length of emplacement drifts, and the total areal footprint of the repository.

Table 3-2. Comparison of repository characteristics for generic configurations using 12-, 24- and 37-PWR assembly waste packages, compiled from Mariner et al. (2017b) and Sevougian et al. (2019c).

Repository Characteristics	2017 Reference Case (12-PWR)	2019 Reference Case (24-PWR)	2019 Reference Case (37-PWR)
Waste Package (WP)			
WP length (m)	5.20	5.00	5.00
WP outer diameter (m)	1.37	1.67	1.67
WP center-to-center spacing (m)	20.0	20.0	30.0
Inventory per WP (MTHM)	5.225	11.28	17.39
Number of WPs	13,398	3150	2100
Emplacement Drift			
Drift diameter (m)	4.5	5.0	5.0
Drift center-to-center spacing (m)	30	40	40
Number of WPs per drift	50	75	50
Drift seal length (m)	25	25	25
Drift length, including seals (m)	1035	1535	1535
Repository			
Repository Depth (m)	500	515	515
Number of drifts	268	42	42
Number of shafts	Not specified	4	4
Shaft access size (m ²)	Not specified	5x10	5x10
Emplacement footprint (km ²)	8.3	5.00	2.6

In addition to in-drift emplacement, the 2017 generic reference case (Mariner et al. 2017b) analyzed a repository concept in which waste packages would be emplaced in boreholes drilled horizontally from the emplacement drift, as shown schematically in Figure 3-5. This disposal concept would only be applicable if the waste packages were small, such as the 4-PWR assembly packages. The emplacement boreholes would be steel-lined, 1.82 m in diameter and 100 m long, containing 9 waste packages that were 0.82 m in diameter, spaced 9 m apart. The packages would be emplaced in a bentonite/sand buffer, which would also be used to backfill the spaces between packages.

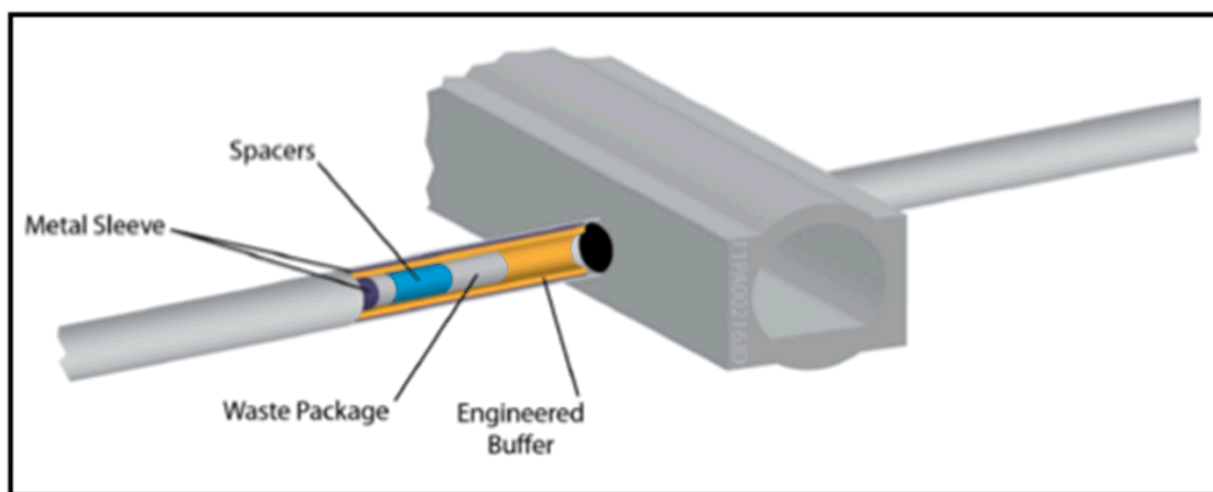


Figure 3-5. Sketch of generic disposal in emplacement boreholes showing elements of the engineered barriers (Jové Colón et al. 2014).

As described in Mariner et al (2017), the use of 4-PWR waste packages would require the disposal of a far greater number of packages (over 40,000), the drilling of over 4400 emplacement boreholes, and a far larger repository footprint (over 15 km²), than in-drift emplacement.

Waste Form: For simplicity, reference case PA simulations assume that the inventory consists entirely of commercial PWR SNF assemblies composed of polycrystalline ceramic uranium oxide (UO₂), which is stable both at high temperatures and in ambient environmental conditions and would degrade slowly in the disposal environment. Cladding protects the fuel from degradation in the reactor, and likely also in the repository. Cladding is generally made from Zircaloy, an alloy that is chemically stable and resistant to corrosion. Spent fuel undergoes physical changes due to heating, radiation damage, and the build-up of fission products, which become concentrated in voids and the outer margins of the UO₂ matrix. As a result, the waste form will release radionuclides in two fractions: instant-release of the void fraction (upon waste package breach), and slow-release (according to the UO₂ matrix dissolution rate). Mariner et al. (2016) provides a description of the UO₂ waste form degradation model in PFLOTRAN. The radionuclide inventory for the reference case is described in Mariner et al. (2017b).

Waste Package: The 2017 shale reference case considered two waste package configurations: a 12-PWR waste package and a 4-PWR waste package. Both were assumed to consist of a stainless-steel canister and a stainless-steel overpack. The 12-PWR waste package is 5.2 meters in length and has a diameter of 1.37 m and contains 12-PWR SNF assemblies (5.22 MTHM) (Hardin and Kalinina 2016). The 4-PWR waste package is 5 meters in length and has a diameter of 0.84 m and contains 4-PWR SNF assemblies (1.74 MTHM) (Hardin and Kalinina 2016). The 2019 shale reference case considered two DPC waste package configurations: a 24-PWR waste package (11.28 MTHM) and a 37-PWR waste package (17.39 MTHM).

Both are assumed to consist of a stainless-steel canister and a stainless-steel overpack. The waste package is 5 meters in length with a diameter of 2 m.

Buffer and Other EBS Materials: The 2017 and 2019 reference cases for 12-PWR, 24-PWR and 37-PWR waste packages assume horizontal, in-drift emplacement with packages elevated on plinths of compacted bentonite and drifts buffered and filled with compacted bentonite pellets and/or bricks in one or two layers as shown in Figure 3-4. The 4-PWR reference case assumes emplacement of 4-PWR waste packages within rings of compacted bentonite buffer in horizontal emplacement boreholes. For simplicity, PA simulations assume that access drift and shafts are filled with compacted bentonite buffer. Compacted bentonite has low permeability, high sorption capacity and may be engineered to achieve desirable thermal properties; for instance, quartz sand or graphite can be added to increase thermal conductivity. The current simulations assume a single bentonite buffer with material properties appropriate for a compacted mixture of 70% bentonite and 30% quartz sand.

For stability, access drifts and emplacement drifts would be lined with shotcrete (Jové Colón et al. 2014) or concrete liners (Hardin and Kalinina 2016). Seals of compacted bentonite supported by cement plugs would be placed at ends of disposal drifts, within shafts, and possibly at intervals within disposal and/or access drifts. Access drifts and shafts except where sealed are likely to be filled with backfill rather than compacted bentonite, for instance crushed rock, or a mixture of crushed rock and clay (e.g., ANDRA 2005). Shotcrete, cement, steel liner and other backfill materials are not simulated in the current PA.

3.2.1.3 Natural System

The natural barrier system (NBS) comprises the shale formation hosting the repository, the disturbed rock zone (DRZ) adjacent to the repository, and geological formations above and below the host formation, including surface overburden. Based on stratigraphic sequences observed in sedimentary basins throughout the U.S. (Perry et al. 2014), the NBS is conceptualized as a thick (on the order of thousands of meters) marine depositional sequence consisting of thick layers of low permeability sediments such as shales and marls alternating with thinner layers of higher permeability sediments such as limestones and sandstones.

The generic stratigraphic column for the argillite/shale reference case (Figure 3-6) was updated for consistency with a regional geologic evaluation conducted by Perry and Kelley (2017). It consists of: a 450-m thickness of indurated shale interrupted by a 30-m thick sandstone aquifer; a 75-m thick limestone aquifer; a 585-m thickness of sealing shale (the host rock) including a 90-m thickness of a silty shale unit; a 60-m thick sandstone aquifer; and a 30-m thickness of unconsolidated overburden. Layer thicknesses and material properties are loosely based on the regional stratigraphy surrounding the Cretaceous Pierre Shale (Perry and Kelley 2017). The stratigraphic column and rock properties are consistent with those used in previous models of generic clay repositories (Hansen et al. 2010; Bianchi et al. 2015) and within the range of those found in other marine depositional sequences in the U.S. (Perry et al. 2014).

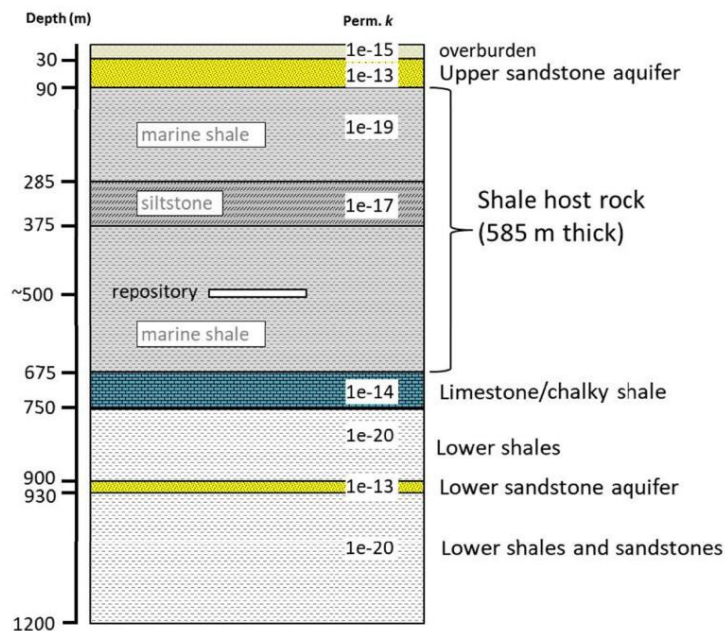


Figure 3-6. Stratigraphic section used for generic argillite/shale reference case.

The 2019 update to the reference case (Sevougian et al. 2019c) describes development of a new GFM to simulate a representative shale environment, based on the Pierre Shale in the Northern Great Plains province. The Pierre Shale was selected because it has numerous characteristics considered favorable to a repository, including a stable tectonic environment, large aerial extent, accessible depth, adequate thickness, high clay content, and an overall lack of natural resources that could lead to human intrusion (Perry and Kelley 2017).

The construction of the GFM will enable modelers to export the relevant features of the model for gridding and meshing, and subsequent use in flow and transport modeling in PFLOTRAN. Figure 3-2 is a 3D regional-scale depiction of the stratigraphy and surface features included in the GFM. As the figure shows, there are aquifers above and below the repository host rocks (as described in Section 3.1.2) that represent potential pathways for radionuclide migration.

The DRZ is defined as the portion of the host rock adjacent to the engineered barrier system that experiences durable (but not necessarily permanent) changes due to the presence of the repository. The DRZ is addressed separately in the PA model because stresses induced by mining operations will impact the hydrologic properties of this zone, and the changes could result in the creation of potential pathways for radionuclide migration.

3.2.1.4 Post-Closure Performance Assessment

Mariner et al. (2017b) describes the conceptual framework for the generic post-closure PA analysis. The updated reference case includes simulation of important processes that affect performance of the engineered barrier, the natural barrier, and the biosphere in the undisturbed scenario. Key processes and key characteristics of each system are summarized in Table 3-3.

Table 3-3. Key characteristics and processes included in the reference case PA.

Repository Subsystem	Model Component	Key characteristics	Key processes included in PA
Engineered Barrier	Waste Form	Commercial SNF (UO ₂)	Radionuclide decay, instant release fraction, waste form dissolution
	Waste Package	Stainless steel	Degradation and breach
	Bentonite Buffer	Low permeability, high sorption capacity	Radionuclide advection, diffusion, sorption, decay
Natural Barrier	Shale Host Rock	Low permeability, high sorption capacity	Radionuclide advection, diffusion, sorption, decay
	DRZ	Enhanced permeability	Radionuclide advection, diffusion, sorption, decay
	Upper Sandstone Aquifer	High permeability, potable water	Radionuclide advection, diffusion, sorption, decay
Biosphere	Pumping Well	500 gallons/day	Well water extraction, adsorption enhancement, dose by well water ingestion

Mariner et al. (2017b) also describes the numerical implementation of the PA model, including the model domain and approach to discretization, initial and boundary conditions, thermal output and decay of waste package heat sources, waste package degradation and failure rate, radionuclide source terms, and the material properties of both engineered and natural materials. Compared to the 2014 and 2015 iterations of the argillite/shale reference cases, the 2017 version incorporated numerous substantive improvements to PFLOTRAN and the submodels used to simulate performance, such as:

- Updated techniques for significantly improved performance of multiphase flow calculations;
- A new reference biosphere dose model for ingestion of well water;
- An improved waste form degradation model for HLW glass;
- The ability to simulate a single waste package using multiple grid cells;
- A new implicit solution for decay and ingrowth of isotopes in both the transport domain and in the waste form;
- Extensive verification testing of flow and transport problems, and documentation of this testing;
- Development and simulation of two new generic shale repository models.

The deterministic and probabilistic results of the PA model are discussed in terms of concentrations of the long-lived radionuclides ¹²⁹I ($t_{1/2} = 1.57 \times 10^7$ yr) and ²³⁷Np ($t_{1/2} = 2.14 \times 10^6$ yr). ¹²⁹I is assumed to have unlimited solubility and to be non-adsorbing; it thus behaves nearly conservatively. ²³⁷Np is solubility-limited and adsorbing.

Simulation Results: The 2017 clay/shale reference case model presented major advances to previous versions in terms of the extent, resolution, features, processes, and number of radionuclides simulated in the model (Mariner et al. 2017b). The generic shale host rock is 585-m thick and is conceptualized as a sealing shale (a shale with high clay content, low permeability, and low compressive strength). Moderately permeable aquifers overlie (sandstone) and underlie (limestone) the host rock. Waste packages fail largely between 6,000 and 200,000 years, and the spent nuclear fuel degrades at a mean fractional rate of 10^{-7} yr⁻¹.

In the 2017 simulations, waste package temperatures peak at approximately 20 years, with the 12-PWR simulation peaking at 151 °C and the 4-PWR simulation peaking at 104 °C. Because of the temperature differences in the two reference cases, the mean waste package breach time is slightly lower for 12-PWR (31,000 yr) than for 4-PWR (41,000 yr); however, concentrations of ^{129}I in the aquifers over time are very similar for the two cases. As shown in Figure 3-7, simulations show that radionuclides move diffusively through the host rock and do not reach the aquifers in significantly elevated concentrations until about 100,000 years. Two radionuclides make it to the aquifers within the one-million-year modeling period, ^{129}I and ^{36}Cl . Because of its low solubility and sorptive properties, ^{237}Np remains in or near the repository environment.

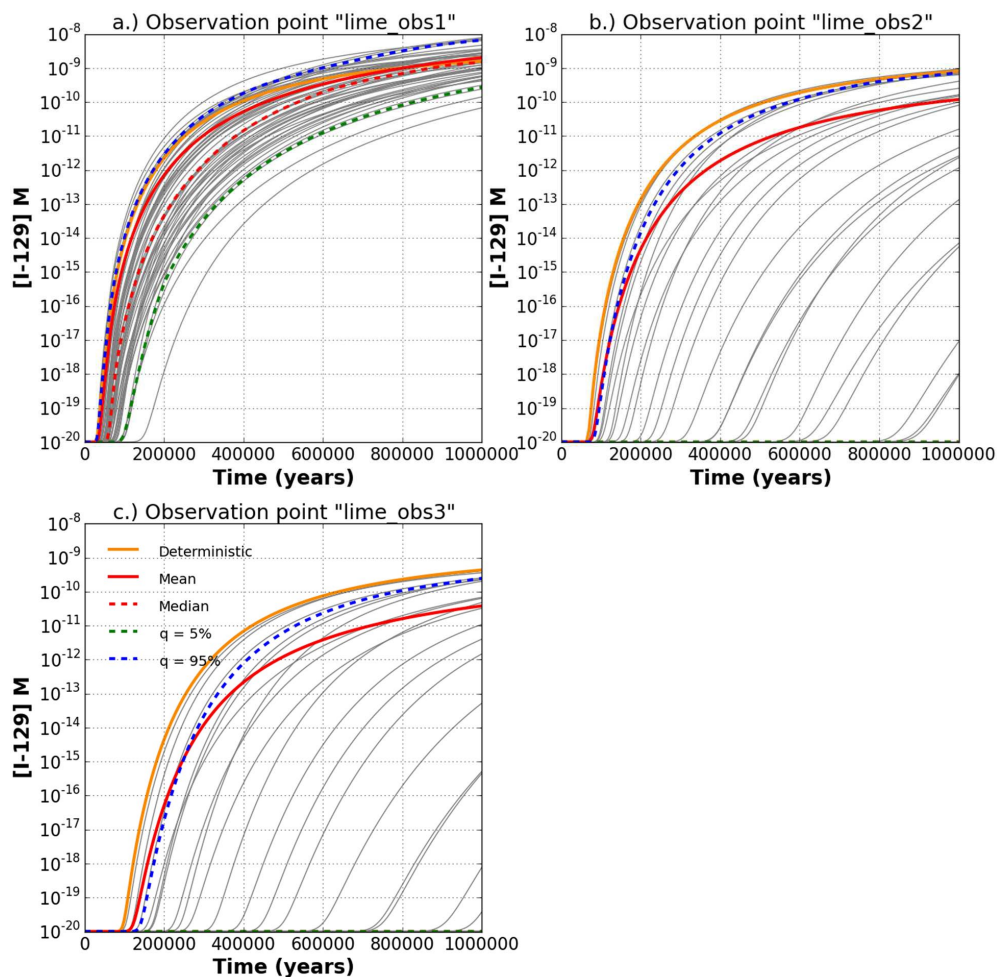


Figure 3-7. ^{129}I concentration versus time at three observation points in the limestone aquifer: 30 m (a), 2500 m (b), and 5,000 m (c) downgradient of the repository.

The ingestion dose rate at an extraction well located five kilometers down gradient in the upper aquifer indicates a mean breakthrough of 10^{-15} Sv yr $^{-1}$ after 400,000 years and an increase in the mean dose rate to nearly 3×10^{-11} Sv yr $^{-1}$ by one million years. None of the probabilistic realizations result in dose rates exceeding 5×10^{-10} Sv yr $^{-1}$ within the one-million-year modeling period.

Sensitivity Analyses: Spearman rank correlation coefficients (SRCCs) (Helton et al. 2006) were calculated using Dakota to assess the sensitivity of the maximum concentration of ^{129}I to sampled parameters.

Sensitivity analyses indicate that uncertainty in shale porosity has a large effect on ^{129}I concentrations in the aquifers at locations above and below the repository. As observation points move down gradient in the aquifers, aquifer permeability overtakes shale porosity as the input parameter most highly correlated with ^{129}I concentrations. This happens because low permeability aquifers and low head gradients provide significant natural barriers to ^{129}I transport.

3.2.1.5 Ongoing Work

As described briefly above, a new GFM is being developed for a representative generic shale environment. The new model is the first step in developing a workflow that will enable modelers to simulate and export the features and properties of the GFM for meshing and use the mesh for flow and transport modeling in PFLOTRAN.

Work is also underway on a set of near-field simulations with a highly discretized grid, as a precursor to coupling more detailed process models into PFLOTRAN and the GDSA Framework. The objective of this analysis is to investigate the near-field thermal-hydrologic behavior of pore fluids in an argillite/shale repository. The focus of the effort is to assess the impact of hydrogeological properties of the engineered buffer and disturbed rock zone (DRZ) on the near-field performance of a typical bentonite back-filled shale repository. This near-field model development will continue for the remainder of FY 2019, with a goal of using this domain in a PA-GDSA model (i.e., GDSA Framework) to represent near-field thermal-hydrologic-mechanical coupled process effects. Surrogate modeling will be used to couple a mechanical response to thermal loading by linking permeability and porosity with the pressure and temperature distribution in the near-field.

Lastly, 2019 updates to the GDSA Shale Reference Case include incorporation of the capability to analyze 24-PWR and 37-PWR waste packages (DPCs) for disposal, as proposed in Section 4 of Mariner et al. (2017b).

3.2.2 Crystalline

The crystalline reference case was initially presented in Wang et al. (2014). The reference case has been significantly updated in Mariner et al. (2016) for commercial SNF and in Sevougian et al. (2016) for DOE-managed (as) HLW and DOE SNF (DSNF). The reference case includes engineered and natural barriers associated with a geologic repository in fractured crystalline rock (Figure 3-8). This section presents a high-level description of the engineered system, including repository layout, inventory, waste form, waste package, and characteristics of the buffer, and drifts and the natural system, including geologic setting, host rock characterization, disturbed rock zone, and overburden. Significant differences between the reference case for commercial SNF and the reference case for DOE-managed (as) HLW and DSNF are highlighted. Preliminary results from the GDSA model are presented and briefly discussed to illustrate model capabilities.

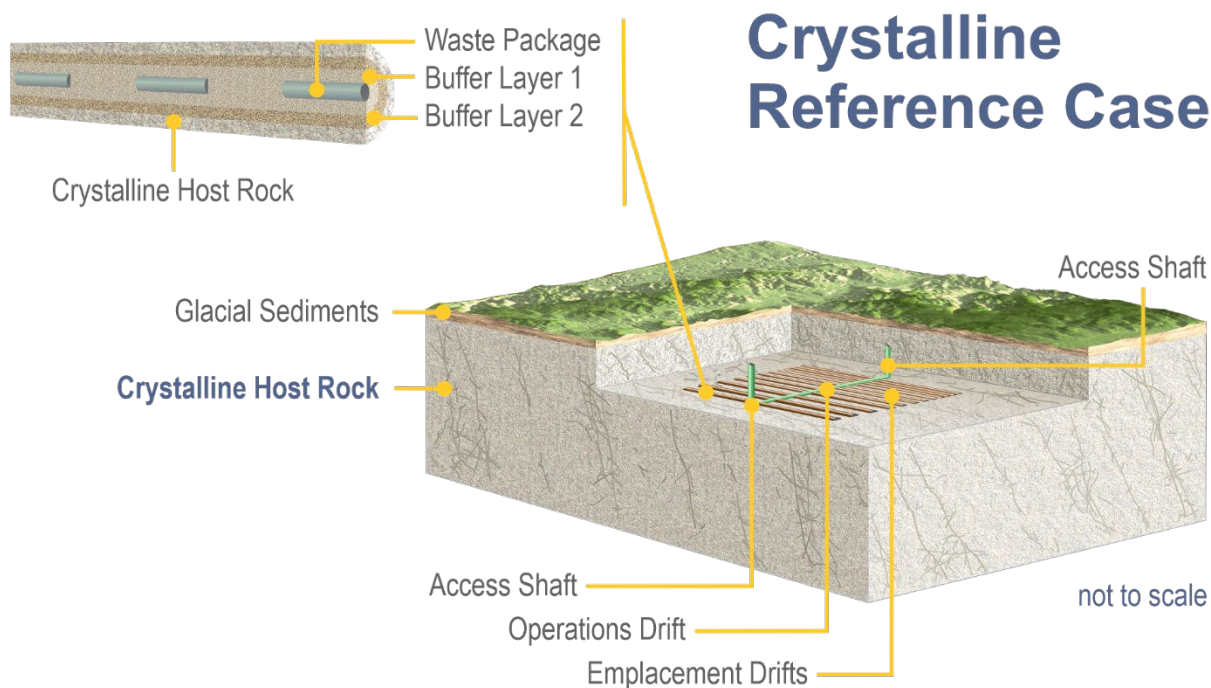


Figure 3-8. Schematic illustration of the Crystalline Reference Case.

Engineered System: The definition of features of the engineered system in the crystalline reference case focuses on those features that can have an impact on the performance of the repository. The repository layout (Figure 3-8) includes drifts that are 805-m long and are separated by 20 m (center to center). Commercial SNF waste packages and HLW waste packages are emplaced lengthwise. DSNF waste packages are emplaced in short vertical boreholes drilled into the floor of the disposal drifts. The repository is located 600 m below the land surface.

The commercial repository is assumed to hold 70 MTHM of commercial SNF. The inventory is restricted to pressurized water reactor (PWR) assemblies. The repository for DOE-managed wastes includes approximately 67% of the inventory of existing and projected glass HLW from Savannah River and Hanford and approximately 67% of the inventory of DSNF with a heat output of ≤ 1500 W/canister (calculated on the basis of 2010 wattages), based on information in Wilson (2016). Radionuclide inventory and decay heat curves are taken from Carter et al. (2013).

The waste form for commercial SNF is spent uranium oxide (UO_2) with zircaloy cladding. Radionuclide releases from the waste form are modeled as an instantaneous release (upon waste package breach) of fission products in voids of the waste form and a slower release that is governed by the dissolution rate of the UO_2 matrix. The waste package is modeled as a 5-m long stainless-steel canister containing 12-PWR UNF fuel assemblies, with a stainless steel overpack. Waste package failure is not instantaneous but is modeled using a degradation rate equation as discussed below.

Table 3-4. Dimensions for the crystalline reference case repository (modified from Wang et al. 2014).

Parameters	Reference Case Value	Simulated Value
Waste Package (WP)		
WP length (m)	5.00	5.00
WP outer diameter (m)	1.29	1.67 (on a side)
WP center-to-center spacing in-drift (m)	10.0	10.0
Inventory per 12-PWR WP (MTHM)	5.225	5.225
Number of WPs	13,398	3360
Emplacement Drift		
Drift diameter (m)	4.5	5.0 (on a side)
Drift center-to-center spacing (m)	20	20
Number of WPs per drift	80	80
Drift seal length (m)	10	5
Drift length, including seals (m)	805	805
Shaft access diameter (m)	5.4	NA
Access hall/ramp height (m)	5	5
Access hall/ramp width (m)	8	8.35
Number of drifts	168	42
Number of access halls	1	2
Repository		
Number of drift pairs (rounded up)	84	NA
Repository length (m)	1,618	822
Repository width (m)	1,665	825
Repository Depth (m)	600	585

The waste form for DOE-managed (as) HLW is borosilicate glass. PA simulations calculate glass dissolution using a rate law formulated by Kienzler et al. (2012, Equation 6) that is discussed in Sassani et al. (2016, Table 3-4). DSNF includes several different waste types and associated waste forms. Currently, the PA calculations assume that the DSNF instantaneously degrades when it is exposed to water.

Waste packages are emplaced within the drifts horizontally on plinths of compacted bentonite. DSNF waste packages in vertical emplacement boreholes are assumed to be emplaced within prefabricated rings of bentonite buffer as in the Swedish KBS-3V concept (Pettersson and Lonnerberg 2008). The drifts are filled with compacted bentonite pellets and/or bricks (Wang et al. 2014). In PA simulations all access halls and drifts are filled with compacted bentonite buffer. Mariner et al. (2016) and Sevougian et al. (2016) present complete descriptions of the engineered systems for commercial SNF and the DOE-managed waste repositories respectively.

Natural System: The geologic setting of the repository system plays an important role in the development of scenarios that will be analyzed in the performance assessment. The repository setting is conceptualized as a sparsely fractured crystalline mass in a stable cratonic terrain with low probabilities of seismicity, igneous activity, and human intrusion. These characteristics allow disruptive events to be excluded from the preliminary performance assessments. This conceptualization is consistent with international concepts of nuclear waste disposal in crystalline rock (SKB 2007).

There is a large body of international work that is available to assist in the development of a representation of a repository in crystalline rock (SKB 2007; Follin et al. 2014; Joyce et al. 2014). In particular, the extensive work done at the Forsmark site in Sweden provides a substantial database to draw upon. At Forsmark, geologic mapping has identified volumes of relatively undeformed, i.e. sparsely fractured, rock bounded by deformation zones characterized by concentrated brittle and/or ductile deformation. Fractures in the relatively undeformed domains occur as sets defined by orientation.

The relatively undeformed domains are the potential host rock for a repository in crystalline rocks. The fracture sets create fracture-controlled flow channels that provide the dominant form of permeability in the host rock in the vicinity of the repository. Detailed studies at the Forsmark site provide hydrologic properties data, i.e. porosity and permeability, for the fractured crystalline rock that hosts the site (SKB 2007).

The definition of fracture networks is especially important for crystalline rocks, because of the importance of fracture-controlled flow in the host rock. Discrete fracture networks (DFNs) for hydrogeologic modelling of crystalline rock typically are generated by computer programs that perform random sampling guided by user input of the properties of multiple fracture sets. Fracture set properties include fracture orientation, fracture size, fracture intensity, and fracture transmissivity. Each of these properties may be represented by distributions to capture and propagate uncertainty. They may also account for known correlations, such as between fracture size and fracture transmissivity. The DFNs for the Crystalline Reference case are generated using the code `dfnWorks` (Hyman et al. 2015a). The generated fractures are mapped to a gridded equivalent continuous porous medium domain using `mapDFN.py`, a code that approximates hydraulic fracture properties by calculating and assigning permeability and anisotropy on a cell by cell basis in the crystalline rock (Stein et al. 2017).

Temperature changes, resulting from decay heat, will affect radionuclide diffusion rates, solubility and sorption, but these processes are not currently modeled as a function of temperature in PA. Details of pore water chemistry, the calculation of solubility limits and sorption are given in Mariner et al. (2016). The crystalline reference case assumes a linear sorption characterized by a distribution coefficient K_d for each element. The GDSA model implements sorption to the bentonite buffer and natural barrier (host rock, DRZ, and sediments) but not to the waste package.

The DRZ is defined as the portion of the host rock adjacent to the engineered barrier system that experiences durable (but not necessarily permanent) changes due to the presence of the repository. The DRZ is addressed separately in the PA model because stresses induced by mining operations will impact the hydrologic properties of this zone. In-situ measurements in URLs in crystalline rock in Korea (Cho et al. 2013) and Canada (Martino and Chandler 2004) provide important data and insights to improve the model representation of this zone. To date, the representation of the natural system is completed with a 15-m thick layer of glacial sediments above the crystalline rock.

Post-Closure Performance Assessment: The preliminary generic GDSA PA includes a conceptualization of engineered and natural barriers in an undisturbed scenario. Key aspects of this conceptualization are summarized on Table 3-5 and Figure 3-9. The performance metric for these calculations is maximum radionuclide concentration.

Table 3-5. Conceptual representation of the engineered and natural barriers in PA.

Region	Component	Key characteristics	Key processes included in PA
Engineered Barrier	Waste Form	Commercial SNF (UO ₂) HLW Glass DSNF	Radionuclide decay, instant release fraction, waste form dissolution
	Waste Package	Stainless steel	Degradation and breach
	Bentonite Buffer	Low permeability, high sorption capacity	Radionuclide advection, diffusion, sorption, decay
Natural Barrier	Crystalline Basement	Sparsely fractured, low permeability	Radionuclide advection, diffusion, sorption, decay
	DRZ	Enhanced permeability	Radionuclide advection, diffusion, sorption, decay
	Sediments	Thin, unconsolidated	Radionuclide advection, diffusion, sorption, decay

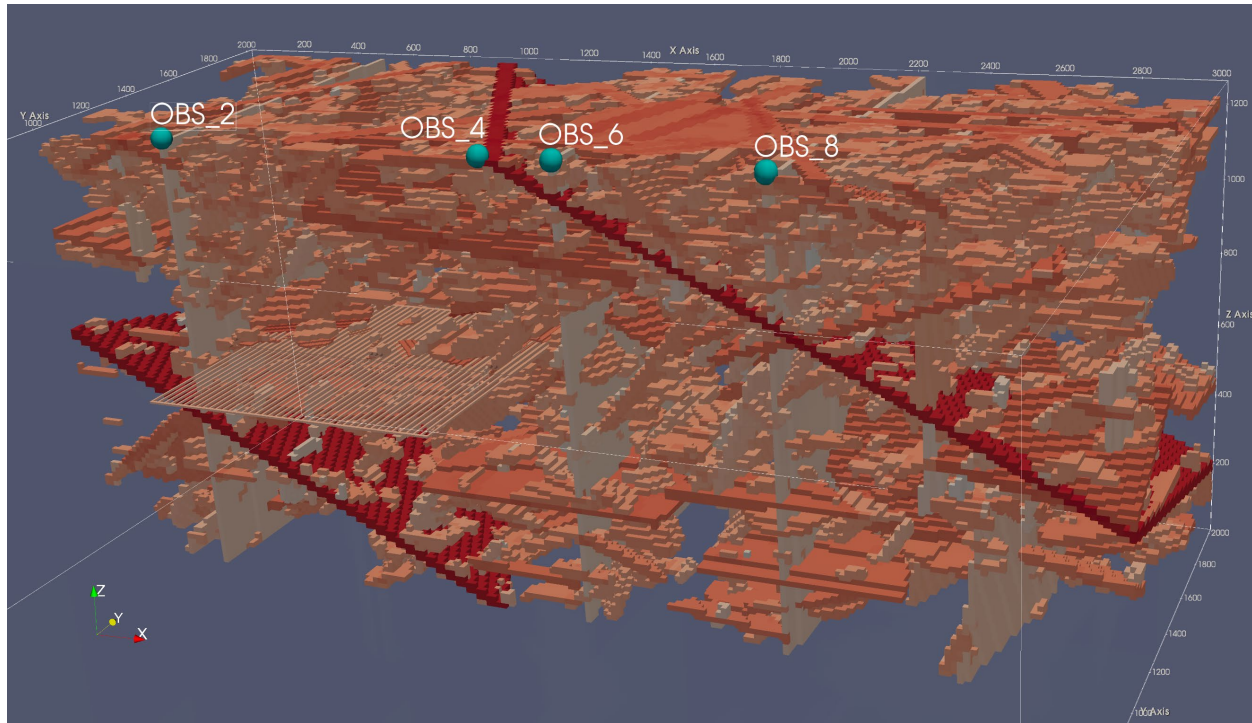


Figure 3-9. Cutaway of a DFN realization mapped to the porous medium grid, showing the far half of the model host rock domain and the full repository. The overlying alluvial sediments are not shown. Fractures of the DFN realization are shown in orange. Unconnected fractures are removed. Five deterministic fracture zones, three sub-vertical (gray) and two with a dip of approximately 30 degrees (red), are common to each DFN realization. Observation points are located above the midline of the repository where the deterministic fracture zones intersect the top boundary.

Reference case simulations assume (1) a mined repository at 585-m depth in fractured crystalline rock; (2) 15 m of unconsolidated sedimentary overburden; (3) a head gradient of -0.0013 m/m from west to east; (4) a regional heat flux of 60 mW/m², a mean annual surface temperature of 10 °C; and (5) a saturated domain.

PA simulations, using the GDSA framework, commonly include deterministic simulations and a suite of probabilistic simulations for uncertainty and sensitivity analyses. Probabilistic inputs for the simulations are prepared using Dakota's Latin Hypercube Sampling (LHS) capability.

Initial conditions for the model simulations are established to represent a geothermal temperature gradient and hydrostatic pressure gradient in the vertical direction, and a horizontal pressure gradient that drives flow from west to east. A full discussion of the parameters used in the calculations can be found in Mariner et al. (2016). A few of the important parameters are discussed here.

Thermal load is calculated using an initial value for PWR UNF 100 yr out of reactor (OoR). Waste package failure is modeled using a canister degradation rate. For the deterministic simulations, a base canister degradation rate is assigned to each waste package from a sampled rate distribution. Probabilistic simulations sample on the mean distribution rate. Upon waste package failure, the decayed radionuclide inventory is released in two fractions, instant-release and slow-release, as discussed above. The crystalline reference case assumes a non-zero instant-release fraction for ¹³⁵Cs, ¹²⁹I, ⁹⁹Tc, and ³⁶Cl, and zero for all other radionuclides. The slow-release fraction is modeled using a fractional dissolution rate of 10⁻⁷ yr⁻¹ for the deterministic case and fractional rate that is sampled from a log uniform distribution, 10⁻⁸ yr⁻¹ to 10⁻⁶ yr⁻¹, for the probabilistic simulations.

To evaluate the importance of fracture networks, multiple fracture network realizations are generated. These realizations are defined by variations in fracture orientations, fracture size, i.e. fracture radii, and fracture abundance. Note that all of the realizations include deterministic fracture zones, where high fracture abundances create high permeability zones. The five deterministic fracture zones illustrated in Figure 3-9 are included in the latest iteration of the GDSA framework model (Mariner et al. 2018a). Standard sensitivity analyses that evaluate the impact of an individual uncertain parameter on a numerical model output are ineffective for evaluating the impact of the fracture network. This is because there are several individual model parameters that contribute to the impact of the fracture network on permeability and fluid flow. The fracture network realizations provide a tool to supplement the standard sensitivity analyses, as discussed below.

Simulation Results: In FY 2019, the crystalline reference case domain shown in Figure 3-9 was extensively exercised to examine the relative sensitivity of aleatory and epistemic uncertainties. Aleatory uncertainties include (1) the randomized locations and sizes of fractures in each DFN realization and (2) the randomized assignment of waste package degradation rates to different waste packages in the domain to represent the variability in waste package degradation rates among waste packages within a single PA realization. Epistemic uncertainties in the current crystalline reference case include the mean of the coefficient of the waste package degradation rate equation, permeabilities and porosities of buffer materials and natural barriers, and the waste form fractional degradation rate.

An example snapshot of one of the plumes for DFN realization 1 of the current crystalline reference case is shown in Figure 3-10. In this realization, several waste packages fail in less than 300 years, and a small minority of them are located near well-connected fractures that allow relatively rapid migration of ¹²⁹I through the host rock. To mimic what would likely occur at an actual site, future simulations will be designed to avoid waste emplacement near fractures that would seep in an open excavation above a predetermined flow rate.

The FY 2019 study, which is ongoing, is presented in detail in Chapter 8 of Swiler et al. (2019, in progress) and will not be discussed further here. Instead, to demonstrate the implementation of the crystalline reference case, selected results from previous analyses are discussed in the remainder of this section.

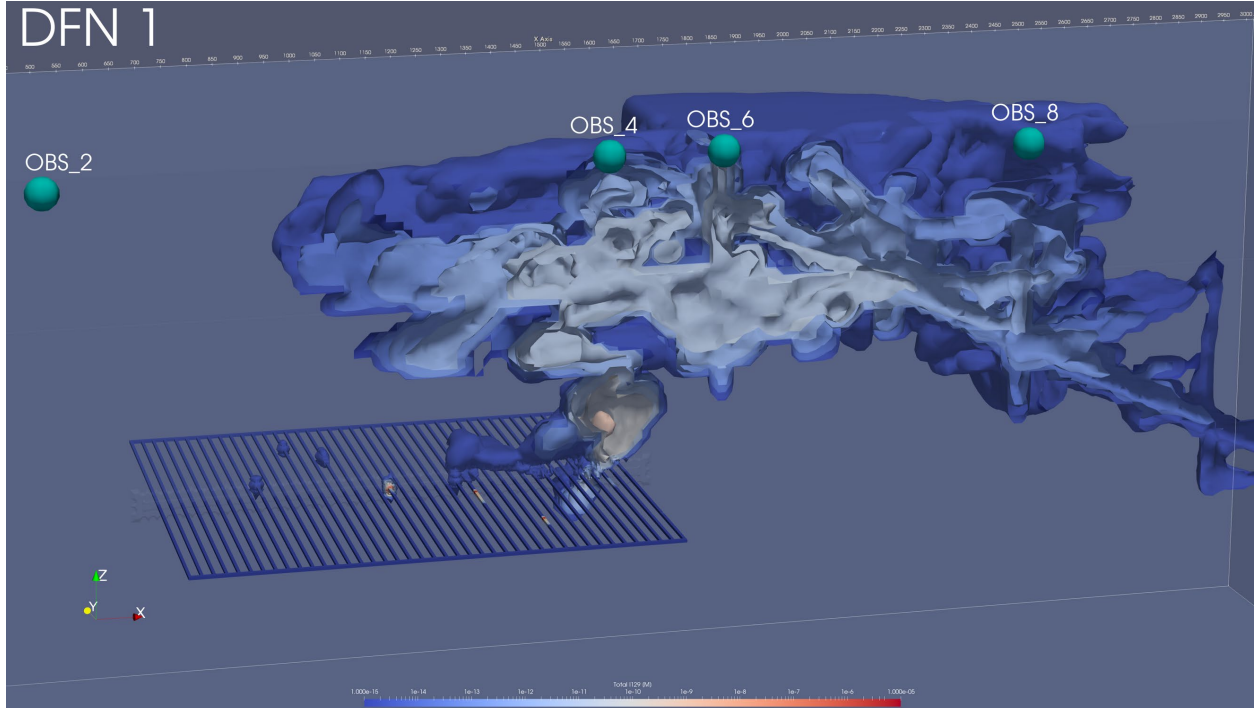


Figure 3-10. ^{129}I concentration contours for DFN 1 at 300 years, showing the full repository and a section of the plume.

GDSA/Domain 6

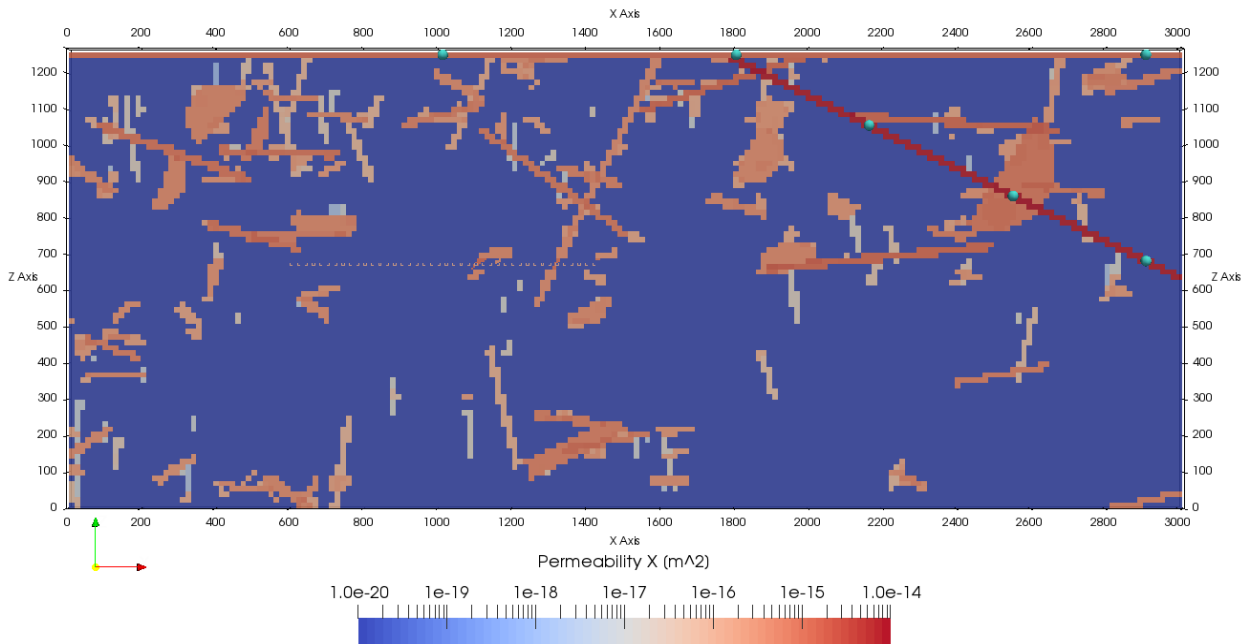


Figure 3-11. XZ cross section at the Y midpoint of the domain showing the locations of observation points (small teal spheres) (Mariner et al. 2016).

In FY 2016, deterministic analyses were completed using fifteen fracture network realizations (Mariner et al. 2016). A cross section of that domain is shown in Figure 3-11. The observation points for the model included three points at the top of the host rock directly above the midline of the repository (similar to the arrangement of observation points in Figure 3-9). In this earlier model, the observation points were named *glacial1*, *glacial2*, and *glacial3* and were located at 1,000 m, 1,800 m, and 2,900 m, as shown in Figure 3-11.

Break through curves for ^{129}I are shown on Figure 3-12. The fracture network, i.e. fracture realization, can be seen to have a significant effect on the arrival times and the concentration out to 100,000 years. Among the sediment observation points, the spread in time of earliest arrival is almost three orders of magnitude, from a few hundred years to approximately 100,000 years. At which observation point ^{129}I first arrives depends on the fracture realization. In Figure 3-12, the two dashed lines indicate two simulations in which ^{129}I arrived at the furthest point from the repository first (approximately 300 years into the simulation) and at closer observation points thousands to tens of thousands of years later. The spread in maximum concentration of ^{129}I is approximately four orders of magnitude. The timing of maximum concentration varies between approximately 10^4 and 10^6 years. The time of earliest arrival and the timing and magnitude of maximum concentration at any given point in the domain depend heavily on the fracture connectivity (or lack thereof) between that point and the repository.

A suite of 50 probabilistic simulations was run using a single fracture network realization (Domain6) and sampling of seven uncertain parameter distributions (Mariner et al. 2016, Table 4-12). Concentrations of ^{129}I were observed at the same observation points used to compare fracture realizations.

The variation among the probabilistic simulations in metrics associated with concentration and arrival times of ^{129}I is less than the variation observed among fracture realizations. For example, at all observation points except the one most distant from the repository, the time of earliest arrival in the probabilistic simulations varies by less than a factor of two, falling between approximately 300 and 500 years. At *glacial3*, the furthest observation point from the repository, the time of earliest arrival in the probabilistic simulations varies between approximately 400 and 10,000 years; this variation may indicate a travel path through the sediment and the influence of sediment properties (permeability, K_d) on travel time. In contrast, the variation in time of earliest arrival is almost three orders of magnitude, from a few hundred years to approximately 100,000 years for the deterministic analyses based on the fifteen different fracture network realizations (Mariner et al. 2016).

Spearman rank correlation coefficients were calculated to assess the sensitivity of maximum concentration of ^{129}I and ^{237}Np to sampled parameters (Mariner et al. 2016). Maximum concentrations of ^{129}I and ^{237}Np were found to be sensitive to properties of the engineered and natural barriers, including waste package degradation and waste form dissolution rates in the engineered barrier, and sorption coefficients and permeability of flow pathways in the natural barrier.

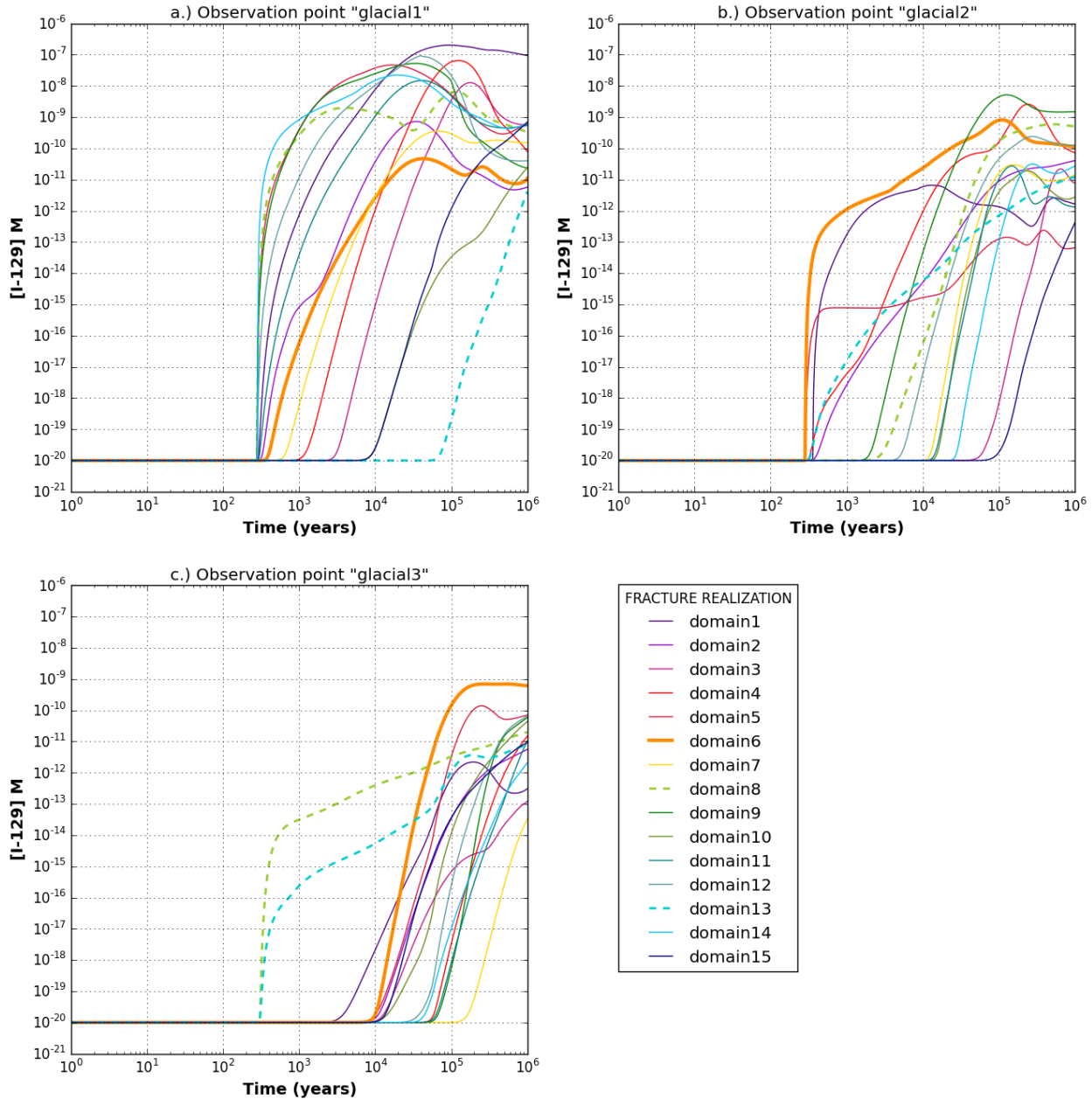


Figure 3-12. Predicted concentration of ^{129}I versus time for 15 fracture realizations at three observation points at the top of the model. The heavy orange line is Domain6, the fracture realization used in probabilistic simulations.

Future Crystalline Reference Case Development: Ongoing work will focus on adding mechanistic processes that affect waste package degradation and improving methods for characterization of natural fracture networks in crystalline rocks. Sensitivity analyses are underway to examine the importance of aleatory uncertainty in realizations relative to other major processes (Swiler et al. 2019, Chapter 8, in progress). Additional studies will investigate next-generation buffer materials and the effects of corrosion products (e.g. iron oxides) of EBS components. The incorporation of field data, such as including topographic relief, into modeling applications will also be pursued. Results from International activities, especially the Swedish underground research laboratory (URL) and Development of COupled models and

their VALidation against Experiments (DECOVALEX) activities, may also provide important contributions.

3.2.3 Salt

The salt reference case was initially presented in Sevougian et al. (2012). The reference case was updated in Freeze et al. (2013a) for commercial SNF and in Sevougian et al. (2016) for DOE-managed (as) HLW and DSNF. Further development occurred early in FY 2019 (Sevougian et al. 2019c), including incorporating DPC size waste packages, i.e. 37-PWR and 24-PWR, into the reference case. Since then, additional improvements have been made and will be documented in Sevougian et al. (2019d, in progress).

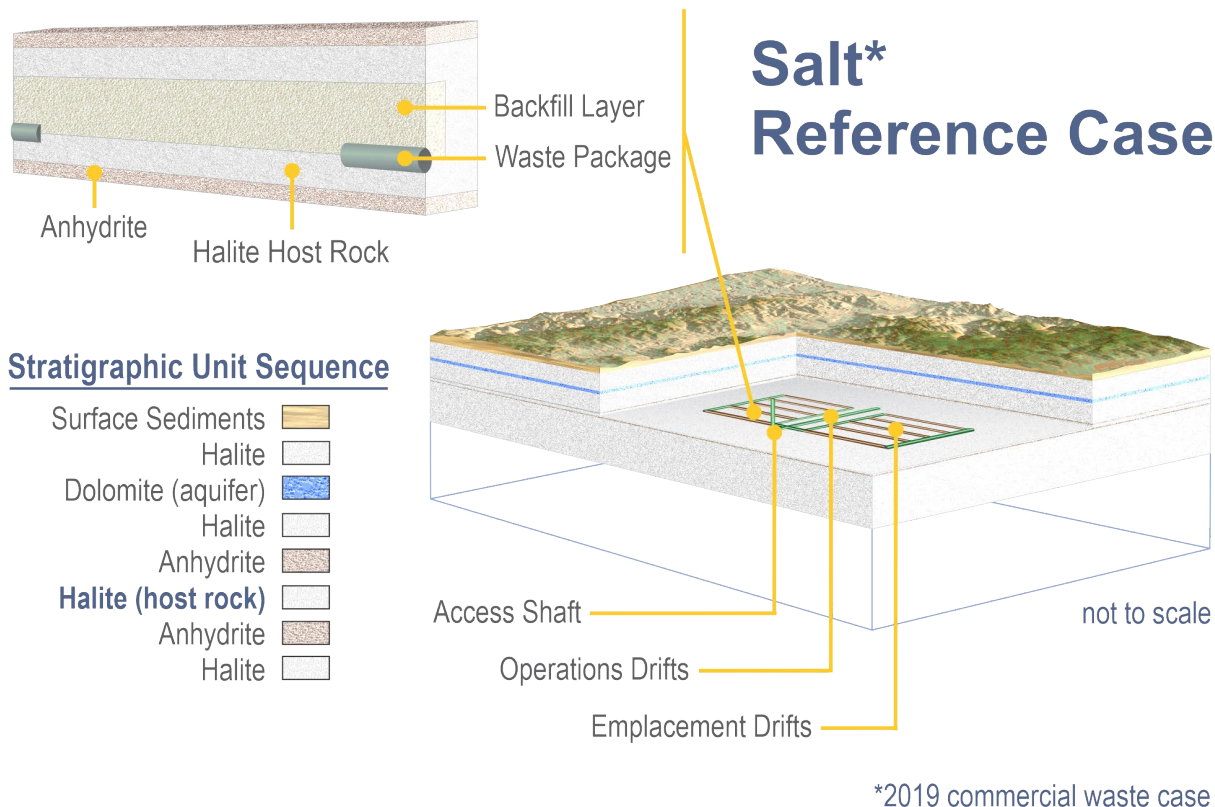


Figure 3-13. Schematic illustration of the Salt Reference Case (Based on Sevougian et al. (2019d, in progress)). The “Stratigraphic Unit Sequence” is the conceptualized stratigraphic section that is included in the reference case model. Note that the “Backfill Layer” is granular salt. The enlarged view, showing the EBS represents the central portion of the drift. The first waste package is set back 25 m from the entrance of the drift. The bottom portion of the model volume is empty, because the thickness of the rock units included in the Salt Reference Case model is less than the other reference case models. The extra volume is included in this figure to facilitate comparisons between the reference cases.

The reference case includes engineered and natural barriers associated with a geologic repository in bedded salt (Figure 3-13). This section presents a high-level description of the engineered system, including repository layout, inventory, waste form, waste package, and characteristics of the buffer, and drifts and the natural system, including geologic setting, host rock characterization, disturbed rock zone, and overburden. Significant differences between the reference case for commercial SNF (Sevougian et al. 2019c) and the

reference case for DOE-managed (as) HLW and DSNF (Sevougian et al. 2016) are highlighted. Preliminary results from the GDSA model are presented and briefly discussed to illustrate model capabilities.

Engineered System: The differences between the reference cases for commercial and DOE-managed waste begin with the repository layout. The reference case for DOE-managed waste includes a repository layout consisting of excavated, rectangular, emplacement drifts separated by intact salt “pillars”. Drifts are laid out in pairs, separated by a central access hallway (Note- in some reports these are referred to as rooms). Number of drift pairs, drift dimensions, and drift spacing are determined by total inventory, waste package size, and thermal and mechanical design considerations (Table 3-6). Waste packages are emplaced lengthwise and are covered by crushed salt backfill. The reference case for commercial SNF includes 102, 1525-m long, emplacement drifts. Each drift contains 50 waste packages emplaced lengthwise and spaced 30 m center-to-center. A 25-m long seal is placed at either end of each emplacement drift. Drifts are 5.0 m per side spaced 30 m center-to-center (Table 3-7).

The commercial repository is assumed to hold 70 MTHM of commercial SNF. The inventory is restricted to pressurized water reactor (PWR) assemblies. The repository for DOE-managed wastes includes the entire inventory of existing and projected glass HLW from Savannah River and Hanford and of DSNF with a heat output at the time of disposal (2038) of $\leq 1\text{kW/canister}$. Radionuclide inventory and decay heat curves are taken from Carter et al. (2013).

Table 3-6. Dimensions and counts for the DOE-managed waste bedded Salt Reference Case (Sevougian et al. 2016, Table 4-1).

Parameters	Reference Value	Simulated Value
HLW Waste Package (WP)		
WP length (m)	4.5 ^a	4.44
WP outer diameter (m)	0.61 ^a	0.56 (on a side) ^g
Number of Hanford WPs	11800 ^b	11800
Number of Savannah River WPs	7824 ^b	7824
DSNF Waste Package (WP)		
WP length (m)	4.6 ^c	4.44
WP outer diameter (m)	0.61 ^c	0.56 (on a side) ^g
Number of DSNF WPs (< 50 W bin)	1163 ^b	1164
Number of DSNF WPs (50-100 W bin)	234 ^b	234
Number of DSNF WPs (100-200 W bin)	940 ^b	940
Number of DSNF WPs (200-300 W bin)	12 ^b	12
Number of DSNF WPs (300-500 W bin)	41 ^b	42
Number of DSNF WPs (500-1000 W bin)	88 ^b	88
Number of DSNF WPs (1000-1500 W bin)	4 ^b	4
Disposal Rooms		
Room height (m)	3.05 ^d	3.33

Room width (m)	6.10 ^d	6.67
Room center-to-center spacing (m)	36.58 ^d	36.67
Room seal length (m)	15.24 ^d	15
Room length, including seals (m)	182.9 ^d	185
Number of WPs per room	166 ^d	140
WP center-to-center spacing (m)	0.91 ^d	1.11
Number of rooms per panel	10 ^d	10
Repository		
Number of HLW panels	14 ^d	14
Number of DSNF panels	3 ^d	2
Access hall height (m)	6.10 ^d	5
Access hall width (m)	9.14 ^d	10
Number of shafts	5 ^d	4
Shaft diameter (m)	7.38 ^d	5 (on a side) ^g
Repository length (m) ^e	NA ^d	1925
Repository width (m) ^f	NA ^d	753
Repository Depth (m)	655 ^d	601

^a Hanford glass HLW canister (DOE 2008, Table 1.5.1-16)

^b On the basis of canister counts reported in Wilson (2016) and Carter et al. (2013)

^c Large, long standardized canister (DOE 2008, Figure 1.5.1-9)

^d Carter et al. (2012, Section 4.2, Case 4). Dimensions are converted from feet. Overall repository dimensions are not explicitly calculated.

^e Equivalent to the length of the long hall extending from the shafts to the furthest disposal panel

^f Equivalent to the length of the short halls connecting pairs of disposal panels

^g PFLOTRAN simulations represent waste packages as rectangular cuboids instead of right circular cylinders, in order to simplify the gridding.

The waste form for commercial SNF is spent uranium oxide (UO₂) with zircaloy cladding. Radionuclide releases from the waste form are modeled as an instantaneous release (upon waste package breach) of fission products in voids of the waste form and a slower release that is governed by the dissolution rate of the UO₂ matrix. The waste package is modeled as a 5-m long stainless-steel canister containing 12-PWR SNF fuel assemblies, with a stainless steel overpack. The latest update changes the repository design to accept 24- and 37-PWR DPCs, in a 50/50 split by weight of heavy metal for each canister size (Sevougian et al. 2019c). Waste package failure was instantaneous in early versions of the reference case but in the latest version is modeled using a degradation rate equation as discussed below.

The waste form for DOE-managed (as) HLW is borosilicate glass. PA simulations calculate glass dissolution using a rate law formulated by Kienzler et al. (2012, Equation 6) that is discussed in Sassani et al. (2016, Table 3-4). DSNF includes several different waste types, and associated waste forms. Currently, the PA calculations assume that the DSNF instantaneously degrades when it is exposed to water.

In the salt reference case waste package degradation rate is an uncertain parameter represented by a truncated lognormal distribution with a mean of 10^{-4.5} yr⁻¹, a standard deviation of 0.5 (log units) and an

upper truncation of -3.0 (log units). This distribution is used to assign a base canister degradation rate for each waste package in deterministic analyses. Probabilistic simulations sample on the mean degradation rate using a log uniform distribution from $10^{-5.5} \text{ yr}^{-1}$ to $10^{-4.5} \text{ yr}^{-1}$.

Table 3-7. Dimensions and counts for the commercial SNF bedded Salt Reference Case (Sevougian et al. 2019c, Table 5-1).

Parameters	Reference Case Value	Simulated Value
Waste Package (WP)		
WP length (m) [24-PWR and 37-PWR]	5.20 ^a	5
WP outer diameter (m) [24-PWR and 37-PWR]	1.37 ^a	1.67 / side
WP center-to-center (m) [24-PWR and 37-PWR]	30	30
Inventory per 24-PWR WP (MTHM)	11.28 ^c	11.28 ^c
Inventory per 37-PWR WP (MTHM)	17.39 ^c	17.39 ^c
Number of 24-PWR WPs	3100	1550 / 3100 ^b
Number of 37-PWR WPs	2000	1000 / 2000 ^b
Emplacement Drift		
Drift diameter (m)	4.5 ^a	5.0 (on a side)
Drift center-to-center spacing (m)	30 ^a	30
Number of WPs per drift	50 ^a	50
Drift seal length (m)	25	25
Drift length, including seals (m)	1525	1525
Repository		
Repository Depth (m)	600	600
Number of drifts	102	51 / 102 ^b
Number of shafts	Not specified	3 / 6 ^b
Shaft access size (m ²)	Not specified	5 x 10
Emplacement footprint (km ²)	4.88	2.44 / 4.88 ^b

^a Hardin and Kalinina (2016, Section 3)

^b half-symmetry domain / with reflection

^c Hardin et al. (2013, Table 4-2)

Natural System: The reference repository site occurs in a geologically stable sedimentary basin with low probabilities of seismicity and igneous activity. The present concept for a mined repository in a bedded salt formation places the repository in a stratum of relatively pure halite (> 50%) at least 76-m thick. Bedded salt formations, often hundreds of meters thick, form in near-shore and shallow-marine environments during cycles of marine transgression and regression. In addition to beds of very low permeability and low porosity

halite (the target for waste isolation), they may contain beds rich in other evaporite minerals (anhydrite, polyhalite), and carbonate and clastic (shale, sandstone) interbeds (Perry et al. 2014, Section 4.2.1).

The generic stratigraphic section which comprises the natural barrier in the PA simulations, for the DOE-managed Waste Reference Case, consists of beds of halite and anhydrite with overlying mudstone and siltstone, and a fractured dolomite aquifer (Figure 3-14). A 15-m thick aquifer, modeled as fractured dolomite which is assumed to provide a potential pathway for radionuclide release, is separated from the halite by a 15-m thickness of mudstone. A 105-m thick unit of mudstone interrupted by the dolomite aquifer overlies the halite. Thicker anhydrite beds are located at depth. The generic stratigraphic section used in the Commercial SNF Reference Case has been modified by the removal of the siltstone and mudstone units and the thicker anhydrite beds at depth (Sevougian et al. 2019d, in progress). The representation of the units in the salt reference cases relies heavily, but not exclusively, on information from WIPP. Specific information can be found in the supporting reports.

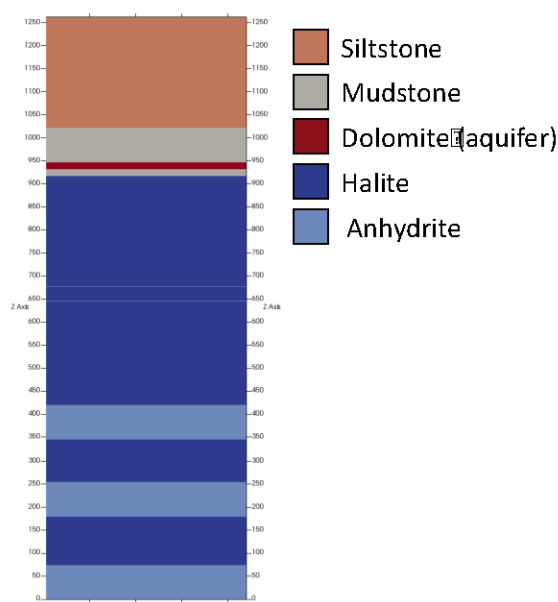


Figure 3-14. Generic stratigraphic column for salt reference case. The repository horizon is centered between the two thin beds of anhydrite at $z = 661$ m (Sevougian et al. 2016, Figure 4-3).

The DRZ is defined as the portion of the host rock adjacent to the engineered barrier system that experiences durable (but not necessarily permanent) changes due to the presence of the repository (Freeze et al. 2013a). The DRZ is expected to have elevated permeability and porosity with respect to the properties of the host rock matrix due to the changes in stress induced by mining. The reference cases assume 1-m thick anhydrite interbeds located immediately above and below the repository DRZ. Anhydrite beds and interbeds are more permeable than the surrounding halite. Near the repository, they may become fractured as a result of the excavation, and therefore serve as potential pathways for radionuclide transport.

Post-Closure Performance Assessment: The generic GDSA model for a salt repository has evolved. The model of the reference case used by Freeze et. al. (2013, Figure 3-7) includes only a single 805-m drift containing 80 waste packages. The bottom of the model domain is a horizontal (X-Y plane) symmetry boundary imposed through the vertical center of the EBS, and the top of the model domain is the top of the overlying aquifer. The PA model for the 2019 salt reference case is under development.

The generic GDSA PA model for DOE-managed (as) HLW and DSNF provides a good illustration of the capabilities of post-closure PA modeling (Sevougian et al. 2016). The model includes a conceptualization of engineered and natural barriers in an undisturbed scenario. The key aspects of this conceptualization are summarized on Table 3-8. The performance metric for these calculations is maximum radionuclide concentration because there is no representation of the biosphere in the model.

Table 3-8. Conceptual representation of the engineered and natural barriers in PA (Sevougian et al. 2016, Table 4-6).

Region	Component	Key characteristics	Key processes included in PA
Engineered Barrier	HLW (source term)	Glass waste form	Radionuclide decay, waste form dissolution
	DSNF (source term)	Metallic fuel waste form	Radionuclide decay, instantaneous dissolution
	Waste Package (control on source terms)	Carbon steel	Degradation and breach
	Waste Package (region of domain)	Package plus contents	Radionuclide advection, diffusion, and decay
	Crushed Salt Backfill	Enhance permeability and porosity compared to intact halite	Radionuclide advection, diffusion, decay
Natural Barrier	Halite	Low permeability and porosity	Radionuclide advection, diffusion, decay
	DRZ	Enhanced permeability and porosity compared to intact halite	Radionuclide advection, diffusion, decay
	Anhydrite	Higher permeability than halite, potential pathway for release	Radionuclide advection, diffusion, sorption, decay
	Mudstone	Moderately low permeability	Radionuclide advection, diffusion, sorption, decay
	Aquifer	Fractured dolomite	Radionuclide advection, diffusion, sorption, decay
	Siltstone	Moderately high permeability	Radionuclide advection, diffusion, sorption, decay

Simulations assume (1) a mined repository at 600-m depth in relatively pure halite; (2) a 15-m thick fractured dolomite aquifer overlying the halite; (3) a head gradient of -0.0013 m/m from west to east; (4) a regional heat flux of 60 mW/m² with a mean annual surface temperature of 10 °C; and (5) a saturated domain. Figure 3-15 shows the 3D model domain.

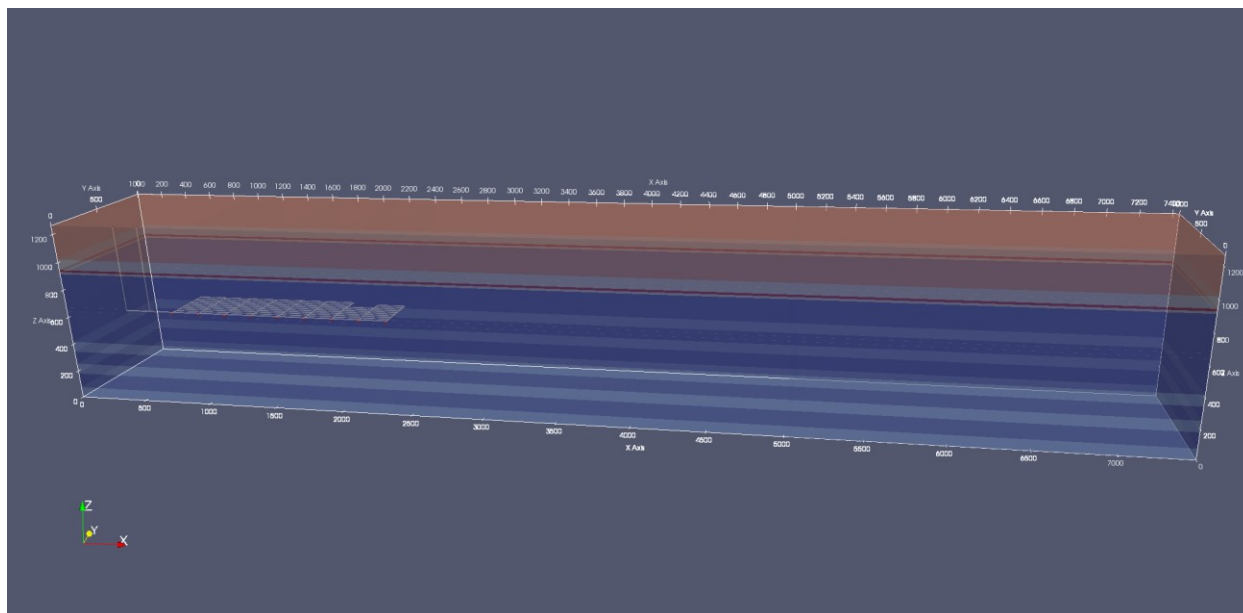


Figure 3-15. Transparent view of the model domain. The 3D structure inside the half-symmetry domain is the repository, including 8 disposal panels and 2 shafts (Sevougian et al. 2016, Figure 4-4).

Initial conditions specified are pressure, temperature, and radionuclide concentrations. Initial pressures and temperatures throughout the model domain are calculated by applying a liquid flux of 0 m/s and an energy flux of 60 mW/m² to the base of the domain, holding temperature (10°C) and pressure (approximately atmospheric) constant at the top of the domain, and allowing the simulation to run to 106 years. Pressure at the top of the domain decreases from west (left) to east (right) with a head gradient of -0.0013 (m/m). This technique results in initial conditions that represent a geothermal temperature gradient and hydrostatic pressure gradient in the vertical direction, and a horizontal pressure gradient that drives flow from west to east.

In PA simulations, each waste package is a single region containing a radionuclide source term (due to waste form dissolution/degradation) and a heat source term. The radionuclide source term is activated when a waste package is breached. This iteration of the salt reference case takes credit for a 7.5 cm thick carbon steel overpack, which is assumed to degrade via general corrosion. Each waste package is modeled as a transient heat source. Deterministic simulations assign a base canister degradation rate for each waste package by sampling on a truncated log normal distribution with a mean of 10^{-3.4} yr⁻¹, a standard deviation of 0.5 (log units), and an upper truncation of -3.0 (log units). Probabilistic simulations sample on the mean degradation rate using a log triangular distribution over the range 10^{-4.7} yr⁻¹ to 10^{-3.4} yr⁻¹, with a mode of 10^{-3.6} yr⁻¹.

Simulation Results: Deterministic and probabilistic analyses were completed using the PA model. The deterministic analysis evaluated the evolution of temperature and flow fields as the repository cooled. It also evaluated radionuclide releases as waste packages breached. Slightly more than 10% of the waste packages have breached 1000 years into the simulation, and all waste packages have breached by 25,000 years. Figure 3-16 shows the distribution of nearly conservative ¹²⁹I at 100,000 years into the simulation.

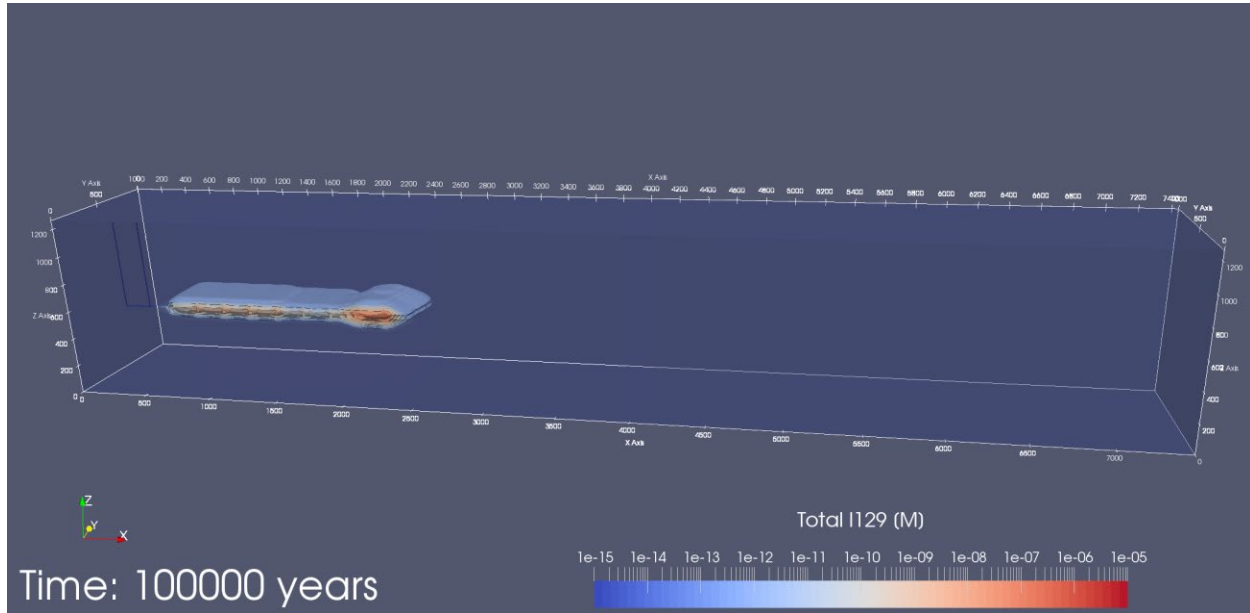


Figure 3-16. ^{129}I concentration at 100,000 years in the deterministic simulation (Sevougian et al. 2016, Figure 4-13).

A suite of 50 probabilistic simulations were completed to the transport of ^{129}I and ^{237}Np in the aquifer overlying the repository. Breakthrough curves show that ^{129}I concentrations are low, i.e. 10^{-16} mol/L or less, at all times out to 1,000,000 years at three observation points in the aquifer and ^{237}Np concentrations never exceed background values.

Future Salt Reference Case Development: The BATS (Brine Availability Test in Salt) test at WIPP is expected to produce a wealth of new information and the analyses of these new data will lead to significant enhancements to the salt reference case. The main focus of BATS is to explore brine availability. These tests are the first part of a wider systematic field investigation campaign to improve the existing long-term repository safety case for disposal of heat-generating radioactive waste in salt. BATS will also provide data on the quantification of inflow rates and brine composition in the near-field (at scales of cm to m from the heat source) with the aim to improve: 1) our understanding and observations of coupled thermal-hydrological-mechanical-chemical (THMC) processes affecting prediction of near-field conditions; 2) conceptual models of near-field behavior that inform the safety case; and 3) the numerical models, constitutive relationships, and parameterizations that are implemented in PA models. Also, the unique brine geochemical data to be obtained during the tests are potentially relevant to long-term repository safety cases, including benchmarks for adjusting and validating thermodynamic databases for geochemical modeling of brine chemistry in salt (Mills et al. 2019).

3.2.4 Alluvium

The performance assessment of a generic geologic repository in an unsaturated alluvium host rock was first described and analyzed in Mariner et al. (2018b), with additional work done by Sevougian et al. (2019c) and Sevougian et al. (2019d, in progress). The GDSA reference case includes the engineered and natural barrier systems for a mined geologic repository in variably-saturated alluvium formation. Ongoing work on model building, simulation studies and development of new PFLOTRAN capabilities are described.

Natural System: Multiple barriers are necessary to contribute to the safety of waste isolation and delaying or limiting radionuclide releases and transport. There are three main siting features in the unsaturated zone generic case that contribute to isolation of waste and delay and limit radionuclide releases: Alluvial basins

of the western U.S. are in arid climates and have deep water tables with low recharge rates, which minimizes the potential for groundwater contact with radionuclides. The thickness of alluvial formations is typically on the order of 100s of meters, which provides longer transport paths to the assessable environment. Finally, alluvial basins have stacked playa and lacustrine deposits that will impede radionuclide migration due to low permeability of the playa and sorption onto sediment. There is also a reliance on engineered barriers.

A schematic of the hydrology and geology of an unsaturated alluvium repository is presented in Figure 3-17. The Great Basin has been the subject of several programs of study as well as smaller-scope projects. Notable programs include the Regional Aquifer-System Analysis conceptual model (Prudic et al. 1995), the Death Valley Regional Flow System study (Belcher 2004), the Basin and Range Carbonate Aquifer System study (Welch et al. 2007), and the Great Basin Carbonate and Alluvial Aquifer System study (Heilweil and Brooks 2010).

The physical geography of the Great Basin is characterized by north or northeast trending mountain ranges separated by broad valleys. Surface-water is relatively uncommon and tends to originate in mountains on the western and eastern edges and in the northern part of the Great Basin. All surface water drains internally to the Great Basin as terminal lake or playa systems (Mariner et al. 2018b). Consolidated rock and basin-fill aquifers tend to be well connected hydraulically. Other sediment within alluvial basins may host local, perched aquifers (Sweetkind et al. 2010).

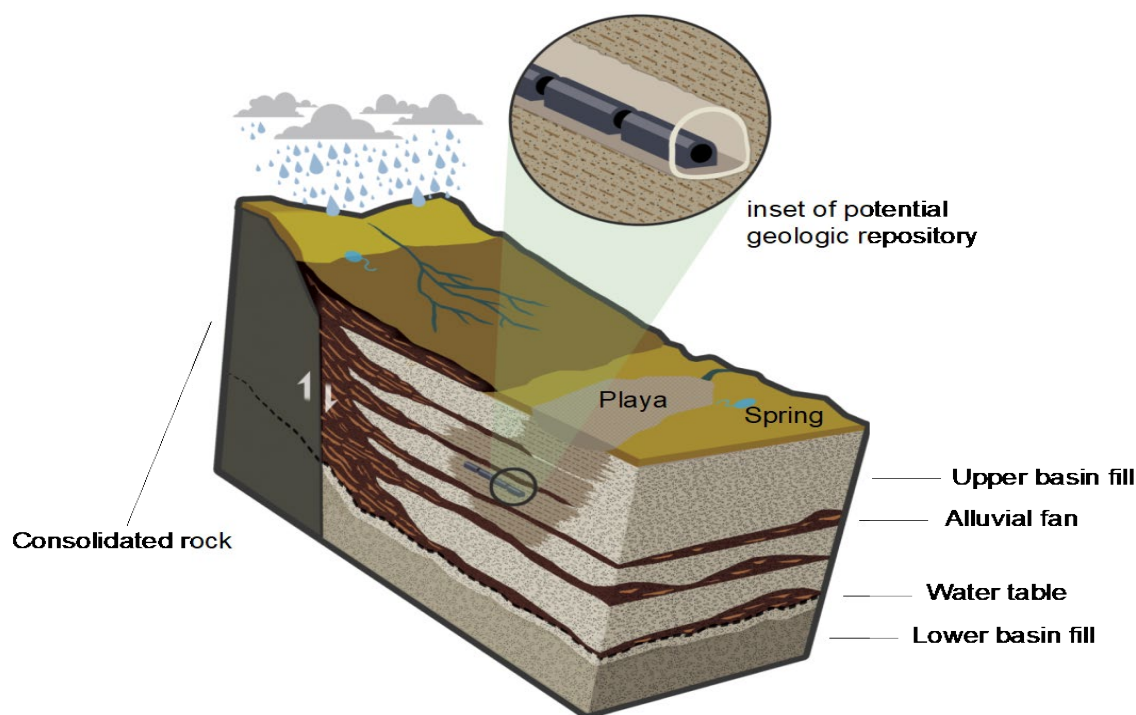


Figure 3-17. Schematic of potential unsaturated zone geologic repository. The lithologic heterogeneity that is expected in basin-fill valleys is depicted. Alluvial fans, fluvial systems, spring discharge areas, and playas are common features.

Thermal Conductivity: DPCs emit a great deal of energy into the subsurface after disposal. Though there is little data available, thermal conductivity of alluvium is low, which may result in extremely high temperatures. As part of the present work, dry thermal conductivity was measured on a fine- and coarse-grained samples were in the range of 0.3-0.45 W/mK, with a slight increase in conductivity over the temperature range 35-300°C. Thermal conductivity of the fine-grained sample was on the order of 0.05

W/mK higher than the coarse sample. These numbers are lower than any of the measurements found from an extensive literature review (Mariner et al. 2018b).

Radionuclide Inventory and Transport: PA simulations assume that the waste form and waste packages are identical to the 12-, 24- and 37-PWR DPCs considered for the other reference cases. For the purposes of long-term geologic storage of spent nuclear fuel, understanding the transport of long-lived transuranic elements are most important. The chief sources of radioactivity are ^{273}Np and isotopes of americium and plutonium. Isotopes such as ^{233}U , ^{234}U , ^{99}Tc , ^{14}C , ^{129}I , and ^{226}Ra have also been included in total system performance assessments because they are soluble and weakly sorb onto geologic media (SNL 2008, Chapter 2; Simmons and Neymark 2012). As radionuclides migrate from low oxidation potential conditions in the engineered barrier system to the higher oxidation potential condition in the natural barrier system, some may precipitate, effectively reducing the mobility of those radionuclides. Solute transport and ranges of key radionuclides for oxidizing conditions are discussed in more detail in (Mariner et al. 2018b).

Conceptual Model: This conceptual model includes the delineation of hydrogeologic units within the alluvial fill of a basin with similar characteristics to the Great Basin in the western United States (Perry et al. 2018). The natural barrier system is subdivided into two hydrogeologic units. The upper basin-fill aquifer unit is generally taken to be variably saturated with low to moderate permeability. Playa/lacustrine sediment in the upper basin fill unit has lower permeability and provides the first barrier to radionuclide transport. The occurrence and juxtaposition of permeable and impermeable units is important in determining the potential for radionuclide migration within and between hydrographic areas. A small west to east hydraulic gradient is assumed. Hydraulic properties based on an extensive literature review are presented in Table 5-1 of Mariner et al. (2018b).

Repository Characteristics: The GDSA reference alluvium case is focused on disposal of 12-, 24-, and 37-PWR assemblies. The disposal facility design includes engineered and natural barrier systems associated with a mined geologic repository as discussed above.

The performance assessment model assumes (1) a mined repository at 255-m depth; (2) a head gradient of 0.005 m/m from west to east; and (3) a variably-saturated model domain to a depth of around 500 m with water saturated media below. There are a number of flow processes occurring for storage of high energy PWR assemblies within the unsaturated zone that do not occur in the other GDSA reference cases considered to date, such as water/air phase partitioning, formation dry out, advection and diffusion of vapor through the matrix, adsorption at the air-water interface, vapor adsorption to solid, and transport of radionuclides in the gas phase.

Processes accounted for in the simulations will include waste package degradation, waste form (UO_2) dissolution, equilibrium-controlled radionuclide sorption and precipitation/dissolution, radioactive decay and ingrowth in all phases (aqueous, adsorbed, precipitate), coupled heat and fluid flow, and radionuclide transport via advection and diffusion in both the liquid and vapor phases. Mariner et al. (2018b), Sevougian et al. (2019c) and Sevougian et al. (2019d, in progress) describe the development of the repository models in more detail.

Engineered Barrier System: Engineered backfill is required due to the low thermal conductivity of the alluvium. The conceptual model has a well-compacted backfill engineered to have wet and dry thermal conductivity that may be as high as 2.0 W/mK. This is necessary to moderate temperature in and near the waste packages.

Simulations: The coupled thermal and multiphase flow problem is being simulated on a performance assessment domain with 25 waste packages per drift and 27 drifts (Sevougian et al. 2019c). Figure 3-18 shows the model for the repository in the subsurface. The meshes are unstructured and gridded with Cubit (Blacker et al. 2016). Probabilistic inputs for the simulations will be prepared using Dakota's Latin Hypercube Sampling (LHS) capability. Simulations of flow and transport will be run with PFLOTRAN.

Drift spacing is 50 m while center-to-center spacing of WP along drift is 20 m. This configuration was chosen as the waste packages should be far enough apart to prevent complete dry out of the formation for 37-PWR assemblies, based on sector model simulations (Sevougian et al. 2019c). The half-symmetry model domain is 3,915 m in length (X), 1,065 m in width (Y), and 1,005 m in height (Z). A variety of simulation grids have been studied. The coarsest has 64,000 cells and does not resolve the individual waste packages. The finest mesh has 2,402,205 grid cells and has sufficient refinement across the full domain for both near-field heat and advection and far-field radionuclide transport. Biosphere and radionuclide transport are not yet considered in the models. Sevougian et al. (2019c) and Sevougian et al. (2019d, in progress) describe numerical implementation for 24 and 37 PWRs in the performance assessment-scale and sector models in more detail.

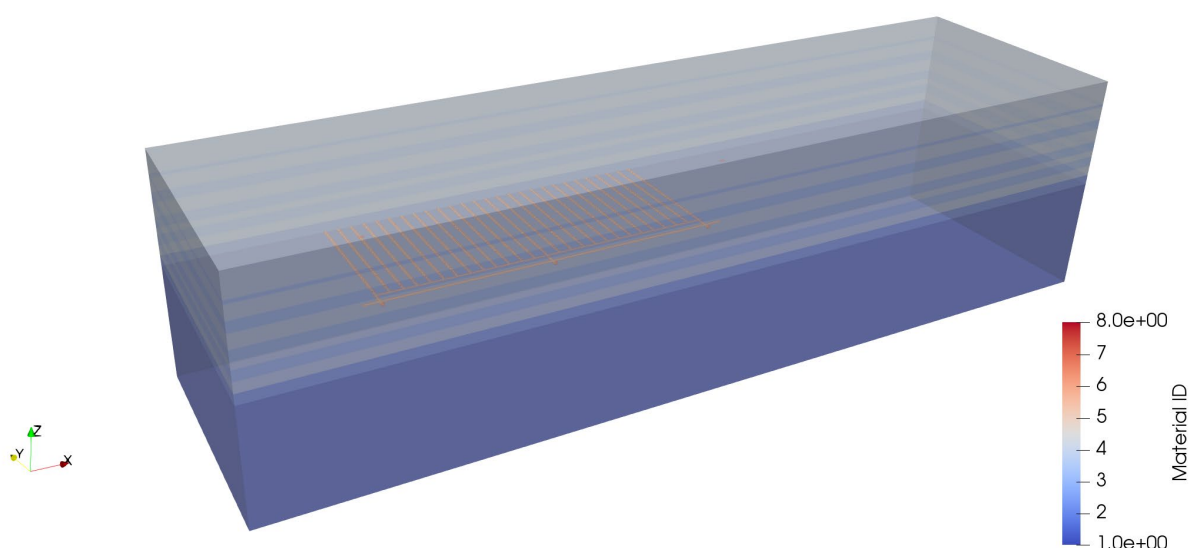


Figure 3-18. The simulation model for the configuration of the repository and natural barrier system. Upper basin fill is shown in light blue and grey, lower basin fill is in dark blue, repository and damage zone are pink and red.

Ongoing Work: Simulations focused on the thermal and fluid flow problem are in progress. Considerable numerical development of PFLOTRAN has been necessary for the new alluvium case with DPCs that release so a great deal of heat into the formation after disposal. New developments include the ability to simulate at temperatures in excess of 350°C, transport of radionuclides in dried-out porous media, and improved Newton solvers to handle rapid temperature and phase changes. These are discussed in more detail in Section 2.2.

A simulation study is currently underway to compare the results of finely gridded single-waste package models with sector models and PA-scale models with coarser grids. This is a first step towards developing a workflow that uses upscaling or nested models to develop accurate simulations without prohibitive computation time. Multiscale modelling allows resolution of short-term heat and transient flow processes on small models, while the large-scale long-term radionuclide transport problem is resolved on large models.

Los Alamos scientists are currently developing a more realistic geological model for a representative alluvium environment. This will be used as the basis of the natural system domain in future iterations of the alluvium reference case.

4. SUPPORTING DISPOSAL R&D

The SFWST R&D program has made significant progress developing experimental methods to test and analyze the chemical and physical phenomena that could impact the long-term safety assessment of nuclear waste disposal, and in modeling those processes. The Argillite, Crystalline, Salt, EBS, and International R&D programs are all highly collaborative, coordinating and communicating extensively with other programs. Much of the ongoing research related to the development of generic EBS and DPC conceptual designs and performance is applicable to each of the media-specific R&D programs and many of the experimental tests in the International program are being conducted in European and Asian Underground Research Laboratories (URLs).

The sections below describe recent progress and the current status of R&D in the various programs. Integration of the individual programs with the effort to develop improved GDSA capability to support future decisions related to disposal, storage and transportation of SNF and HLW in the U.S. To that end, considerable effort is being dedicated to developing improved models to link analyses of specific process models (particularly models of complex coupled processes) to the PA capability in the GDSA Framework. As part of this effort, simplified models (or surrogate models) are being developed by the R&D programs for incorporation in PFLOTRAN or the larger GDSA Framework.

4.1 Argillite R&D Activities

The primary goal of the Argillite R&D program is to improve our understanding and ability to simulate how environmental conditions would evolve in a repository such as one hosted in argillite, particularly in response to the increased temperatures caused by the emplacement of SNF. The experiments range from long-term, large scale simulations of repository performance to laboratory scale detailed studies of mineralogical and geochemical changes. Jové Colón et al. (2018) describes recent progress in Argillite R&D and summarizes future priorities and goals for the program, including integration with PFLOTRAN and GDSA Framework and development of the argillite reference case (Section 3.2.1). Similar progress reports have been published annually since 2012. The discussions are generally organized in several categories or types of R&D activities, which include:

- Development of a reference case GDSA model for a generic repository in shale/argillite
- Large scale URL investigations of coupled THMC processes and reactive transport in the EBS and near field environment
- Laboratory scale experimental activities investigating buffer/backfill interactions at elevated pressure and temperature
- Development and implementation of a Fuel Matrix Degradation Model (FMDM)
- Thermodynamic database development

GDSA Generic Reference Case Analysis: The development and updating of the reference case analysis for a generic repository in argillite is described in Section 3.2.1. Additional improvements to the model are anticipated as new subsystem process models and surrogate models are developed and incorporated in PFLOTRAN.

Large Scale URL Investigations: Large scale coupled process experiments relevant to repositories in argillite have been and are being performed in URLs in Switzerland (Mont Terri and Grimsel), France (Bure), and Japan (Mizunami). The experiments have generally been designed to investigate the effects of a repository environment on the host rock, and the engineered materials that would be used to emplace and isolate SNF and/or high-level waste (e.g., steel waste packages, bentonite buffers, other backfill materials and concrete).

Figure 4-1 is a schematic drawing of the Mont Terri URL, showing the location of several major experiments that have been performed since the facility opened in 1996. Site 7 is the location of a long-term full-scale heater test using three steel canisters to simulate waste packages. The canisters were placed on bentonite blocks and bentonite was used to backfill around them. Heating began in 2015 and is planned to continue until 2025. Instrumentation in the engineered barriers, and in boreholes in the Opalinus clay host rock, is used to monitor environmental conditions. The U.S. program is utilizing the TOUGH and FLAC codes to model the THM effects of the test. The results to date indicate that thermal pressurization, temperature and humidity can be reasonably well simulated in both the backfill and the clay host rock (Jové Colón et al. 2018). After 3.5 years of heating and water infiltration, no significant swelling stress has been detected in the bentonite buffer.

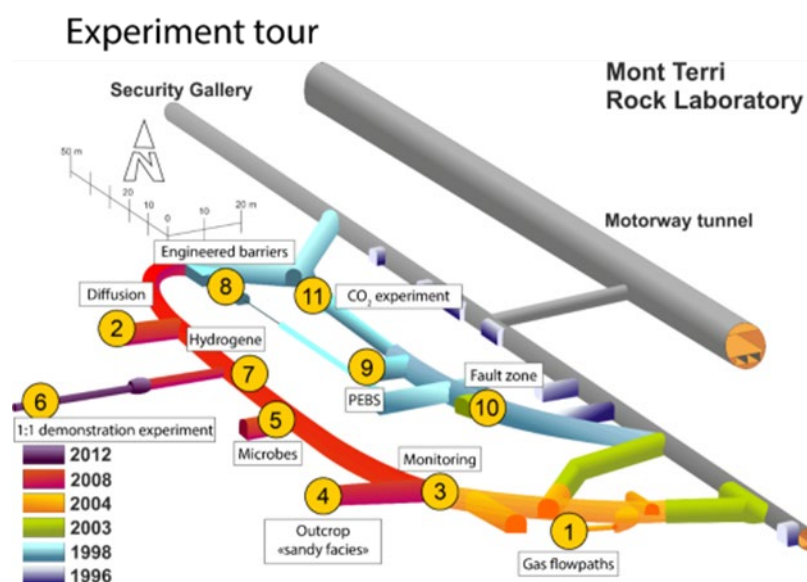


Figure 4-1. Schematic drawing of the Mont Terri URL (from Mont Terri website at <https://www.mont-terri.ch/en/experiments/the-most-important-experiments.html>).

The Full-scale Engineered Barriers Experiment (FEBEX) “In-Situ” Test at Grimsel is a long-term full-scale heater test that began in 1994 to analyze the effects of high temperature on engineered barrier materials. The test began in 1997 with two heaters designed to heat the near-field environment to a temperature of 100°C. One heater was shut down in 2002, while the second continued heating until 2014. Throughout the operational phase of the experiment, international teams of scientists monitored an extensive network of sensors measuring physical and chemical conditions including temperature, pressure, moisture content, and the geochemical environment. Figure 4-2 is a schematic drawing of the FEBEX test showing the configuration of the heaters and EBS materials.

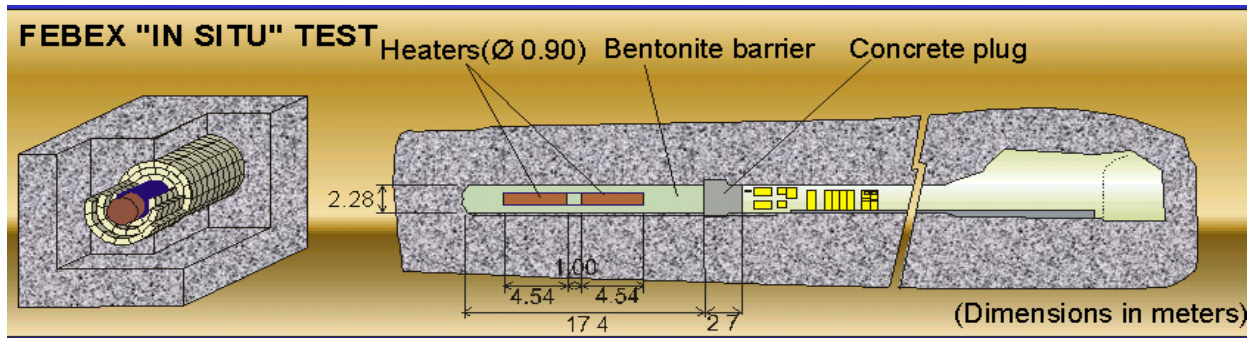


Figure 4-2. Schematic drawing of the FEBEX "In-Situ" Test at the Grimsel Switzerland URL.

The FEBEX Dismantling Project (FEBEX-DP) began in late 2014 and continues today. FEBEX-DP is systematically removing the heaters and materials used in the experiment and performing numerous studies to investigate the effects of heating on bentonite, steel and concrete. The Argillite R&D program (Jové Colón et al. 2018) is analyzing postmortem samples to assess chemical and structural changes to clay mineralogy, such as changes to bentonite composition, sorption behavior, and swelling in response to heating. The analyses revealed Mg enrichment in samples closest to the heater. This observation is consistent with other studies and demonstrates the extent of swelling is less variable for samples closest to the heater. Measured water content was consistent with the results of other studies.

The Argillite R&D program is participating in the GREET (Groundwater REcovery Experiment in Tunnel, Mizunami URL, Japan) project as part of Development of COupled models and their VALidation against Experiments (DECOVALEX) Task C, which includes 3D Reactive transport modeling (PFLOTTRAN) of the closure test drift (CTD), focusing on interactions between ground water and the cement liner in the water-filled tunnel (Jové Colón et al. 2018). This effort is part of an inter-comparison exercise between different modeling teams. Model predictions of pH and Cl⁻ concentrations are compared to measured data at specific locations and times to calibrate and improve the ability of PFLOTTRAN to simulate geochemical conditions relevant to transport.

As part of the TED and ALC Experiments at the Bure URL in France (DECOVALEX-2019 Project), the Argillite R&D program has used experimental data to calibrate THM parameters and the TOUGH-FLAC codes to model THM behavior in the COx claystone. The model parameters and results are in good agreement with theoretical solutions, and with experimental results at both small and large scales (Jové Colón et al. 2018). Ongoing work will expand the model to repository scale (an area with several high-level waste cells).

Laboratory Scale Investigations of Coupled Processes: The Argillite R&D program is modeling gas migration in clay as part of DECOVALEX-2019 using continuum (TOUGH-FLAC) and discrete fracture network (TOUGH-RBSN) approaches. The two approaches are designed to be complementary, and both are used to simulate the results of gas migration experiments in a 60 mm x 120 mm cylinder filled with bentonite. The TOUGH-FLAC model captures the main features of the experiment (pressure, stress, and flow evolution), but there are large deviations from model predictions at the end of the experiment where gas flow shuts down. The TOUGH-RBSN simulator with enhanced fracture permeability demonstrated the gas breakthrough with simulated pore pressure evolutions that matched the experimental data well. However, the simulated outflow rate deviates from the experiment in terms of the flow activation time and the overall shape of the evolution curve (Jové Colón et al. 2018).

Extensive detailed laboratory scale geochemical investigations of both EBS materials and natural host rocks are being performed by LANL. Hydrothermal experiments (at 200°C and 300°C) have involved Opalinus Clay (wall rock), Wyoming bentonite, Portland cement, and steel (low-carbon and stainless). Characterization studies have involved SEM-EMPA, XRD, and aqueous solution compositional data of

hydrothermal experiments. SEM-EMPA and XRD analyses were also completed for a set of FEBEX-DP bentonite samples from Section 49. Several significant observations can be drawn from the investigations:

- The Opalinus Clay experiments appears to show an increase in the illite-smectite distribution. However, there was negligible illitization in the bentonite fraction for the mixed experiment. The overall high silica saturation appears to inhibit illite formation and favor precipitation of high-silica zeolites such as analcime/wairakite.
- A mixture of Opalinus Clay plus bentonite produces higher corrosion rates for low-carbon steel relative to bentonite alone experiments. The higher corrosion rates are attributed to the high pyrite content in the Opalinus Clay fraction.
- The addition of cement to a clay favors the formation of an analcime-wairakite phase at lower temperatures (200°C). This is most probably due to the high concentration of Si and Ca liberated into the groundwater from the cement.
- The FEBEX-DP bentonite clay sample characterization study indicates feldspar compositions (both plagioclase and K-feldspar) vary in the outer and middle location, but more homogeneous compositions in the region closer to the heater surface. MgO and SiO₂ in smectite generally varies from the different sample block locations with distance from the heater surface.

LBNL is developing a tool (the SIMFIP borehole probe) that can simultaneously measure fluid pressure and three-dimensional displacements at high frequency. The probe could be used to probe fault movements and estimate fault permeability variations during in situ fault activation experiments at depths relevant to nuclear repository sites. Data gathered to date indicate that large fault permeability variations correlate with periods of large fault slip rate events. However, these permeability changes do not correlate well with the imposed pressure, which suggests that fault displacement rate might play a larger role than displacements in fault permeability variations. A sensor such as the SIMFIP probe could track minor fault displacements and slip rates to help assess their effects on potential leakage in low permeability argillite host rock. Field observations and numerical results show that the initial stress on a fault, affecting the permeability change and friction during fluid pressurization, has an important effect on fluid pressure diffusion and slip growth (Jové Colón et al. 2018).

Development of the Spent Fuel Degradation and Waste Package Degradation Models: The parameter database for the FMD (Fuel Matrix Degradation) model was updated based on comparisons between model results and existing spent fuel, and UO₂ dissolution rate data. An electro-kinetic mixed potential model for the corrosion of steels was coupled with the spent fuel dissolution reactions through the H₂ generation reactions.

Sensitivity analyses with the new FMD model reiterate the need for additional experimental data to parameterize and validate the steel corrosion module added to the FMD model. Results from scoping experiments demonstrated a straightforward electrochemical method that provides the electrokinetic information needed for model parameterization and validation.

Model simulations using the new FMD model agree with previous model results showing that the presence of metals that corrode at different rates can extend the time over which H₂ generation will attenuate the fuel degradation rate.

Thermodynamic Database Development: In recent years, there have been several significant advances in thermodynamic databases, particularly with respect to integration and coordination with other international efforts. In 2017, the program implemented the International Association for the Properties of Water and Steam (IAPWS-95) equation of state (EoS) for water. It is also consistent with the recommendations of CODATA. EoS was implemented as a stand-alone code (H2OI95) that will be interfaced to SUPCRT92.

Code results have been validated in various ways with exact match to tabulated results from the original EoS developers and by using NIST calculations of water thermophysical properties (Jové Colón et al. 2017).

The SFWST campaign is now integrating with and represented within the NEA-TDB project. Ongoing work is underway on sorption database development and modeling strategies using a PhreeqC-PEST fitting routine using various surface complexation models (Jové Colón et al. 2018).

Overall Status and Future Priorities for Argillite R&D: Jové Colón et al. (2018) summarized the status of ongoing work and identified future goals and objectives for the Argillite R&D program. The recommendations are organized by categories related to the types of R&D needed, including:

- Experimental and thermodynamic modeling studies of barrier material interactions
- Coupled-process model development for simulation of near-field thermal, chemical, mechanical, and transport (THMC) interactions
- Development of source term models for (spent nuclear) fuel matrix degradation (FMD) and integration with GDSA

The primary goal of the overall Argillite R&D program is to build a credible GDSA model that can be used to support decisions regarding the U.S. used fuel and high-level waste disposal program, including the siting and design of future repositories in argillite or other host rocks. As a result, the GDSA model must reflect a broad understanding of the characteristics of such sites, including both natural and engineered systems, and the processes that may affect the ability of the site to isolate waste. That understanding must also be supported by defensible process models, or surrogate models, that can be incorporated into the PFLOTRAN total system model.

4.2 Crystalline R&D Activities

Crystalline Disposal R&D work conducted to support the development of the crystalline reference case (Section 3.2.2) and integration of near-field processes important to the crystalline reference case into PFLOTRAN and GDSA Framework includes field and laboratory testing, conceptual model development, and computer code enhancements. Some studies have focused on features and processes that are most important in the crystalline rocks that could host a potential repository. Other studies have focused on features and processes that are important in the engineered barrier system of a potential repository in any host rock environment. Details about the studies that are summarized here can be found in several SFWST reports, especially Wang et al. (2014) and Wang et al. (2018b).

Modeling Studies: A simulation tool (dfnWorks) for fracture network generation and for simulating fluid flow and transport in discrete fracture network has been developed at Los Alamos National Laboratory (Hyman et al. 2015a) (Figure 4-3). This tool, adopted by GDSA Framework, generates interconnected networks of explicitly represented fractures. A network of fractures is stochastically generated using a stochastic model derived from site data. Each fracture plane is represented by a computational mesh and flow equations are solved using this computational mesh. Radionuclide transport can be simulated using the computed flow field and particle tracking techniques (Wang et al. 2017). The discrete fracture networks (DFNs) generated by dfnWorks can be used for theoretical studies and for analysis of field data.

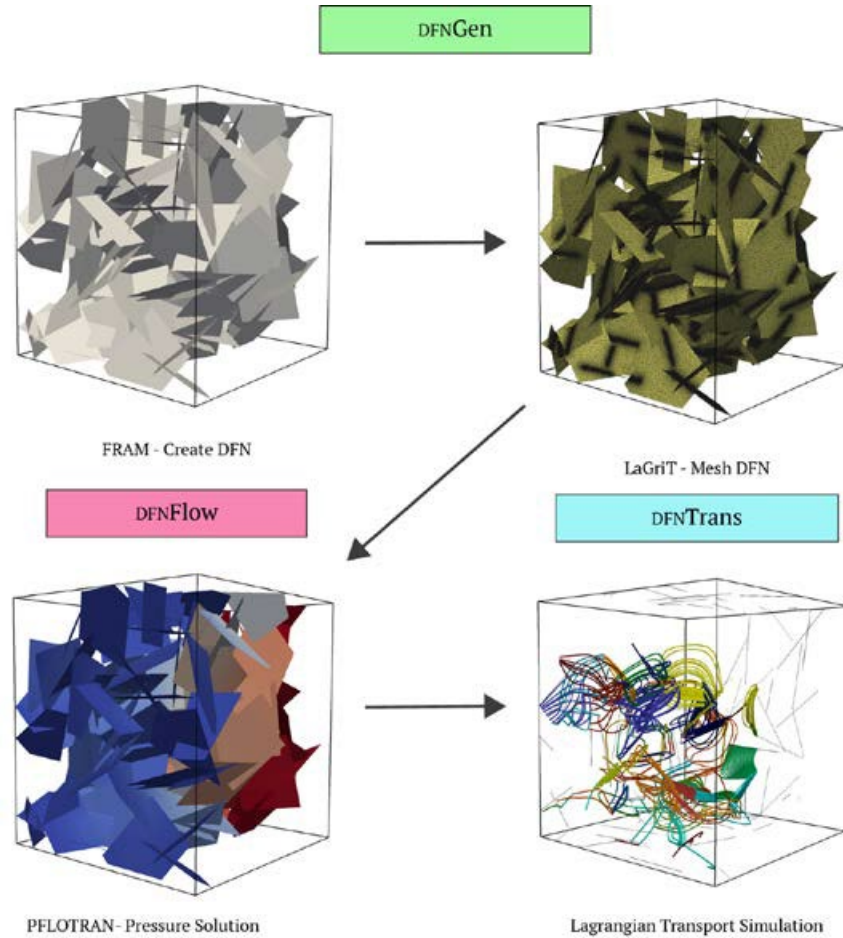


Figure 4-3. dfnWorks Workflow. The input for dfnWorks is a fractured site characterization that provides distributions of fracture orientations, radius, and spatial locations. **DFNGEN:** 1) **FRAM - Create DFN:** Using the fractured site characterization networks are constructed using the feature rejection algorithm for meshing. 2) **LaGriT - Mesh DFN:** The LaGriT meshing toolbox is used to create a conforming Delaunay triangulation of the network. 3) **DFNFlow PFLOTRAN-Compute Pressure Solution:** The steady-state pressure solution in the DFN is obtained using PFLOTRAN. **DFNTRANS:** 4) **Lagrangian Transport Simulation.** A Lagrangian particle tracking method is used to determine pathlines through the network and simulate transport. (Wang et al. 2017)

Using a DFN model, dispersion and mixing within three-dimensional fracture networks were simulated. The result shows that, as hydraulic heterogeneity increased, both longitudinal and traverse dispersion increases; the less mechanical dispersion observed in the structured network appears to be linked to the higher levels of connectivity than in the poorly connected random network; for moderate levels of hydraulic heterogeneity, fracture network structure is the principal control on transport times and dispersion within fracture networks (Wang et al. 2018b).

DFN models have also been used as data analysis tools in conjunction with field experiments. A DFN model was used to simulate the Long Term Sorption Diffusion Experiment (LTDE) conducted at the Aspo URL. The model was used to validate the hypothesis, which states that the LTDE results were strongly influenced by heterogeneity in the micro-structure and the major diffusion of injected tracer into crystalline rock occurs through multiple micro fractures, which are observed in the rock samples. The conclusion from the performed numerical simulations is that microstructure is present in the experimental sample and the

injected tracer is driven by both, diffusion and advection (Wang et al. 2018b). A DFN model was also used to analyze hydrologic and chemical data from a research tunnel at 500-m depth, at the Japan Atomic Energy Agency (JAEA) Mizunami URL. The fracture model was used to generate 10 DFN realizations which were used in flow and transport analyses. Predictions of inflow into an inclined drift for the 10 realizations are reasonable when compared with experimental data. Other inflow predictions were over-predicted and future modeling efforts will attempt to improve the simulation results.

Laboratory Studies: A series of laboratory experiments were conducted on granite slabs with a special geometry to replicate the stresses and rock deformation responses that are expected to occur in larger circular excavations of the excavation damage zone (EDZ) in a mined crystalline repository. The stressed samples were used to assess the changes in rock permeability as an indicator of how these microcracks could affect hydraulic properties of rock in the EDZ. Preliminary modeling studies of flow and transport coupled process and the effects of the rock deformation on hydrological and transport properties were initiated using a rigid body spring network modeling approach. Another aspect of the study investigated the use of flowing fluid electrical conductivity logs to identify borehole inflow zones. The logs were used to study the 2.5 km deep “Collisional Orogeny in the Scandinavian Caledonides” scientific borehole in central Sweden. It appears that the majority of inflow zones, in the borehole, are associated with foliation-parallel fractures.

Bentonite is a major component of the EBS for crystalline repository models. Consequently, it is important to understand the role that bentonite plays in barrier performance. The effect of bentonite heating on U(VI) adsorption was investigated using bentonite samples from the FEBEX *in situ* experiment. The adsorption seems to decrease with heating but the actual mechanism is not clear.

- A new surface complexation model was developed for U(VI) adsorption onto clay materials. The model specifically accounts for the ‘spillover’ of the electrostatic surface potential of basal cation exchange sites on the surface potential of neighboring edge sites.
- Short-term (< 35 days) study of uranium sorption and diffusion in bentonite was conducted. The results indicate a relevance of so-called anion exclusion effects, the full or partial exclusion of anionic U(VI) solution species from clay interlayer spaces.
- Long-term (6 years) study of uranium diffusion in bentonite was conducted. The K_d values obtained from the long-term experiment is one order of magnitude lower than those from batch sorption measurements. The apparent U(VI) diffusion coefficient determined from the long-term experiment is about two orders lower than obtained from short-term experiments, which may be attributed to a reduction of clay porosity.
- A study of Pu sorption and desorption in bentonite was performed. The result suggests the importance of montmorillonite phases in controlling Pu sorption/desorption reactions on FEBEX bentonite.
- An analysis was performed to examine the consistency of macroscopic measurements, electrical double layer (EDL)-based models, and molecular-scale simulations of clay media for adsorption and diffusion of trace levels of calcium (Ca^{2+}), bromide (Br^-), and tritiated water in a loosely compacted, water-saturated Na-montmorillonite.
- The concept of the control of nanopore confinement on radionuclide interaction with compacted clay materials was explored and applied to iodide sorption. The work shows that iodide can potentially interact with interlayer sites of a clay material.

Ongoing studies will continue to explore the role of bentonite in EBS barrier performance.

Batch and column transport experiments were conducted to interrogate the effects of colloid aging on colloid-facilitated transport of ^{137}Cs through crushed analcime columns. The batch experiments were conducted to quantify the effect of colloidal aging on Cs partition coefficients and characterize the colloids injected into the columns. The column experiments were designed to characterize the desorption of Cs from strong sites on colloids. This was accomplished by using a very low concentration of total Cs ($\sim 10^{-10}$ M) so that ^{137}Cs would preferentially sorb to the fewer but stronger sorption sites. The first set of column experiments involved spiking a solution of FEBEX colloids with ^{137}Cs and letting the colloids age for a few hours, whereas the second set of experiments let the colloids age for 1200 hours prior to injecting through the analcime column. For both sets of column experiments, the eluent that passed through a first analcime column was collected and injected into a second fresh analcime column. The sequential injection method allows characterization of the ^{137}Cs bound to the strong sites on the colloid, and the use of a strongly sorbing column material (analcime) promotes desorption from the colloids. Both batch and column experiments demonstrate analcime's ability to outcompete colloids for ^{137}Cs sorption. In the presence of analcime, 12-23% of ^{137}Cs sorbed to the colloids and only 2-6% was in the dissolved phase, with the remainder sorbed to the analcime. Compared to previous batch experiments, the experiments of the present study report a higher K_d value for sorption of Cs onto colloids owing to the lower total Cs concentration and aging effects. Additionally, the present batch experiments demonstrate that the sorption rate onto the strong sorption site of the colloid is very slow compared to the sorption rate onto the weaker colloid sorption site. Furthermore, the desorption rate constant of the strong colloid sorption site had to be lowered for the aged colloid column experiment relative to the un-aged column experiment, suggesting that with a progressively smaller Cs concentration, the remaining Cs is proportionally more sorbed to the stronger sites.

Studies have been conducted to evaluate the potential for radionuclide sequestration by corrosion products to significantly contribute to EBS barrier performance. A small number of binary (RN-mineral) coprecipitation experiments were conducted to test radionuclide (Pu, Am, Np, and U) partitioning. Experiments were designed to quantify coprecipitation partitioning and also examine the effects of aging and the potential iron oxide recrystallization effects associated with the presence of aqueous phase Fe(II). The experimental results reveal that (1) upon aging of a Pu-doped ferrihydrite precursor into more crystalline phase, plutonium associates more strongly with goethite (FeOOH) than hematite (Fe_2O_3); and (2) the timing of Pu addition in the synthetic procedures affects the final form of plutonium associated with goethite. This process could significantly inhibit the release of radionuclides following waste package breach. The process deserves further study and consideration for incorporation into PA models.

FMD Model: The fuel matrix degradation (FMD) model (Figure 4-4) was developed based on fundamental electrochemistry and thermodynamics.

- A recent sensitivity analysis with the FMD model shows that the dissolved H_2 concentration is the dominant environmental variable affecting the UO_2 spent fuel dissolution rate.
- A simplified version of the FMD model was implemented in the GDSA model (no steel corrosion).
- A new glass degradation model was developed by considering the nonlinear dynamics of involved glass dissolution processes.

The FMD model has been directly coupled to PFLOTRAN. Surrogates of this model have also been developed and are being coupled with PFLOTRAN so that the effects of this model can be propagated in full-scale PA calculations (Section 2.3.1.6 and Appendix A).

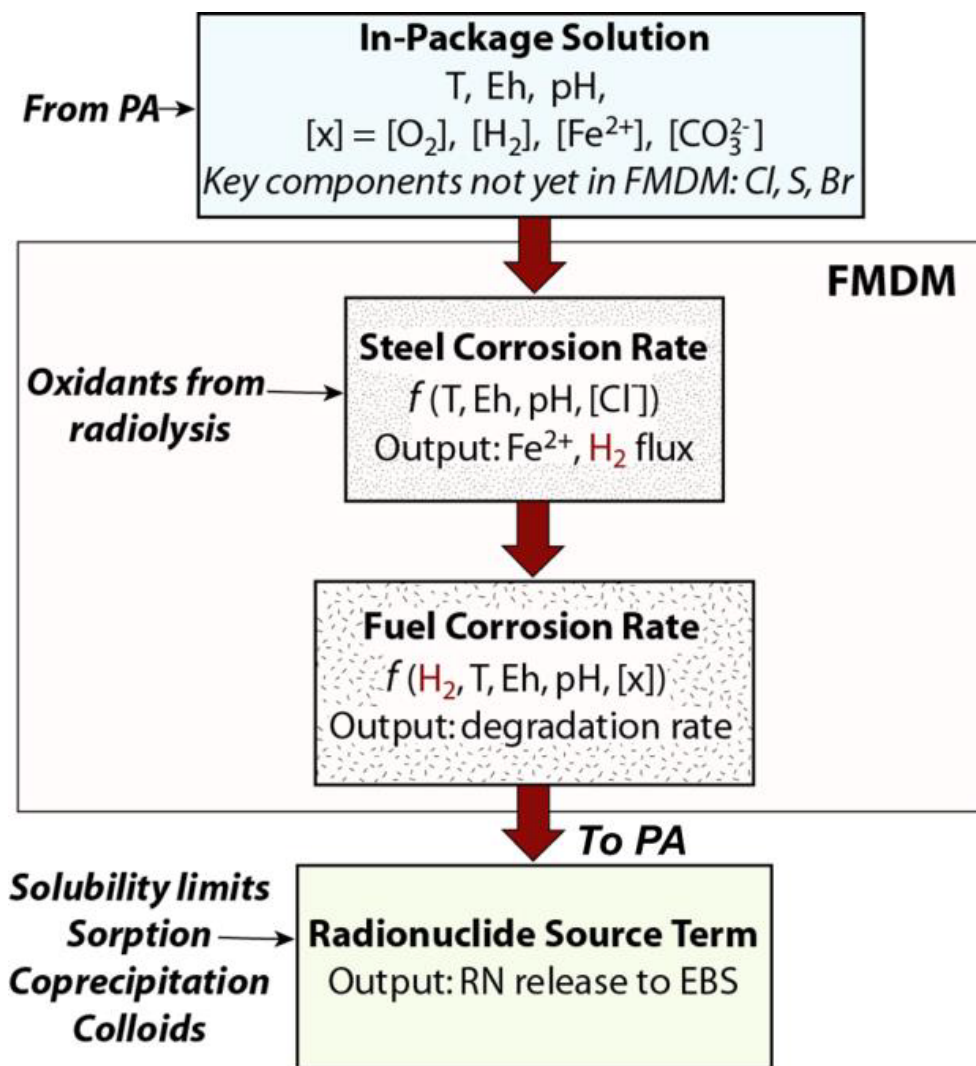


Figure 4-4. Summary figure showing the context of the FMDM within the source term calculation information flow (adapted from Jerden et al. 2017). (Wang et al. 2018b)

Future Crystalline R&D Activities: Future crystalline R&D activities include:

- Continue to focus on two key topics related to deep geologic disposal of spent fuel in crystalline rocks: better characterization and understanding of fractured media and fluid flow and transport in such media and designing effective engineered barrier systems (EBS) for waste isolation.
- Help the GDSA team to develop a PA model and provide the parameter feeds to the model.
- Synthesize technical results obtained in prior years in a few selected areas including the stability of bentonite and the modeling approach for fluid flow and transport in fractured geologic media.
- Move towards model demonstrations and applications using actual field data. For process model development, an emphasis will be placed on integration with GDSA Framework.
- Fully leverage international collaborations, especially with the URL in Sweden and DECOVALEX.

4.3 Salt R&D Activities

Salt Disposal R&D Work conducted to support the development of the salt reference case (Section 3.2.3) and integration of near-field processes important to the salt reference case into GDSA Framework includes field and laboratory testing, conceptual model development, and computer code enhancements. Some studies have focused on features and processes that are most important in bedded salt that could host a potential repository. Other studies have focused on features and processes important in the evolution of the repository environment, especially the mechanical behavior of the salt. Details about the studies that are summarized here can be found in several SFWST reports, especially Kuhlman et al. (2018) and Kuhlman et al. (2017).

Laboratory Studies: Laboratory studies have been conducted to address a variety of topics (Kuhlman 2014; Kuhlman et al. 2017). Space restrictions do not allow a summary of all of these studies. A few of them are summarized below.

An international consensus has emerged on the use of borosilicate glass as a matrix for immobilizing HLW such as the liquid filling tanks at Hanford and Savannah River. Extensive studies have been carried out over the years investigating the kinetics of borosilicate glass dissolution. However, relatively few of these studies have included brine solutions such as those found in salt formations. Consequently, studies were conducted to evaluate how sodium and magnesium chloride bearing brines impact dissolution rates for borosilicate glass. Preliminary results suggest that addition of even low concentrations of NaCl to solution enhances the dissolution rate of borosilicate glass. This behavior is similar to that observed for the SiO₂ polymorphs (β -quartz and amorphous silica). The similarity in behavior argues that the principal mechanism by which multicomponent borosilicate glass dissolves is by rupture of the Si—O bond. At higher concentrations of NaCl the rates decrease, due to a decrease in the activity of water (Kuhlman et al. 2017).

The partitioning of fission products, such as Cs, Sr, and I, into salt phases could be an important process in a future scenario where heat producing waste is emplaced in a salt repository. In such a scenario the heat produced by the waste could cause heating of the near field that leads to intrusion of groundwater into the repository.

Studies were conducted and preliminary results indicate that if aqueous solutions intruded a mined salt repository and dissolved waste containing the fission products ¹³⁵Cs, ¹³⁷Cs, ⁹⁰Sr and ¹²⁹I, precipitation of typical salt phases could reduce the mobility of these fission products. Specifically, precipitation of gypsum would harbor large amounts of ⁹⁰Sr while langbeinite and leonite would sequester moderate amounts of ¹³⁵Cs and ¹³⁷Cs at higher temperatures (>70 °C). At all temperatures studied, carnallite is a major host for ¹³⁵Cs and ¹³⁷Cs and precipitation of this phase will greatly impact the concentration of Cs in solution. None of the phases that we studied selectively sequestered iodine. A more complete set of data could be used to consider the possibility that “natural attenuation” processes will remove much of the radionuclide load and limit the extent to which mass transport can occur. Such attenuation processes could be incorporated into safety assessments for repository systems.

Caporuscio et al. (2013) and Caporuscio et al. (2014) performed laboratory characterization studies related to brine content and movement in bedded geologic salt. Using thermogravimetric analysis and X-ray diffraction, they characterized brine and mineral content of clay and bedded salt samples from WIPP. Microscope-scale laboratory experiments were conducted to monitor migration of brine inclusions in single (Caporuscio et al. 2013) and multiple (Caporuscio et al. 2014) salt crystals on a heated microscope stage. Scanning electron microscopy was used to image salt crystals after brine inclusions had migrated through them under a thermal gradient, illustrating a network of small-scale brine transport tubes. Caporuscio et al. (2014) showed nuclear magnetic resonance to be a viable method for characterizing brine distribution in salt, distinguishing relative amounts of mineral-bound water, water in clays, and free water (sum of intergranular and intragranular water) (Kuhlman 2014).

Laboratory studies have also been conducted to characterize the compositions of brines at WIPP. Kuhlman et al. (2018) compile existing data and identify compositional groupings and trends (Figure 4-5). They also present preliminary results of ongoing laboratory experimental work and EQ3/6 brine composition modeling as part of the Salt R&D heater test. This laboratory effort is developing and improving analytical methods for analyzing brines and solids collected before, during and after the upcoming heater test. The modeling effort is developing comprehension regarding brine composition and evolution and assembling the modeling tools and approaches needed to interpret the brine and precipitant composition data that will be collected during the heater test.

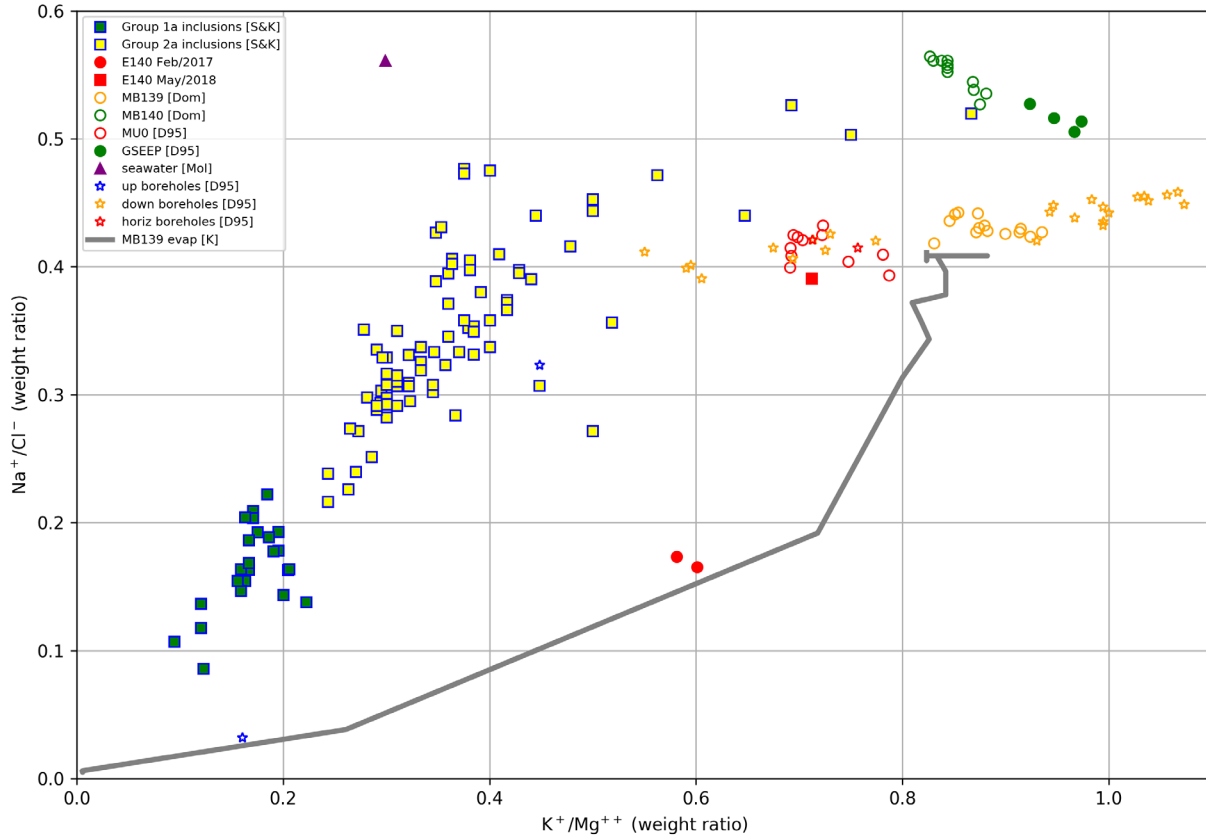


Figure 4-5. Mass ratios of WIPP brines. Blue ellipse: WIPP fluid inclusions; yellow ellipse: near MB-139; green ellipse: near MB-140; red dashed ellipse: E-140 boreholes. (Kuhlman et al. 2018, Figure 7)

Lewis and Holness (1996) state the connectivity of the network of pores in halite (NaCl-water brine system) can be related to the dihedral angle, which is the angle where two salt grains meet with a compatible brine. This connectivity defines the permeability in the salt, as the halite crystals are impermeable themselves. Microscopic analyses of salt core samples collected before and after heating in the upcoming WIPP heater test could be analyzed to estimate the dihedral angle and quantify any changes that might occur to it due to heating or changes in pressure. Of course, the WIPP brines will have a more complicated composition than the pure NaCl-water system. Kuhlman et al. (2018) investigate the impacts of brines that have ions that are not in halite (NaCl) crystals. Several different lines of investigation illustrate that the interfacial tension would be increased compared to pure NaCl solutions, due to the overall increase in ionic strength. An increase in the interfacial tension necessarily increases the dihedral angle. Increasing the dihedral angle makes the pore network less connected (i.e., lower permeability) at a given pressure and temperature.

Increasing the ionic strength of the brine beyond that of a pure NaCl brine equilibrated with the halite crystals and adding divalent cationic constituents tends to make the pore network less connected, and the salt less permeable.

Field Studies: The recent focus of the DOE-NE Salt R&D field testing program has been on brine availability in repository excavations in salt (Kuhlman et al. 2017). Availability of brine includes the characterization of how much brine of each type is present in the evaporite formation, and the conditions under which this brine moves through excavation damage to an opening (i.e., a borehole or drift). The movement of brine through salt to excavations is controlled by the interaction of the excavation, the DRZ, and the drift-scale stratigraphy of the host rock. Geologic salt is impermeable without the overprint of fracturing and damage accumulation associated with excavations or the heterogeneity of more permeable and more brittle nonsalt units (e.g., clay, anhydrite, polyhalite, carnallite) in evaporite formations. Migration of brine in a two-phase system is non-linear and depends on the state of the system, too (e.g., liquid and gas pressure, temperature, stress, liquid and brine saturation, and brine composition). Availability of brine is an important part of the safety case because it controls waste package corrosion and transport of radionuclides and can provide back-pressure to slow down creep closure of excavations.

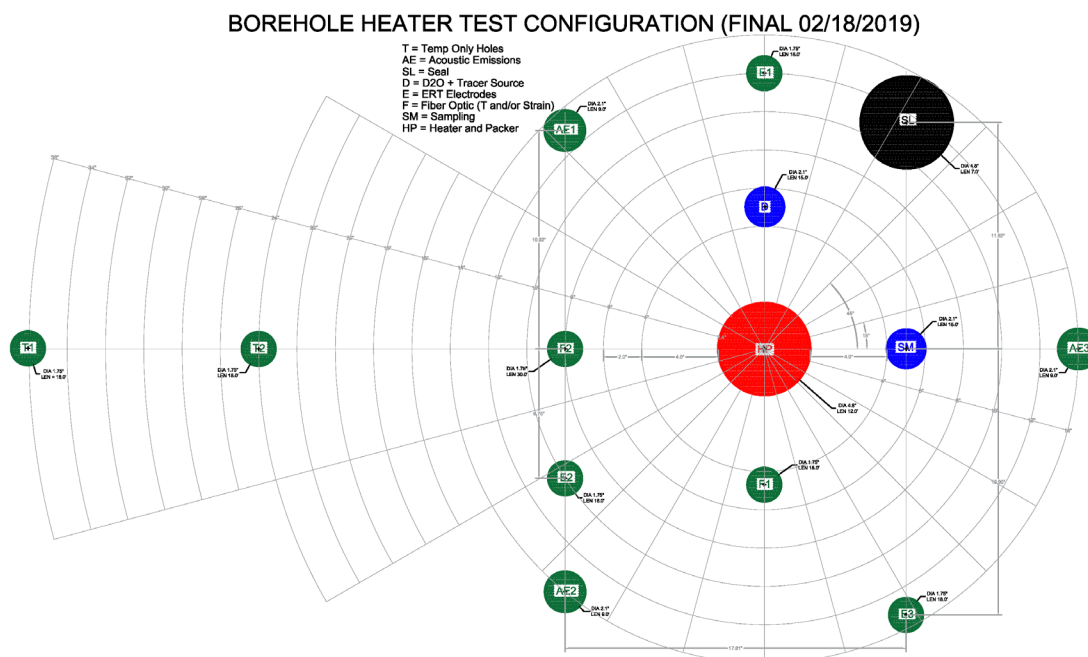


Figure 4-6. Schematic drift view of satellite observation boreholes and central borehole (Mills et al. 2019, Figure 2).

The BATS (Brine Availability Test in Salt) test at WIPP comprises two initial horizontal borehole heater tests. One test array will be heated (heater in central HP borehole, Figure 4-6) and the other pattern will be similar, but unheated. Each array will be configured with instruments in the central HP borehole and the

surrounding satellite boreholes. Temperature distribution, strain, and brine movement will be monitored with thermocouples, fiber-optic distributed strain and temperature sensing, acoustic emissions monitoring, ultrasonic travel-time tomography, electrical resistivity tomography, introduced liquid and gas phase tracers, and sampling of liquid and vapor phases for natural and introduced tracers (Mills et al. 2019).

The borehole heater test will sample brine produced from the salt under both unheated and heated conditions. Water comes from three primary sources from within the salt:

- Brine between grains in pores (intergranular brine);
- Fluid inclusions (intragranular brine); and
- Hydrous minerals (e.g., clay, gypsum, epsomite or polyhalite).

One of the objectives of the heater test is to attempt to discern the contributions from these brine sources through time at different temperatures. The three brine sources produce water under different conditions and due to different driving forces, illustrated as follows:

- Intergranular brine exists in a connected pore network near excavations and can move due to a pressure gradient. Water can evaporate into mine ventilation air and move in the vapor phase. Both brine and vapor can move in response to applied temperature (i.e., pressure increase from thermal expansion).
- Fluid inclusions cannot move under fluid pressure gradients and typically only move under temperature gradients (away or towards the heat source depending on their gas content). Fluid inclusions will be liberated at the decrepitation point (~250 °C). When fluid inclusions move to grain boundaries or are liberated through decrepitation, they can then flow to the borehole through the intergranular pore network (see previous bullet).
- Water of hydration cannot move under pressure gradients and is only liberated when minerals are heated above their dehydration temperature. This water is given off as steam, which can move through the intergranular porosity as vapor. Depending on the salt temperature, the vapor can condense and dissolve salt to create a brine that can flow to the borehole through the intergranular pore network (see first bullet).

Fluid inclusions and hydrous minerals can act as spatially distributed sources for additional intergranular brine, depending on the conditions. Given the complex spatial and temporal response of these different brine sources to temperature, temperature gradient, mine ventilation humidity, and fluid pressure, the goal of this work is to discern whether these three water sources can be differentiated compositionally.

A full discussion of all pre- and post-test analyses planned for BATS can be found in Mills et al. (2019).

Project WEIMOS: Joint Project WEIMOS is a collaboration between U.S. and German salt researchers. WEIMOS stands for *Weiterentwicklung und Qualifizierung der gebergmechanischen Modellierung für die HAW-Endlagerung im Steinsalz* (Further Development and Qualification of the Rock Mechanical Modeling for the Final HLW Disposal in Rock Salt). The participants calibrate their salt constitutive models against simple laboratory tests and benchmark the models against more complex laboratory or underground experiments. This process helps identify deficiencies in both the constitutive model and the methods used to simulate the complex experiments.

An example of laboratory testing involves characterizing the shear behavior of stratigraphic interfaces. The interfaces between stratigraphic layers are known to slide relative to one another as waste emplacement drifts close, and the sliding is thought to have first-order effects on roof collapse, room closure, and interface permeability to fluid flow. A study is beginning to test salt cores (with interfaces) similar to those found at the WIPP. Core drilling sites have been selected with salt/clay/salt, anhydrite/salt, and polyhalite/salt

interfaces and direct shear testing on 4-inch diameter specimens should begin shortly. Another example of laboratory testing involves microscopic studies to evaluate the creep mechanism of salt at low deviatoric stresses.

Monitoring of the closure of Room D at WIPP is an example of data from an underground experiment that was used to improve a constitutive model. Analysis of the data identified shortcomings of the Munson-Dawson (MD) constitutive model for the thermomechanical behavior of salt.

- The MD model failed to capture the creep behavior of salt at low deviatoric stresses, so a new steady-state creep term and a new transient creep term were added to the model.
- The MD model originally used von Mises equivalent stress, but the equivalent stress measure was changed to Tresca in order to better match experimental data.
- The numerical formulations of the MD model in Sierra/Solid Mechanics were improved to make the analysis more robust.

The new MD model implementation, including the changes discussed above, was verified against two analytic solutions and by comparing the model formulations in a room closure simulation (Kuhlman et al. 2017).

Future Salt R&D Activities: The top priority of the Salt R&D program in the near term is to implement and complete the BATS underground test. This test is expected to produce a wealth of new information useful to GDSA PA. The analyses of these new data will be a significant effort, but this will not be the only work that is undertaken.

Integration of new information, including new information from BATS, will be a second priority for the Salt R&D program. The GDSA integration focus includes uncertainty quantification with process models and strategies for both “tight” and “loose” coupling of processes with PFLOTRAN. Additional processes or behaviors that could be integrated into PA/GDSA modeling include (Kuhlman et al. 2018):

- Pitzer or specific ion interaction theory model for activity coefficients at high ionic strength allowing process models to consider full chemistry (i.e., all observed ionic species) in evaporites. This would be directly implemented in PFLOTRAN; it is currently done either with EQ3/6 or TOUGH-REACT.
- Consider physical thermal-hydrologic-chemical (THC) effects of dense, saline brines (e.g., impacts of salinity on vapor pressure, capillarity changes during significant porosity changes, and non-linear thermal conductivity) into GDSA models. This would be directly implemented in PFLOTRAN; some of these capabilities are currently implemented in FEHM.
- Consider high-temperature environments above brine boiling point (e.g., around hot waste canisters with dry-out and heat pipes) in GDSA models while treating full chemistry. This would be directly implemented in PFLOTRAN; some of these capabilities are currently implemented in TOUGH-REACT and FEHM.
- Incorporation of thermal-hydrological-mechanical (THM) coupled processes or THM predictions into GDSA models. It is well known that permeability and porosity in salt is related to excavation-induced damage. Time-dependent hydrologic properties should be explicitly linked to damage evolution in an appropriate geomechanical model. This either would involve a significant effort to implement these features into PFLOTRAN (i.e., large-deformation capabilities and viscoplastic constitutive models would be needed), or a loose coupling of the output of an existing THM code like TOUGH-FLAC into the initial conditions or parameters of PFLOTRAN.

- Validation of existing process models in GDSA, with implementation of new process models as needed (some of these processes given in previous bullets), to explain field data collected from borehole heater tests.

These are mostly GDSA modeling integration efforts, that may also be useful for interpreting aspects of the data collected during the BATS field test. The field test data will provide a physically relevant validation data set for checking if implemented processes are correct, and to show the processes are physically important under relevant conditions. Numerical model prediction of field observations is a complex and iterative process, requiring close work between those collecting the data and those developing the numerical models. Uncertainty quantification and parameter estimation methods from GDSA can be applied to the process of matching validation observations from the field tests.

4.4 International R&D Activities

The SFWST Campaign has ongoing collaborations with international groups that have supported several aspects of the SFWST research program. This work is valuable to the development of GDSA Framework and development of the reference cases because it provides field data and helps keep process modelers and PA modelers updated with new international approaches to modeling. Details of the collaborations and the research results are documented in annual reports, i.e., Birkholzer et al. (2018) and references therein.

Birkholzer et al. (2018) identify several key research questions that are being addressed by the international program.

- **Near-Field Perturbation:** How important is the near-field damage to a host rock (such as clay and salt) due to initial mechanical and thermal perturbation, and how effective is healing or sealing of the damage zone in the long term? How are reliable existing constitutive models for the deformation of elastoplastic and plastic geomaterials as affected by temperature and water-content changes?
- **Engineered Barrier Integrity:** What is the long-term stability and retention capability of backfills and seals? Can bentonite mixtures be developed that allow for gas-pressure release while maintaining sealing properties for water? Can bentonite be eroded when in contact with water from flowing fractures? How relevant are interactions between engineered and natural barrier materials, such as metal-bentonite-cement interactions?
- **Radionuclide Transport:** Can the radionuclide transport in fractured rock be predicted with confidence? What is the potential for enhanced transport with colloids? How can the diffusive transport processes in nanopore materials, such as compacted clays and bentonites, best be described? What is the effect of high temperature on the swelling and sorption characteristics of clays (i.e., considering the heat load from dual-purpose canisters)?
- **Demonstration of Integrated System Behavior:** Can the behavior of an entire repository system, including all engineered and natural barriers and their interaction, be measured and demonstrated? Are the planned construction/emplacement methods feasible?

Ongoing in-situ testing in URLs is focused on addressing these questions. The spectrum of tests and analyses is broad and it is difficult to summarize in a brief format. The testing is being conducted in numerous facilities spread across Europe and east Asia. The testing also addresses a wide range of technical topics. It is impossible, in a brief discussion, to specifically identify all of the important efforts that are underway. The following discussion uses broad technical topics as a framework for discussing ongoing, and recently completed, work in the International program. The discussion is very high level with references for those interested in the details.

FE Heater Test Mont Terri Switzerland: The thermal perturbation that would be caused by a nuclear waste repository is being addressed from several different perspectives. The Full-scale Emplacement

Experiment (FE Heater Test) at the Mont Terri URL in Switzerland (Figure 4-7) is a long-term heater test in argillaceous claystone (Opalinus Clay) that is designed to evaluate the impacts of waste heat on EBS materials and argillaceous host rock. Pre-test activities included predictive THM modeling to support design and implementation of the test as well as to provide testable predictions of test results. The heaters were turned on February 2015 and are expected to continue for 15-20 years. Thermal effects to be evaluated include temperature and relative humidity evolution of the bentonite buffer and thermal pressurization of the argillaceous host rock. Initial results, based on ~3.5 years of heating, are encouraging.

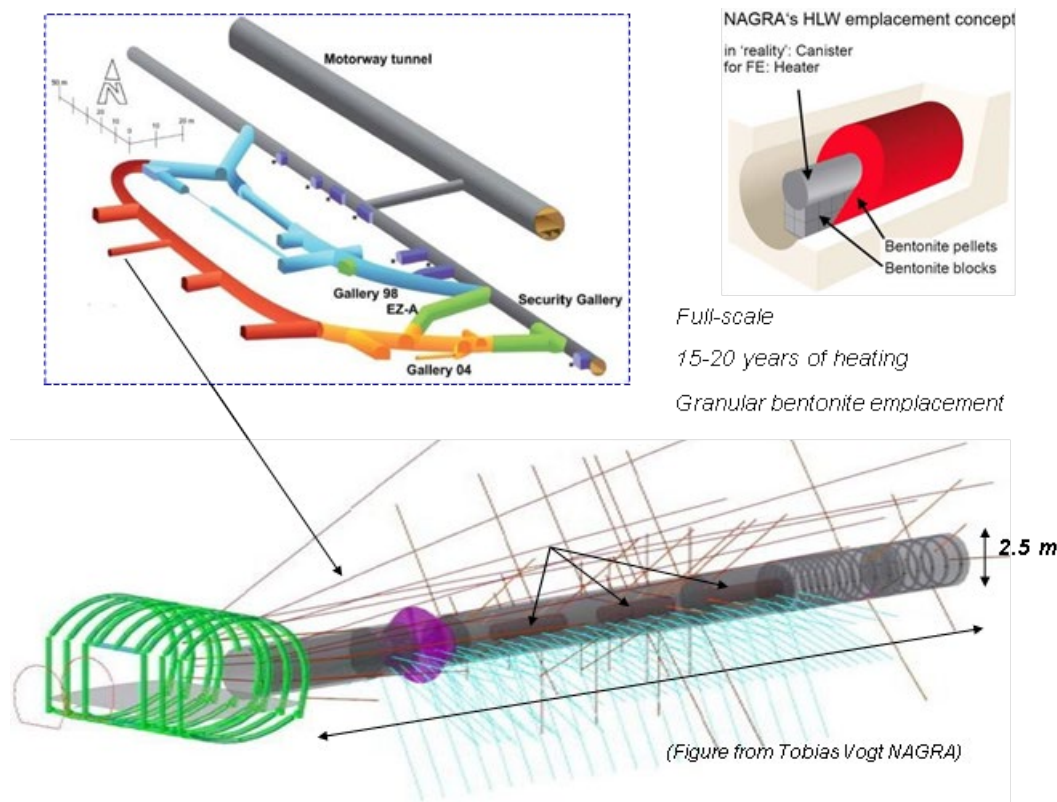


Figure 4-7. FE Heater Test at Mont Terri URL: experiment setup and borehole layout (from Zheng et al. 2015). (Birkholzer et al. 2018, Figure 3.1-5)

Meuse/Haute-Marne URL near Bure France: Heater tests at the Meuse/Haute-Marne URL near Bure in France are also evaluating thermal effects on argillaceous host rock, i.e. Callovo-Oxfordian claystone. These tests involve THM modeling with a specific focus on upscaling THM modeling from small size experiments (cubic meters) to emplacement cells (ten cubic meters) and up to the scale of a waste repository (cubic kilometers). An initial small-scale heater test, the TED experiment, started in 2010 and ended in 2013. The TED experiment involved three heaters in three parallel boreholes. A full-scale heater test, the ACL experiment, is currently underway. The ACL experiment is based on the French conceptual design and is a single full-scale emplacement micro-tunnel. Comparisons between model predictions and measured data have produced good results so far and are ongoing. The final step in this analysis will predictions and testing at the repository scale with several high-level waste cells.

FEBEX Grimsel Switzerland: The FEBEX, Full-scale EBS, heater test at the Grimsel URL in Switzerland evaluated the thermal evolution and resaturation of bentonite backfill surrounding a heated waste package (Figure 4-8) during 18 years of heating. Subsequently, the FEBEX Dismantling Project (FEBEX-DP) is focusing on studying the impacts of 18 years of heating and resaturation on EBS components, including

bentonite, metals, instruments, etc. Primary data/objectives of the FEBEX-DP are (Gaus and Kober 2014; NAGRA 2014):

- Key physical properties (density, water content) of the bentonite and distribution
- Corrosion on instruments and coupons under evolving redox conditions and saturation states
- Mineralogical interactions at interfaces and potential impacts on porosity
- Integration of monitoring results and modeling

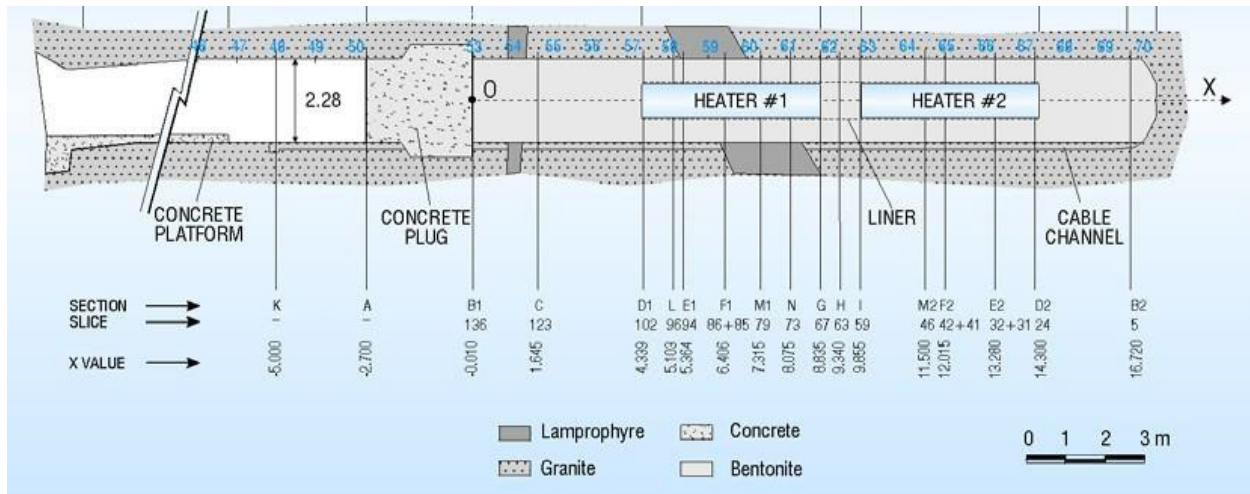


Figure 4-8. Schematic cross section of the FEBEX Test at Grimsel Test Site (NAGRA 2014). (Birkholzer et al. 2018, Figure 3.3-6)

GREET Mizunami Japan: GREET (Groundwater REcovery Experiment in Tunnel) is a full-scale drift closure experiment conducted at the Mizunami URL (crystalline rock) in Japan. The project examines hydro-mechanical-chemical-biological processes during natural groundwater recovery into a sealed gallery, or drift (Figure 4-9). The goals of the experiment are to (Birkholzer et al. 2018):

- Understand the water recovery processes and mechanisms of the geological environment during facility closure
- Verify coupled hydrological-mechanical-chemical and -biological simulation methods for modeling these processes
- Develop monitoring techniques for the facility closure phase and appropriate closure methods taking recovery processes into account.

The experiment is currently in the recovery stage and monitoring will continue after steady-state conditions are established. The crystalline group is supporting this effort by developing DFN realizations and implementing them in flow and transport models using PFLTRAN and DAKOTA for statistical analyses (Wang et al. 2018b).

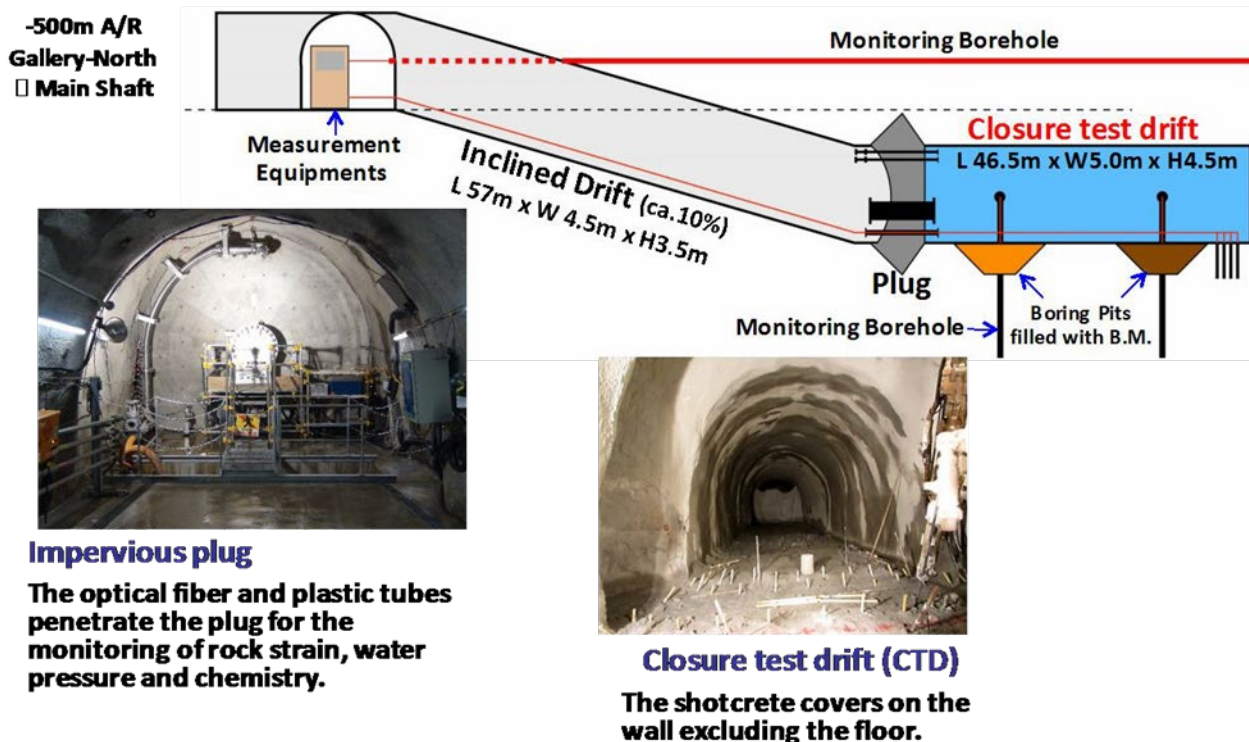


Figure 4-9. Schematic showing GREET tunnel design in a cross-section and photos taken during construction (Iwatsuki 2016). (Birkholzer et al. 2018, Figure 3.2-5)

U.S./German Collaboration on Salt: Thermal-mechanical coupled processes are especially important in a salt repository because the excavated emplacement drifts will close over time, and thermal effects will accelerate this process. Joint projects between Germany and the U. S., i.e. KOSINA and WEIMOS, have addressed important issues related to thermal-mechanical processes. KOSINA was based on thermomechanical calculations and resulted in new repository designs. KOSINA stands for Konzeptentwicklung für ein generisches Endlager für wärmeentwickelnde Abfälle in flach lagernden Salzschichten in Deutschland sowie Entwicklung und Überprüfung eines Sicherheits- und Nachweiskonzeptes (Concept development for a generic final repository for heat-generating wastes in flat-bedded salt layers in Germany as well as development and examination of a safety and verification concept). WEIMOS is ongoing and is based on analysis of in-situ data from the WIPP repository in New Mexico. These analyses are leading to significant improvements in constitutive model for thermomechanical behavior in salt (Kuhlman et al. 2017).

The BenVaSim (Benchmarking for the verification and validation of TH²M simulators) Initiative is another U.S./German collaboration. The initiative is focused on benchmarking and validation of computer codes used for the analysis of coupled processes associated with nuclear waste disposal in salt. The program involves the analysis of benchmark problems of increasing complexity, i.e. 1D, 2D, and 3D problems. The final stage will include in-situ and laboratory tests for code validation.

Another interesting problem that is being investigated through international collaborations is the migration of brine inclusions in salt. Brine inclusion migration could impact the performance of rock salt, which otherwise has an extremely low permeability. It is important to characterize the distribution, volume, and interconnectivity of such fluid inclusions. A model for brine inclusion migration has been developed that can predict (Wang et al. 2018b):

- A linear increase in migration velocity with increasing thermal gradient

- A nonlinear increase in migration velocity with the inclusion size
- An overall acceleration in fluid migration with temperature
- The dependence of migration velocity on mechanical loadings.

A bifurcation point in vapor/liquid volume ratio for the direction of fluid migration has been derived.

Gas Migration Impacts: Modeling and laboratory experiments are being employed to improve our understanding of processes and mechanisms governing the advective movement of gas in compact bentonite and clay-based materials, and its impact on performance assessment.

Four primary phenomenological concepts describing gas flow have been identified:

- Gas movement by diffusion and/or solution within interstitial fluids along prevailing hydraulic gradients
- Gas flow in porous media, commonly referred to as viscocapillary (or two-phase) flow
- Gas flow along localized dilatant pathways, which may or may not interact with the continuum stress field
- Fracturing of the rock similar to that performed during hydrocarbon stimulation tests (Harrington 2016)

A series of laboratory experiments have been completed that demonstrate the complexity of gas migration in clay rich low permeability materials. Modeling approaches are being developed to help unravel and understand these complexities.

International Opportunities: There are several benefits of DOE engagement in these international collaborations: (1) they provide access to a deep knowledge base with regards to alternative repository environments developed over decades, (2) provide access to experimental data from many past, ongoing, and future in situ tests conducted in several URLs in different host rocks, (3) allow for active research participation in international groups, which conduct, analyze, and model performance-relevant processes, and (4) provide the opportunity to conduct SFWD experiments in international URLs. Promising opportunities exist for further expansion of the international program, for example the new HotBENT Project, a full-scale high-temperature heater experiment to be conducted at the Grimsel Test Site in Switzerland.

4.5 Engineered Barrier System

The goal of the EBS R&D program is to improve our understanding of, and ability to simulate how environmental conditions would evolve in a repository, particularly in response to the increased temperatures caused by the emplacement of SNF. EBS R&D activities range from long-term, large scale simulations of repository performance to detailed laboratory scale experimental studies of mineralogical and geochemical changes. Matteo et al. (2018) describes recent progress in EBS R&D and summarizes future priorities and goals for the program. The discussions are organized in eight distinct activities, which are investigating various aspects of EBS performance:

- THMC Modeling Investigation of the Impact of High Temperature Limits in Clay-Based Buffer materials
- Coupled THMC Modeling of the Evolution of Bentonite in FEBEX-DP
- Comparative Analysis of Modeling Approaches to Support the HOTBENT Field Test

- Code Comparison of Semi-Analytical Thermal Analysis Software
- Thermal Analysis for Disposal of Spent Nuclear Fuel in Alluvium Host Rock Using the Semi-Analytical Method
- Thermal Hydrology Modeling for Disposal of Spent Nuclear Fuel in Crystalline Rock
- Experimental Investigations of Bentonite and Other Clay-Based Buffer Materials
- High Temperature Experiments of EBS Component Interactions

THMC Modeling Investigation of the Impact of High Temperature Limits in Clay-Based Buffer Materials: There is growing interest in the international EBS community to investigate the feasibility of raising the limit of the waste package surface temperature above 100 °C. For EBS designs in granite and argillite, which rely significantly on bentonite buffer and/or backfill, raising the thermal limit could have a significant impact on repository operations (e.g., surface storage time), the repository design concept, and/or site selection. A higher temperature limit could, in theory, allow waste packages to be in placed after a shorter surface storage time-period, which may impact operational workflows, and would also allow waste packages and drifts to be spaced more closely, thus decreasing the overall size of the repository footprint. A smaller footprint, in turn, may impact the site selection process, as disposal formation thickness and especially areal extent are critical parameters in site selection.

A coupled THMC model facilitates evaluating the direct impact of chemical changes on the mechanical behavior. In previous THMC model simulations (e.g., Zheng et al. 2015), the coupling between chemical and mechanical processes assumed an extended linear swelling model, which is simple and its key parameters were relatively easy to calibrate. However, the model does not accurately describe the transient state of swelling, neglects the history of mechanical change, and is unable to account for the impact of cation exchange on the swelling. In FY 2017, the THMC models were improved based on the double structure Barcelona Expansive Model (BExM) (Sanchez et al. 2005) to link the mechanical process with chemistry, and to incorporate simultaneously the effects of exchangeable cations, the ionic strength of pore solution and the abundance of swelling clay on the swelling stress of bentonite. In FY 2018, the parameters of BExM were recalibrated for FEBEX bentonite to account for the effects of chemical reactions and to align with the reference state of in-situ bentonite.

The improved THMC model, and calibrated parameters, was used to simulate high (200 °C) and low (100 °C) temperature disposal options in clay. The analyses indicate that dissolution of smectite leads to a decrease in the volume fraction of smectite, which, in turn, decreases the stress. In contrast to the 2017 model, the new model predicts the reduction of exchangeable sodium in the interlayer, which also causes a decrease in stress. Infiltration of higher salinity water from the surrounding clay formation to the EBS bentonite leads to the increase in osmotic suction and subsequently lowers the stress. The combination of these effects reduces both the total stress and the effective/net stress in the bentonite buffer in the “high T” cases.

The revised THMC model, using BExM, has significantly improved our understanding of the coupled processes contributing to chemical and mechanical alteration in EBS bentonite and natural system argillite formations (Matteo et al, 2018). This knowledge will help better address questions regarding the thermal limit of EBS bentonite in the clay repository. Nevertheless, our ability to model coupled THMC processes causing the alteration of bentonite and clay formations needs further improvement.

Future work will include investigation of chemical controls on montmorillonite structure and swelling pressure using TOUGHREACT-FLAC (incorporating BExM) to derive an improved constitutive model to describe variations of the swelling pressure in compacted clay barriers. The importance of bentonite alteration and its impact on mechanical behavior needs to be integrated in the GDSA model to assess its relevance to the safety of a repository. A variety of swelling models will be evaluated using the parallel

THMC simulator TREATMECH. A reduced order model will be developed based on the simulations that can be incorporated into the GDSA performance assessment model.

Coupled THMC Modeling of the Evolution of Bentonite in FEBEX-DP: The FEBEX in situ test, which lasted for more than 18 years, generated extremely valuable data for validating the coupled THMC model and improving our understanding of the processes affecting the temporal and spatial evolution of the bentonite barrier over the course of long-term heating and hydration. Figure 4-2 presents a schematic drawing of the test configuration. In the FEBEX-DP project, Heater #2 was dismantled and extensive THMC characterization was conducted. The goal of FEBEX-DP is to validate THMC models and further enhance our understanding of coupled processes in bentonite.

Since FY 2015, the model for the FEBEX in situ test has evolved from a TH model to the current THMC model, and particularly to understand the lower-than-expected relative humidity data near the heater. Numerous approaches have been tested, including the Non-Darcian flow model, investigation of swelling via the Barcelona Expansive Clay model, linear swelling model, state surface model, and various constitutive relationships for saturated permeability in bentonite as functions of either stress or dry density. After extensive calibration, the THMC models developed (Zheng et al. 2016) reasonably simulated the measured temporal evolution of temperature, relative humidity and stress in the bentonite barrier and the measured spatial distribution of water content and dry density at 5.3 years (when Heater #1 was dismantled), and at 18.3 years (when Heater #2 was dismantled). However, the model failed to explain the spatial profile of chloride concentration at 5.3 years. In FY 2017, the THMC model was further revised by adding thermal osmosis and using a revised permeability-dry density relationship, and eventually was able to reproduce the THM data and the spatial profile of chloride concentration at 5.3 years. In FY 2018, after obtaining the geochemical data, including ion concentration in pore water of bentonite and granite, mineral phases and element contents in solid phase of bentonite, and detailed characterization of montmorillonite, the modeling efforts focused on the interpretation of geochemical data. The major findings from the current modeling work (Matteo et al. 2018) are as follows:

- Chemical data is important. Models calibrated with more types of data are more reliable.
- The key coupling processes required to match the THM data and concentration of conservative species (e.g., chloride) include vapor diffusion, porosity change due to swelling, permeability change as a function of dry density (and porosity), and thermal osmosis.
- Because geochemical data in solid phases were either too scattered to constrain the model or incomparable with model outputs, the current model predominantly relied on the ion concentration in the aqueous phase to understand the geochemical change in the bentonite.
- The model matched the spatial profiles of most chemical species in pore water, but discrepancies still exist.
- Based on the match between model and data, an increase in sulfur was caused by the formation of anhydrite, and the higher content of calcium in the solid phase resulted from calcite precipitation. However, the model offered no insight into the increase in measured sodium content in the solid phase from the heater toward the granite and the decrease of magnesium content in the solid phase from the heater toward the granite.
- Measured mass fractions of illite in the illite/smectite mixed layer varied depending on the laboratory samples, showed no clear spatial trend, and were indistinguishable from the reference bentonite. The model results suggested illite precipitation and montmorillonite dissolution near the heater, which is neither proved nor disapproved by the data.

Future work will focus on the evolution of redox conditions, interaction between steel corrosion products and bentonite, and geochemical changes at the interface between concrete and bentonite. Specifically, the model will tackle the following problems:

- Modeling of redox conditions in the bentonite barrier is critical for understanding canister corrosion and waste form degradation but is a significant challenge because of the difficulty simulating redox-sensitive species such as $\text{Fe}^{+2}/\text{Fe}^{+3}$ transformation. Obtaining reliable concentrations of these species in the initial pore water before or after the FEBEX test is difficult. A synthesis of measured gas concentrations, biological data and redox sensitive minerals and aqueous species may help understand the evolution of redox conditions.
- The model of bentonite-canister interaction, causing the corrosion of the canister and interaction of corrosion products with bentonite will be improved, and the model will be tested against measured mineralogical phase changes in the bentonite and the canister.
- Bentonite-concrete interactions will be modeled to understand mineralogical changes at the interface between concrete and bentonite.

Comparative Analysis of Modeling Approaches to Support the HOTBENT Field Test: The HotBENT Field Test has been proposed as a successor to the long-term FEBEX “In-Situ” test at Grimsel to evaluate the potential impacts on bentonite and other EBS materials at temperatures up to 200 °C. Numerous international HotBENT partners and DOE are participating in the effort to define the test plan and configuration. This effort could be beneficial for all parties, as substantial cost savings could be achieved in the design of a repository if HotBENT demonstrates that the temperature of bentonite backfill can be raised without drastic changes in the performance implications.

To support the Preliminary Design Study, numerical models are being used to study the evolution of bentonite. Coupled THMC processes are highly interactive in bentonite, which requires coupled models. However, a fully coupled THMC model with a 3D simulation of HotBENT and all EBS components would likely be computationally too demanding to be carried out in a reasonable amount of time. Therefore, this report considers models with a simple geometric 1D or 2D setup that can be used to (1) simulate coupled THMC processes; (2) study the hydrological evolution of bentonite when the impact of mechanical changes (swelling) on porosity and permeability is considered; and (3) evaluate the chemical evolution in bentonite over the course of the test. The objective of the analysis (Matteo et al, 2018) is to identify existing models that can simulate coupled THMC processes that will occur over the course of the test, and that can be used to evaluate the results without implementing the fully coupled 3D model. These modeling exercises supplement the 3D TH model (Finsterle et al., 2017).

The first set of models are 1D axi-symmetric coupled THMC models based on the model for the FEBEX in situ test (Zheng et al. 2017) to illustrate the expected THMC response in the hot cross-sections that cut through the middle of the heater. The second set of models consists of 2D cross-sectional models with THMC processes for one of the scenarios reported in Finsterle et al. (2017). Figure 4-10 shows the cross-sectional mesh developed for the 2D models.

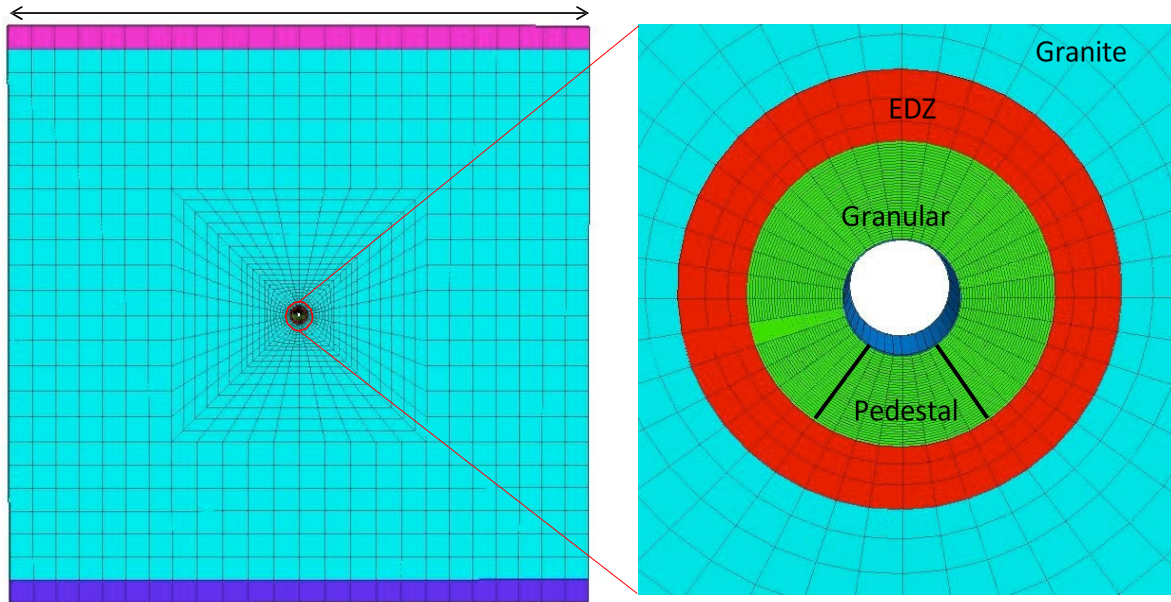


Figure 4-10. 2D cross-sectional mesh for the THMC model.

Major observations from the 1D axi-symmetric coupled THMC models include:

- HotBENT with a heater temperature of 200 °C will lead to a temperature of around 90 °C in granite, thus boiling in granite would probably not be a concern.
- Most of the bentonite barrier for HotBENT with a heater temperature of 200 °C will stay dry for a very long time
- Despite the higher temperature in HotBENT, the stress is lower than in the FEBEX in situ test
- HotBENT needs a longer cooling period at the end of test than the FEBEX in situ test, and stronger redistribution of moisture in the bentonite during the cooling period is expected.
- The TH model that ignores porosity and permeability changes due to swelling/shrinkage overestimates relative humidity by 20-25% over the entire simulation period compared with the THMC model, if it is FEBEX bentonite. However, if the bentonite has higher permeability than the FEBEX bentonite, the difference between TH and THMC models is smaller and short-lived.
- If HotBENT uses FEBEX bentonite:
 - High concentrations of major ions are expected.
 - Minerals with high solubility (e.g., calcite and gypsum) tend to dissolve in the area near the granite and precipitate in areas near the heater, and
 - Dissolution of montmorillonite and precipitation of illite are not expected, but rather the opposite is observed in the model.

The 2D cross-sectional THMC model simulates one of the scenarios in Finsterle et al. (2017), which assumes the mechanical and chemical parameters for the granular bentonite and the pedestal are the same as FEBEX bentonite. The relatively high permeability for granular bentonite is expected to create conditions

with high temperature and water saturation that foster significant chemical changes. The main observations from modeling results include:

- The 3D TH model (Finsterle et al. 2017) and the 2D cross-sectional TH model provide a similar saturation of the bentonite barrier in terms of the thickness of the full saturation area at 10 years but differ slightly at 1 and 5 years.
- A comparison between TH and THMC models suggests that the THMC model leads to faster hydration of bentonite because, in the bentonite near the granite, saturation leads to swelling and a decrease in dry density and subsequently to higher permeability.
- Consistent with the prediction based on the THMC model, high concentrations of major ions (except bicarbonate and pH) in granular bentonite near the heater are expected. A high concentration zone near the heater also appears in the pedestal within a short time (< 1 year) but disappears later.
- Bicarbonate and pH show complex spatial patterns because they are affected by dissolution/precipitation of carbonate minerals and surface protonation.
- Despite the 2D cross-sectional model having a higher permeability for granular bentonite than the 1D model, similar mineralogical changes occur in the 1D THMC model: calcite and gypsum tend to dissolve in the area near the granite and precipitate in the area near the heater; illitization (dissolution of montmorillonite and precipitation of illite) is not expected, but rather the precipitation of montmorillonite and dissolution of illite are observed.

The pedestal behaves differently from granular bentonite in terms of the change in ion concentration in pore-water despite the current model hypothesis that they have the same initial geochemical conditions. The high initial water saturation in the pedestal makes it become fully saturated soon, and, therefore, the pedestal generally has lower ion concentrations than granular bentonite. However, in terms of clay mineral alteration (montmorillonite and illite), the pedestal behaves similarly.

Code Comparison of Semi-Analytical Thermal Analysis Software: Semi-analytical codes are used for evaluating the thermal field of heat-generating nuclear waste in a repository. They offer an ease of use that is ideally applied at the design-phase, where quick scoping calculations can be made to understand waste package surface temperature as a function of waste package spacing and drift spacing. Semi-analytical models are ideal for these calculations, as changes can easily be made without the complication of re-meshing. The trade-off is less accurate temperature prediction. The objective of this study (Matteo et al. 2018) was to perform code-to-code benchmarking between semi-analytical codes used by the SFWST Program, and the German nuclear waste program, and to compare both calculations to a more robust solver TH solver (i.e., FLAC3D).

The comparative benchmark in this study is based on a repository disposal layout in bedded salt. Conduction-only thermal analysis was performed at Sandia using the semi-analytical method implemented in Mathcad 14. A numerical simulation with PFLOTRAN was also used to test the Mathcad-based semi-analytical simulations. Thermal analysis of the benchmark was also done by DBE TECHNOLOGY GmbH with the codes LinSour and FLAC3D. The simulations at both DBE and Sandia used the same original input parameters. The studies include comparisons of results, which will be used to assess and improve the performance of the codes.

The Mathcad-based thermal model calculates the heat distribution produced by a central waste package including contributions from adjacent waste packages, and from waste packages in adjacent drifts. The model also includes convection, radiant heat transfer, ventilation and other processes.

LinSour (LINE SOURces) was developed to manage the complexity that arises when thermal analysis is performed on an entire repository with large dimensions (up to several km²) and over a time scale of >100 years. LinSour relies on the analytical solution of the heat transfer differential equation for a finite, linear, stationary heat source emplaced in an infinite, homogeneous and isotropic medium.

A repository is characterized by complex geometry, and heterogeneous materials whose parameters can be nonlinear with respect to time, temperature and pressure. In addition to thermal conduction, convection and radiation also occur. In such conditions, thermal analysis is usually performed with numerical codes. Therefore, the example problem was also solved using FLAC3D, a finite difference code developed by Itasca Inc. FLAC3D has a thermal option for analyzing conduction and advection.

The analysis includes conduction-based thermal simulations for waste packages emplaced in two configurations, with identical parameter values applied to all materials. The first configuration involves a single waste package emplaced in an infinite medium. The second configuration represents a repository layout with arrays of waste packages in different drifts. Each code was used to calculate the temperature at the drift wall and waste package surface as a function of time.

The results show that predictions of the three codes for both configurations were comparable under identical initial and boundary conditions. A separate simulation was conducted with PFLOTRAN numerical code to test results of the Mathcad-based semi-analytical calculations for Configuration 1. The results of that simulation were also very close. Comparison of the results of the different software and simulation methods provides confidence in our ability to perform thermal analyses.

Future work in this area could include comparisons of TH or THM models at the drift- scale or partial-repository scale.

Thermal Analysis for Disposal of Spent Nuclear Fuel in Alluvium Host Rock Using the Semi-Analytical Method: Thermal-only, semi-analytical analysis was conducted for the disposal of spent nuclear fuel in alluvium host rock. The simulations were conducted in support of the generic GDSA analysis to provide estimates of temperature at the surface of the waste package and the drift wall to help define a generic repository layout. Thermal responses were investigated to estimate temperatures at the surface of the waste package and the drift wall, and to examine the effect of drift and waste package spacing, backfill thermal conductivity, burnup, PWR assembly size, and the length of surface storage (Matteo et al. 2018).

The repository was assumed to be at 250-m depth. Ambient average ground surface temperature of 25°C, and a natural geothermal gradient of 30°C/km were used. The disposal concept assumed waste packages emplaced horizontally, encapsulated in swelling clay-based buffer material. The geometry includes a drift diameter of 5.5 m and a waste package diameter of 3.2 m and 5-m length. Both 21-PWR and 12-PWR waste packages were analyzed, with assumed surface storage periods of 100, 150 and 200 years. Two values of thermal conductivity (0.5, 1.5 W/m K) for backfill materials were also evaluated.

Peak temperatures for 100 years storage time average in the range of 230 - 240 °C for the 21-PWR waste package surface and 110 – 125 °C for the drift wall, using the lower value of backfill thermal conductivity. Temperatures are lower for longer surface storage times, and lower thermal output (12-PWR) waste packages. Assuming the higher thermal conductivity in the backfill results in maximum temperatures at the waste package surface of 150 – 160 °C for 100 years storage time.

The peak temperature was not significantly affected by the combinations of waste package spacing and drift spacing selected. Drift wall temperatures were much lower than the waste package surface temperatures. For all cases, the plots show that temperatures significantly drop after the peak is reached due to thermal decay.

Thermal-Hydrology Modeling for Disposal of Spent Nuclear Fuel in Crystalline Host Rock: This analysis is a continuation of the modeling of the disposal of DOE managed DHLW and DSNF waste in a crystalline medium documented in (Matteo et al. 2018). The current work concentrates on modeling disposal of commercial spent nuclear fuel to estimate thermal effects due to the disposal of SNF. The model

includes a preliminary analysis of two-phase flow in the near field with possible evaporation and condensation. In the analysis, fractured crystalline host rock is represented as a homogenous system with a single average permeability. Future work will include fracture characterization of the host rock.

This study (Matteo et al. 2018) follows the analysis by Mariner Mariner et al. (2017b) and uses similar properties and parameter values to represent the waste and the host rock. The SNF is 12-PWR, 60 GWd/MTHM burn-up, and is assumed to be 100 years out of reactor (surface storage time). The model domain includes only a portion of the repository, in order to allow detailed thermal analysis with a refined mesh. The domain contains 9 drifts with 9 waste packages in each drift. The drift diameter is 4.5 m with a 2 m Disturbed Rock Zone (DRZ) surrounding each drift. Each waste package is surrounded by buffer material. The domain includes a 10.5 m wide access drift.

After evaluation of several grid generation tools, Meshmaker was used to generate a 3D cartesian mesh which was exported to the TOUGH3 code for the numerical simulations. The study investigates thermal behaviors due to the disposal of SNF with higher thermal power than previous analyses, and related vapor migration. The simulations assumed base case material properties and provided a venue for testing the newest version of TOUGH3. High peak temperatures can be expected with the disposal of SNF (Figure 4-6). Limited sensitivity analyses were also conducted that investigated the effects of buffer thermal conductivity and contributions of adjacent waste packages to thermal effects. The analyses showed that the use of buffer materials with higher thermal conductivity could reduce peak temperatures. Other parameters such as longer surface storage, optimum repository footprint and thermal loading considerations would also lower peak temperatures.

Future work will include running of simulations for longer time, varying homogenous rock properties such as permeability, varying surface storage time, incorporating fracture characterization of the host rock, and incorporating different waste types.

Experimental Investigations on Bentonite and Other Clay-Based Materials: Geologic media with high clay content (e.g., argillite or shale), are being evaluated to determine if they could be suitable host rocks for a geologic repository storage for spent fuel and high-level nuclear waste. Clay-based materials such as bentonite have also been proposed as an engineered barrier within a repository, because they have hydrologic and geochemical properties that could contribute to waste isolation, including low hydraulic conductivity, and high adsorption capacity for contaminants such as radionuclides. Montmorillonite, a smectite mineral, is the dominant clay mineral found in bentonite. It is a phyllosilicate with a large specific surface area and cation exchange capacity. Although clay minerals are known to exhibit these favorable properties at low temperatures, it is not clear whether they would continue to function as effective barriers in the high temperature environments created by a repository.

Experiments were designed to test the effect of bentonite heating on U(VI) adsorption, and mineral alteration (Matteo et al. 2018). U(VI) adsorption onto bentonite samples from the FEBEX in-situ experiment, which were subjected to 18 years of heating at temperatures of 50-100 °C, was compared to adsorption on FEBEX bentonite that was not heated during the test. U(VI) adsorption is 5-10% lower on a sample heated to 95°C compared to a 20°C cold-zone sample for both bulk bentonite and purified bentonite clay. The observed difference in adsorption appears to be due to structural differences in the clay minerals. By contrast, U(VI) adsorption onto an intermediate (50°C) heated purified clay sample is nearly identical to the cold-zone sample. This suggests that effects of heat may only be observed at the highest temperatures experienced during the test (100 °C) and indicates that the overall effect on the EBS would be limited to the area immediately surrounding waste canisters (i.e., within 25 cm).

Based on analyses of heated and unheated FEBEX samples, it also appears that small differences in illitization (i.e., 5% vs 10%) will likely have a small to negligible effect on U(VI) adsorption. The structural differences in the clay minerals from heated and unheated samples are not well understood, but do not appear related to alteration of montmorillonite to illite. Instead, they may be due to differences in edge structure or the number of edge adsorption sites in the montmorillonite or electrostatic characteristics.

This study provides important information relevant to performance assessment. Decreased adsorption as a result of bentonite heating may impact the rate of diffusion of U(VI) through engineered clay barriers. Because the decreased U(VI) adsorption was due to changes in the clay mineral structure and not to aqueous U(VI) speciation, other radionuclides may be similarly affected.

Future work related to bentonite heating and alteration is planned to combine the existing FEBEX bentonite data set with previously collected U(VI) adsorption data on laboratory-heated bentonite. Additional mineralogical analyses of the samples which showed the largest difference in U(VI) adsorption is planned, as are diffusion experiments under realistic waste disposal conditions to investigate how differences in U(VI) adsorption affect the diffusive transport of U(VI).

High Temperature Experiments of EBS Component Interactions: There have been numerous investigations of bentonite stability under various repository conditions, but questions remain, including specifically whether montmorillonite will remain relatively unaltered through the repository life-time. It is expected that the initial heat pulse will start to decay after about 100 to 1,000 years. After the high temperature pulse passes and temperatures begin to decrease, retrograde reactions have the potential to further change the mineralogy.

In order to increase our understanding of potential chemical and mineralogical reactions and interactions that could occur during the heating and cooling periods associated with a repository, two high-temperature, high-pressure hydrothermal experiments ($T = 250\text{ }^{\circ}\text{C}$ for 6 weeks), were performed. The experiments are known as Grimsel Granodiorite wall rock experiments IEBS-1 and IEBS-2. After the heating and cooling phase of the experiments was complete, detailed mineralogical and geochemical studies were conducted including 1) SEM imaging, 2) XRD (QXRD and clay determination) analyses, 3) electron microprobe data for major mineral phases, and 4) aqueous geochemistry data from both starting materials and the reaction products from the experiments conducted so far. The experiments represented all major EBS components, including buffer materials (bentonite sourced from Colony, Wyoming, USA), canister materials (stainless steel coupons), and Grimsel Granodiorite (the host rock in the FEBEX tests). The experiments were designed to investigate potential interactions at the waste canister/buffer boundary, and at the buffer/host rock boundary, at higher temperatures than have been investigated in field tests to date.

Several mineral alterations were observed in experiments with Grimsel Granodiorite and Wyoming Bentonite. The primary mineral reaction is the retention of clinoptilolite in volcanic glass shards and formation of a calcium (aluminum) silicate hydrate (C(A)SH) mineral (tobermorite, zeophyllite?) in the Wyoming Bentonite. Interpreting clay mineral evolution in experiments with the Grimsel EBS materials is complicated due to the variety of clay minerals already present in the system. However, it does appear that muscovite genesis occurs in the bentonite fraction in the mixed reactions at the current experimental conditions. With any of these experiments that are intended to represent the repository system, kinetics is always an issue that must be considered when interpreting data.

Observations based on the experiments conducted so far include (Matteo et al. 2018):

- Illitization of smectites may be restricted due to the bulk chemistry of the overall system
- The interface between bentonite and steel develops a well characterized new mineral phase, Fe-saponite (especially at $300\text{ }^{\circ}\text{C}$), that grows perpendicular to the steel surface
- Another Fe layered phyllosilicate, stilpnomelane, grows in the presence of native iron (one of our solid buffer materials), which suggests that oxygen fugacity may be quite variable, depending on scale
- Zeolites transform as temperature increases. Mine-run bentonite contains clinoptilolite, which was preserved in relict glass shards
- C(A)SH minerals formed within the Wyoming Bentonite mixed with Grimsel Granodiorite

- No abundant zeolites have been observed
- Future research is needed to enhance our understanding of the geochemical environment and mineralogical evolution in the EBS:
- Continue to build an experimental data base of Grimsel Granodiorite and EBS materials
- Perform transmission electron microscope (TEM) investigation looking at very local chemical changes within a pit corrosion metal surface
- Continue analysis of the corrosion of steels and interface silicate mantling effects
- Develop models to incorporate experimental results into Generic GDSA models
- Continue work to understand formation of C(A)SH minerals at relatively low pH (< 7)

The experimental database, along with summary conclusions, should be useful to other experimental teams within DOE, system modelers, and the international repository science community.

4.6 Dual Purpose Canisters

Research in dual-purpose canister (DPC) performance in direct geologic disposal concepts has also been a major focus of R&D for the SFWST Campaign. Due to widespread usage of DPCs in recent years for dry storage of spent nuclear fuel, there is significant interest in examining the potential for long-term direct disposal of DPCs in permanent geologic repositories without repackaging. While these canisters have been designed to ensure safety from biosphere exposure to radioactive waste forms during storage and transportation, they have not been designed specifically based on considerations for how they may perform when disposed of in a geologic repository. If DPCs are to be disposed of in a geologic repository, one question that remains to be answered concerns the potential consequences that could arise should the spent nuclear fuel contained in these canisters go critical during the post-closure period.

To screen out the exposure potential of a criticality event occurring in a DPC subjected to long-term geologic disposal, one approach is to screen out criticality on the basis of consequence. In FY 2019, a new module was developed in PFLOTRAN to account for the potential consequences of an in-package criticality event, which can include a rapid increase in thermal loading as well as a change in radionuclide inventory in the waste form. If a DPC is breached, moderation of criticality by water could prolong the criticality event, and the heat of the criticality could boil off the water. Therefore, this module will primarily be used to study multiphase, multicomponent flow and transport problems using PFLOTRAN's General mode.

4.6.1 Criticality Module

The criticality module has been designed as an extension of the waste form process model in PFLOTRAN. Just as each waste form in a simulated repository can be uniquely described, the criticality parameters can also be uniquely defined and applied to each individual waste form. The criticality event is currently parameterized as a change in both the heat source term and the radionuclide inventory in the waste form.

The heat source term is currently defined by a pseudo steady state formulation, whereby a critical event occurs over a specified period of time with a constant heat of criticality. The heat of criticality is superimposed on top of the radionuclide decay heat. The heat of criticality is assumed to distribute evenly throughout each waste package. Criticality start and end time define the period over which the additional heat source is emitted from the waste package. These times are read in separately for each waste package, allowing for flexible and heterogeneous implementation of criticality events for different waste packages.

Radionuclide inventory in a waste package changes dynamically with a critical event and is not mechanistically simulated in PFLOTRAN. The radionuclide inventory during the criticality event is

designed to be read in from external neutronics simulations; similarly, the change in decay heat due to changes in radionuclide inventory is also designed to be read in from an external neutronics code.

4.6.2 Results

The criticality module was applied to a repository in a fully water-saturated shale host rock. This nearfield simulation modeled a single waste package in the center of a repository in a half symmetry domain, using reflection boundary conditions in both lateral dimensions at the center of the waste package. A decay heat source for an as-loaded MAGNASTOR TSC 37 DPC loaded with 37 Westinghouse 15x15 assemblies and 100 years out of reactor was calculated externally using a neutronics code (Painter et al. 2019). In addition to the decay heat, 2.1 kW of heat was added throughout the duration of the criticality event, which was specified to start at 9,000 years and last until 20,000 years after repository closure. The center of the repository is set at 500 m below ground level, and pressure in the system is initially hydrostatic. Temperature follows a geothermal gradient of 25°C per km. Therefore, pressure and temperature at the waste package are initially about 5 MPa and 31°C, respectively. Physical properties of the host rock, DRZ, buffer material, and waste package are consistent with GDSA shale host rock reference case.

Temperature profiles depicted in Figure 4-11 show significant early contribution to the temperature history by the decay heat (from < 1 year to 1000 years) followed by a second temperature spike resulting from the criticality event. Throughout the entire simulation, water temperature remains below the boiling point (about 264°C at 5 MPa). Although peak temperatures occur at early times during which the decay heat is still significant, the criticality event does contribute significantly to the thermal load of the system and only avoids increasing the system temperature to the boiling point because the critical event is sufficiently offset in time from the peak decay heat.

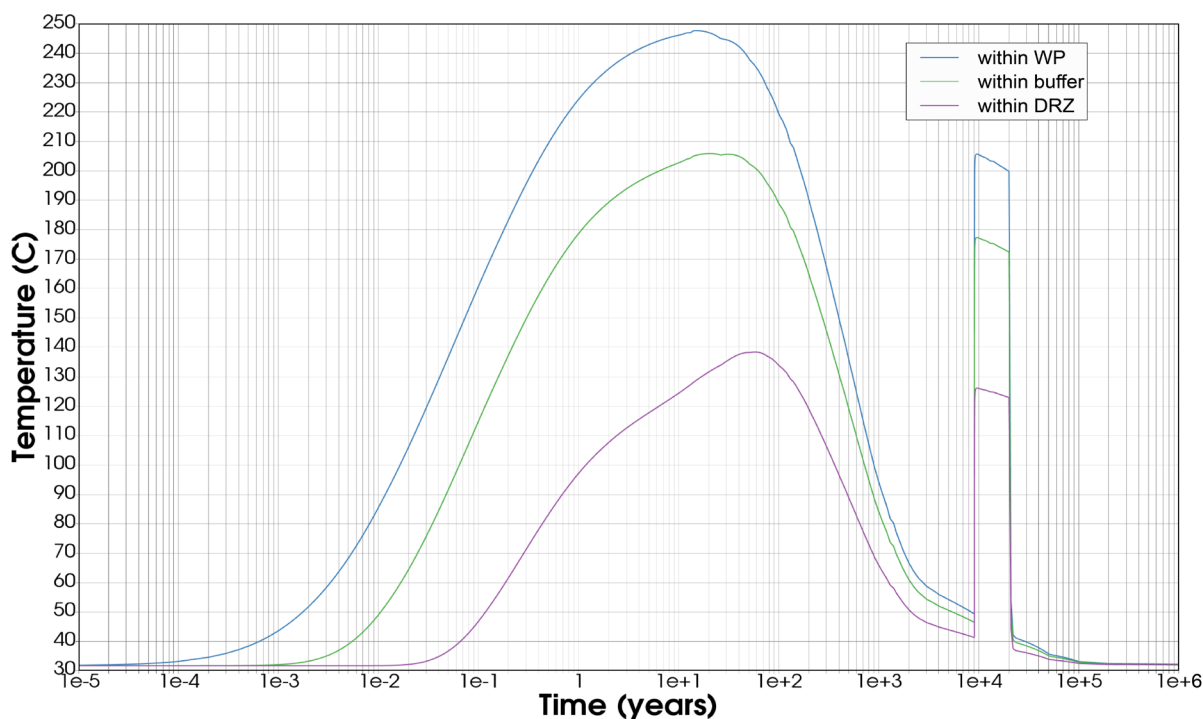


Figure 4-11. Temperature profiles at the center of the waste package (Cell 27), in the buffer (Cell 149), and in the DRZ (cell 342).

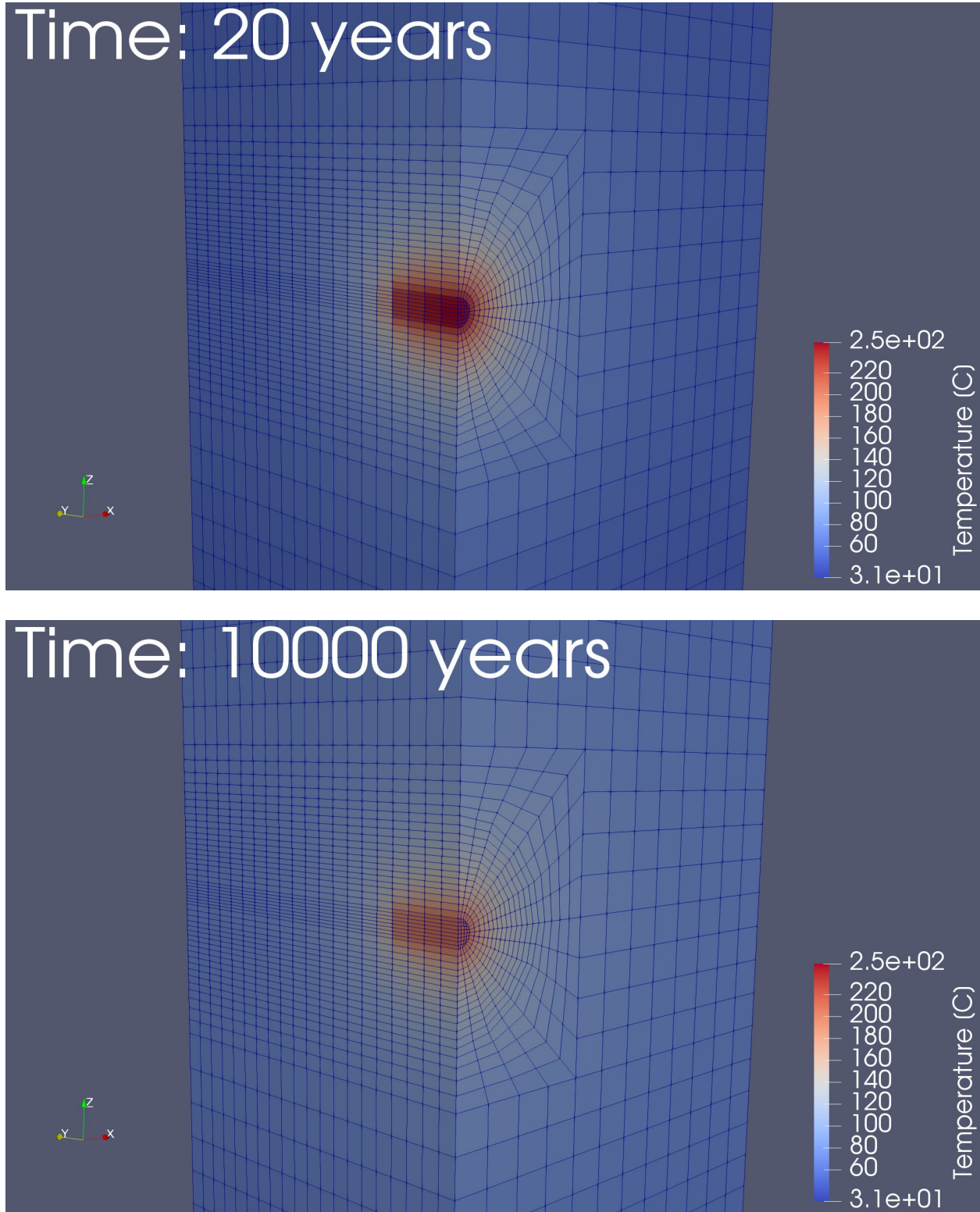


Figure 4-12. 3D rendering of the simulation domain at 2 times where temperature near the waste package spikes.

Pictured in 3D in Figure 4-12, the heat source generated in the waste package at the corner of the domain produces two temperature spikes centered at the middle of the waste package at 20 years and 10,000 years respectively. As alluded to previously, the temperature peak at 20 years is due to the decline in decay heat matching the speed of heat conduction away from the waste package, while the temperature peak at 10,000 years is due to the introduction of the heat of criticality.

4.6.3 Future Work

This work is currently being expanded to include an unsaturated alluvium repository host rock, and the criticality module is being modified to include the effects of water saturation and density in moderating the criticality event. If the heat of a criticality event boils off water, the criticality may not be sustainable without moderation and thus could cease, which could potentially result in cycles of resaturation and boiling which could turn the criticality event on and off.

4.7 SDA Legacy Document Archive

As a result of the DOE-NE reorganization that created the Office of Spent Fuel and Waste Disposition (SFWD), the Document Management System (DMS)—the former repository for UFD milestone deliverable documents—became unavailable. This gap is now being filled with a new restricted-access SharePoint website, called the SFWD Document Archive (SDA). This new document repository captures reports generated in the Disposal Research (DR), Storage and Transportation (S&T), and Integrated Waste Management (IWM) areas of SFWD.

The SDA includes copies of both UUR (unclassified unlimited release) and unclassified limited release (ULR) deliverable documents and concise information about their pedigree (e.g., “downloaded from OSTI,” “best available draft from author,” etc.) and their release status (e.g., “ULR,” “internal use only, do not cite or release,” etc.), and it is a searchable and sortable resource for SFWD participants. Although the SDA is not open to the general public, the section of it called the “NE 81 Public Milestones Library,” which contains UUR DR and S&T milestone deliverable documents, has been made available to most of the SFWD staff who are DOE employees or contractors and who attended the SFWD Working Group Meeting in Las Vegas, Nevada, in May 2019.

We have collected or accounted for almost all NE 81 and NE 82 milestone deliverable documents from FY 2010 through FY 2019. Some of the FY 2019 deliverables are still due between now and the end of September. FY 2020 milestone deliverables will be added to the master list in mid-October 2019, some of which will supersede some of the remaining FY 2019 deliverables.

Table 4-1, Table 4-2, and Table 4-3 show the current status of the SDA. Figure 4-13 is a screenshot of the SDA SharePoint website indicating the display format and the type of information available.

Table 4-1. NE 81 Disposal Research (DR) documents.

Total DR milestone deliverable documents referenced in PICS:NE ¹		527	
Total DR documents collected in the SDA ²		560	
Total DR deliverables that still need to be collected		4	
Level	Total DR milestone deliverable documents referenced in PICS:NE	Total DR milestone documents collected in SDA	Documents outstanding
1	1	1	0
2	105	109	0
3	142	148	1
4	269	281	3
5	10	9	0

¹ Program Information Collection System: Nuclear Energy (PICS:NE) is a web-based tool used by the Department of Energy, Office of Nuclear Energy (DOE-NE) for tracking program scope, schedule, budget, and deliverables.

² There is a small discrepancy between the number of milestone documents from PICS:NE and the milestone documents collected in the SDA because sometimes multiple documents are associated with single milestones (e.g., like the current document, which has two revisions, Rev.0 and Rev.1). Also, a very small number of other important documents have been added to the SDA. 504 of the 532 collected DR documents in the SDA are UUR and can be found in the NE-81 Public Milestones Library section of the SDA.

Table 4-2. NE 81 Storage and Transportation (S&T) documents.

Total S&T milestone deliverable documents referenced in PICS:NE	291
Total S&T documents collected in the SDA ^{2,3}	291
Total S&T deliverables that still need to be collected	0

³ All of the 291 S&T documents are in the SDA and can be found in the NE 81 Public Milestones Library or the NE 81 Non-Public Milestones Library.

Table 4-3. NE 82 Integrated Waste Management (IWM) documents.

Total IWM milestone deliverable documents referenced in PICS:NE	501
Total IWM documents collected in the SDA ⁴	354
Total IWM deliverables that still need to be collected	147 (Levels 3, 4, and 5)

⁴ These documents will be made available to SFWD staff at a later date.

File Name	WFS	WP Manager	WP Number	DMS Tracking Number	Milestone ID Number	R&D	Title	First Author	WP Title	Key Word	Deliverable Description	FY	Lab Report Number
M2F1-17SN010302011 Evaluation of Spent Fuel Disposition in Crystalline Rocks FY17 Progress Report	1.08.01.03.02.01	Wang, Yifeng	SF-17SN01030201	SFWD-SFWST-2017-00007	M2F1-17SN010302011	NE 81 Disposal Research	Evaluation of Used Nuclear Fuel Disposition in Crystalline Rocks FY17 Progress Report	Wang, Yifeng	Crystalline International Collaborations - SNL	Crystalline	EOFY17 status update for crystalline disposal R&D	FY17	None
M2SF-17SN010301011 Evaluation of Used Fuel Disposition in Clay-bearing Rock rev.1	1.08.01.03.01.01	Jove-Colon, Carlos	SF-17SN01030101	SFWD-SFWST-2017-00006, Rev.1	M2SF-17SN010301011	NE 81 Disposal Research	Evaluation of Used Nuclear Fuel Disposition in Clay-bearing Rock rev.1	Jove-Colon, Carlos	Argillite Disposal R&D - SNL	Argillite	End of FY17 status update on argillite disposal R&D	FY17	SAND2017-10533R
M2SF-17SN010303011 Proceedings of the 7th US German Workshop on Salt Repository Research, Design, and Operation	1.08.01.03.03.01	Kuhlman, Kris	SF-17SN01030301	SFWD-SFWST-2017-00008	M2SF-17SN010303011	NE 81 Disposal Research	Proceedings of the 7th US German Workshop on Salt Repository Research, Design, and Operation	Hansen, Francis	Salt R&D - SNL	Salt	This report will present the collaborative efforts between technical peers in the US, Germany and the Netherlands on topics in salt repository research that were the focus of the 7th US/German Workshop in Washington DC	FY17	SAND2017-1057R
M2SF-17SN010501014 Inventory and Waste Characterization Status Report	1.08.01.05.01.01	Sassani, David	SF-17SN01050101	SFWD-SFWST-2017-00014	M2SF-17SN010501014	NE 81 Disposal Research	Inventory and Waste Characterization Status Report	Sassani, David	Complete and Populate Online Waste Library (OWL) - SNL	Online Waste Library (OWL) DOE NW	EOFY17 status update on the DOE Managed HLW & SNF Characterization and Inventory work activities.	FY17	SAND-2017-10260R
M2SF-17L8010307011 International Collaboration Activities in Different Geologic Disposal Environments	1.08.01.03.07.01	Birkhofer, Jens	SF-17L801030701	SFWD-SFWST-2017-00013	M2SF-17L8010307011	NE 81 Disposal Research	International Collaboration Activities in Different Geologic Disposal Environments	Birkhofer, Jens	International Disposal Research Coordination - LBNL	International Collaboration	EOFY17 status update on international collaborations in disposal research.	FY17	LBNL-2001063
M2SF-17SN010304011 Advances in Geologic Disposal	1.08.01.03.04.01	Mariner, Paul	SF-17SN01030401	SFWD-SFWST-2017-00044	M2SF-17SN010304011	NE 81 Disposal Research	Advances in Geologic Disposal	Mariner, Paul	Generic Disposal	Generic Disposal	This report will describe the development of the	FY17	SAND2017-10304R

Figure 4-13. Screenshot of the SFWD Document Archive SharePoint site.

5. DISPOSAL R&D ROADMAP

Following the suspension of the Yucca Mountain Project and the dissolution of the Office of Civilian Radioactive Waste Management in 2010, DOE reorganized its radioactive waste management program in the Office of Nuclear Energy (NE). The Used Fuel Disposition Campaign (UFDC), and later the Spent Fuel and Waste Science and Technology (SFWST) Campaign were organized to conduct research and development (R&D) on deep geologic disposal of SNF and HLW. The R&D program was designed to be “generic” (i.e., “non-site-specific”), so that its results could be used to support any of several potential programmatic decisions regarding the focus of the future program, including the siting of alternative sites for storage and or disposal. In 2011, recognizing the need to identify and prioritize R&D activities that would be most useful for supporting future decisions, DOE formulated an R&D Roadmap outlining generic R&D activities and their priorities appropriate for developing safety cases and associated performance assessment (PA) models for generic deep geologic repositories in several potential host-rock environments in the contiguous United States. This UFDC Roadmap (DOE 2012) also identified the importance of re-evaluating priorities in future years as knowledge is gained from the DOE’s ongoing R&D activities. In addition to identifying and evaluating activities specific to the U.S., DOE also decided to increase cooperation with several international radioactive waste management programs, especially with countries operating underground research laboratories (URLs). These collaborations enable DOE to cost effectively perform experiments, and develop models, in alternative geologic media. Working with other international programs also enables DOE to develop confidence in the reliability of models used to assess the potential performance of future repositories.

5.1 2012 Roadmap

The 2012 UFDC Roadmap (DOE 2012) defined and utilized a systematic, decision-analysis-based approach to develop and prioritize the R&D portfolio. The approach involved several steps, including the identification of potential “R&D issues” (information needs and knowledge gaps) and the prioritization of these R&D issues based on evaluation metrics, primarily their importance to the safety case and the state of knowledge regarding the issue. The R&D issues were derived from the generic list of 208 FEPs (Features, Events, or Processes) developed by the U.S. and International programs that were considered important to repository performance. A total suite of 354 R&D Issues were identified, which is greater than the original list of 208 FEPs, because each FEP could have a different importance to the safety case or a different state-of-the-art knowledge level depending on which of the three generic, host-rock concepts (argillite, crystalline, or bedded salt) was being evaluated.

Figure 5-1 summarizes the calculated scores for each individual R&D issue. Using the graph, the UFDC development team selected two cutoffs (priority scores of 2.4 and 3.5) to identify Low, Medium, and High priority issues. These cutoffs were selected to correspond to the two slope changes shown in Figure 5-1. A significant number of individual issues had a priority score of zero. This could occur because (1) the issue could not be addressed through generic R&D; (2) it could be fully addressed by conducting R&D on other issues, or; (3) the current level of information was judged to be sufficient.

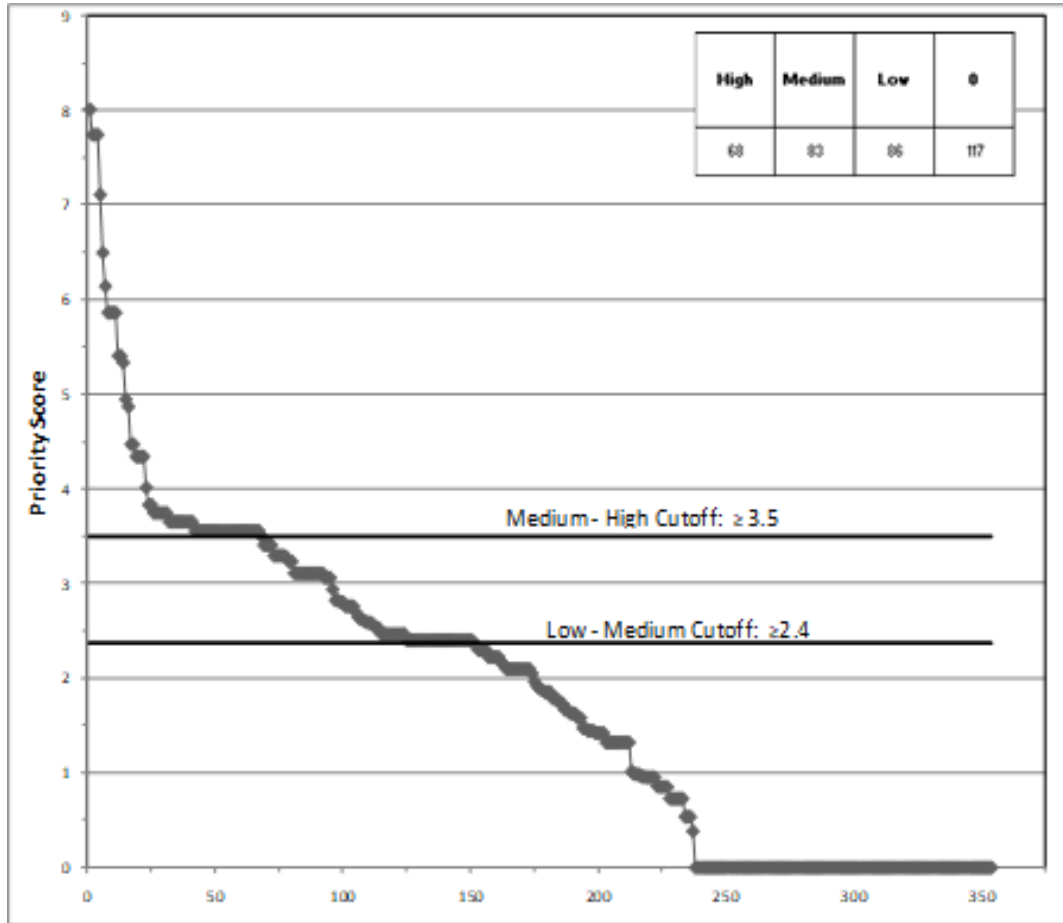


Figure 5-1. Priority scores for UFDC R&D issues.

Table 5-1 shows the results of an analysis by UFDC experts of the overall priority of categories of FEPs (listed by Process types) applicable to the natural system, sorted by geologic media (crystalline, salt and shale or argillite). The analysis demonstrated that certain categories of issues/FEPs had a consistently high priority (e.g., Host Rock properties), whereas others could vary considerably between media. The prioritization rankings related to the natural system were assessed separately for repositories in crystalline, salt, and argillite or shale media. In general, the highest ranked issues in crystalline media repositories included flow and transport pathways in the host rock and EDZ; for argillite or shale repositories, the highest ranked issues included the excavation disturbed zone, chemical processes, and thermal processes; for salt repositories, understanding of hydrologic processes was the highest priority (DOE 2012, Table 7).

Table 5-1. Relative priority of groups of R&D issues sorted by processes and geologic media.

Geosphere	Crystalline	Salt	Shale
1.2.01. LONG-TERM PROCESSES (tectonic activity)	Low	Low	Low
1.2.03 SEISMIC Activity			
Effects on EBS	High	High	High
Effects on NS	Low	Low	Low
1.3.01. CLIMATIC PROCESSES AND EFFECTS	Low	Low	Low
2.2.01. EXCAVATION DISTURBED ZONE (EDZ)	Medium	Medium	High
2.2.02 HOST ROCK (properties)	High	High	High
2.2.03 OTHER GEOLOGIC UNITS (properties)	Medium	Medium	Medium
2.2.05. FLOW AND TRANSPORT PATHWAYS	Medium	Medium	Medium
2.2.07. MECHANICAL PROCESSES	Low	Medium	Medium
2.2.08. HYDROLOGIC PROCESSES	Low	High	Medium
2.2.09. CHEMICAL PROCESSES - CHEMISTRY	Low	Low - Medium	Medium - High
2.2.09. CHEMICAL PROCESSES - TRANSPORT	Medium	Medium - High	Medium
2.2.10. BIOLOGICAL PROCESSES	Low	Low	Low
2.2.11. THERMAL PROCESSES	Low	Low	Medium
2.2.12. GAS SOURCES AND EFFECTS	Low	Low	Low
2.2.14. NUCLEAR CRITICALITY	Low	Low	Low

For engineered barriers, the rank scoring was not based on specific barrier materials, but rather on the main components of the system (e.g., waste form, waste package, buffer materials, backfill, seals, liners, etc.) and key potential processes to performance. Therefore, the results are organized by the primary engineered component(s) and the likely types of materials that would be considered to provide the engineered function. The main reason for this approach is that specific engineered system materials are highly dependent on repository design concepts and these still need to be developed to the point where the engineered components important to waste isolation can be identified and evaluated. Moreover, engineered barrier system materials can be considered, to a large extent, independent of the host media, but their performance is inherently important to the safety case. Waste form issues ranked higher than those for inventory. Waste container issues and chemical processes generally ranked higher than those for specific processes such as hydrologic and biologic. Buffer and backfill materials and issues related to chemical processes generally ranked higher than others. For seal and liner materials, issues related to chemical, mechanical, and thermal processes generally ranked higher than those for radiation or nuclear criticality effects. For other engineered barrier materials, issues related to chemical processes and radionuclide speciation/solubility ranked slightly higher than issues related to thermal, mechanical, and hydrological processes. Overall, chemical processes in the engineered barrier system components ranked higher than others but these are strongly coupled to thermal, hydrological, and even mechanical processes within the engineered barrier system. The ability to address coupled thermal- hydrologic-mechanical-chemical processes is emphasized in several subsequent sections of the report.

Evaluation of the prioritization rankings also revealed an important set of broad cross-cutting R&D categories that were helpful for defining the future R&D program. These categories were not explicitly evaluated as “R&D Activities,” but were recognized as potentially significant. They are listed in Table 5-2, along with qualitative priority levels that were assigned to them.

Table 5-2. Priority ranking of cross cutting technical issues.

Cross Cutting Technical Issue	Rank
Design Concept Development	High
Disposal System Modeling	High
Operations-Related Research and Technology	Low
Knowledge Management	Medium
Site Screening and Selection Tools	Medium
Experimental and Analytical Techniques for Site Characterization	Medium
Underground Research Laboratories	Medium
Research and Development Capabilities Evaluation	Medium

Although Table 5-2 demonstrates that the participants in the 2012 exercise clearly understood that the development of Disposal System Modeling capability was a high priority, the 2012 Roadmap did not explicitly consider or evaluate any activities related to the development of the GDSA Framework, or the GDSA Model (PFLOTRAN), because the decision to develop and implement the GDSA capability was not made until 2013.

5.2 2019 Roadmap Update

The original 2012 UFDC Roadmap promised a re-evaluation of priorities in future years as knowledge was gained from ongoing activities in the U.S. and abroad (DOE 2012, Section 2.4). Thus, a re-assessment of R&D priorities was initiated during fiscal year 2018, culminating in a workshop of Campaign experts in early 2019, held at the University of Nevada in Las Vegas from January 15 to 17. The results of the workshop and subsequent analyses are documented in the *DOE SFWST Campaign R&D Roadmap Update* (Sevougian et al. 2019a; Sevougian et al. 2019b). In addition, a new document archive was developed to organize and store the various reports generated by the disposal R&D work packages over the course of the UFD and SFWST Campaigns.

The 2019 R&D Roadmap Update summarized the progress of ongoing generic disposal R&D activities, re-assessed R&D priorities, and identified new activities of high priority, such as R&D on disposal of DPCs (dual purpose canisters), which now contain a significant fraction of the Nation’s commercial SNF activity. The objectives of the 2019 R&D Roadmap Update included the following:

1. Recap the original 2012 Roadmap results and conclusions
2. Document the 2019 Roadmap Update Workshop approach, process, and evaluations
3. Summarize the status, progress, and priority of current (as of 2019) SFWST R&D Activities and their relation to the FEPs identified as important to various host rocks and repository designs (those identified in the 2012 Roadmap)

4. Formulate the generic R&D still needed to advance the state-of-the-art for important R&D Activities and their associated 2012 FEPs
5. Identify any important 2012 FEPs that have not been addressed adequately by Campaign R&D Activities in the intervening years
6. Present a new document archive for UFD and SFWST milestone reports

Objectives 3 and 4 are primarily addressed in a series of appendices to the Roadmap Update report that capture the wealth of consensus information compiled by Campaign experts during the three-day Roadmap Update Workshop. In order to accomplish Objective 5, the update exercise identified “gap” activities that represent future R&D necessary to adequately advance the state-of-the-art understanding of several 2012 high- and medium-priority FEPs.

5.2.1 Methods

The 2019 Roadmap Update utilized a systematic process that was similar in many ways to that used in the 2012 Roadmap, but with important differences in both the definition of the items to be prioritized, and in the criteria and process used for prioritization. Specifically, there were five basic steps in the 2019 process:

- Identify a set of items to be evaluated (e.g., R&D activities, issues, or options)
- Identify criteria and associated metrics for assessing the set of items, such as:
 - *Importance* to the safety case (ISC) (e.g., to performance assessment (PA) calculations, technical bases, confidence-building potential)
 - Potential to reduce key *uncertainties*, i.e., to advance the state-of-the-art level (SAL) or knowledge
 - Other factors
- Evaluate each item (R&D Activity) against the metrics
- Define a “utility function” (or ranking function) to combine the metric values and produce an overall ranking or score for each item (R&D Activity)
- Compare rankings of the items (R&D Activities)

The goal was to identify R&D items that provide maximum value to DOE in terms of advancing the program’s ability to support future decisions regarding the siting, selection, design, licensing and construction of a geologic repository. For the 2019 R&D Roadmap Update, the SFWST Campaign decided to redefine the R&D items to be prioritized. Instead of prioritizing individual FEPs, as was done in 2012, the items to be prioritized were based on ongoing and proposed R&D work scope activities (or tasks) being performed by project participants and are herein referred to as R&D Activities. For completeness and for a high-level evaluation of R&D progress since 2012, the generic FEPs list was used to both map the R&D Activities to FEPs, and to help identify “gap” activities where existing R&D Activities did not completely address particular FEPs.

The activity-based approach is believed to have several advantages over the FEPs-based approach utilized in 2012. Scientists and engineers planning and executing the R&D program generally do not design experiments or perform analyses that are specific to individual FEPs. Instead, work is conceived and conducted at a broader conceptual level, which provides information on multiple FEPs. For example, experimental test programs typically address both engineered and natural features of the system, as well as multiple processes (e.g., thermal, hydrologic, geochemical and geomechanical) that act on the features.

Similarly, the analyses and models developed to simulate the test results and predict long term behavior must likewise address multiple FEPs. The 2019 activity-based approach has the additional benefit of allowing program participants and managers to directly assess the resources (both personnel and costs) required to conduct prioritized R&D, and to understand the costs and benefits of various “multi-FEP” R&D tasks.

The initial list of R&D Activities for the 2019 Update was compiled by the Technical Leads for the SFWST Program, and several additional activities were added to this list during the Update Workshop. Although R&D Activities are generally described more broadly than individual FEPs, they do still vary in their level of discretization—some are quite narrow in scope and some are broad. To ensure that the 2019 Roadmap Update addressed all the R&D Issues identified in the 2012 Roadmap, SWFST staff identified and correlated all the medium- and high-priority FEPs from 2012 with the R&D Activities defined for 2019. In this way, the 2012 FEPs list also served as a completeness check on the R&D Activities list and facilitated gap identification. The R&D Activities Excel spreadsheet compiled for the 2019 Workshop had 109 Activities, with more than 20 columns of information for each Activity. This spreadsheet was actively revised by consensus during the Update Workshop and has since been converted to a Microsoft Access® database, which can be used in the future for tracking and prioritizing project R&D.

The same two primary criteria were used in 2019 to assess the overall importance of each R&D Activity: “Importance to the Safety Case” and “State-of-the-Art.” However, the guidance provided to workshop participants about what to consider and how to rank activities was significantly different. As an example, the 2012 UFD Roadmap attempted to address the time-value of R&D by considering the relative (and variable) importance of its evaluation metrics at different stages of the repository development timeline, such as at site screening, site selection, site characterization, etc. For the 2019 Roadmap Update, this weighting scheme was considered unnecessary, in part because the U.S. Program is currently in the R&D stage for generic repository sites, so the focus is on developing generic safety cases. Furthermore, the overall scores for R&D Activities were assessed more qualitatively in 2019, such that detailed discretization of the utility function is not warranted. Instead of assessing the value of R&D activities at multiple decision points, the 2019 Roadmap Update process established a simpler near-term goal. The SFWST experts were asked to define the generic R&D needed to develop and implement credible and defensible total system PA models for generic sites with “baseline capability” by the year 2022. This meant a capability to run PA models for generic sites that would simulate the effect of important post-closure FEPs. In addition to the requirement for a baseline PA, a goal was established to improve understanding of important systems and processes by advancing the state-of-the-art metric for each R&D activity by at least one level. Achieving this goal would represent a significant reduction in uncertainty for the overall program, and a meaningful evolution of the generic repository safety cases.

The 2019 R&D Roadmap Update Workshop was organized around the rock types that are the basis for the generic R&D in the SFWST Campaign, i.e. argillite (e.g., clay or shale), crystalline (e.g., granite), and bedded salt. The primary results of the Update Workshop are summarized in the report’s appendices. The organization of the appendices includes these generic host rock divisions, as well as other cross-cut groupings of R&D Activities. Specifically, the information presented in the appendices is organized into eight groups of R&D: Argillite, Crystalline, Salt, EBS, International, DPC, PA, and Other. Each group has a defined set of technical activities, or tasks, that form the basis of the prioritization presented in this report. A total of 109 R&D Activities have been defined. The Activities are described in Appendix B, along with their workshop-derived, consensus metric values and computed priority scores.

As noted above, the R&D Activities were assessed from two different perspectives or criteria, and evaluation metrics were defined for these two criteria before the Workshop. Importance to the Safety Case (ISC) was evaluated as High, Medium, or Low, with specific definitions of the three scale values being dependent on the importance of the R&D Activity relative to various components or elements of the generic safety case. The State-of-the-Art Level (SAL) was assigned one of five values based on the level of knowledge currently available and what yet needs to be obtained. The highest priority rating (5) was

assigned to activities investigating processes for which little or no data or modeling capability is available. The lowest rating (1) would apply to activities investigating processes which are well understood and supported by ample data and analyses. All the activities in the current R&D program received a SAL score of 3 or higher, reflecting the level of uncertainty that currently exists in repository modeling, and the need for continued R&D. The two metrics were combined after the Workshop to define an overall Priority Score: High, Medium-High, Medium, or Low for each R&D Activity.

Consensus on ISC and SAL metric values was obtained within “breakout” sessions comprised of about ten to fifteen experts each, using the provided metric scales, and with guidance by the session chairs and the overall Workshop chair. There were six breakout sessions: first, there were three host-rock (Argillite, Crystalline, Salt) day-long, concurrent sessions; these were followed by half-day concurrent sessions on EBS, DPC, and International R&D Activities. PA and Other R&D Activities did not have individual sessions but were assigned to the six aforementioned sessions, at the discretion of the technical leads.

In addition to providing consensus metric values, the technical specialists also identified the R&D necessary to change each Activity from its current SAL level to the next improved level, as well as other comments and suggestions for future R&D opportunities, integration needs, and emerging issues. The “raw” consensus information (metric values, comments, and other suggestions) is primarily documented in Appendices B and K. Post-workshop mappings of FEPs to Activities and vice-versa are given in Appendices D through I, which help show the comprehensiveness of the current Campaign R&D Activities relative to the important FEPs identified in 2012 (primarily those FEPs identified as of high and medium priority).

Probably the most important categorization of R&D Activities shown here is by generic host-rock breakout session: Argillite, Crystalline, and (Bedded) Salt. These three host rocks form the three core generic repository concepts (and associated safety cases) being developed within the Campaign; however, the R&D Activities that need to be evaluated for these concepts are not just geologic (or natural system) related R&D Activities, since each repository concept consists of both natural and engineered barriers. Therefore, each host-rock breakout session was asked to also consider EBS, DPC, International, and PA R&D Activities that are relevant to their generic repository concept. This resulted in a number of these other R&D Activities being evaluated in more than one host-rock breakout session. Any inconsistencies in the ISC and SAL metric values developed in the host-rock sessions were then resolved in the later EBS, DPC, and International breakout sessions. Inconsistencies in PA metric values were resolved by PA experts after the Workshop.

5.2.2 Analysis and Results

The primary goal of the Workshop was to develop a consensus of the technical experts on the priority and state-of-the-art of the current (and gap) R&D Activities. Metric scores (for SAL and ISC), the associated Rationale for these scores, and the future R&D Needed (to move the R&D to the next improved SAL), are the primary results and information gathered in the Update Workshop from the 50+ Campaign experts. The consensus information is presented in several ways in the appendices to the Update report. For example, because the 2012 Roadmap was based on FEPs and the 2019 Roadmap Update is based on R&D Activities, the appendices have several mappings between FEPs and Activities, to ensure completeness relative to the original 2012 R&D Roadmap prioritization. The FEPs mapping to the 2019 R&D Activities focuses on FEPs that were identified as high or medium priority FEPs in the original Roadmap report (DOE 2012) because these formed the basis of the UFD/SFWST R&D program during these years. In a few cases, low priority FEPs are mapped to current R&D Activities, but in most cases FEPs rated as low priority in 2012 are omitted from the appendices, since most of those FEPs are still considered as not important to generic repository research, or enough information is known about them during the generic repository phase. Exceptions include, for example, criticality events which have a higher probability in used fuel canisterized in DPCs, which only made up a small fraction of stored fuel in 2012 but now are a greater fraction.

Each R&D Activity was further characterized by identifying the element(s) of the Safety Case that it supports. The assignments were made using the categories defined in Figure 5-2. Most of the Activities support elements 3.3 (Post-closure Bases (FEPs)) and/or 4.2 (Post-closure Safety Assessment). These assignments were an important part of the ISC metric evaluation during the Workshop.

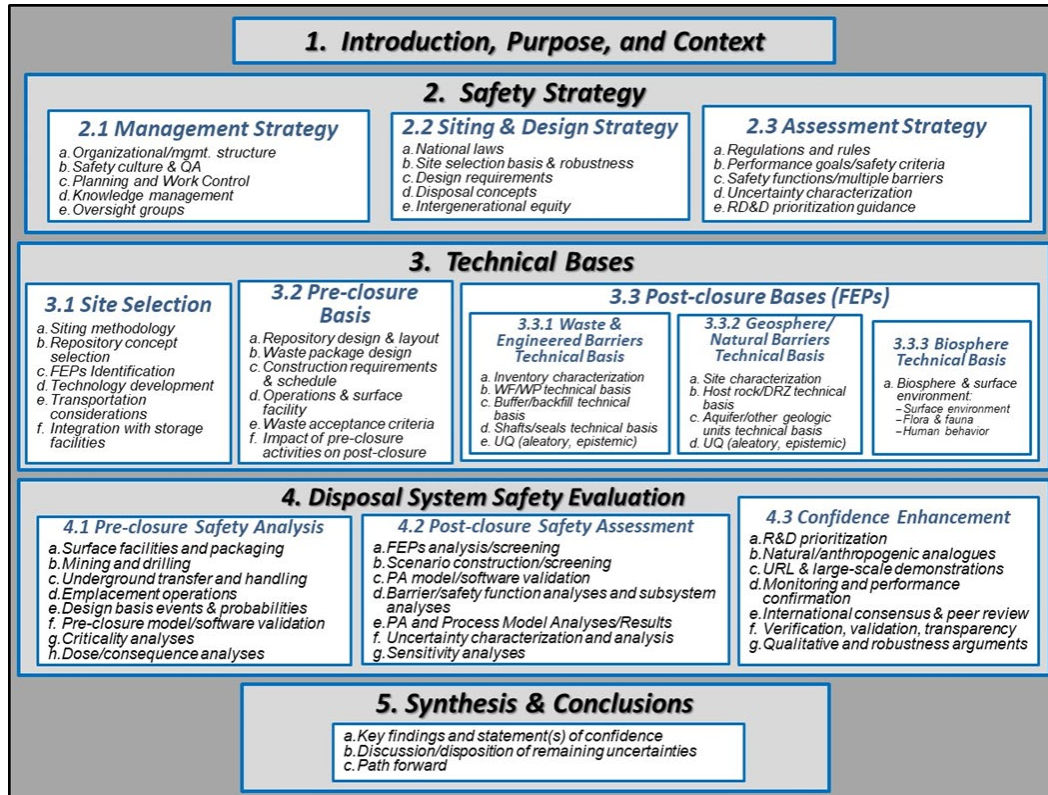


Figure 5-2. Typical elements of the safety case for geologic disposal.

Following the Update Workshop, the SAL and ISC metric scores (reached by expert consensus within each breakout session) were combined to derive an overall Priority Score (Low, Medium, Medium-High, High) for each R&D Activity, similar to the qualitative rankings (Low, Medium, High) or groupings of R&D Issues (FEPs) in the 2012 Roadmap (see Figure 5-1). Figure 5-3 and Figure 5-4 are graphical presentations of the R&D Activity Priority Scores from the three host-rock breakout sessions, based on the suite R&D Activities included in each of these sessions. Figure 5-3 is a histogram representation of the Priority Score results, whereas Figure 5-4 is a discrete cumulative distribution functions (CDFs) showing the cumulative fraction of R&D Activities having each of the four possible Priority Scores: Low, Medium, Medium-High, and High. A given cross-cutting R&D Activity from Appendix C may be included in more than one bar (or curve) in Figure 5-3 and Figure 5-4 because it may have been reviewed by two or three host-rock breakout sessions. A total of thirty-eight cross-cutting R&D Activity reviews were completed in the host rock sessions (i.e., a total of thirty-eight EBS, International, and PA Activities).

It is clear from Figure 5-3 that the Crystalline breakout reviewed the most R&D Activities, followed by Argillite and Salt. Figure 5-4 indicates remarkable uniformity in priority assignment among the three sessions, with all three host-rock sessions resulting in about 50% Medium-priority Activities, 30% Medium-High-priority Activities, and 20% High-priority Activities. This uniformity across host-rock breakout sessions is perhaps indicative of a rather uniform “calibration” of the experts across the sessions.

By comparison, Figure 5-1 shows that about 55% of Issues were scored Medium and 45% scored High in the 2012 Roadmap—after subtracting out the Low- and Zero-scoring Issues because the latter were not used to design the R&D program following the 2012 Roadmap.

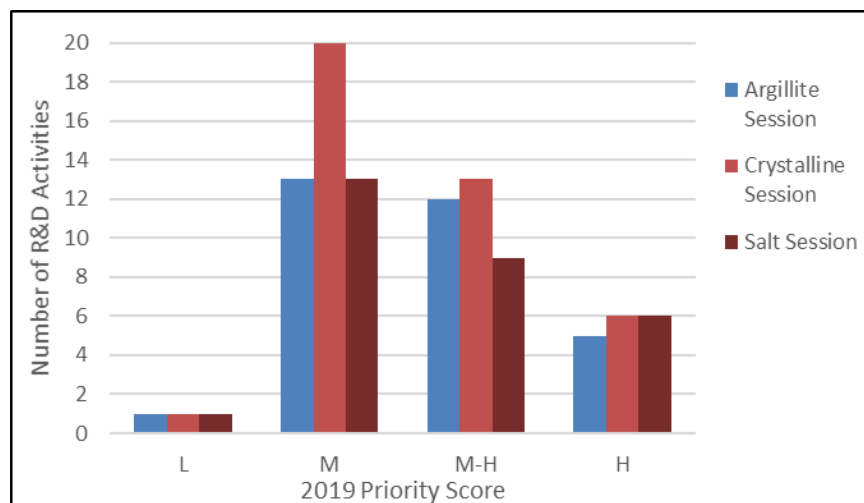


Figure 5-3. Histogram of priority scores for each host-rock breakout session (including gaps).

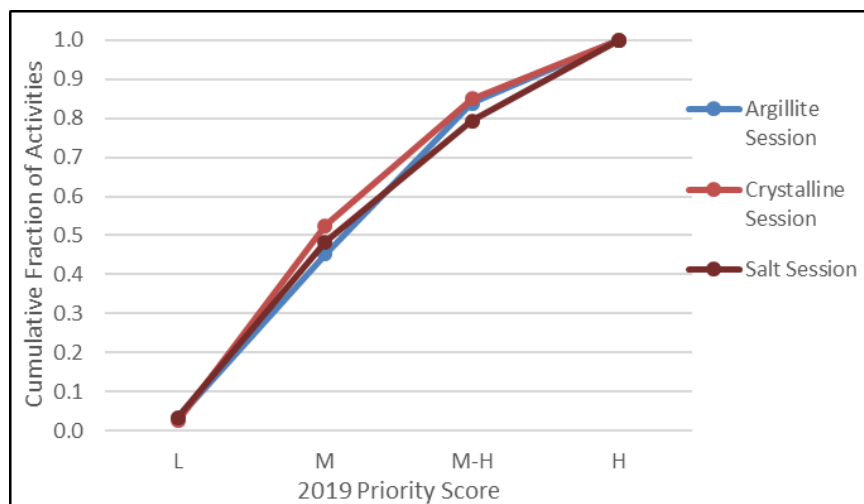


Figure 5-4. Fraction CDF of priority scores for each host-rock breakout session (including gaps).

Figure 5-5 is a histogram of Priority Scores for each of the eight topical R&D Activity groupings described above (Argillite, Crystalline, Salt, DPC, EBS, International, PA and Other), while Figure 5-6 is a cumulative fraction CDF of the same information, which emphasizes the relative percentage of R&D Activities in each Priority Score class for each R&D Activity group. The DPC R&D Activity group had, by far, the highest percentage of High-Priority Activities (about 70% of its total), primarily because the recent emphasis on evaluating direct disposal of DPCs in generic deep geologic repository concepts has led to a number of new, emerging issues that are being addressed by these R&D Activities.

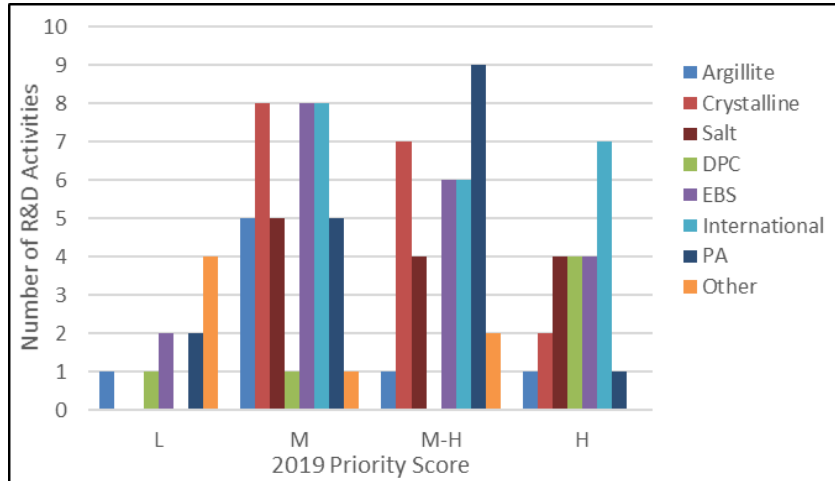


Figure 5-5. Histogram of priority scores for each R&D activity grouping (including gaps).

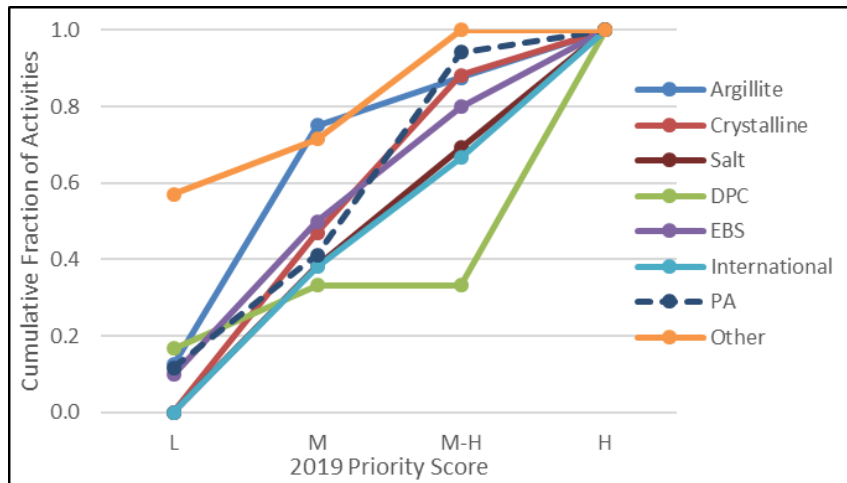


Figure 5-6. Fraction CDF of priority scores for each R&D activity grouping (including gaps).

Future long-term R&D still thought to be necessary, but not being conducted presently, is identified as a series of “Gap Activities;” and the 2019 prioritization results are presented graphically with and without the Gap Activities, i.e., as charts of Priority Scores for all R&D Activities (current and future), as well as Priority Scores of only current R&D (“without Gap Activities”).

Twenty-three R&D Activities were scored as High priority (Table 5-3). One Argillite Activity, two Crystalline Activities, four DPC Activities, four EBS, seven International Activities, one PA Activity, and four Salt Activities rank as High priority. The large number of International Activities that rank as High priority reflects the importance of the data collection from tests being conducted in the international URLs. The high priority Salt Activities include in-situ thermal testing at the Waste Isolation Pilot Plant (WIPP). The relatively large number of EBS Activities that are ranked as High priority reflect a transition in the emphasis of SFWST work from initial development of generic host-rock PA models to improvement of the representation of model elements important to barrier capability. A relatively large number of DPC Activities are ranked as High priority because this is a new area of research emphasis.

Table 5-3. High priority R&D activities.

High Priority R&D Activities	
A-08	Evaluation of ordinary Portland cement (OPC)
C-15	Design improved backfill and seal materials
C-16	Development of new waste package concepts and models for evaluation of waste package performance for long-term disposal
D-01	Probabilistic post-closure DPC criticality consequence analyses Task 1 - Scoping Phase Task 2 - Preliminary Analysis Phase Task 3 - Development Phase
D-03	DPC filler and neutron absorber degradation testing and analysis
D-04	Coupled multi-physics simulation of DPC postclosure (chemical, mechanical, thermal-hydraulic) including processes external to the waste package.
D-05	Source term development with and without criticality
E-09	Cement plug/liner degradation
E-11	EBS High Temp experimental data collection- To evaluate high temperature mineralogy /geochemistry changes.
E-14	In-Package Chemistry
E-17	Buffer Material by Design
I-04	Experiment of bentonite EBS under high temperature, HotBENT
I-06	Mont Terri FS Fault Slip Experiment
I-08	DECOVALEX-2019 Task A: Advective gas flow in bentonite
I-12	TH and THM Processes in Salt: German-U.S. Collaborations (WEIMOS)
I-13	TH and THM Processes in Salt: German-U.S. Collaborations (BENVASIM)
I-16	New Activity: DECOVALEX Task on Salt Heater Test and Coupled Modeling
I-18	New Activity: Other potential DECOVALEX Tasks of Interest: Large-Scale Gas Transport
P-12	WP Degradation Model Framework
S-01	Salt Coupled THM processes, hydraulic properties from mechanical behavior (geomechanical)
S-03	Coupled THC advection and diffusion processes in Salt, multi-phase flow processes and material properties in Salt
S-04	Coupled THC processes in Salt, Dissolution and precipitation of salt near heat sources (heat pipes)
S-05	Borehole-based Field Testing in Salt

Note: The alphanumeric identifier (first column) includes the Activity Group and number of the activity within the group. Information about each activity is provided in Appendix B of Sevougian et. al. (2018).

Thirty-five R&D Activities were scored as Medium-High priority (Table 5-4). One Argillite Activity, seven Crystalline Activities, six EBS Activities, six International, two “Other” Activities, nine PA Activities, and four Salt Activities rank as Medium-High priority. PA, International and EBS Activities are prominent among the Medium-High-priority Activities because of their cross-cutting nature. The two “Other” Activities involve geologic mapping and visualization tools and products. The large number of Crystalline medium-high priority Activities reflects the complexity of the Crystalline PA model, arising from host-rock spatial heterogeneity and fast transport in the fracture field. The long-term (“gap-like”) nature of most of these Crystalline Activities is also a factor in the Medium-High prioritization. The importance of completing research on these long-term Activities will increase later during detailed site characterization and design.

Table 5-4. Medium-high priority R&D activities.

Medium-High Priority R&D Activities	
A-04	Argillite Coupled THM processes modeling including host rock, EBS, and EDZ (TOUGH-FLAC)
C-01	Discrete Fracture Network (DFN) Model
C-06	Buffer Erosion (is this a gap in our program?) is it too site specific for generic R&D
C-08	Interaction of Buffer w/ Crystalline Rock
C-11	Investigation of fluid flow and transport in low permeability media (clay materials).
C-13	Evaluation and upscaling of the effects of spatial heterogeneity on radionuclide transport
C-14	Radionuclide sorption and incorporation by natural and engineered materials: Beyond a simple K_d approach
C-17	Model DFN evolution due to changes in stress field
E-02	SNF Degradation testing activities
E-03	THC processes in EBS
E-04	Waste Package Degradation Model (mechanistic)
E-06	Waste Package Degradation Testing
E-10	High-Temperature Behavior
E-20	Colloid source terms
I-02	FEBEX-DP Modeling: Dismantling phase of the long-term FEBEX heater test - Modeling
I-03	FEBEX-DP Experimental Work: Dismantling phase of the long-term FEBEX heater test
I-07	DECOVALEX-2019 Task E: Upscaling of modeling results from small scale to one-to-one scale based in heater test data in Callovo-Oxfordian claystone (COx) at MHM underground research laboratory in France.

I-09	DECOVALEX-2019 Task C: GREET (Groundwater REcovery Experiment in Tunnel) at Mizunami URL, Japan
I-14	TH and THM Processes in Reconsolidating Salt: German-U.S. Collaborations (KOMPASS)
I-21	New Activity: SKB Task 10 Validation of DFN Modeling
O-02	GDSA Geologic Modeling
O-03	Web Visualization of Geologic Conceptual Framework for GDSA Geologic Modeling
P-01	CSNF repository argillite reference case
P-02	CSNF repository crystalline reference case
P-04	CSNF repository unsaturated zone (alluvium) reference case
P-11	Pitzer model
P-13	Full Representation of Chemical processes in PA
P-14	Generic Capability Development for PFLOTRAN
P-15	Species and element properties
P-16	Solid solution model
P-17	Multi-Component Gas Transport
S-02	Salt Coupled THM processes, creep closure of excavations
S-07	Brine Origin, Chemistry, and Composition in Salt (in support of field test S-5)
S-08	Evolution of run-of-mine salt backfill
S-11	THMC effects of anhydrites, clays, and other non-salt components

Review of the Priority Scores of all R&D Activities allows for the identification of several “High Impact R&D Topics.” The listing of the Activities with High or Medium-High Priority Scores (Table 5-3 and Table 5-4) is the starting point. These tables reveal a spectrum of types of Activities with High and Medium-High Priority Scores. However, there are commonalities among these Activities that can be used to compile R&D Activities into topical areas. Table 5-5 presents just such a grouping of the High and Medium-High-priority Activities into “High Impact R&D Topics” that are the current focus of R&D in the SFWST Campaign. Note that the effect of high repository temperatures is a common aspect of a number of High- and Medium-High-priority Activities. In part, this is a result of the new interest in DPCs. But there is also International interest in this topic, as reflected in HotBENT and the long term FEBEX heater test. These heat effects play a role in evaluation of EBS barrier performance.

Buffer and seal studies are included in several High- and Medium-High-priority R&D Activities. International testing, including HotBENT, FEBEX-DP, and DECOVALEX-2019 Task E, are addressing issues related to buffers and seals. R&D Activities are looking at materials that are currently being used and novel new materials that could be used in the future. The performance of buffer and seal materials during potential future repository operation is also being evaluated.

Table 5-5. High impact R&D topics.

High Impact R&D Topics	High-Priority R&D Activities	Medium-High-Priority R&D Activities
High Temperature Impacts	D-1, D-4, I-4, I-6, I-16, E-11, S-5	I-2, I-3, I-7, E-10
Buffer and Seal Studies	I-4, E-9, E-17, A-8, C-15	I-2, I-3, I-7, A-4, C-6, C-8, C-11
Coupled Processes (Salt)	S-1, S-3, S-4, I-12, I-13	I-14, S-2, S-7, S-8, S-11
Gas Flow in the EBS	I-6, I-8, I-18	I-9, P-17
Criticality	D-1, D-3, D-4, D-5	
Waste Package Degradation	C-16, P-12	E-4, E-6
In-Package Chemistry	E-14	E-2, E-20, P-15, P-16
Generic PA Models		P-1, P-2, P-4, P-11, P-13, P-14
Radionuclide Transport		C-11, C-13, C-14, P-15, P-16
DFN Issues		I-21, C-1, C-17
GDSA Geologic Modeling		O-2, O-3
THC Processes in EBS		E-3

Generic PA model development and implementation continue to be High-priority Activities and is a High Impact Topic. A lot has been accomplished with the generic rock type models, but there is still a lot to be done especially integration of new results from process model developments. The generic unsaturated zone (alluvium) reference case is only beginning development.

Coupled process testing and modeling for a salt repository is a High-Impact Topic. Although extensive modeling of salt repositories at low temperature (e.g., WIPP) has been performed, significantly less work has been conducted for disposal of HLW/SNF at higher temperatures. Significant uncertainties remain regarding coupled THM processes, especially for the evolution of the EDZ and backfill. Activities include proposed field scale heater tests at WIPP.

Gas flow in the EBS is another High Impact Topic. Significant work related to the development, testing and implementation of coupled models including chemical processes and thermodynamic databases has been completed both within the U.S. (e.g., FMDM – see Sevougian et al. (2019b, Appendix B, Activity E-01)), and through U.S. participation internationally (e.g., FEBEX, HOTBent, GREET). However, direct incorporation of the process models into GDSA Framework (PFLOTTRAN) has not yet been accomplished, and it is not yet clear which modeling/simulation strategies will prove the most effective and efficient in terms of model confidence building and model validation.

Criticality is a new High Impact Topic. It was excluded from the 2012 prioritization evaluation. The potential for direct disposal of DPCs has led to a higher priority for criticality studies, e.g., see Activities D-01 and D-04.

The discussions and interactions that took place during the Workshop were part of an important information exchange between the technical experts of the SFWST Campaign. The interactions occurred formally during the breakout sessions, and informally throughout the Workshop. An integration session at the end of the Workshop provided an opportunity to discuss and document cross-cutting issues that had been identified in the breakout sessions. The topics and issues included:

- Technical integration between R&D Activities is essential because of the complexity of developing generic PA models and generic safety cases
- The temporal framework (or timeline) for “Generic R&D Needed” appeared to vary a lot between breakout sessions and could improve in the future with more intensive inter-group calibration prior to, and at the beginning of, the Workshop
- “Calibration” on the assignment of ISC and SAL metric values is important to develop prior to, and at the beginning of, the Workshop
- Adding a metric for level of effort (LOE) for individual activities would be very useful
- Integration of DPC-relevant parameters into all modeling activities is needed

Much has been accomplished since 2012, through R&D in the U.S. Program and through international collaborations. Appendix J of the 2019 Roadmap Update illustrates the amount of progress made by the R&D program by providing a comparison between the consensus SAL descriptive values developed in the 2019 Update Workshop with the comparable “State-of-the-Art” assignments in the 2012 Roadmap (DOE 2012, Appendix A). This comparison is not exact because FEPs (“Issues”) were evaluated in 2012, while R&D Activities were evaluated in 2019. However, a comparison of the 2019 R&D Activity SAL values with the “primary” FEP state-of-the-art values from 2012 indicates that significant progress has been made because many SAL scores have improved. Table 5-6 is an example of this, extracted from Appendix J of Sevougian et al. (2019b), illustrating the progress that has been made for a few selected activities, across the various R&D groupings. [See Table 5-7 for a definition of the SAL values used in 2019.]

Although significant R&D progress has been made since 2012, as indicated in Table 5-6 (and in more detail in Appendix J of Sevougian et al. (2019b)), the 2019 R&D Roadmap Update reflects the need for continuing R&D on many of the 2012 R&D Issues, plus some obvious new priorities, such as R&D on disposal of DPCs (dual purpose canisters), which now contain a significant fraction of the Nation’s spent fuel.

The 2019 R&D prioritization effort is now closely integrated with the development of the SFWST Campaign’s generic performance assessment model/software framework (the GDSA Framework), so that much of the ongoing R&D work is designed to directly support the development of improved process models that feed the PA model and software. Given the importance of post-closure performance assessment in building confidence in the safety case, this is believed to be appropriate and essential. Section 4 of this report provided additional detail regarding the integration of individual R&D Activities and associated models with the GDSA Framework. This integration will be essential for enhancing understanding and confidence in a safety case for a repository in any geologic media, and in support of future decisions regarding site screening, selection and characterization.

Table 5-6. Comparison of 2012 “State-of-the-Art” with 2019 SAL values for R&D activities.

R&D Activity	R&D Activity Name	Primary FEP	2012 Roadmap “State of the Art” (for the Primary FEP)	2019 Roadmap Update “State of the Art” Level (SAL)
A-2	Simplified Representation of THMC processes in EBS and host rock, e.g., clay illitization	2.1.04.01 Evolution and Degradation of Backfill/buffer	Fundamental Gaps in Method, Fundamental Data Needs	Improved Representation
A-7	Analysis of clay hydration/dehydration and alteration under various environmental conditions	2.2.08.06 Flow through EDZ (clay/shale)	Fundamental Gaps in Method, Fundamental Data Needs	Fundamental Gaps in Method or Fundamental Data Needs, or Both
C-1	Discrete Fracture Network (DFN) Model	2.2.09.51 Advection of Dissolved Radionuclides in Host Rock (crystalline)	Fundamental Gaps in Method, Fundamental Data Needs	Improved Representation
C-15	Design improved backfill and seal materials (GAP)	2.1.04.01 Evolution/Degradation of Backfill/buffer	Fundamental Gaps in Method, Fundamental Data Needs	Fundamental Gaps in Method or Fundamental Data Needs, or Both
E-1	SNF Degradation (& FMDM)	2.1.02.01 SNF Degradation	Fundamental Gaps in Method, Fundamental Data Needs	Improved Defensibility
E-2	SNF Degradation testing activities	2.1.02.01 SNF Degradation	Fundamental Gaps in Method, Fundamental Data Needs	Improved Representation
E-5	Corrosion Products - incorporation of radionuclides	2.1.09.02 Chemical Characteristics of Water in Waste Packages	Fundamental Gaps in Method, Fundamental Data Needs	Fundamental Gaps in Method or Fundamental Data Needs, or Both/
I-1	Radionuclide transport as pseudo-colloids, Grimsel	2.2.09.64 Radionuclide Release from Host Rock (crystalline or clay/shale/salt)	Fundamental Gaps in Method, Fundamental Data Needs	Improved Defensibility
I-2	FEBEX-DP Modeling: Dismantling phase of the long-term FEBEX heater test - Modeling	2.1.04.01 Evolution and Degradation of Backfill/buffer	Fundamental Gaps in Method, Fundamental Data Needs	Improved Representation
P-1	CSNF repository argillite reference case	FEP (0.1.10.01 Model Issues) not explicitly scored, but “Disposal System Modeling” rated as a “High” priority “Cross-Cutting” issue in 2012	Not Evaluated	Improved Representation
P-6	(Pseudo) Colloid-Facilitated Transport Model	2.2.09.61 Radionuclide Transport thru EDZ	Fundamental Gaps in Method, Fundamental Data Needs	Improved Defensibility
S-2	Salt Coupled THM processes, creep closure of excavations	2.2.07.01 Mechanical Effects on Host Rock (Salt)	Fundamental Gaps in Method Fundamental Data Needs	Improved Representation
S-13	Acid gas generation, fate, and transport (GAP)	2.2.12.02 Effects of Gas on Flow Through the Geosphere (Salt)	Fundamental Gaps in Method, Fundamental Data Needs	Fundamental Gaps in Method or Fundamental Data Needs, or Both

Table 5-7. 2019 SAL (State-of-the-Art Level) metric values and definitions.

SAL	SAL Descriptive Value	SAL Definition
5	<i>Fundamental Gaps in Method or Fundamental Data Needs, or Both</i>	The representation of an issue (conceptual and/or mathematical, experimental) is under development, and/or the data or parameters in the representation of an issue (process) is being gathered
4	<i>Improved Representation</i>	Methods and data exist, and the representation may be reasonable but there is not widely-agreed upon confidence in the representation (scientific community and other stakeholders).
3	<i>Improved Defensibility</i>	Focuses on improving the technical basis and defensibility of how an issue (process) is represented by data and/or models
2	<i>Improved Confidence</i>	The representation of an issue is technically defensible, but improved confidence would be beneficial (i.e., lead to more realistic representation).
1	<i>Well Understood</i>	The representation of an issue (process) is well developed, has a strong technical basis, and is defensible. Additional R&D would add little to the current understanding

6. SUMMARY AND PATH FORWARD

This report documents progress made in Geologic Disposal Safety Assessment (GDSA) R&D in FY 2019 and provides an overview of GDSA development since 2010. In 2010, the Department of Energy initiated the Used Fuel Disposition (UFD) Campaign. The purpose of the UFD Campaign was, in part, to focus GDSA R&D on generic repository concepts and new potential host rocks. This report summarizes the evolution of GDSA performance assessment (PA), how PA priorities were initially determined and have been recently updated, and how GDSA PA capabilities have advanced under the UFD Campaign through FY 2017 and under the SFWST Campaign thereafter.

In the early years of the UFD Campaign, a major effort was made to assess and prioritize disposal R&D priorities (DOE 2012). In 2013, after a review of available codes and methodologies (Freeze and Vaughn 2012), a new GDSA computational framework was established. This framework today is known as GDSA Framework. The primary codes of this framework are PFLOTRAN and Dakota. PFLOTRAN is a multiphase flow and reactive transport code designed for simulating flow and reactive transport in the subsurface. Dakota is an uncertainty quantification and sensitivity analysis code. These codes are open source, freely available, and built for high performance computing. The full set of codes and tools in GDSA Framework is used to probabilistically simulate the various possible mechanisms and pathways for release and migration of radionuclides from waste packages in a deep geologic repository to the biosphere.

Since 2013, many new capabilities have either been added to PFLOTRAN or are in the process of being added. They include:

- Radionuclide processes (decay and ingrowth in all phases, isotope partitioning between phases, solubility limits, mineral-specific linear sorption, species-specific diffusion, colloids);
- Source term processes (waste form process models, waste package degradation, waste form dissolution, instantaneous release fractions, decay and ingrowth within the waste form, criticality);
- Geophysical properties (discrete fracture networks, density-driven flow, permeability scaling, buffer evolution);
- Biosphere processes (well water ingestion dose model, dose effects of sorption enhancement of unsupported radionuclides);
- Uncertainty quantification and sensitivity analysis (uncertainty sampling, stepwise linear regression, partial correlation coefficients, rank transformations, sensitivity indices); and
- Coupled surrogate models (polynomial chaos, neural network, nearest neighbors).

Features and improvements since 2013 are summarized in this report with an emphasis on advances in FY 2019.

An overview of computational improvements to PFLOTRAN and GDSA Framework is also provided in this report. Computational improvements include:

- A process model coupling framework added to PFLOTRAN;
- Improved analytical derivatives for PFLOTRAN;
- New and improved nonlinear solvers for PFLOTRAN;
- A tool for calculating physically consistent boundary conditions for cells in which a new phase appears or an initial phase disappears;
- Enhanced restart capability; and

- New mesh generation tools.

In FY 2019, code development primarily focused on four activities. One involved the development of a reduced-order criticality model, which is being added to PFLOTRAN to investigate potential impacts to repository performance of criticalities that may occur in dual purpose canisters (DPCs) in an underground repository. This new capability effectively simulates the changes in radionuclide inventories and heat output resulting from a critical event. Another code development activity involved optimizing the Newton-Raphson nonlinear solvers for the unsaturated alluvium reference case and developing a new trust region nonlinear solver. Development of these solvers is needed to improve convergence in unsaturated reference cases with high heat loads. Surrogate models to simulate the fuel matrix degradation (FMD) model is the third code development activity in FY 2019. The new FMD surrogate models are highly accurate relative to the FMD process model with faster execution and, when coupled to PFLOTRAN, will allow PA simulations to account for the effects of radiolysis and growth of an alteration layer when calculating spent fuel dissolution rates. The fourth code development activity in FY 2019 involves the testing and development of an open source meshing generator, VoroCrust, which may become a standard mesh generator for GDSA Framework.

In addition to code development, the GDSA team increased its efforts in FY 2019 regarding PFLOTRAN quality assurance (QA). Major progress was made in developing QA documentation for PFLOTRAN, including drafts of a software quality assurance plan, a requirements document, and a verification and validation document. Such documentation will be needed when PFLOTRAN is applied in a regulatory environment. In addition, a QA test harness was developed for the verification test suite, and several new 1D and 2D verification tests were successfully performed and added to the test suite.

An important responsibility of the GDSA team is to integrate with disposal R&D activities across the SFWST Campaign to ensure that R&D activities support the safety cases being developed. In FY 2019, the GDSA team conducted a special multi-day, campaign-wide meeting to assess progress in disposal R&D since the 2012 roadmap and to update roadmap priorities going forward. This work produced the 2019 roadmap update (Sevougian et al. 2019b), a report that will be highly useful for planning and prioritizing disposal R&D activities over the next several years. A comparison of the 2019 R&D Activity SAL values with the “primary” FEP state-of-the-art (SAL) values from 2012 indicates that significant progress has been made because many SAL scores have improved. The 2019 R&D Roadmap Update reflects the need for continuing R&D on many of the 2012 R&D Issues, plus some obvious new priorities, such as R&D on disposal of DPCs (dual purpose canisters), which now contain a significant fraction of the Nation’s spent fuel. The 2019 R&D prioritization effort is now closely integrated with the development of the SFWST Campaign’s generic performance assessment model/software framework (the GDSA Framework), so that much of the ongoing R&D work is designed to directly support the development of improved process models that feed the PA model and software. Given the importance of post-closure performance assessment in building confidence in the safety case, this is believed to be appropriate and essential. Integration will be essential for enhancing understanding and confidence in a safety case for a repository in any geologic media, and in support of future decisions regarding site screening, selection and characterization.

Each year, our GDSA Framework improves as additional modelers and programmers from around the world use, apply, and contribute to its development (Section 2.3.4). GDSA Framework is accessible to everyone because the primary codes, PFLOTRAN and Dakota, are open source, available for free download, and have supporting documentation online. The GDSA team has worked to increase the number of users and participants by

- Maintaining a collaborative web site (pa.sandia.gov);
- Expanding online documentation of verification testing, generic reference cases, and code features;
- Developing quality assurance documentation and a user manual;

- Conducting PFLOTRAN short courses (in FY 2019 in New Mexico, Australia, and Switzerland); and
- Presenting multiple papers and posters on GDSA Framework capabilities at international forums.

Outreach like this supports a primary objective of the GDSA work package by facilitating testing of, and feedback on, PFLOTRAN and GDSA Framework and by increasing the likelihood outside users will contribute directly to code development in the future.

The ability to simulate increasingly complex repository reference cases continues to affirm that HPC-capable codes can be used to simulate important multi-physics couplings directly in a total system safety assessment. The generic repository systems modeled to date indicate that PFLOTRAN and its coupled codes can simulate complex coupled processes in a multi-kilometer domain while simultaneously simulating sub-meter-scale coupled behavior in the repository. Continued development is needed to ensure GDSA Framework is ready for application to potential sites that may be selected in the future. The challenge is to address the remaining needs using available resources. Meeting this challenge will require close integration with technical teams across the SFWST Campaign.

7. REFERENCES

- Aaltonen, I. (ed.), Engstrom, J., Front, K., Gehor, S., Kosunen, P., Karki, A., Mattila, J., Paananen, M., and Paulamaki, S., 2016. Geology of Olkiluoto, POSIVA Report 2016-16. 404 p.
- Aaltonen, I. e., J. Engstrom, K. Front, S. Gehor, P. Kosunen, A. Karki, J. Mattila, M. Paananen and S. Paulamaki (2016). Geology of Olkiluoto. POSIVA Report 2016-16. POSIVA, Finland.
- Adams, B. M., K. R. Dalbey, M. S. Eldred, L. P. Swiler, W. J. Bohnhoff, J. P. Eddy, D. M. Vigil, P. D. Hough and S. Lefantzi (2012). DAKOTA, A Multilevel Parallel Object-Oriented Framework for Design Optimization, Parameter Estimation, Uncertainty Quantification, and Sensitivity Analysis: Version 5.2+ User's Manual. SAND2010-2183. Sandia National Laboratories, Albuquerque, New Mexico.
- Adams, B. M., M. S. Ebeida, M. S. Eldred, G. Geraci, J. D. Jakeman, K. A. Maupin, J. A. Monschke, J. A. Stephens, L. P. Swiler, D. M. Vigil, T. M. Wildey and e. al. (2018a). Dakota, A Multilevel Parallel Object-Oriented Framework for Design Optimization, Parameter Estimation, Uncertainty Quantification, and Sensitivity Analysis: Version 6.8 User's Manual. Sandia National Laboratories. Albuquerque, NM: 384.
- Adams, B. M., M. S. Ebeida, M. S. Eldred, G. Geraci, J. D. Jakeman, K. A. Maupin, J. A. Monschke, J. A. Stephens, L. P. Swiler, D. M. Vigil, T. M. Wildey, W. J. Bohnhoff, K. R. Dalbey, J. P. Eddy, J. R. Frye, R. W. Hooper, K. T. Hu, P. D. Hough, M. Khalil, E. M. Ridgway, J. G. Winokur and A. Rushdi (2018b). Dakota, A Multilevel Parallel Object-Oriented Framework for Design Optimization, Parameter Estimation, Uncertainty Quantification, and Sensitivity Analysis: Version 6.8 Theory Manual. SAND2014-4253, Updated May 8, 2018. Sandia National Laboratories, Albuquerque, New Mexico.
- Adams, B. M., M. S. Ebeida, M. S. Eldred, J. D. Jakeman, L. P. Swiler, W. J. Bohnhoff, K. R. Dalbey, J. P. Eddy, K. T. Hu, D. M. Vigil, L. E. Baumann and P. D. Hough (2013). Dakota, a Multilevel Parallel Object-Oriented Framework for Design Optimization, Parameter Estimation, Uncertainty Quantification, and Sensitivity Analysis, Version 5.3.1+ Theory Manual. SAND2011-9106, Updated May 22, 2013, <http://dakota.sandia.gov/>. Sandia National Laboratories, Albuquerque, New Mexico.
- ANDRA (2005). Dossier 2005 Argile: Phenomological evolution of a geological repository. National Radioactive Waste Management Agency, Paris, France.
- ASME (2015). Quality Assurance Requirements for Nuclear Facility Applications. ASME NQA-1-2015. American Society of Mechanical Engineers (ASME), New York, New York.
- Avasarala, S., P. C. Lichtner, A. M. S. Ali, R. Gonzalez-Pinzon, J. M. Blake and J. M. Cerrato (2017). "Reactive Transport of U and V from Abandoned Uranium Mine Wastes," *Environmental Science & Technology*, **51**(21):12385-12393.
- Balay, S., J. Brown, K. Buschelman, V. Eijkhout, W. D. Gropp, D. Kaushik, M. G. Knepley, L. Curfman McInnes, B. F. Smith and H. Zhang (2013). PETSc Users Manual. ANL-95/11 – Revision 3.4. Argonne National Laboratory, Argonne, Illinois.
- Belcher, W. R. e. (2004). Death Valley regional ground-water flow system, Nevada and California—Hydrogeologic and transient ground-water flow model. U.S. Geological Survey Scientific Investigations Report 2004–5205.
- Bianchi, M., H.-H. Liu and J. T. Birkholzer (2015). "Radionuclide transport behavior in a generic geological radioactive waste repository," *Ground Water*, **53**(3):440-451.
- Birkholzer, J., B. Faybishenko, P. Dobson, P. M. Fox, J. Rutqvist, L. Zheng, F. A. Caporuscio, P. Reimus, H. Viswanathan, C. F. Jové Colón, Y. Wang, K. Kuhlman, E. Matteo, K. McMahon and M. Zavarin (2018). International Collaboration Activities in Different Geologic Disposal Environments. LBNL-2001178. Lawrence Berkeley National Laboratory, Berkeley, California.
- Blacker, T., S. J. Owen, M. L. Staten, R. W. Quador, B. Hanks, B. Clark, R. J. Meyers, C. Ernst, K. Merkley, R. Morris, C. McBride, C. Stimpson, M. Plooster and S. Showman (2016). CUBIT Geometry and

- Mesh Generation Toolkit 15.2 User Documentation. SAND2016-1649 R. Sandia National Laboratories, Albuquerque, New Mexico.
- Brady, P. V., B. W. Arnold, G. A. Freeze, P. N. Swift, S. J. Bauer, J. L. Kanney, R. P. Rechard and J. S. Stein (2009). Deep borehole disposal of high-level radioactive waste. Sandia National Laboratories, Albuquerque, New Mexico.
- Caporuscio, F. A., H. Boukhalfa, M. C. Cheshire and M. Ding (2014). Brine Migration Experimental Studies for Salt Repositories. LA-UR-26603. Los Alamos National Laboratory, Los Alamos, New Mexico.
- Caporuscio, F. A., H. Boukhalfa, M. C. Cheshire, A. B. Jordan and M. Ding (2013). Brine Migration Experimental Studies for Salt Repositories. LA-UR-13-27240. Los Alamos National Laboratory, Los Alamos, New Mexico.
- Carter, J. T., A. J. Luptak, J. Gastelum, C. Stockman and A. Miller (2013). Fuel Cycle Potential Waste Inventory for Disposition. FCRD-USED-2010-000031 Rev 6. Savannah River National Laboratory, Aiken, South Carolina.
- Carter, J. T., P. O. Rodwell, B. Robinson and B. Kehrman (2012). Defense Waste Salt Repository Study. FCRD-UFD-2012-000113, May 5, 2012.
- Chen, X., G. Hammond, C. Murray, M. Rockhold, V. Vermeul and J. Zachara (2013). "Applications of ensemble-based data assimilation techniques for aquifer characterization using tracer data at Hanford 300 area," *Water Resources Research*, **49**:7064-7076.
- Chen, X., H. Murakami, M. Hahn, G. E. Hammond, M. L. Rockhold, J. M. Zachara and Y. Rubin (2012). "Three-Dimensional Bayesian Geostatistical Aquifer Characterization at the Hanford 300 Area using Tracer Test Data," *Water Resources Research*, **48**.
- Cho, W. J., J. S. Kim, C. Lee and H. J. Choi (2013). "Gas permeability in the excavation damaged zone at KURT," *Engineering Geology*, **164**:222-229.
- Clayton, D., G. Freeze, T. Hadgu, E. Hardin, L. Lee, J. Prouty, R. Rogers, W. M. Nutt, J. Birkholzer, H. H. Liu, L. Zheng and S. Chu (2011). Generic Disposal System Modeling - Fiscal Year 2011 Progress Report. SAND 2011-5828P, FCRD-USED-2011-000184. Sandia National Laboratories, Albuquerque, New Mexico.
- de Vries, L. M., J. Molinero, H. Ebrahimi, U. Svensson, P. Lichtner and E. Abarca (2013). "Regional Scale HPC Reactive Transport Simulation of Nuclear Spent Fuel Repository in Forsmark, Sweden," Joint 8th International Conference on Supercomputing in Nuclear Applications (SNA) / 4th Monte Carlo Meeting (MC), Paris, France, Oct 27-31.
- DOE (2008). Yucca Mountain Repository License Application Safety Analysis Report. DOE/RW-0573, Revision 1, <http://www.nrc.gov/waste/hlw-disposal/yucca-lic-app/yucca-lic-app-safety-report.html#1>. US Department of Energy, Washington, DC.
- DOE (2011). Used Fuel Disposition Campaign Disposal Research and Development Roadmap. FCRD-USED-2011-000065 REV 0. Fuel Cycle Technologies, Office of Nuclear Energy, US Department of Energy, Washington, DC.
- DOE (2012). Used Fuel Disposition Campaign Disposal Research and Development Roadmap. FCR&D-USED-2011-000065, REV 1. U.S. DOE Office of Nuclear Energy, Used Fuel Disposition, Washington, D.C.
- DOE (2013a). Administrative Changes to DOE O 414.1d, Quality Assurance. DOE O 414.1D CHG 1 5-8-2013. US Dept. of Energy (DOE) National Nuclear Security Administration (NNSA), Washington, D.C.
- DOE (2013b). Strategy for the Management and Disposal of Used Nuclear Fuel and High-Level Radioactive Waste, January 2013. U.S. Department of Energy, Washington, DC. <http://energy.gov/downloads/strategy-management-and-disposal-used-nuclear-fuel-and-high-level-radioactive-waste>.
- DOE (2014). Title 40 CFR Part 191 Subparts B and C Compliance Recertification Application 2014 for the Waste Isolation Pilot Plant, Appendix SOTERM-2014, Actinide Chemistry Source Term. DOE/WIPP 15-3503. U.S. Department of Energy, Carlsbad, New Mexico.

- Driscoll, D. G., C. J.M., J. E. Williamson and L. D. Putnam (2002). Hydrology of the Black Hills area, South Dakota. Water-Resources Investigations Report 02-4094. U.S. Geological Survey Washington, D.C.
- Fahrenback, M. D., F. V. Steece, J. F. Sawyer, K. A. McCormick, G. L. McGillivray, L. D. Schultz and J. A. Redden (2010). South Dakota Stratigraphic Correlation Chart. Oil and Gas Investigation 3. South Dakota Geological Survey, South Dakota.
- Finsterle, S., M. Kowalsky, F. Kober and S. Vomvoris (2017). HotBENT – Preliminary Design Study of Phenomenological Aspects. NAB 17-30.
- Follin, S., L. Hartley, I. Rhen, P. Jackson, S. Joyce, D. Roberts and B. Swift (2014). "A methodology to constrain the parameters of a hydrogeological discrete fracture network model for sparsely fractured crystalline rock, exemplified by data from the proposed high-level nuclear waste repository site at Forsmark, Sweden," *Hydrogeology Journal*, **22**(2):313-331.
- Freeze, G., W. P. Gardner, P. Vaughn, S. D. Sevougian, P. Mariner, V. Mousseau and G. Hammond (2013a). Enhancements to the Generic Disposal System Modeling Capabilities. SAND2013-10532P, FCRD-UFD-2014-000062. Sandia National Laboratories, Albuquerque, New Mexico.
- Freeze, G., P. E. Mariner, J. A. Blink, F. A. Caporuscio, J. E. Houseworth and J. C. Cunnane (2011). Disposal System Features, Events, and Processes (FEPs): FY11 Progress Report. FCRD-USED-2011-000254. SAND2011-6059P. Sandia National Laboratories, Albuquerque, New Mexico.
- Freeze, G., E. Stein, P. V. Brady, C. Lopez, D. Sassani, K. Travis and F. Gibb (2019). Deep Borehole Disposal Safety Case. SAND2019-1915. Sandia National Laboratories, Albuquerque, New Mexico.
- Freeze, G., E. Stein, L. Price, R. J. Mackinnon and J. Tillman (2016). Deep Borehole Disposal Safety Analysis. FCRD-UFD-2016-000075 Rev. 0, SAND2016-10949R. Sandia National Laboratories, Albuquerque, New Mexico.
- Freeze, G. and P. Vaughn (2012). Development of an Advanced Performance Assessment Modeling Capability for Geologic Disposal of Nuclear Waste: Methodology and Requirements. SAND2012-10208. Sandia National Laboratories, Albuquerque, New Mexico.
- Freeze, G., M. Voegele, P. Vaughn, J. Prouty, W. M. Nutt, E. Hardin and S. D. Sevougian (2013b). Generic Deep Geologic Disposal Safety Case. FCRD-UFD-2012-000146 Rev. 1, SAND2013-0974P. Sandia National Laboratories, Albuquerque, New Mexico.
- Freeze, G. A., E. R. Stein, P. V. Brady, C. Lopez, K. Travis and F. Gibb (2017). Deep Borehole Disposal Safety Case. SFWD-SFWST-2017-000009; SAND2017-xxxxR (in progress). Sandia National Laboratories, Albuquerque, New Mexico.
- Gardner, W. P., G. Hammond and P. Lichtner (2015). "High Performance Simulation of Environmental Tracers in Heterogeneous Domains," *Groundwater*, **53**:71-80.
- Gaus, I. and F. Kober (2014). FEBEX-DP Project Plan. NAGRA, Switzerland.
- Hammond, G., P. Lichtner and C. Lu (2007). "Subsurface multiphase flow and multicomponent reactive transport modeling using high performance computing," *Journal of Physics: Conference Series* **78**:1-10.
- Hammond, G. E. and P. Lichtner (2010). "Field-scale modeling for the natural attenuation of uranium at the Hanford 300 area using high performance computing," *Water Resources Research*, **46**.
- Hammond, G. E., P. C. Lichtner, C. Lu and R. T. Mills (2011a). "PFLOTRAN: Reactive Flow and Transport Code for Use on Laptops to Leadership-Class Supercomputers." Groundwater Reactive Transport Models. F. Zhang, G. T. Yeh and J. Parker. Bentham Science Publishers.
- Hammond, G. E., P. C. Lichtner, R. T. Mills and C. Lu (2008). "Toward petascale computing in geosciences: application to the Hanford 300 Area," *Journal of Physics Conference Series*, **125**:12051-12051.
- Hammond, G. E., P. C. Lichtner and M. L. Rockhold (2011b). "Stochastic simulation of uranium migration at the Hanford 300 Area," *Journal of Contaminant Hydrology*, **120-121**:115-128.
- Hansen, F. D., E. L. Hardin, R. P. Rechar, G. A. Freeze, D. C. Sassani, P. V. Brady, C. M. Stone, M. J. Martinez, J. F. Holland, T. Dewers, K. N. Gaither, S. R. Sobolik and R. T. Cygan (2010). Shale

- Disposal of U.S. High-Level Radioactive Waste. Sandia National Laboratories, Albuquerque, New Mexico.
- Hanson, B., H. Alsaed, C. Stockman, D. Enos, R. Meyer and K. Sorenson (2012). Gap Analysis to Support Extended Storage of Used Nuclear Fuel, Rev. 0. PNNL-20509, FCRD-USED-2011-000136 Rev. 0. Pacific Northwest National Laboratory, Richland, Washington.
- Hardin, E., D. Clayton, R. Howard, J. M. Scaglione, E. Pierce, K. Banerjee, M. D. Voegelé, H. Greenberg, J. Wen, T. A. Buscheck, J. T. Carter, T. Severynse and W. M. Nutt (2013). Preliminary Report on Dual-Purpose Canister Disposal Alternatives (FY13). FCRD-UFD-2013-000171 Rev. 0.
- Hardin, E. and E. Kalinina (2016). Cost Estimation Inputs for Spent Nuclear Fuel Geologic Disposal Concepts. Sandia National Laboratories. Albuquerque, NM: 57.
- Harrington, J. (2016). DECOVALEX 2019, Specification for DECOVALEX-2019: Task A: modElliNg Gas INjection ExpERiments (ENGINEER).
- Heilweil, V. M. and L. E. Brooks (2010). Conceptual model of the Great Basin Carbonate and Alluvial Aquifer System. US Geological Survey Scientific Investigations Report 2010-5193. US Geological Survey, Washington, D.C.
- Helton, J. C. and F. J. Davis (2000). "Sampling-Based Methods." *Sensitivity Analysis*. A. Saltelli, K. Chan and E. M. Scott. Wiley, Chichester, U.K., 102-153.
- Helton, J. C. and F. J. Davis (2003). "Latin hypercube sampling and the propagation of uncertainty in analyses of complex systems," *Reliability Engineering & System Safety*, **81**(1):23-69.
- Helton, J. C., J. D. Johnson, C. J. Sallaberry and C. B. Storlie (2006). Survey of Sampling-Based Methods for Uncertainty and Sensitivity Analysis. Sandia National Laboratories, Albuquerque, New Mexico.
- Howard, B. A., M. B. Crawford, D. A. Galson and M. G. Marietta (2000). "Regulatory basis for the Waste Isolation Pilot Plant performance assessment," *Reliability Engineering & System Safety*, **69**(1-3):109-127.
- Hyman, J. D., S. Karra, N. Makedonska, C. W. Gable, S. L. Painter and H. S. Viswanathan (2015a). "dfnWorks: A discrete fracture network framework for modeling subsurface flow and transport," *Computers & Geoscience*, **84**:10-19.
- Hyman, J. D., S. L. Painter, H. Viswanathan, N. Makedonska and S. Karra (2015b). "Influence of injection mode on transport properties in kilometer-scale three-dimensional discrete fracture networks," *Water Resources Research*, **51**(9):7289-7308.
- IAEA (2003). "Reference Biospheres" for Solid Radioactive Waste Disposal. International Atomic Energy Agency, Vienna, Austria.
- IAEA (2006). Geological Disposal of Radioactive Waste. International Atomic Energy Agency, Vienna, Austria.
- IAEA (2011). Disposal of Radioactive Waste, Specific Safety Requirements. IAEA Safety Standards Series No. SSG-23. IAEA, Vienna, Austria.
- IAEA (2012). The Safety Case and Safety Assessment for the Disposal of Radioactive Waste. Specific Safety Guide SSG-23. International Atomic Energy Agency, Vienna, Austria.
- Iraola, A., P. Trinchero, S. Karra and J. Molinero (2019). "Assessing dual continuum method for multicomponent reactive transport," *Computers & Geosciences*, **130**:11-19.
- Iwatsuki, T. (2016). Task C: GREET, Hydro-mechanical-chemical-biological processes during groundwater recovery. Presentation given at 1st DECOVALEX 2019 Workshop, May 2016. Berkeley, California.
- Jerden, J., K. E. Frey and W. Ebert (2017). Spent Fuel Matrix Degradation and Canister Corrosion: Quantifying the Effect of Hydrogen. Spent Fuel and Waste Science and Technology Project, SFWD-SFWST-2017-000039. Argonne National Laboratory, Lemont, Illinois.
- Jerden, J., G. Hammond, J. M. Copple, T. Cruse and W. Ebert (2015). Fuel Matrix Degradation Model: Integration with Performance Assessment and Canister Corrosion Model Development. FCRD-UFD-2015-000550. US Department of Energy, Washington, DC.

- Jové Colón, C. F., C. Payne, A. Knight, T. Ho, J. Rutqvist, K. Kim, H. Xu, Y. Guglielmi, J. Birkholzer, F. A. Caporuscio, K. B. Sauer, M. J. Rock, L. M. Houser, J. Jerden, V. K. Gattu and W. Ebert (2018). Evaluation of Used Fuel Disposition in Clay-Bearing Rock. M2SF-18SN010301051, SAND2018-12044 R. Sandia National Laboratories, Albuquerque, New Mexico.
- Jové Colón, C. F., Y. Wang, T. Hadgu, L. Zheng, J. Rutqvist, H. Xu, K. Kim, M. Voltolini, X. Cao, P. M. Fox, P. S. Nico, F. A. Caporuscio, K. E. Norskog, M. Zavarin, T. J. Wolery, C. Atkins-Duffin, J. Jerden, V. K. Gattu, W. Ebert, E. C. Buck and R. S. Wittman (2017). Evaluation of Used Fuel Disposition in Clay-Bearing Rock. M2SF-18SN010301051, SAND2018-12044 R. Sandia National Laboratories, Albuquerque, New Mexico.
- Jové Colón, C. F., P. F. Weck, D. C. Sassani, L. Zheng, J. Rutqvist, C. I. Steefel, K. Kim, S. Nakagawa, J. Houseworth, J. Birkholzer, F. A. Caporuscio, M. Cheshire, M. S. Rearick, M. K. McCarney, M. Zavarin, A. Benedicto-Cordoba, A. B. Kersting, M. Sutton, J. L. Jerden, K. E. Frey, J. M. Copple and W. L. Ebert (2014). Evaluation of Used Fuel Disposition in Clay-Bearing Rock. FCRD-UFD-2014-000056, SAND2014-18303 R. Sandia National Laboratories, Albuquerque, New Mexico.
- Joyce, S., L. Hartley, D. Applegate, J. Hoek and P. Jackson (2014). "Multi-scale groundwater flow modeling during temperate climate conditions for the safety assessment of the proposed high-level nuclear waste repository site at Forsmark, Sweden," *Hydrogeology Journal*, **22**(6):1233-1249.
- Karra, S., S. L. Painter and P. C. Lichtner (2014). "Three-phase numerical model for subsurface hydrology in permafrost-affected regions (PFLOTTRAN-ICE v1.0)," *Cryosphere*, **8**(5):1935-1950.
- Kienzler, B., M. Altmaier, C. Bube and V. Metz (2012). Radionuclide Source Term for HLW Glass, Spent Nuclear Fuel, and Compacted Hulls and End Pieces (CSD-C Waste). KIT Scientific Reports 7624. Karlsruhe Institute of Technology, Baden-Württemberg, Germany.
- Kuhlman, K. L. (2014). Summary Results for Brine Migration Modeling Performed by LANL, LBNL, and SNL for the UFD Program. FCRD-UFD-2014-000071, SAND2014-18217R. Sandia National Laboratories, Albuquerque, New Mexico.
- Kuhlman, K. L., C. M. Lopez, M. M. Mills, J. M. Rimsza and D. C. Sassani (2018). Evaluation of Spent Nuclear Fuel Disposition in Salt (FY18). M2SF-18SN010303031, SAND2018-11355R. Sandia National Laboratories, Albuquerque, New Mexico.
- Kuhlman, K. L., E. N. Matteo, T. Hadgu, B. Reedlunn, S. R. Sobolik, M. M. Mills, L. D. Kirkes, Y. L. Xiong and J. P. Icenhower (2017). Status Report on Laboratory Testing and International Collaborations in Salt. SFWD-SFWST-2017-000100. Sandia National Laboratories, Albuquerque, New Mexico.
- Kumar, J., N. Collier, G. Bisht, R. T. Mills, P. E. Thornton, C. M. Iversen and V. Romanovsky (2016). "Modeling the spatiotemporal variability in subsurface thermal regimes across a low-relief polygonal tundra landscape," *Cryosphere*, **10**(5):2241-2274.
- Le Gratiet, L., S. Marelli and B. Sudret (2017). "Metamodel-Based Sensitivity Analysis: Polynomial Chaos Expansions and Gaussian Processes." *Handbook of Uncertainty Quantification*. R. G. e. al. Springer International Publishing, Switzerland 1289-1325.
- Lewis, S. and M. Holness (1996). "Equilibrium halite-H₂O dihedral angles: High rock-salt permeability in the shallow crust?," *Geology*, **24**(5):431-434.
- Lichtner, P. C. and G. E. Hammond (2012). Quick Reference Guide: PFLOTTRAN 2.0 (LA-CC-09-047) Multiphase-Multicomponent-Multiscale Massively Parallel Reactive Transport Code. LA-UR-06-7048. December 8, 2012. Los Alamos National Laboratory, Los Alamos, New Mexico.
- Lichtner, P. C., G. E. Hammond, C. Lu, S. Karra, G. Bisht, B. Andre, R. Mills and J. Kumar. (2015). "PFLOTTRAN User Manual: A Massively Parallel Reactive Flow and Transport Model for Describing Surface and Subsurface Processes," http://www.pflotran.org/docs/user_manual.pdf.
- Lu, C. and P. C. Lichtner (2007). "High resolution numerical investigation on the effect of convective instability on long term CO₂ storage in saline aquifers," *Journal of Physics Conference Series*, **78**:U320-U325.

- Mariner, P. E., W. P. Gardner, G. E. Hammond, S. D. Sevougian and E. R. Stein (2015). Application of Generic Disposal System Models. FCRD-UFD-2015-000126, SAND2015-10037 R. Sandia National Laboratories, Albuquerque, New Mexico.
- Mariner, P. E., G. E. Hammond and J. M. Frederick (2017a). "Isotope Partitioning, Decay, and Ingrowth across Multiple Phases in PFLOTRAN Code of GDSA Framework," Migration 2017 - 16th International Conference on the Chemistry and Migration Behaviour of Actinides and Fission Products in the Geosphere, Barcelona, Spain, September 10-15, 2017.
- Mariner, P. E., E. R. Stein, E. Basurto and M. Nole (2018a). "Performance assessment of a reference nuclear waste repository in crystalline rock: effects of variability in fracture network realizations," Proceedings of the 2018 IGSC Symposium, Rotterdam, Netherlands, October 10-11, OECD Nuclear Energy Agency.
- Mariner, P. E., E. R. Stein, J. M. Frederick, S. D. Sevougian and G. E. Hammond (2017b). Advances in Geologic Disposal System Modeling and Shale Reference Cases. SFWD-SFWST-2017-000044, SAND2017-10304 R. Sandia National Laboratories, Albuquerque, New Mexico.
- Mariner, P. E., E. R. Stein, J. M. Frederick, S. D. Sevougian, G. E. Hammond and D. G. Fascitelli (2016). Advances in Geologic Disposal System Modeling and Application to Crystalline Rock. FCRD-UFD-2016-000440, SAND2016-9610 R. Sandia National Laboratories, Albuquerque, New Mexico.
- Mariner, P. E., E. R. Stein, S. D. Sevougian, L. J. Cunningham, J. M. Frederick, G. E. Hammond, T. S. Lowry, S. Jordan and E. Basurto (2018b). Advances in Geologic Disposal Safety Assessment and an Unsaturated Alluvium Reference Case. SFWD-SFWST-2018-000509, SAND2018-11858 R. Sandia National Laboratories, Albuquerque, New Mexico.
- Mariner, P. E., L. P. Swiler, D. T. Seidl, B. J. Debusschere, J. Vo, J. M. Frederick and J. L. Jerden (2019). "High Fidelity Surrogate Modeling of Fuel Dissolution for Probabilistic Assessment of Repository Performance," International High-Level Radioactive Waste Conference, Knoxville, Tennessee, April 15-18, 2019.
- Martino, J. B. and N. A. Chandler (2004). "Excavation-induced damage studies at the Underground Research Laboratory," *International Journal of Rock Mechanics and Mining Sciences*, **41**(8):1413-1426.
- Matteo, E. N., T. Hadgu, L. Zheng, H. Xu, P. M. Fox, P. S. Nico, J. Birkholzer, F. A. Caporuscio, K. B. Sauer, M. J. Rock and L. M. Houser (2018). Evaluation of Engineered Barrier Systems in the Disposition of Spent Nuclear Fuel. M2SF-18SN010308042, SAND2018-12124 R. Sandia National Laboratories, Albuquerque, New Mexico.
- McCormick, K. A. (2010). Elevation Contour Map of the Precambrian Surface of South Dakota. Available online at <http://www.sdgs.usd.edu/publications/index.html>. South Dakota Geological Survey, South Dakota.
- Meacham, P. G., D. R. Anderson, E. J. Bonano and M. G. Marietta (2011). Sandia National Laboratories Performance Assessment Methodology for Long-Term Environmental Programs: The History of Nuclear Waste Management. SAND2011-8270. Sandia National Laboratories, Albuquerque, New Mexico.
- Mills, M. M., K. Kuhlman, E. Matteo, C. Herrick, M. Nemer, J. Heath, Y. L. Xiong, M. Paul, P. Stauffer, H. Boukhalfa, E. Guiltinan, T. Rahn, D. Weaver, B. Dozier, S. Otto, J. Rutqvist, Y. Wu, J. Ajo-Franklin and M. Hu (2019). Salt Heater Test (FY 19), April 30, 2019. M2SF-19SN010303031, SAND2019-4814 R. Sandia National Laboratories, Albuquerque, New Mexico.
- Mills, R., C. Lu, P. C. Lichtner and G. Hammond (2007). "Simulating subsurface flow and transport on ultrascale computers using PFLOTRAN," 3rd Annual Scientific Discovery through Advanced Computing Conference (SciDAC 2007), Boston Journal of Physics Conference Series, U387-U393.
- NAGRA (2014). FEBEX-DP Kick-Off Meeting. Presentation given at the kick-off meeting for the FEBEX-DP project. Thun, Switzerland.
- Navarre-Sitchler, A., R. M. Maxwell, E. R. Siirila, G. E. Hammond and P. C. Lichtner (2013). "Elucidating geochemical response of shallow heterogeneous aquifers to CO₂ leakage using high-performance

- computing: implications for monitoring CO₂ sequestration," *Advances in Water Resources*, **53**:44-55.
- Oberkampf, W. L. and T. G. Trucano (2007). Verification and Validation Benchmarks. SAND2007-0853. Sandia National Laboratories, Albuquerque, New Mexico.
- OECD (2004). Post-Closure Safety Case for Geological Repositories Nature and Purpose. Nuclear Energy Agency No. 3679, ISBN 92-64-02075-6. Organisation for Economic Co-Operation and Development, Nuclear Energy Agency, Paris, France.
- Olszewska-Wasiolek, M. A. and B. W. Arnold (2011). "Radioactive Disequilibria in the Saturated Zone Transport Model and the Biosphere Model for the Yucca Mountain Repository — The Case of Radon-222," International High-Level Radioactive Waste Management Conference, Albuquerque, New Mexico, 767-772.
- Painter, S., Z. Fang, R. Howard and K. Banerjee (2019). ORNL Input to GDSA Repository Systems Analysis FY19. M4SF-19OR010304072. Oak Ridge National Laboratory, Oak Ridge, Tennessee.
- Perry, F. V. and R. E. Kelley (2017). Regional Geologic Evaluations for Disposal of HLW and SNF: The Pierre Shale of the Northern Great Plains. SFWD-SFWST-2017-000119. Los Alamos National Laboratory, Los Alamos, NM.
- Perry, F. V., R. E. Kelley, P. F. Dobson and J. E. Houseworth (2014). Regional Geology: A GIS Database for Alternative Host Rocks and Potential Siting Guidelines. FCRD-UFD-2014-000068, Unlimited Release Report LA-UR-14-20368. Los Alamos National Laboratory, Los Alamos, New Mexico.
- Perry, F. V., E. Swanson, D. M. Milazzo, G. Y. A. Bussod and R. E. Kelley (2018). Regional Geologic Evaluations for Disposal of HLW and SNF: Alluvial Basins of the Basin and Range Province. LA-UR-18-28909. Los Alamos National Laboratory, Los Alamos, New Mexico.
- Pettersson, S. and B. Lonnerberg (2008). Final Repository for Spent Nuclear Fuel in Granite - The KBS-3V Concept in Sweden and Finland. Paper presented at the International Conference Underground Disposal Unit Design & Emplacement Processes for a Deep Geologic Repository, Prague.
- Pollok, L., M. Savnowski, T. Kuhneneze, V. Gundelach, J. Hammer and C. Pritzkow (2018). "Geological exploration and 3D model of the Asse salt structure for SE expansion and Asse II mine," Proceedings Mechanical Behavior of Salt IX. ISBN-978-3-9814108-6-0.
- Prudic, D. E., J. R. Harrill and T. J. Burbey (1995). Conceptual evaluation of regional ground-water flow in the Carbonate-Rock Province of the Great Basin, Nevada, Utah, and adjacent states. U.S. Geological Survey Professional Paper 1409-D. U.S. Geological Survey, Washington, D.C.
- Rechard, R. P. (1995). Performance Assessment of the Direct Disposal in Unsaturated Tuff of Spent Nuclear Fuel And High-Level Waste Owned by US Department of Energy. SAND94-2563/1,2,3. Sandia National Laboratories, Albuquerque, New Mexico.
- Rechard, R. P. (2002). "General approach used in the performance assessment for the Waste Isolation Pilot Plant," Scientific Basis for Nuclear Waste Management XXV, Boston, Massachusetts, November 26-29, 2001, Materials Research Society.
- Rechard, R. P., T. A. Cotton and M. D. Voegelé (2014). "Site selection and regulatory basis for the Yucca Mountain disposal system for spent nuclear fuel and high-level radioactive waste," *Reliability Engineering & System Safety*, **122**:7-31.
- Rechard, R. P. and C. T. Stockman (2014). "Waste degradation and mobilization in performance assessments of the Yucca Mountain disposal system for spent nuclear fuel and high-level radioactive waste," *Reliability Engineering and System Safety*, **122**(2):165-188.
- Rechard, R. P. and M. S. Tierney (2005). "Assignment of probability distributions for parameters in the 1996 performance assessment for the Waste Isolation Pilot Plant, Part 1: Description of process," *Reliability Engineering and System Safety*, **88**(1):1-32.
- Reimus, P. W. (2017). Mathematical Basis and Test Cases for Colloid-Facilitated Radionuclide Transport Modeling in GDSA-PFLOTRAN. LA-UR-17-26560. Los Alamos National Laboratory, Los Alamos, New Mexico.

- Reimus, P. W., M. Zavarin and Y. Wang (2016). Colloid-Facilitated Radionuclide Transport: Current State of Knowledge from a Nuclear Waste Repository Risk Assessment Perspective. FCRD-UFD-2016-000446. Los Alamos National Laboratory, Los Alamos, New Mexico.
- Sallaberry, C. J., J. C. Helton and S. C. Hora (2008). "Extension of Latin hypercube samples with correlated variables," *Reliability Engineering & System Safety*, **93**(7):1047-1059.
- Saltelli, A., P. Annoni, I. Azzini, F. Campolongo, M. Ratto and S. Tarantola (2010). "Variance based sensitivity analysis of model output. Design and estimator for the total sensitivity index," *Computer Physics Communications*, **181**(2):259-270.
- Saltelli, A., M. Ratto, T. Andres, F. Campolongo, J. Cariboni, D. Gatelli, M. Saisana and S. Tarantola (2008). *Global Sensitivity Analysis The Primer*. Chichester, U.K., Wiley.
- Sanchez, M., A. Gens, L. D. Guimaraes and S. Olivella (2005). "A double structure generalized plasticity model for expansive materials," *International Journal for Numerical and Analytical Methods in Geomechanics*, **29**(8):751-787.
- Sassani, D., J. Jang, P. Mariner, L. Price, R. Rechard, M. Rigali, R. Rogers, E. Stein, W. Walkow and P. Weck (2016). The On-line Waste Library (OWL): Usage and Inventory Status Report. FCRD-UFD-2016-000080. Sandia National Laboratories, Albuquerque, New Mexico.
- Sevougian, S. D., G. A. Freeze, W. P. Gardner, G. E. Hammond and P. E. Mariner (2014). Performance Assessment Modeling and Sensitivity Analyses of Generic Disposal System Concepts. SAND2014-17658. Sandia National Laboratories, Albuquerque, New Mexico.
- Sevougian, S. D., G. A. Freeze, M. B. Gross, J. Lee, C. D. Leigh, P. Mariner, R. J. MacKinnon and P. Vaughn (2012). TSPA Model Development and Sensitivity Analysis of Processes Affecting Performance of a Salt Repository for Disposal of Heat-Generating Nuclear Waste. O. o. U. N. F. Disposition. FCRD-UFD-2012-000320 Rev. 0. US Department of Energy, Washington, DC.
- Sevougian, S. D., G. A. Freeze, P. Vaughn, P. Mariner and W. P. Gardner (2013). Update to the Salt R&D Reference Case. FCRD-UFD-2013-000368, SAND2013-8255P. Sandia National Laboratories, Albuquerque, New Mexico.
- Sevougian, S. D., G. E. Hammond, P. E. Mariner, R. J. Mackinnon, P. N. Swift, R. D. Rogers, D. C. Dobson and M. C. Tynan (2019a). "Re-Evaluation of U.S. DOE R&D Efforts for Generic Deep Geologic Repositories – Roadmap Update," International High-Level Radioactive Waste Management Conference, April 15-18, 2019, Knoxville, Tennessee.
- Sevougian, S. D., P. E. Mariner, L. A. Connolly, R. J. MacKinnon, R. D. Rogers, D. C. Dobson and J. L. Prouty (2019b). DOE SFWST Campaign R&D Roadmap Update, Rev. 1. SAND2019-9033 R, July 22, 2019. Sandia National Laboratories, Albuquerque, New Mexico.
- Sevougian, S. D., E. R. Stein, M. B. Gross, G. E. Hammond, J. M. Frederick and P. E. Mariner (2016). Status of Progress Made Toward Safety Analysis and Technical Site Evaluations for DOE Managed HLW and SNF. Sandia National Laboratories. Albuquerque, NM: 188.
- Sevougian, S. D., E. R. Stein, T. LaForce, F. V. Perry, T. S. Lowry, L. J. Cunningham, M. Nole, C. B. Haukwa, K. W. Chang and P. E. Mariner (2019c). GDSA Repository Systems Analysis Progress Report. SAND2019-5189 R. Sandia National Laboratories, Albuquerque, New Mexico.
- Sevougian, S. D., E. R. Stein, T. LaForce, F. V. Perry, T. S. Lowry, M. Nole and K. W. Chang (2019d). GDSA Repository Systems Analysis FY19 Update. M3SF-19SN010304052. Sandia National Laboratories, Albuquerque, New Mexico.
- Shuai, P., X. Y. Chen, X. H. Song, G. E. Hammond, J. Zachara, P. Royer, H. Y. Ren, W. A. Perkins, M. C. Richmond and M. Y. Huang (2019). "Dam Operations and Subsurface Hydrogeology Control Dynamics of Hydrologic Exchange Flows in a Regulated River Reach," *Water Resources Research*, **55**(4):2593-2612.
- Simmons, A. M. and L. A. Neymark (2012). Conditions and processes affecting radionuclide transport, in Stuckless, J.S., ed., *Hydrology and Geochemistry of Yucca Mountain and Vicinity*, Southern Nevada and California. Geological Society of America Memoir 209.
- SKB (2006). Data report for the safety assessment SR-Can. SKB TR-06-25. Svensk Kärnbränslehantering AB, Stockholm, Sweden.

- SKB (2007). Geology Forsmark. R-07-45. Svensk Karnbranslehantering AB, Stockholm, Sweden.
- SNL (2008). Total System Performance Assessment Model/Analysis for the License Application. Sandia National Laboratories, Albuquerque, New Mexico.
- SNL (2018). Sandia Quality Assurance Program Description REV:5.1, SNL-QAPD-2018-05-31. SAND2018-5378 R. Sandia National Laboratories, Albuquerque, New Mexico.
- Stein, E. R., J. M. Frederick, G. E. Hammond, K. L. Kuhlman, P. E. Mariner and S. D. Sevougian (2017). "Modeling Coupled Reactive Flow Processes in Fractured Crystalline Rock," 16th International High-Level Radioactive Waste Management Conference, Charlotte, North Carolina, April 9-13, American Nuclear Society.
- Stein, E. R., L. P. Swiler and S. D. Sevougian (2019). "Methods of Sensitivity Analysis in Geologic Disposal Safety Assessment (GDSA) Framework," International High-Level Radioactive Waste Management Conference, Knoxville, Tennessee, April 14-18.
- Sudret, B. (2008). "Global sensitivity analysis using polynomial chaos expansions," *Reliability Engineering & System Safety*, **93**(7):964-979.
- Sweetkind, D. S., M. D. Masbruch, V. M. Heilweil and S. G. Buto (2010). Ch. C Groundwater Flow, in, Heilweil, V.M. and Brooks, L.E., eds., Conceptual model of the Great Basin Carbonate and Alluvial Aquifer System. US Geological Survey Scientific Investigations Report 2010-5193.
- Swiler, L. P., J. C. Helton, E. Basurto, D. M. Brooks, P. E. Mariner, L. M. Moore, S. Mohanty, S. D. Sevougian and E. R. Stein (2019). Status Report on Uncertainty Quantification and Sensitivity Analysis Tools in the Geologic Disposal Safety Assessment (GDSA) Framework. M2SF-19SN010304031. Sandia National Laboratories, Albuquerque, New Mexico.
- Trincherro, P., I. Puigdomenech, J. Molinero, H. Ebrahimi, B. Gylling, U. Svensson, D. Bosbach and G. Deissmann (2017). "Continuum-based DFN-consistent numerical framework for the simulation of oxygen infiltration into fractured crystalline rocks," *Journal of Contaminant Hydrology*, **200**:60-69.
- Vaughn, P., G. Freeze, J. Lee, S. Chu, K. D. Huff, W. M. Nutt, T. Hadgu, R. Rogers, J. Prouty, E. Hardin, B. Arnold, E. Kalinina, W. P. Gardner, M. Bianchi, H. H. Liu and J. Birkholzer (2013). Generic Disposal System Model: Architecture, Implementation, and Demonstration. FCRD-UFD-2012-000430 Rev. 1, SAND2013-1539P. Sandia National Laboratories, Albuquerque, New Mexico.
- Wang, J., L. Chen, R. Su and X. Zhao (2018a). "The Beishan underground research laboratory for geological disposal of high-level radioactive waste in China: Planning, site selection, site characterization and in situ tests," *Journal of Rock Mechanics and Geotechnical Engineering*, **10**:411-435.
- Wang, Y., T. Hadgu, E. Kalinina, J. Jerden, V. K. Gattu, W. Ebert, H. Viswanathan, J. Hyman, S. Karra, N. Knapp, N. Makedonska, P. Reimus, K. Telfeyan, P. M. Fox, P. S. Nico, M. Zavarin, E. Balboni and C. Atkins-Duffin (2017). Evaluation of Spent Fuel Disposition in Crystalline Rocks: FY17 Progress Report, Spent Fuel and Waste Disposition. SFWD-SFWST-2017-000007. Sandia National Laboratories, Albuquerque, New Mexico.
- Wang, Y., T. Hadgu, E. Kalinina, C. F. Jové Colón and B. Faybishenko (2018b). International Collaboration on Spent Fuel Disposition in Crystalline Media: FY18 Progress Report. Sandia National Laboratories, Albuquerque, New Mexico.
- Wang, Y. and J. H. Lee (2010). Generic Disposal System Environment Modeling – Fiscal Year 2010 Progress Report. SAND2010-8202P. Sandia National Laboratories, Albuquerque, New Mexico.
- Wang, Y., E. Matteo, J. Rutqvist, J. Davis, L. Zheng, J. Houseworth, J. Birkholzer, T. Dittrich, C. W. Gable, S. Karra, N. Makedonska, S. Chu, D. Harp, S. L. Painter, P. Reimus, F. V. Perry, P. Zhao, J. B. Begg, M. Zavarin, S. J. Tumey, Z. R. Dai, A. B. Kersting, J. Jerden, K. E. Frey, J. M. Coppie and W. Ebert (2014). Used Fuel Disposal in Crystalline Rocks: Status and FY14 Progress. FCRD-UFD-2014-000060, SAND2014-17992 R. Sandia National Laboratories, Albuquerque, New Mexico.
- Weirs, V. G., J. R. Kamm, L. P. Swiler, S. Tarantola, M. Ratto, B. M. Adams, W. J. Rider and M. S. Eldred (2012). "Sensitivity analysis techniques applied to a system of hyperbolic conservation laws," *Reliability Engineering & System Safety*, **107**:157-170.

- Welch, A. H., D. J. Bright and L. A. Knochenmus (2007). Water resources of the Basin and Range carbonate-rock aquifer system, White Pine County, Nevada, and adjacent areas in Nevada and Utah. U.S. Geological Survey Scientific Investigations Report 2007–5261.
- Wilson, J. (2016). Decay Heat of Selected DOE Defense Waste Materials. FCRD-UFD-2016-000636, SRNL-RP-2016-00249. Savannah River National Laboratory, Jackson, South Carolina.
- Zachara, J. M., X. Y. Chen, C. Murray and G. Hammond (2016). "River stage influences on uranium transport in a hydrologically dynamic groundwater-surface water transition zone," *Water Resources Research*, **52**(3):1568-1590.
- Zheng, L., C. F. Jové Colón, M. Bianchi and J. Birkholzer (2014). Generic Argillite/Shale Disposal Reference Case. FCRD-UFDC-2014-000319. Lawrence Berkeley National Laboratory, Alameda County, California.
- Zheng, L., K. Kim, H. Xu and J. Rutqvist (2016). DR Argillite Disposal R&D at LBNL. FCRD-UFD-2016-000437, LBNL-1006013. Berkeley, California, Lawrence Berkeley National Laboratory.
- Zheng, L., J. Rutqvist, K. Kim and J. Houseworth (2015). Investigation of Coupled Processes and Impact of High Temperature Limits in Argillite Rock. FCRD-UFD-2015-000362, LBNL-187644. Lawrence Berkeley National Laboratory, Berkeley, California.
- Zheng, L., J. Rutqvist, H. Xu, K. Kim, M. Voltolini and X. Cao (2017). Investigation of Coupled Processes and Impact of High Temperature Limits in Argillite Rock. SFWD-SFWST-2017-000040, LBNL-2001014. Lawrence Berkeley National Laboratory, Berkeley, California.

Appendix A. SURROGATE MODELING OF THE FUEL MATRIX DEGRADATION (FMD) MODEL

SURROGATE MODELING OF THE FUEL MATRIX DEGRADATION (FMD) MODEL

by

Paul E. Mariner, D. Thomas Seidl, Bert J. Debusschere, Jonathan Vo, Laura P. Swiler, Jennifer M. Frederick, and James L. Jerden

Abstract

Three surrogate models are under development to rapidly emulate the effects of the Fuel Matrix Degradation (FMD) process model in GDSA Framework: a polynomial regression surrogate, a neural network surrogate, and a k-Nearest Neighbors regressor (kNNr) surrogate. The process model simulates chemical and physical processes occurring near the surface of spent fuel to predict aqueous fuel dissolution rates over time and the growth of an altered layer. Direct coupling of the process model to GDSA Framework is too computationally expensive for simulations with large numbers of breached waste packages. Preliminary results indicate the surrogate models will enable GDSA Framework to rapidly emulate the effects of the FMD model for each individual breached waste package in a probabilistic repository simulation. This capability will allow uncertainties in spent fuel dissolution to be propagated to performance metrics and will allow sensitivities in inputs to be quantified and ranked against other inputs.

1. Introduction

High fidelity prediction of waste package and waste form degradation processes for thousands of waste packages in a probabilistic repository performance assessment calculation is computationally expensive. With thousands of waste packages, thousands of time steps, and hundreds of realizations in a simulation, these process models could be called a billion times per simulation.

GDSA Framework is open source repository simulation software built around the massively-parallel multi-physics code PFLOTRAN (SNL 2017). GDSA stands for Geologic Disposal Safety Assessment. An important short-term goal of the development of GDSA Framework (see pa.sandia.gov) is to perform probabilistic repository simulations to identify sources of uncertainty to help prioritize future R&D. To achieve this short-term goal with today's computer resources, developers must consider ways to include the effects of expensive process models in total system simulations.

One way to reduce computational expense is to develop response surface surrogate models that can rapidly emulate the mechanistic process models. An ideal response surface surrogate model runs orders of magnitude faster than its parent process model and provides outputs identical to those of the mechanistic model. In practice, the speed increase is easy to achieve. The challenge is achieving acceptable accuracy.

In 2018, a team of modelers and mathematicians at Sandia National Laboratories began exploring the potential value of developing surrogate models for the Fuel Matrix Degradation (FMD) process model. The FMD model (Jerden et al. 2015a) has been coupled with PFLOTRAN (Mariner et al. 2015), but the coupled model runs too slowly for a set of probabilistic repository-scale simulations. The surrogate modeling work has examined polynomial regression, polynomial basis adaptation methods for dimensionality reduction, tabulation using tree-based lookup methods, and artificial neural networks. Efforts to integrate the regression models as surrogate waste form models within PFLOTRAN are underway. Section 2 describes the FMD process model, and Section 3 presents descriptions and results for the surrogate models studied.

2. Fuel Matrix Degradation Process Model

The FMD process model is a mechanistic spent fuel dissolution model coded in MATLAB and developed at Argonne National Laboratory and Pacific Northwest National Laboratory. The model calculates spent fuel dissolution rates as a function of radiolysis, alteration layer growth, diffusion of reactants through the alteration layer, temperature, and interfacial corrosion potential (Jerden et al. 2015b). During execution it employs a one-dimensional (1D) reactive transport model to simulate diffusion and chemical reactions across this layer over time. The 1D domain, depicted in Figure 1, extends 0.05 m from the fuel surface to the bulk water. It is divided into as many as 100 cells with increasing length toward the bulk water boundary cell.

To couple the FMD process model with PFLOTRAN, a “coupled” FMD process model was coded in Fortran. At each time step, PFLOTRAN calls the coupled FMD process model to obtain a new dissolution rate. Coupling required PFLOTRAN to keep track of the 1D chemical profiles across the domain from the previous time step. It also required relevant inputs from the main PFLOTRAN simulation, such as temperature, time, and environmental concentrations in the boundary cell. Dose rate is calculated in the coupled FMD process model from time and burnup. A full list of FMD process model inputs and outputs available for surrogate modeling is presented in Table 1.

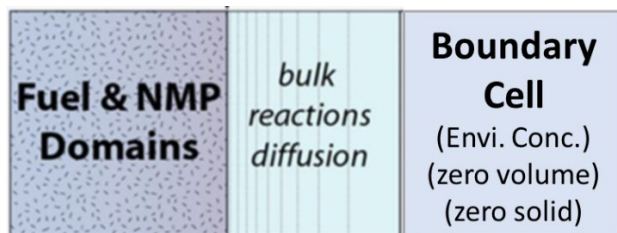


Figure 1. FMD process model domain

Table 1. Inputs/outputs of coupled FMD process model

Available Inputs	Outputs
<ul style="list-style-type: none"> • Initial concentration profiles across 1D corrosion/water layer (UO₂(s), UO₃(s), UO₄(s), H₂O₂, UO₂²⁺, UCO₃²⁻, UO₂, CO₃²⁻, O₂, Fe²⁺, and H₂) • Initial corrosion layer thickness • Dose rate at fuel surface (= f (time, burnup)) • Temperature • Time and time step length • Environmental concentrations (CO₃²⁻, O₂, Fe²⁺, and H₂) 	<ul style="list-style-type: none"> • Final concentration profiles across 1D corrosion/water layer • Final corrosion layer thickness • Fuel dissolution rate

The coupled FMD process model was tested on a problem involving a two-dimensional flow field containing 4 rows of 13 breached spent fuel waste packages. The model successfully simulated fuel dissolution for each of the waste packages over 100 time steps (Mariner et al. 2015). Of the 45 minutes of computational time required to run the simulation, 30 minutes were used calculating the fuel dissolution rates in the coupled process model.

3. Surrogate Modeling

It is often useful to construct a surrogate model to use in uncertainty and sensitivity analysis of a computational physics model when it is computationally demanding. A surrogate model (sometimes called meta-model, emulator, or response surface model) is an inexpensive input-to-output mapping that replaces a simulation code. Once constructed, this meta-model is relatively inexpensive to evaluate so it is often used as a surrogate for the physics model in uncertainty propagation, sensitivity analysis, or optimization problems that may require thousands to millions of function evaluations (Simpson et al. 2008).

There are many different types of surrogate models, including neural networks, regression models, radial basis functions, splines, etc. One popular approach in the literature is to develop an emulator that is a stationary smooth Gaussian process (Santner et al. 2003; Rasmussen and Williams 2006). The popularity of Gaussian processes is due to their ability to model complicated functional forms and to provide an uncertainty estimate of their predicted response value at a new input point. There are many good overview articles that compare various meta-model strategies. Various smoothing predictors and nonparametric regression approaches are compared elsewhere (Santner et al. 2003; Simpson et al. 2008; Storlie et al. 2009). Simpson et al. (2008) provides an excellent overview not just of various statistical meta-model methods but also approaches that use low-fidelity models as surrogates for high-fidelity models. Haftka and his students developed an approach that uses ensembles of emulators or hybrid emulators (Viana et al. 2009). Finally, polynomial chaos expansions (PCE) have become popular surrogate models over the past fifteen years (Ghanem and Spanos 2002; Xiu 2010). These stochastic expansion methods approximate the functional dependence of the simulation response on uncertain model parameters by expansion in an orthogonal polynomial basis. The polynomials used are tailored to the characterization of the uncertain input variables.

Three surrogate modeling approaches are presented, a polynomial regression surrogate model (Section 3.1.1), an artificial neural network surrogate model (Section 3.1.2) and a k-nearest-neighbors surrogate model (Section 3.1.3). The first provides a polynomial expression to emulate the FMD model, the second utilizes a network of artificial neurons with nonlinear activation functions, and the third uses an advanced technique to interpolate between points in a lookup table generated by the FMD model.

3.1 FMD – Standalone MATLAB Version

There are several versions of the FMD process model. The source versions of the code are programmed in MATLAB and are standalone codes. Two versions of the source MATLAB code have been used to generate training data during the development of the surrogate models, a recent 2018 version and an earlier version. The earlier version was translated into Fortran for coupling with PFLOTRAN. In this report, only the 2018 standalone MATLAB version of the code and the coupled Fortran code based on the earlier MATLAB version are used.

The first step of this study was to use the standalone MATLAB code to generate training data. The training data itself can be very large. For example, we may have hundreds of samples of FMD, where each sample involves a multi-dimensional vector sample of inputs such as the environmental concentrations, temperature, burnup, etc. The output is also extensive, since each FMD run involves hundreds of timesteps. So, a few hundred samples and a few hundred timesteps results in a large training matrix with tens of thousands of rows (each row being a training point at one particular timestep) and several columns of inputs (e.g., the left-hand quantities in Table 1) and one column of output (the fuel dissolution rate). Note that for this model, we are only interested in predicting the fuel dissolution rate although the other two output quantities could be treated with a surrogate in similar manner.

3.1.1 Polynomial Regression

In our initial investigation, we decided to use polynomial regression surrogates for FMD, due to the large amount of training data, the smoothing characteristics of a regression model, and the requirement that the evaluation of the FMD surrogate be extremely fast.

A linear regression model \hat{f} as a function of an m -dimensional input vector $\mathbf{x} \in \mathcal{R}^m$ is defined as:

$$\hat{f}(\mathbf{x}) \approx c_0 + \sum_{i=1}^m c_i x_i \quad (1)$$

Similarly, a second order polynomial regression (also called a quadratic regression model) is defined as:

$$\hat{f}(\mathbf{x}) \approx c_0 + \sum_{i=1}^m c_i x_i + \sum_{i=1}^m \sum_{j \geq i}^m c_{ij} x_i x_j \quad (2)$$

To determine the coefficients of the polynomial regression model, a least-squares formulation that minimizes the sum-of-squared error (SSE) between the surrogate model and the actual data is typically used (Seber and Wild 2003). The SSE is the standard error metric for overdetermined polynomial regression. It is a quadratic loss function which tends to find solutions near zero SSE well. We use the training data generated from the uncoupled MATLAB FMD model in the SSE formulation. We have a matrix of n training samples, where each training sample has an input \mathbf{x}_i and a corresponding output y_i . The coefficients minimize the SSE:

$$SSE = \sum_{i=1}^n (\hat{f}(\mathbf{x}_i) - y_i)^2 \quad (3)$$

For general nonlinear regression problems, one needs to use optimization methods to find the vector of coefficients \mathbf{c} which minimize the SSE. However, for linear regression models, the least squares problem reduces to a linear solve. If we write the entire sample matrix of inputs as \mathbf{X} (of dimension $n \times m$) and the sample matrix of outputs as \mathbf{y} (of dimension $n \times 1$), the optimization problem becomes:

$$\hat{\mathbf{c}} = \underset{\mathbf{c}}{\operatorname{argmin}} \|\mathbf{X} \cdot \mathbf{c} - \mathbf{y}\|^2 = (\mathbf{X}^T \mathbf{X})^{-1} \mathbf{X}^T \mathbf{y} \quad (4)$$

In practice, we do not take the explicit inverse of the matrix $(\mathbf{X}^T \mathbf{X})^{-1}$ to solve for the optimal \mathbf{c} but instead use a matrix factorization such as a QR factorization. This makes the determination of $\hat{\mathbf{c}}$ very efficient. Note also that this system is overdetermined for FMD: typically $n = 100\text{K}$ or more but m (the number of coefficients) is on the order of 10 - 100.

A Latin hypercube sampling (LHS) study was performed to generate training and validation data for regression from the standalone MATLAB FMD model. LHS is a stratified sampling technique that generates “well-spaced” samples; it typically gives lower variance statistical estimators than plain Monte Carlo sampling (Helton and Davis 2003). The six-dimensional sample space contained the parameters initial temperature, burnup, and the environmental concentrations of CO_3^{2-} , O_2 , Fe^{2+} , and H_2 . The probability distributions for each parameter are given in Table 2.

Table 2. LHS Sampling Input Parameters and Their Distributions

Parameter	Distribution	Min.	Max.
Init. Temp. (C)	Uniform	298	373
Burnup (Gwd/MTU)	Uniform	20	90
Env. CO_3^{2-} (mol/m ³)	Log-uniform	10 ⁻⁶	10 ⁰
Env. O_2 (mol/m ³)	Log-uniform	10 ⁻⁶	10 ⁻¹
Env. Fe^{2+} (mol/m ³)	Log-uniform	10 ⁻⁶	10 ⁻⁵
Env. H_2 (mol/m ³)	Log-uniform	10 ⁻⁶	10 ⁻¹

Nearly 5000 simulations were executed over the course of the LHS study. The temporal discretization in each problem consisted of 101 logarithmically-spaced (base 10) points from 0 to 10^5 years. In some simulations the UO_2 surface flux would superfluously stagnate after 10^4 years. We filtered the LHS results to remove any such runs. We also removed simulation runs with corrosion layer thickness that exceeded the size of the computational domain. Regression models were trained using data sets comprised of 1908 time series and tested on a set of 465 different time series. The data sets were standardized such that each feature vector was zero mean and unit variance.

We built multiple polynomial surrogate models of differing orders for the UO_2 surface flux (also referred to as fuel dissolution rate) using a feature set that was comprised of temperature, environmental concentrations of CO_3^{2-} , O_2 , Fe^{2+} , and H_2 , and the dose rate at the fuel surface (all at the current timestep). These features were chosen because they are either readily available (the environmental concentrations) or can be computed by PFLOTRAN (temperature and dose rate). The dose rate is determined using a formula that depends on burnup and time (Jerden et al. 2015b). Note that because the fuel dissolution rate, time, and the environmental concentrations varied across orders of magnitude, we used the log-transformed values of these quantities in the regression model.

To assess the accuracy of the models we analyzed the relative pointwise absolute error (RPWAE). At each data point, this error is computed as:

$$RPWAE = \frac{|y_{pred} - y_{true}|}{y_{true}} = \left| 1 - \frac{y_{pred}}{y_{true}} \right| \quad (5)$$

For each data set (i.e., training or test set) size, this error is averaged to obtain the mean RPWAE (M-RPWAE) metric.

Figure 2 displays all the UO_2 surface flux traces from the test set and the corresponding predictions from the regression models. Table 3 contains the number of terms present as well as the two data validation metrics for each model: R-squared (as applied to the log-transformed surface flux used in model construction) and mean absolute error values (measured in original space).

Table 3. Polynomial regression model summary for polynomial order, number of terms, test R-squared value, and mean relative pointwise absolute error (M-RPWAE) for the test and training sets.

P-Order	Terms	Train R^2	Train M-RPWAE	Test R^2	Test M-RPWAE
1	7	0.784	2.86	0.784	2.73
2	28	0.883	1.86	0.885	1.71
3	84	0.916	1.29	0.917	1.17
4	210	0.940	1.09	0.935	1.04
5	462	0.952	0.858	0.942	0.898
6	924	0.964	0.683	0.944	0.907

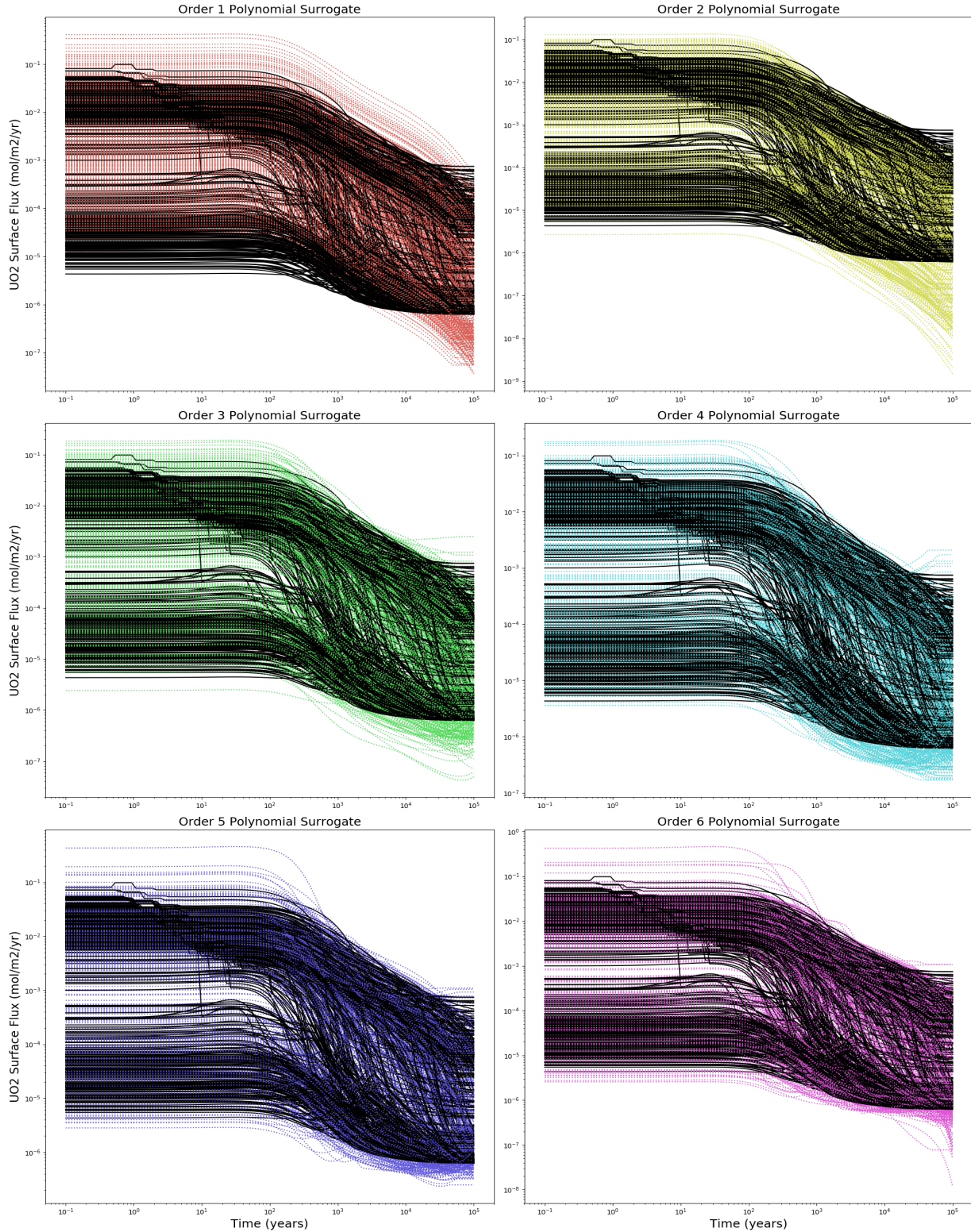


Figure 2. Test set traces (solid black lines) and model predictions (dashed colored lines) for polynomial regression models.

We observe that the sixth order polynomial appears to be overfitting the training data, as the test validation metrics are markedly worse than the training metrics compared to the results from the other models. Visually, the second order polynomial model appears to do the best job of predicting the test data at early (i.e. < 100 years) times.

3.1.1 Polynomial Regression

In this section we describe a neural network model built and assessed using the training and test datasets from the polynomial regression section. We find that it outperforms the polynomial regression models.

A disadvantage of polynomial regression models is the growth of the number of coefficients with increasing polynomial order, as can be seen in Table 3, as well as the restriction to polynomial basis functions. One motivation for the development of neural networks (Rasmussen and Williams 2006; Pedregosa et al. 2011; Ben-David and Shalev-Shwartz 2014) was to enable regression for complex functions by creating intricate networks of “artificial neurons” that are essentially weighted combinations of (usually simple) nonlinear functions.

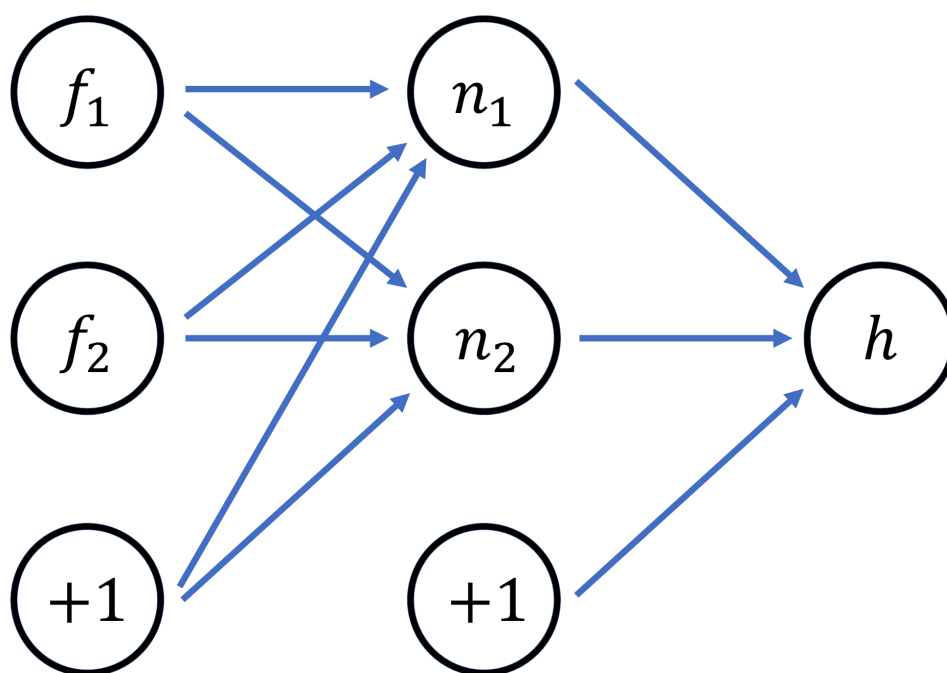


Figure 3. A schematic of a single layer feed-forward neural network with 2 input features and 2 neurons in the hidden layer.

Figure 3 contains a depiction of a single layer feed-forward neural network with two features and a single output. It is called a single layer network because there is one “hidden” layer of neurons between the input and output layers, and the term feed-forward reflects that all the “weights”, the directed connections between neurons, are pointing from the input layer to the output layer. The +1 nodes denote the “bias” or “offset” terms that are independent of the features f_i and neurons. A neural network with more than one hidden layer is often referred to as a “deep” network. We did not observe any appreciable improvement in performance from a model built with two hidden layers and thus did not explore such networks any further.

The inputs to a neuron n_i are weighted by their corresponding weights w , summed, and then fed into a nonlinear “activation function.” In this work we use the popular rectified linear unit (ReLU) function, which is zero for an input less than zero and equal to the input otherwise. The output of each neuron is again

weighted and summed at the output node to produce the model prediction. It's important to note that in regression neural networks there is typically no activation function applied at the output node.

The process of training a neural network involves minimizing a loss function for the weights w (blue arrows in the Figure). A commonly employed loss function is

$$J(w) := \sum_{i=1}^N (h(w, x_i) - y_i)^2 + \alpha ||w||^2, \quad (6)$$

where N denotes the number of data points in the training set and $h(w, x_i)$ is the neural network prediction for features x_i . The second term is a regularization term present to prevent over-fitting and its strength is controlled by a constant α .

We used the machine learning software package Scikit-learn (Pedregosa et al. 2011) to construct a single layer feed-forward neural network with 100 neurons. Table 4 contains the validation metrics for the training and test data sets, and the predictions from the model are displayed in Figure 4.

Table 4. Number of coefficients (i.e. weights) and error metrics for the neural network model

# Coefficients	Train R ²	Train M-RPWAE	Test R ²	Test M-RPWAE
801	0.978	0.40	0.972	0.635

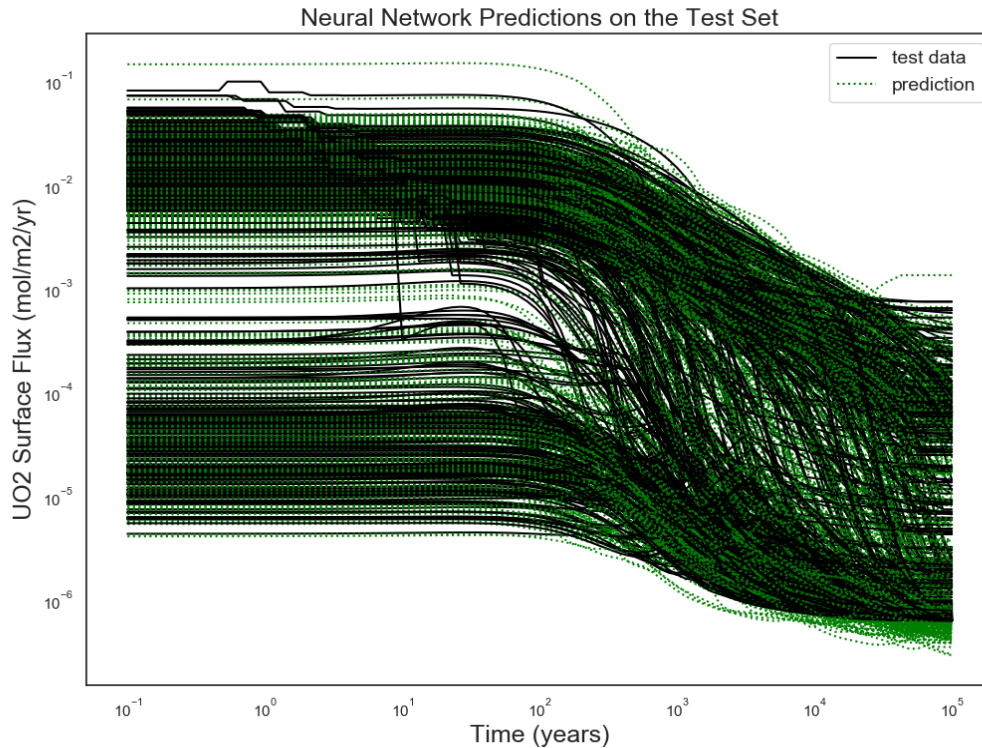


Figure 4. Test data (solid black lines) and neural network model predictions (dashed green lines).

Figure 5 shows the distribution of the mean per-simulation error for each simulation in the test set. The average error value is approximately 28% and the median is 23%, while the runs with the lowest and highest percent error contain approximately 4% and 4800% error, respectively. It's difficult to gauge how well individual truth-prediction pairs match up from Figure 4, so we have plotted a few of the best, middle of the road, and worst results as judged by mean per-simulation error in Figure 6.

The notable improvement in performance of the neural network model described in this section compared to the polynomial regression models of the previous section is encouraging enough to motivate an implementation within PFLOTRAN, and we have begun the process of doing so. There is currently a standalone Fortran version of the model, but it has not yet been added as an option within the waste form object.

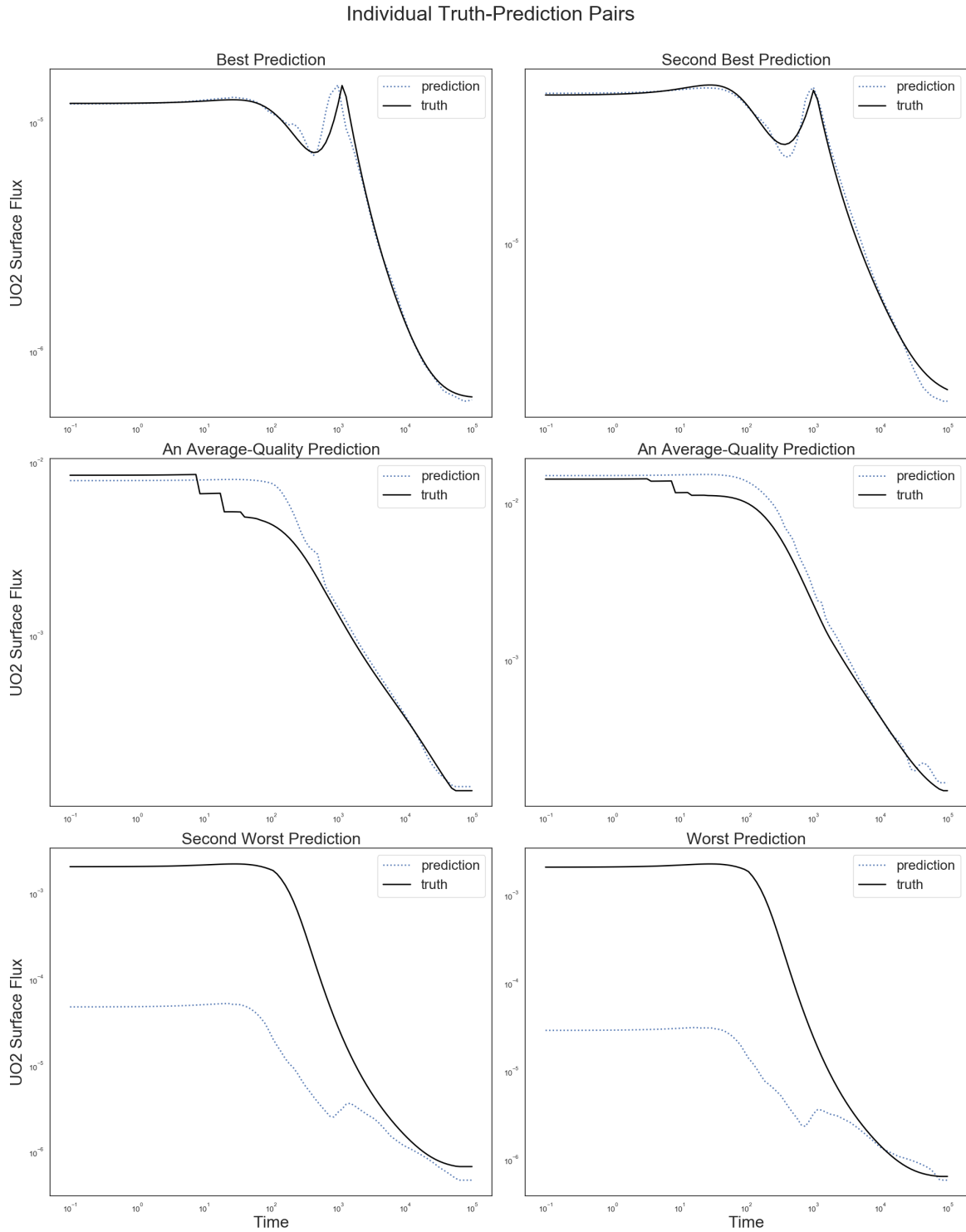


Figure 5. Samples of truth-prediction pairs from the neural network model for excellent, average, and poor predictions.

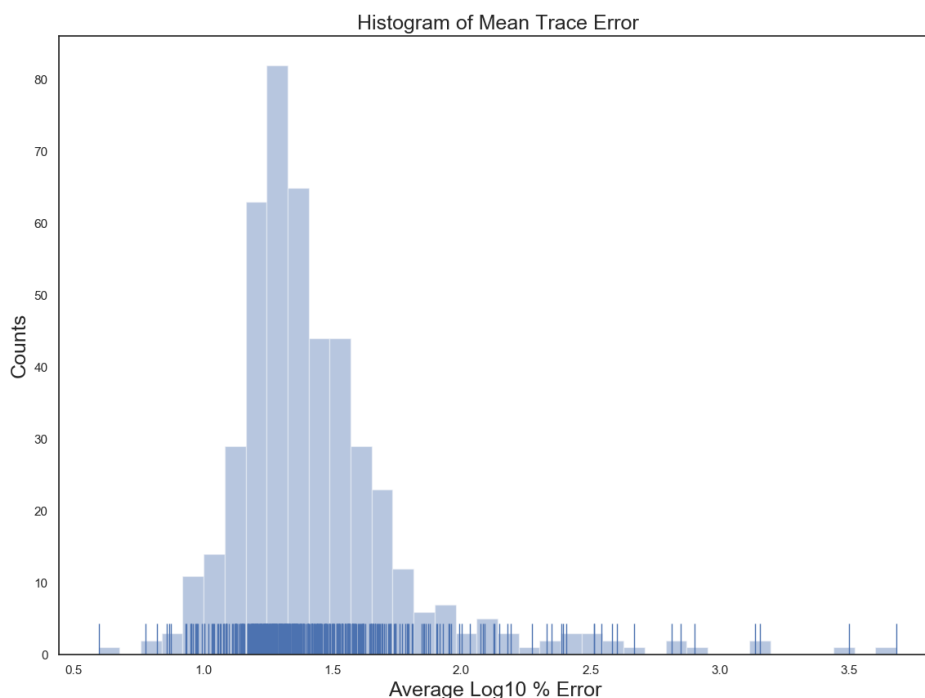


Figure 6. Histogram of the mean per-trace (a single simulation) % error for all 465 runs in the test set.

3.1.3 k-Nearest Neighbor

The k-Nearest Neighbors regressor (kNNr) (Ben-David and Shalev-Shwartz 2014) is a supervised, non-parametric machine learning method that, unlike polynomial regression or neural networks, does not re-express the data in any way in order to make predictions. In contrast to the latter pair of methods, which are active learners, the k-Nearest Neighbors regressor is a lazy learner that tabulates data points inside of a domain X with labels Y to the end of using those values for predictions. This makes the kNNr highly interpretable, as no intermediate hypothesis selection process on the parameters is undertaken as with the aforementioned active learners. Instead, the label for a point within the domain but not in the “table” is obtained as an average of the labels of the k nearest neighbors of this new point, where $k \geq 1$ is fixed. The definition of nearest depends on the metric function one uses, though a typical choice is the Minkowski metric $(\sum_{i=1}^d |x_i - y_i|^p)^{\frac{1}{p}}$, with $p \geq 1$. The case of $p = 2$ is the popular Euclidean metric. The tabulation of data points can be implemented with a matrix representing entries in a table. However, this is less efficient than modern tabulation methods like the K-D Tree or the Ball Tree (Pedregosa et al. 2011). The actual calculation of the predicted value need not be a uniform average. An inverse of the distance to each neighbor may be used to determine how influential that neighbor is in the final calculation of the weighted average.

One of the attractive features of kNNr is that it makes predictions based on local information only, and therefore does not require global smoothness over the input space. On the other hand, the approach requires a sufficiently dense table to get good predictive accuracy, and the cost of table look-ups increases as the table density increases.

3.1.3.1 Formulation

The kNNr is being considered as a surrogate model for predicting the UO_2 surface flux (also called UO_2 dissolution rate) in the waste package model component of PFLOTRAN. To that end, a sufficiently-dense

table is generated based on samples from a MATLAB version of the original model. To improve numerical stability and to put all dimensions on similar footing despite the wide range of tabulated values, we take the log of all the entries of the table.

In this work, we utilized the kNNr method as implemented by scikit-learn, v. 0.19.1 (Pedregosa et al. 2011). This version of kNNr allows for several different kinds of distance metrics, including the Minkowski one. It also provides uniform and distance-based methods of weighting the average. Additionally, it allows for a few different methods of tabulation, one of which scales well with dimension: the BallTree tabulation method.

To assess the suitability of kNNr as a surrogate model, we analyzed the convergence of the kNNr accuracy of UO_2 surface flux predictions as a function of the amount of training data. The training data consists of time-traces of UO_2 surface flux obtained with the detailed FMD model for the sampled values shown in Table 2. In order to have ample amounts of training data, about 24,000 runs were done, resulting in about 2.4×10^6 data points (101 points per run).

For the results that will be discussed in this paper, we picked the Manhattan distance metric, or the Minkowski metric for $p = 1$, as it is better suited to higher-dimensional domain spaces, which is the same reason as to why the BallTree tabulation method was chosen. In the averaging, the distance-weighted approach was used.

To predict the UO_2 surface flux, a table was built using two feature sets. Feature set A includes all externally provided (environmental) conditions:

- Temperature
- Environmental CO_3^{2-}
- Environmental Fe^{2+}
- Environmental H_2
- Environmental O_2
- Dose rate d_0 at the leftmost endpoint of the spatial mesh

Feature set B includes all of those features as well as:

- Corrosion layer thickness

This latter feature, the Corrosion Layer Thickness, is part of the internal state of the FMD model, and therefore would itself have to be predicted for standalone production runs. Further, given the wide ranges in many of the input parameters and the predicted UO_2 surface fluxes, the natural log of all quantities was taken before tabulation. Unless otherwise mentioned, all kNNr results in this report use Feature Set A.

In each numerical experiment, the number of runs from the dataset used for testing was set to 10% of the overall data set, with the remaining data available for training.

As was done for the polynomial surrogate models, the accuracy of the kNNr was analyzed using the relative pointwise absolute error (RPWAE) over the test data set and mean RPWAE (M-RPWAE) metrics over the test data set.

$$RPWAE = \left| \frac{y_{pred} - y_{true}}{y_{true}} \right| \quad (7)$$

This error metric was chosen to normalize the error by the true values, given the wide range in the predicted quantities. We also compute the mean RPWAE (M-RPWAE) error, which is the RPWAE error averaged over one full run of the FMD model. When an ensemble of tests is done, the ensemble average of these M-

RPWAE values is denoted as the EAM-RPWAE. Note that, even though the tabulation and prediction was done with log-transformed quantities, all reported error metrics were computed on the UO_2 flux values at their original scale.

3.1.3.2 Model Selection

The selection of the k value (the number of nearest neighbors to be used for prediction) was done through a model selection experiment. Figure 7 shows the average over the test data set of the relative error at each predicted point, for a set of k -values ranging from 1 to 11. The purple dashed line indicates where the k with minimal error for the different amounts of k considered. Overall, for the data set with 24K training runs, the error seems relatively insensitive to the k -value, but it does show a minimum at $k = 11$.

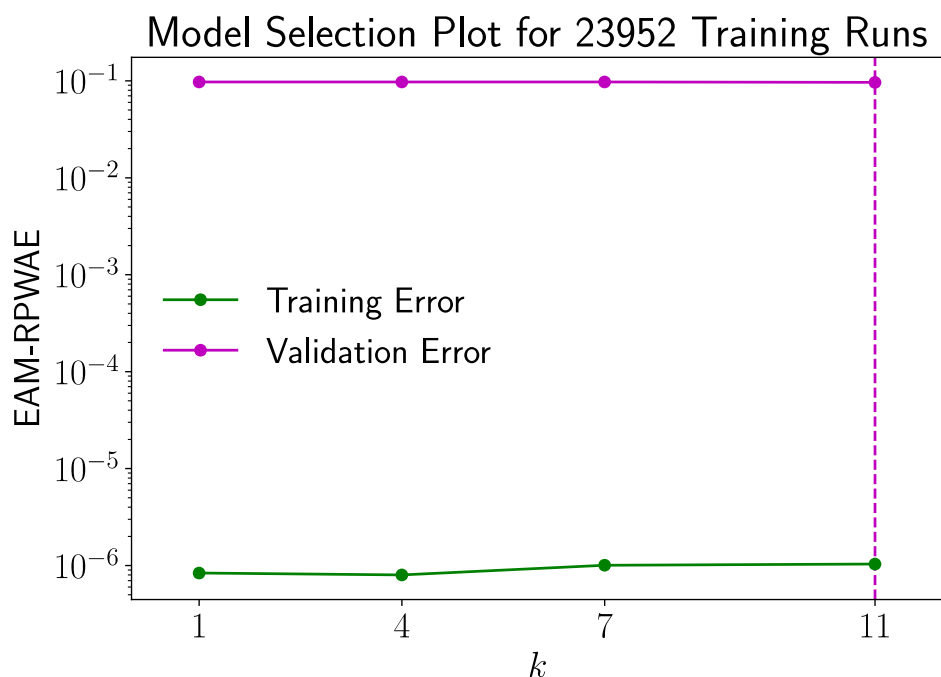


Figure 7. Model selection results to determine the optimal number of nearest neighbors k .

In the remainder of this work, a value k of 7 was used. With this value, we studied the convergence of the kNNr approach as a function of the amount of table data provided. In each experiment, 10 data sets of linearly increasing size were selected as training data sets to study the convergence as a function of the amount of training data. To account for randomness, an ensemble of 15 different permutations of the training data was generated for each training data set size.

3.1.3.3 Sampled Trajectories

To get a qualitative idea of how well the kNNr predicted UO_2 surface flux values compare to the detailed model, Figure 8 and Figure 9 plot an ensemble of 300 predicted UO_2 surface flux trajectories along with their true trajectories.

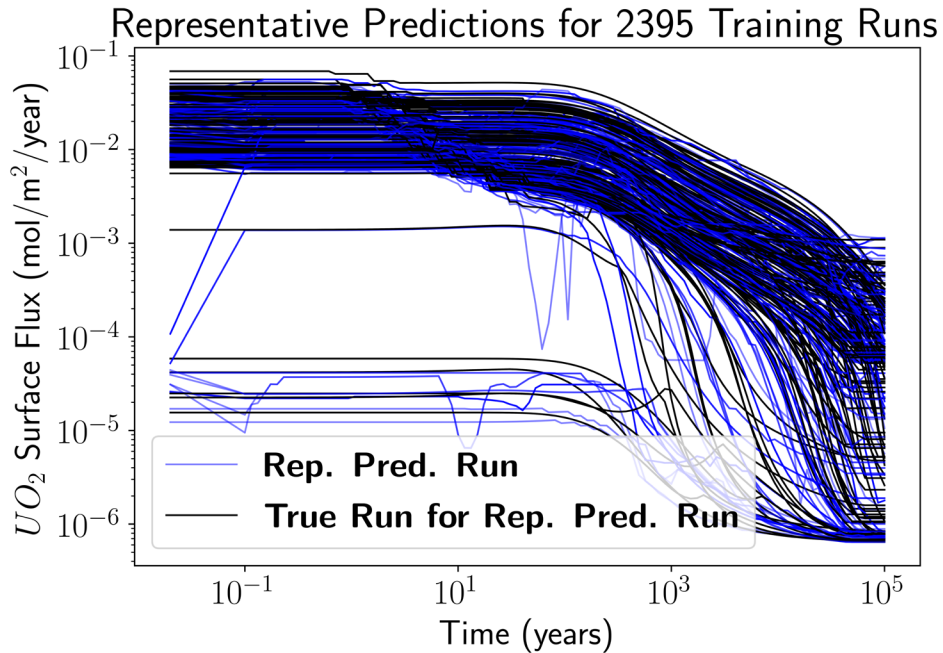


Figure 8. Comparison of kNNr predicted UO_2 surface fluxes and their detailed model counterparts for an ensemble of 300 randomly sampled trajectories for a table based on 2395 training runs. There is quite a bit of discrepancy between the kNNr predictions and the true runs.

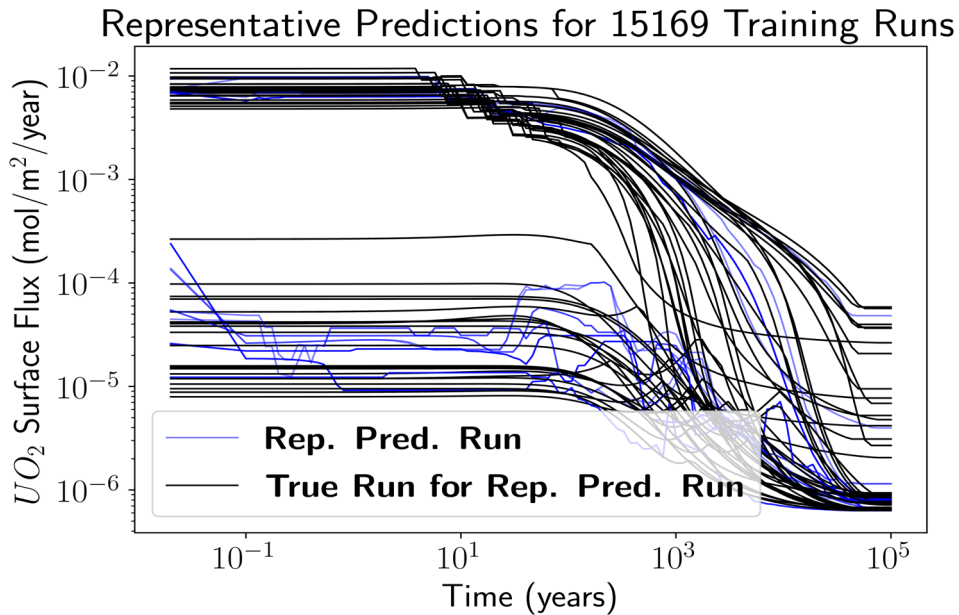


Figure 9. Comparison of kNNr predicted UO_2 surface fluxes and their detailed model counterparts for an ensemble of 300 randomly sampled trajectories for a table based on 15169 training runs. For this case, there is much better agreement between the kNNr predictions and the detailed model except for a few outliers.

For tables that are trained on a small number of data points (data from 2395 training runs), the agreement between the kNNr predictions and the detailed model is not satisfactory. For larger tables though, the agreement gets much better.

3.1.3.4 Predictive Accuracy as a Function of Training Data Size

As shown in Figure 10, the average of the M-RPWAE (green dashed line) decreases with increasing training data sizes, and the range of RPWAE averages per run also decreases, albeit very slowly, as indicated by the distance between the whiskers of the box plot. In this plot, the whiskers of the boxplot are the standard 1.5 * IQR (interquartile range), the orange line in each box represents the median, and outliers are not shown for the sake of readability. This shows the convergence of the kNNr regressor with increasing training data size. However, this convergence of the EAM-RPWAE (green line) is fairly slow. To get a better insight into the nature of the errors, we studied the histogram of the relative errors over all points.

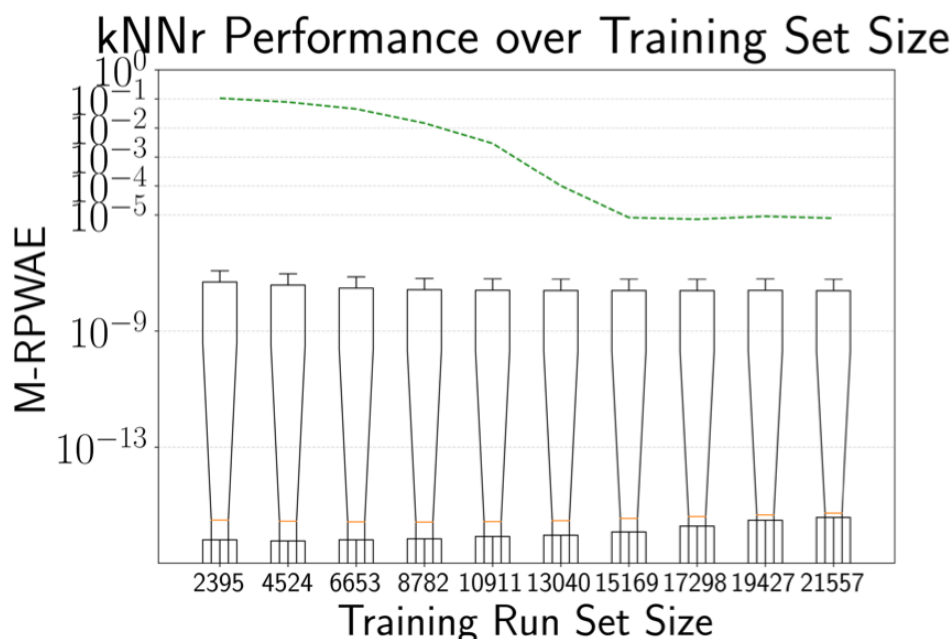


Figure 10. Boxplots of M-RPWAE values as a function of training run set size. The green curve shows the decay of the Ensemble Averaged M-RPWAE. This error decays steadily for training set sizes up to about 15000 runs' worth of data, after which it levels off at a value of about 10^{-5} .

3.1.3.5 Prediction Error Analysis

Figure 11 shows a histogram of the RPWAE values collected from all 15 random permutations of the training data sets for the case with 15169 training runs. To better see the range of values, the histogram is plotted in log scale. Points with zero error were removed from the ensemble to avoid numerical issues with taking the log. Despite the removal of points with zero error, it is clear that most of the RPWAE values are on the order of machine error. However, there are a few clusters of points with relative errors on the order of 10^{-5} and on the order of 1.

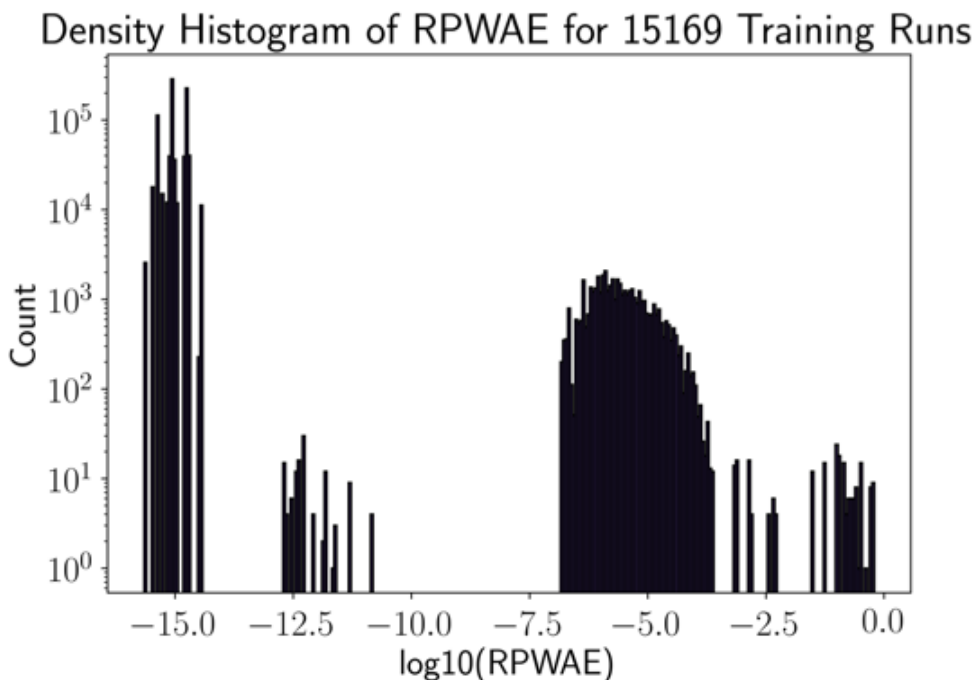


Figure 11. Histogram density plots showing the probability distribution of RPWAE values for a case with 15169 training runs. Most of the values are near zero, but a few clusters exist at higher RPWAE values.

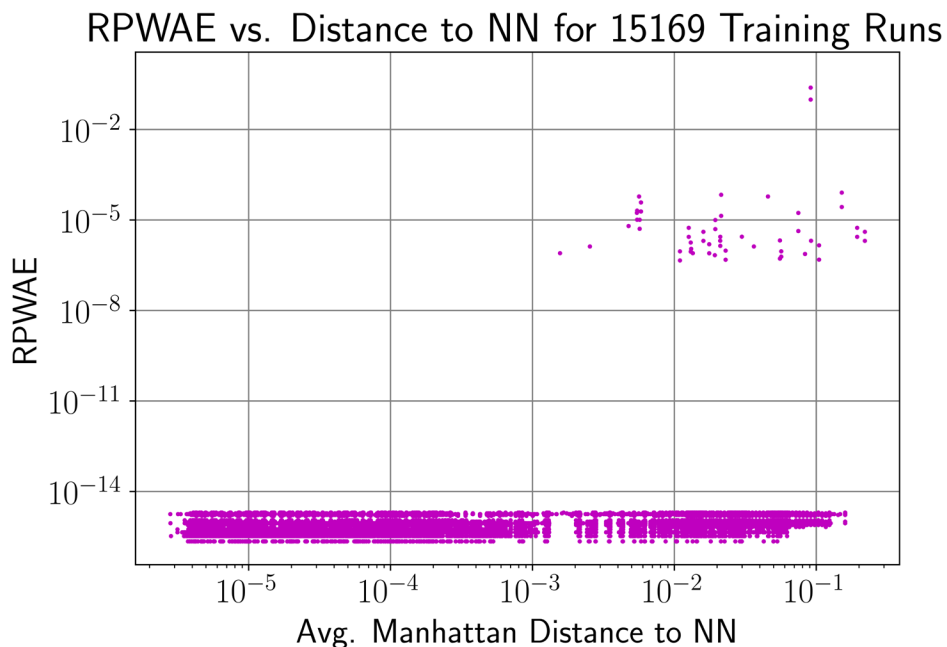


Figure 12. Relative errors compared to the average distance to their nearest neighbors, for the case with 15169 training runs.

When we look at how these errors depend on the average distance to their nearest neighbors, as depicted in Figure 12, we see that for the case with 15169 training runs, the average distances to the nearest neighbors in the table are quite small (less than 10^{-1}) and the corresponding errors are small. As in the previous Figure, we do see the same cluster at an error level of 10^{-5} , for average nearest neighbor distances over 10^{-3} .

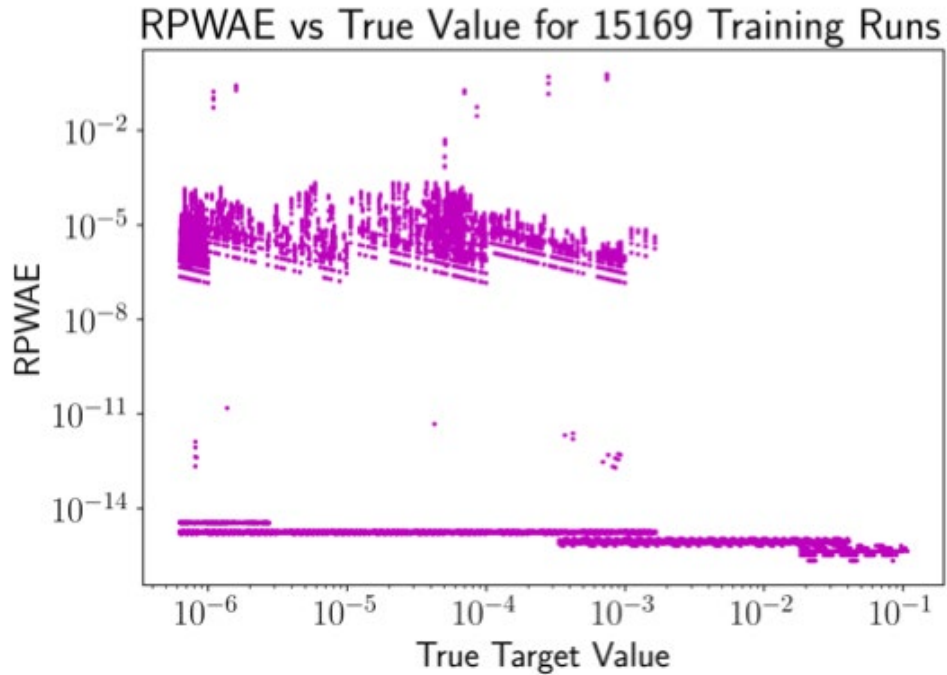


Figure 13. Relative errors compared to the true UO_2 flux values for the case with 15169 training runs.

Figure 13 gives a different view of the errors, showing them as a function of the true target values. This Figure shows that the high errors typically show up for points where the UO_2 surface fluxes are low, which usually happens at later times in the FMD model runs. This is confirmed by Figure 14, which shows the distribution of the errors as a function of time.

Distribution of RPWAE over time; 15169 Training Runs

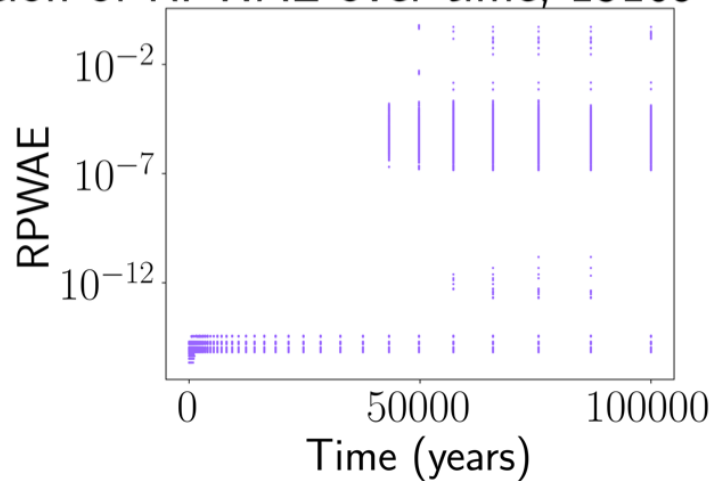


Figure 14. Relative errors as a function of time for the case with 15169 training runs.

Clearly, at later time (after about 40000) years, there is a subset of points for which large errors show up. Determining the nature of the runs that leads to these higher errors is the subject of ongoing work.

Going back to Figure 12, since all errors for lookups with an average distance less than 10^{-3} are very small, introducing a distance cutoff in the table look-up with this particular average Manhattan distance as the threshold may be sufficient to ensure the accuracy of the predictions.

3.1.3.6 Tabulation with Feature Set B

In this subsection, we perform the same analysis as before, but add the Corrosion Layer Thickness (CLT) as an additional feature in the kNN regressor. The CLT was added as a feature as the corrosion layer has a strong impact on the internal concentration profiles in the fuel casks, and as such, it is an important marker of the internal state of the FMD model as a function of time. One caveat of using the CLT is that it is a feature that is not externally provided. For the experiments here, we use the CLT obtained from the detailed FMD model runs. To use a kNNr that relies on the CLT as a feature in standalone mode, it will be necessary to also build a model for CLT as a function of the externally available features.

Figure 15 and Figure 16 show representative samples of kNNr predictions on test data, compared to the true outputs for a kNNr model trained with 2395 and 15169 FMD model runs respectively using the feature set B. While the model trained with 15169 runs performs better than the one based on 2395 runs, both models do better than with feature set A.

Figure 17 shows how the accuracy of the kNNr with feature set B depends on the amount of training data. As with feature set A, the error levels off after about 15000 training runs, but the average error level is a couple of orders of magnitude less than with feature set A. Also, the spread of the errors is much smaller.

This reduction in variability is also apparent in Figure 18, which now shows only two clusters. One near zero (machine precision), and one near 10^{-5} . The cluster near 10^{-5} is quite similar to the one seen with the kNNr based on feature set A.

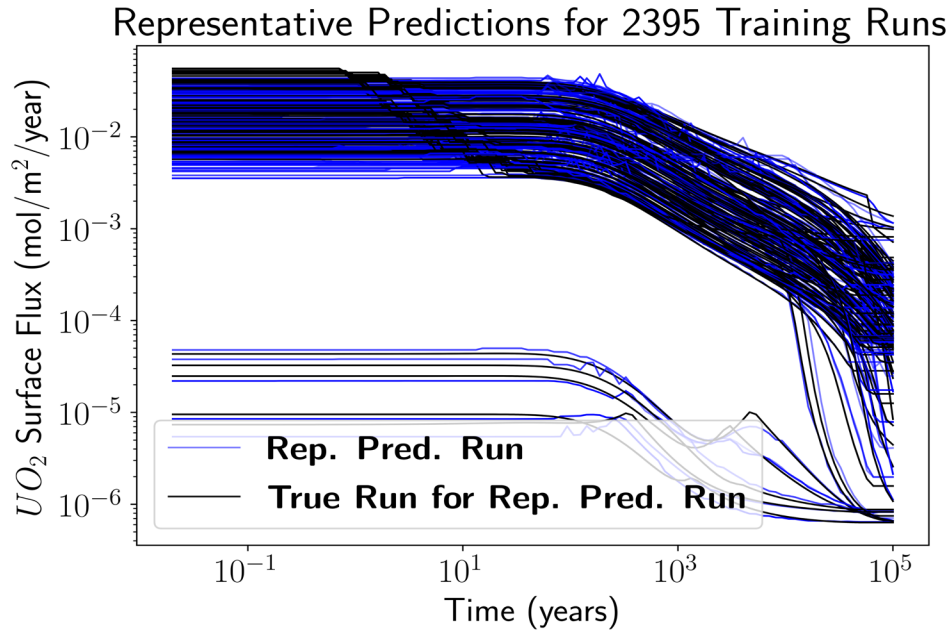


Figure 15. Comparison of kNNr predicted UO_2 surface fluxes and their detailed model counterparts for an ensemble of 300 randomly sampled trajectories for a table based on 2395 training runs, trained with feature set B. Adding the corrosion layer thickness as a feature results in a significantly better prediction accuracy.

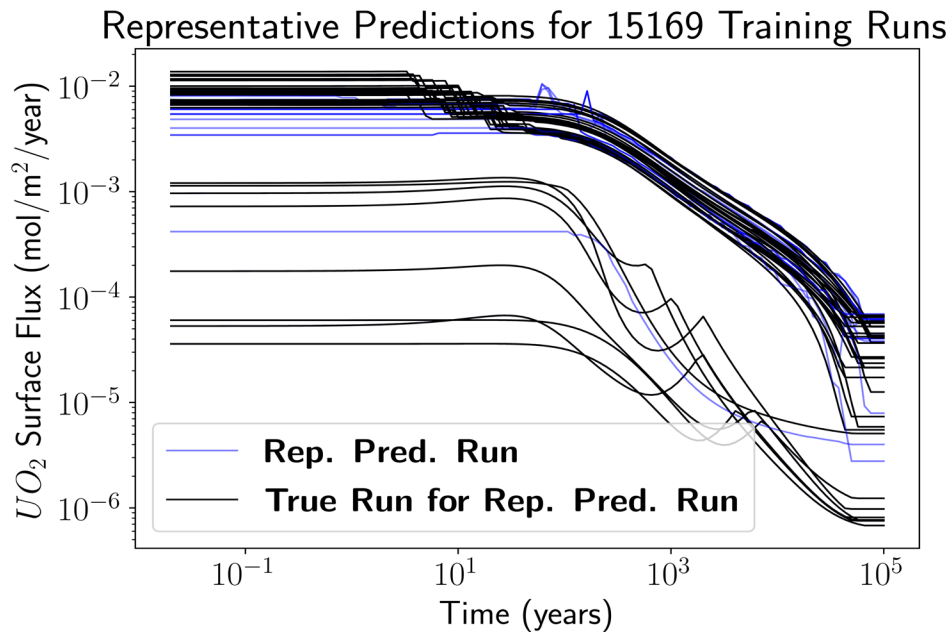


Figure 16. Comparison of kNNr predicted UO_2 surface fluxes and their detailed model counterparts for an ensemble of 300 randomly sampled trajectories for a table based on 15169 training runs, trained with feature set B. For this case, there is much better agreement between the kNNr predictions and the detailed model.

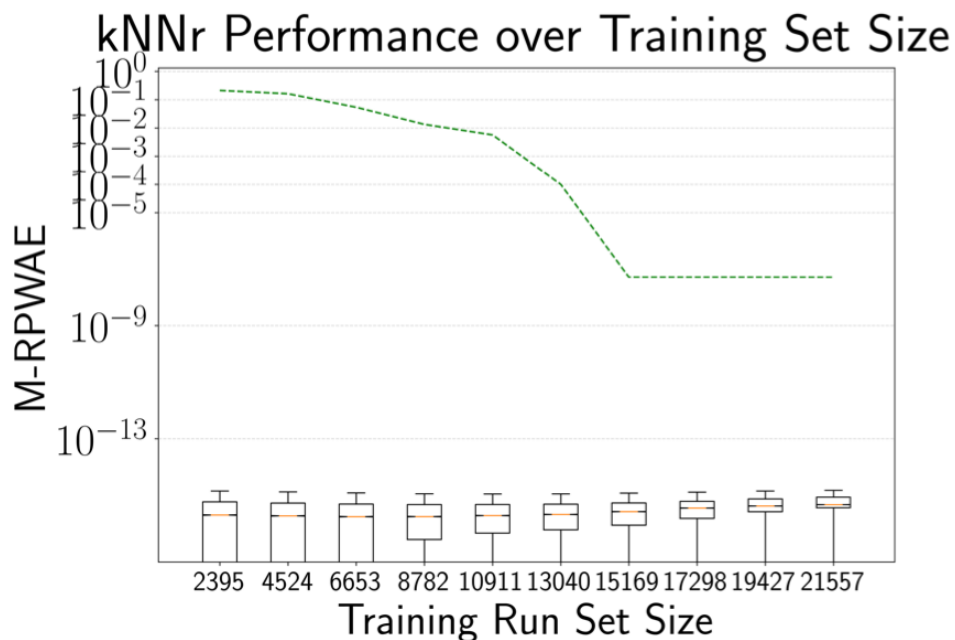


Figure 17. Boxplots of M-RPWAE values as a function of training run set size using feature set B. The green curve shows the decay of the Ensemble Averaged M-RPWAE. This error decays steadily for training set sizes up to about 15000 runs' worth of data, after which it levels off at about 10^{-7} .

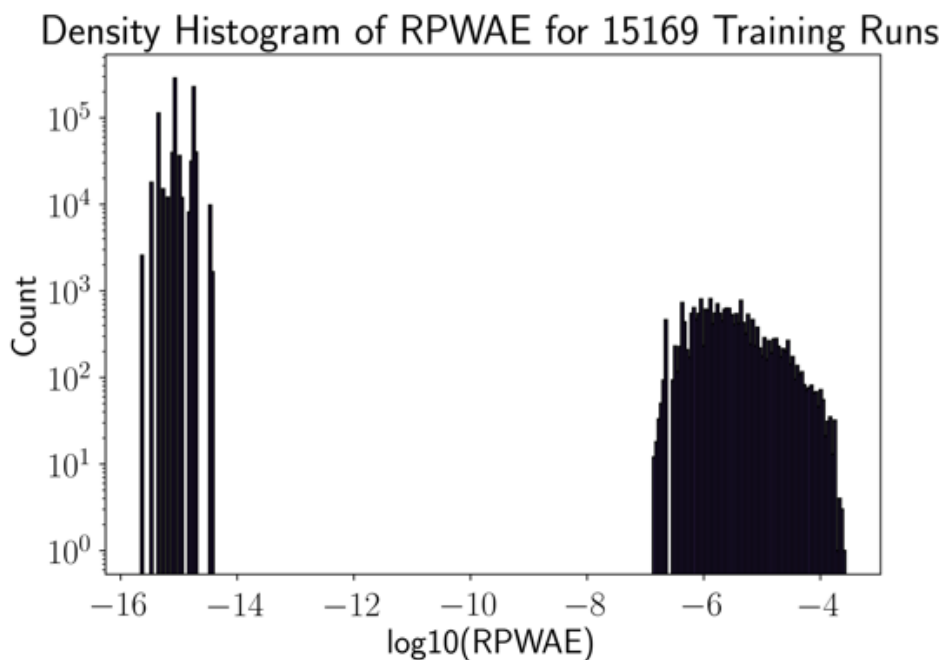


Figure 18. Histogram density plots showing the probability distribution of RPWAE values for a kNNr with 15169 training runs using feature set B. Most of the values are near zero. One cluster remains at higher RPWAE values near 10^{-5} , but the other clusters that were present with feature set A have disappeared.

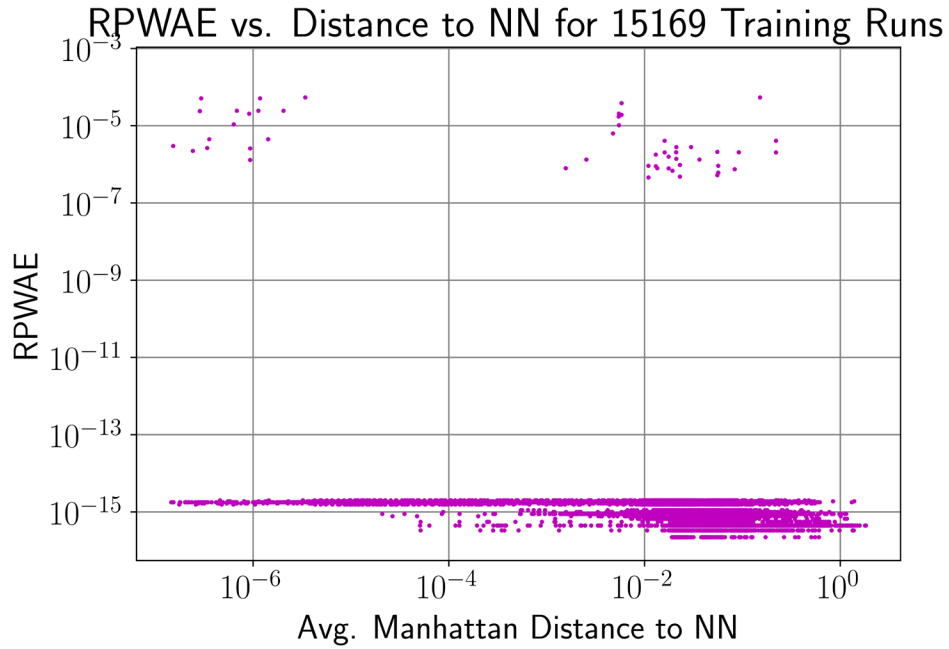


Figure 19. Relative errors compared to the average distance to their nearest neighbors, for the kNNr with 15169 training runs using feature set B.

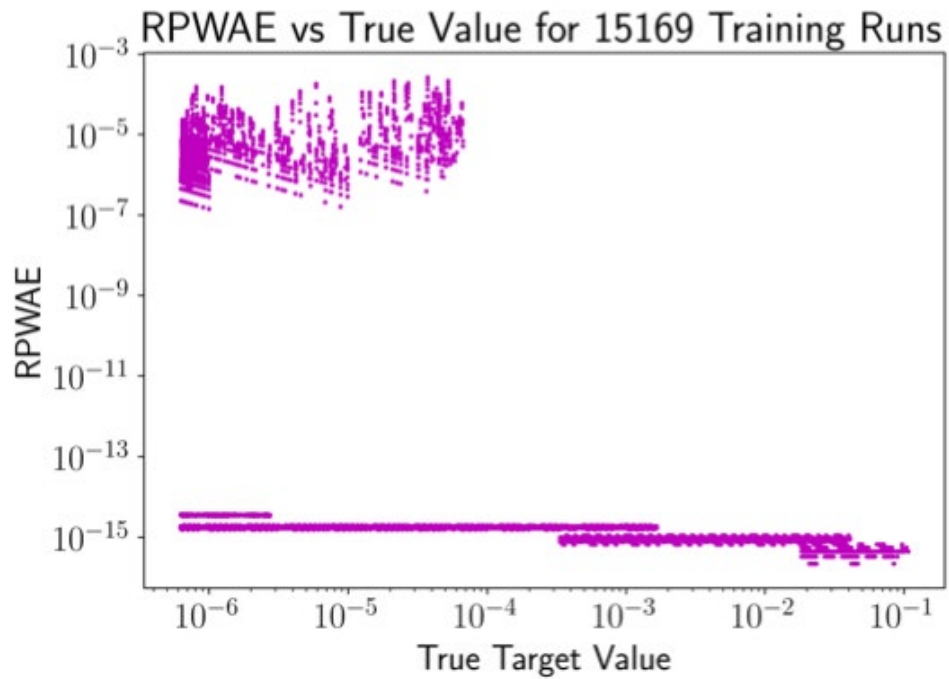


Figure 20. Relative errors compared to the true UO₂ flux values for the kNNr with 15169 training runs using feature set B.

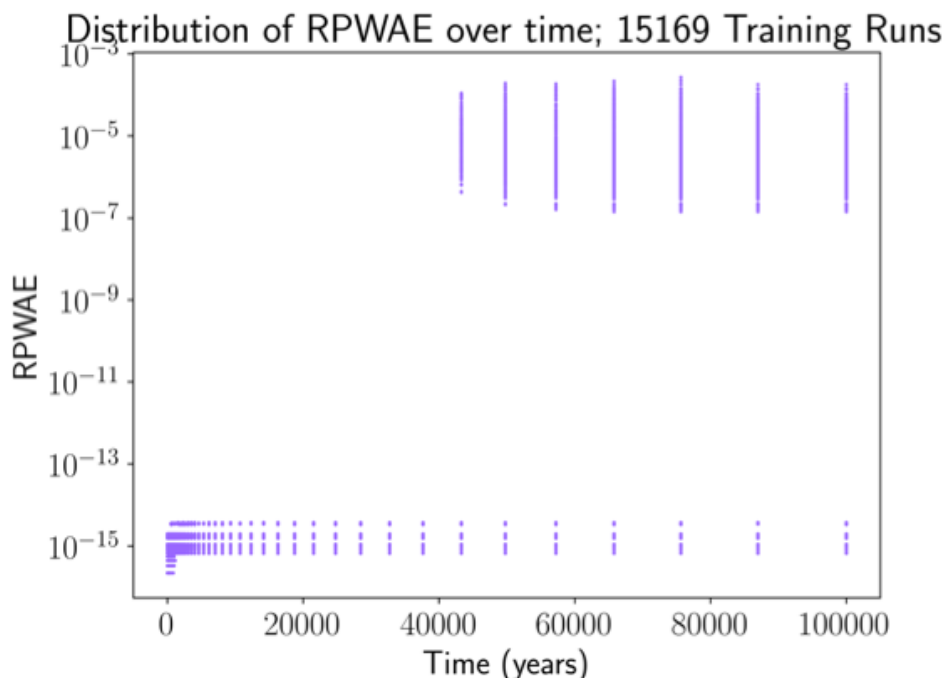


Figure 21. Relative errors as a function of time for the kNNr with 15169 training runs, using feature set B.

As with the kNNr trained on feature set A, Figure 19, Figure 20, and Figure 21, show that the cluster of points with a relative error on the order of 10^{-5} appears to be associated with small values of the UO_2 surface fluxes at late time. More exploration will be required to assess the origin of these points with a large relative error.

Regardless of this higher relative error, however, it is important to note that a relative error on the order of 10^{-5} is actually quite good for engineering purposes.

3.1.3.7 Ongoing Work

Ongoing work focuses on determining the origin of the clusters of points that give a high relative error. The question is whether these clusters are caused by a gap in our training data, or whether they represent outliers that should not be included in our test set.

Further, since the CLT is a property of the internal state of the fuel cask, we will build a table to also predict the CLT at time t , as a function of the current environmental conditions, and the CLT at time $t-1$. We will then assess the impact of the additional approximation in the CLT feature on the prediction of the UO_2 surface fluxes.

For all of these options, we will also assess the computational performance in terms of CPU cost as a function of the table size. While adding more training data improves the accuracy of the predictions, a larger table requires more time to identify the nearest neighbors, and therefore a higher computational cost. Therefore, we will implement approaches to only add more data where it is needed to improve the accuracy, or alternatively, remove data where the table is more than dense enough. The goal is to get an optimal relationship between accuracy and computational cost.

3.2 PFLOTRAN Surrogate Model Integration

This section contains a summary of the efforts spent integrating a polynomial surrogate model developed using data generated from the FMD MATLAB code into PFLOTRAN. One challenge was the

approximately 5-year difference in development time between the MATLAB version of FMD and the older Fortran version that has previously been interfaced to PFLOTRAN.

We originally wanted to update the Fortran code to reflect the more recent version, but after some exploration we found the work required to do so to be overly high relative to the other goals of the surrogate modeling project. It was then decided to build surrogates using the older Fortran FMD code instead, with the aim of comparing their embedded performance with a PFLOTRAN PA simulation to the original FMD model. Unfortunately, we discovered a difficulty along the way related to the time discretization required by the FMD model that made this comparison impossible except for highly contrived scenarios, so this plan was eventually scrapped as well.

The following subsections document the progress that was made in surrogate model integration within PFLOTRAN as well as the difficulties we encountered.

3.2.1 Fortran FMD Modifications

As mentioned in the introduction, we initially thought it would be best to create new surrogates based on data from the Fortran version of FMD for later error assessments, and we made a few modifications to the version of FMD in the PFLOTRAN repository (FMD v2.3) to more closely match the newer MATLAB code. These changes included:

- Cell length changed from 4.5 cm to 5 cm.
- The logical variable “oFlg” was not initialized and thus was determined randomly at compile time. Setting it to “.FALSE.” produced behavior consistent with the MATLAB version.
- The Fortran code used a decay time of 30 years and had no delay time. In the MATLAB version both the decay and delay times were equal to 50 years. An age of fuel (AOF) input variable was added to make this a possible input parameter and set equal to 100 years in the surrogate modeling studies. We ultimately did not pursue varying the AOF because doing so with PFLOTRAN was difficult, as will be discussed in the next section.

Surrogate data was generated using an LHS sampling study as discussed in the section A using the same input parameter distributions described in Table 2. Results from a few traces for both versions of the code are shown in Figure 22. Several of the traces in the MATLAB code display “stair-stepping” for the first 100 years or so, which is absent from the Fortran traces. Some reactions and constants differ between the codes. We found that the stair-stepping can be nearly eliminated by discretizing the 1D domain into 1,000 cells instead of the standard 40 typically used.

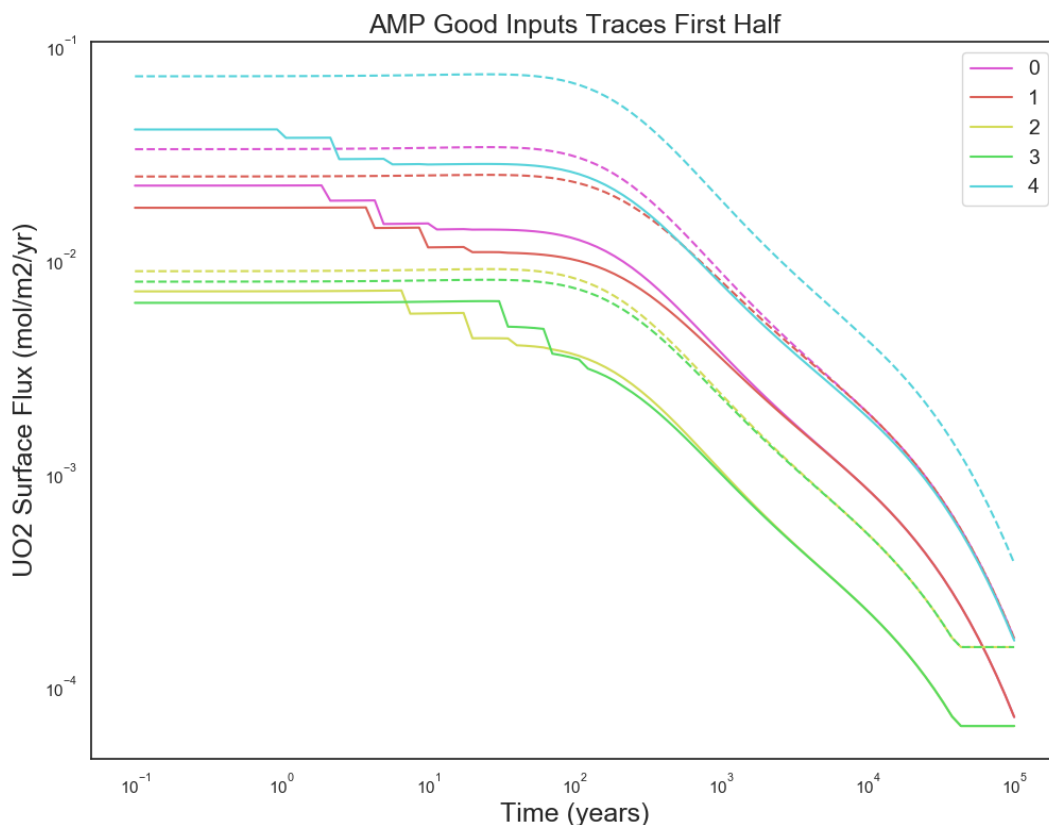


Figure 22. Five traces produced from the modified Fortran (dashed lines) and MATLAB (solid lines) codes using the same input parameters. There is a difference in scale between versions as the shapes of the traces are similar except for the “stair-stepping” observed in the MATLAB results.

3.2.2 Embedded Surrogates

Up until this point in the project, the construction and assessment of surrogate models occurred outside of PFLOTRAN. Our initial exploration focused on the MATLAB FMD code, but we then discovered that updating the Fortran code to match that version would be an undertaking, we instead decided to focus on the Fortran version that is currently callable from PFLOTRAN.

This code, FMD v2.3, has an interface called `AMP_step` that is called from PFLOTRAN at every time step in the simulation. The function call is illustrated in Figure 23. The “`conc`” array is a matrix that contains the concentrations of all 11 species in the FMD model within each cell for a single timestep. The `AMP_step` function takes the previous values of this array as one of its inputs and then updates them within the model. The “environmental” concentrations in our surrogate model data sets are used as boundary conditions at the right end of the `conc` array. The fuel dissolution rate, `fuelDisRate`, is the important output of `AMP_step` that PFLOTRAN uses to compute a source term. `Usource` is not currently used.

```
! FMDM model:$
!=====
interface$
  subroutine AMP_step ( burnup, sTme, temperature_C, conc, &$
    initialRun, fuelDisRate, Usource, success )$
    real ( kind = 8 ), intent( in ) :: burnup $
    real ( kind = 8 ), intent( in ) :: sTme $
    real ( kind = 8 ), intent( in ) :: temperature_C $
    real ( kind = 8 ), intent( inout ), dimension (:,:) :: conc$
    logical ( kind = 4 ), intent( in ) :: initialRun$
    ! sum of fluxes of 3 uranium compounds (UO2,2+;UCO3,2+;UO2)$
    ! units: g/m^2/yr where g = sum of uranium compound mass$
    real ( kind = 8 ), intent(out) :: fuelDisRate $
    ! flux of just the uranium from the 3 uranium compounds $
    ! units: g/m^2/yr where g = uranium mass$
    real ( kind = 8 ), intent(out) :: Usource$
    integer ( kind = 4 ), intent(out) :: success$
  end subroutine$
end interface $
!=====
```

Figure 23. Interface between the Fortran FMD model and PFLOTRAN. Requires storage of the (spatially-varying) concentrations of the species in the FMD model between time steps.

The surrogate model has an interface (Figure 24) like AMP_step, except that there is no concentration array and the four environmental concentrations are input arguments. The surrogates were constructed using mol/m²/yr for the output variable so a multiplication by the proper conversion factor takes place after surrogate evaluation to the expect units of g/m²/yr.

```
$
subroutine AMP_surrogate_step (burnup, sTme, initial_temp_K, &$
  conc, fuelDisRate)$
  implicit none$
  real ( kind = 8 ), intent( in ) :: sTme$
  real ( kind = 8 ), intent( in ) :: burnup$
  real ( kind = 8 ), intent( in ) :: initial_temp_K$
  ! four environmental concentrations$
  real ( kind = 8 ), intent( in ), dimension (:) :: conc$
  real ( kind = 8 ), intent( out ) :: fuelDisRate ! g/m2/yr$
end subroutine$
```

Figure 24. Interface between the Fortran FMD surrogate model and PFLOTRAN. All of the input arguments except for simulation time do not vary during the simulation. The conc array now refers to the four environmental concentrations.

We originally wanted to compare the accuracy of PFLOTRAN simulation that utilizes the FMD process model to one that uses a surrogate version of the FMD model in order to assess the error incurred by the use of a surrogate in the coupled model. This would be done by comparing key quantities of interest in the simulation, such as concentration profiles of radioactive species at observation locations.

In pursuit of this goal we became aware of a limitation of the original FMD process model – it assumes that time discretization is comprised of equally-spaced increments in log10 time. PFLOTRAN performs adaptive time stepping both to save computational cost and enable convergence of the nonlinear solver when the time step is too large.

The incompatibility of the time discretization between PFLOTRAN and FMD explains some of the computational cost of using FMD, as the model was being driven with inappropriate inputs. Figure 25 contains a plot of the time discretization over 10,000 years as would be produced/expected by the default settings in each code respectively. In particular, in this simulation PFLOTRAN adapts its time-stepping

scheme according to its internal rules while the FMD code expects equally time increments that are equally-spaced in log₁₀ time.

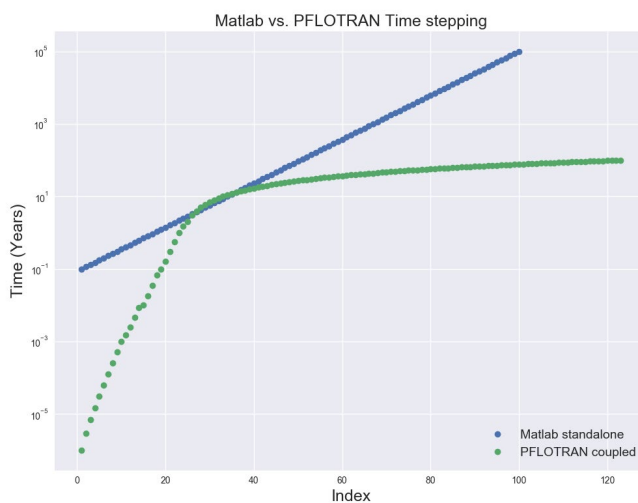


Figure 25. Time discretizations chosen by FMD and PFLOTRAN for a model problem.

fPFLOTRAN can be made to take equally-spaced increments in log space, and we have done so to verify that the coupled model (driven through AMP_step) matches a standalone driver for the Fortran FMD code (see Figure 26).

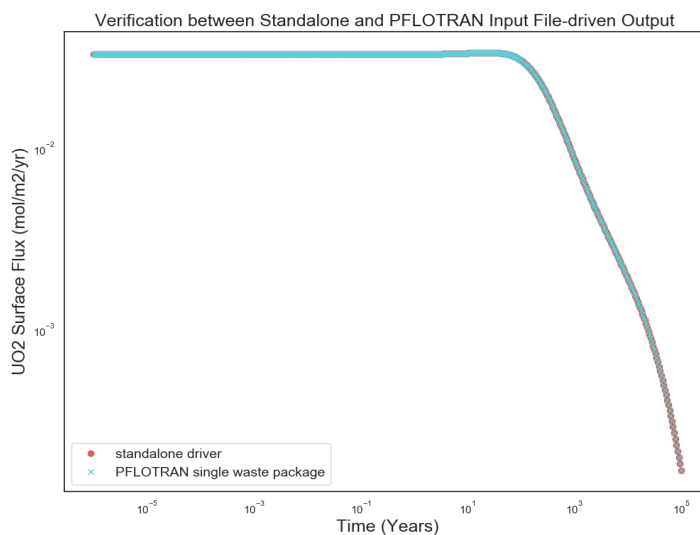


Figure 26. Verification for the standalone driver of Fortran FMD used for surrogate data generation and AMP_step called from PFLOTRAN. The circles and crosses lie on top of each other.

This is a tough limitation to work around, however. The adaptive solver is critical to PFLOTRAN's operation. If it is mandated to use FMD's preferred time discretization and the solver will not converge because a time step is too large, it will be unable to cut the time step and the simulation will end.

Furthermore, the current FMD code assumes that the waste package breaches at time zero. In PA waste packages may breach at arbitrary times. It is conceivable that if a breach time is known *a priori*, PFLOTRAN's time discretization machinery code take whatever time steps it wants until the breach time and then go on a FMD-friendly time march after that, but its implementation would be extremely awkward at best.

A more pressing problem is that PA simulations contain multiple waste packages with different breach times. There is no way that PFLOTRAN will be able to find a time discretization that works for each package post breach. Therefore one of the recommendations of this report is updating the process model to be able to work for arbitrary time steps rather than a rigid (e.g. equally spaced in log or linear time) time discretization.

3.3 Workflow Management

During development of the surrogate models, the importance of several workflow activities, as well as the focus of these activities, was acknowledged. Several of these activities and guidelines are summarized below.

Understand the process model to help identify good predictors that may be internal to the process model. For a process model that runs its own time loop, the set of inputs used at each time step can be much larger than the set of initializing inputs used by the process model. They may also be quite different from the optimal predictors chosen by the surrogate. The surrogate model may also benefit from calculating values for predictors (e.g., corrosion layer thickness) so that the values of these predictors may be stored for use in the following time step.

Perform spatial and temporal convergence testing on the process model and flag outliers that may indicate a potential problem with the process model. Before generating training and testing data with the process model, perform a spatial and temporal discretization convergence study. Plot the results and look for outliers that might indicate issues with the process model under certain circumstances.

Generate training and testing data specifically targeted for the realm of interest and importance. For example, if the PA model will never call the surrogate model until simulated time is high, then including process model results at low simulated time in the training data can be counterproductive or wasteful, depending on the type of surrogate model.

Include in the surrogate model explicit process model calculations where possible. For example, if the process model explicitly calculates an important predictor variable (e.g., dose rate) for the current time step, make this quantity available as a predictor.

Consider how the surrogate model will be applied to the performance assessment model. In this case, the FMD process model starts at time zero. In the PA model, fuel dissolution starts only after waste package breach. This delay, along with time steps that are not synchronized between the PA and process (or surrogate) model, complicates PA integration (e.g. Section 3.2.2).

4. Conclusions

Three surrogate models have been built and are being further developed to rapidly emulate the effects of the Fuel Matrix Degradation (FMD) model to calculate the dissolution rate of UO_2 in repository performance assessment simulations using GDSA Framework. Two of the surrogates, a polynomial regression surrogate and a neural network surrogate, are active learners that use training data to fully develop a multidimensional response surface over the entire domain of interest. The other is a k Nearest Neighbors regressor (kNNr) surrogate, a so-called lazy learner that uses a lookup “table” of solutions to estimate the quantity of interest when called.

As a first step, each of these surrogates were trained using input parameters that would be readily available in GDSA Framework repository simulations at each time step, e.g., temperature, dose rate, and environmental concentrations of CO_3^{2-} , O_2 , Fe^{2+} , and H_2 . These input parameters do not depend on the outputs of the FMD process model or its surrogates. Additional dependent inputs, such as corrosion layer thickness and concentrations of chemical species in the 1D domain of the FMD process model, which would need to be calculated and stored in PFLOTRAN for the next time step, were not used in this first step. In this step, of the two active learners, the neural network surrogate was found to be more accurate than the polynomial surrogate. For the neural network surrogate, where 1,908 simulations were used for training, the mean relative pointwise absolute error (M-RPWAE) on the test data was approximately 63% (Table 4), as opposed to 90% for a fifth-order polynomial surrogate (Table 3). The kNNr surrogate, which was found to work well using seven ($k=7$) nearest neighbors to calculate the UO_2 dissolution rate, produced results that were considerably more accurate. When 2,395 process model simulations were used for training (approximately 25% more than the number used for the active learner surrogates), the M-RPWAE was approximately 10% (Figure 10). When 15,196 process model simulations were used, the mean relative pointwise absolute error dropped to less than 0.001% (Figure 10), and the maximum error among the nearly one million data points tested dropped to less than 100% (Figure 11).

Considerable improvement in the accuracy of these models are realized when a dependent input, such as corrosion layer thickness, is added to the set of predictors. For example, a kNNr surrogate that uses 15,196 training runs, and includes the corrosion layer thickness as a predictor, causes the ensemble M-RPWAE to decrease by approximately two orders of magnitude to 0.00001% (Figure 17) and the maximum error among all tested data points to fall to less than 0.001% (Figure 18). However, this preliminary test uses the corrosion layer thickness predicted by the process model as if it were an independent input. The next step is to create a surrogate for predicting the change in the corrosion layer thickness resulting from the UO_2 dissolution rate surrogate so that it can be stored in PFLOTRAN for the next time step. Without a corrosion layer thickness surrogate, this approach cannot be used in repository simulations.

During the development of these surrogate models, several workflow activities and best practices were found to be highly important. They include:

- Understand the process model to help identify good predictors that may be internal to the process model.
- Perform spatial and temporal convergence testing on the process model to ensure the generation of accurate training and testing data sets and to flag outliers that may indicate a potential problem with the process model.
- Generate training and testing data specifically targeted for the realm of interest and importance.
- Include in the surrogate model explicit process model calculations where possible.
- Consider how the surrogate model will be applied to the performance assessment model, e.g., periods of time and time stepping.

Ultimately, the aim of these surrogate models is to enable GDSA Framework to simulate spent fuel dissolution for each individual breached spent fuel waste package in a probabilistic repository simulation. Having the ability to emulate spent fuel dissolution in probabilistic PA simulations will have the added capability of allowing uncertainties in spent fuel dissolution to be propagated and sensitivities in FMD inputs to be quantified and ranked against other inputs.

5. References

- Ben-David, S. and S. Shalev-Shwartz (2014). Understanding Machine Learning: From Theory to Algorithms. Cambridge, United Kingdom, Cambridge University Press.
- Ghanem, R. and P. Spanos (2002). Stochastic Finite Elements: A Spectral Approach. New York, New York, Springer Verlag.
- Helton, J. C. and F. J. Davis (2003). "Latin hypercube sampling and the propagation of uncertainty in analyses of complex systems," *Reliability Engineering & System Safety*, **81**(1):23-69.
- Jerden, J., J. M. Copple, K. E. Frey and W. Ebert (2015a). Mixed Potential Model for Used Fuel Dissolution - Fortran Code. O. o. U. N. F. Disposition. FCRD-UFD-2015-000159. U.S. Department of Energy, Washington, DC.
- Jerden, J., G. Hammond, J. M. Copple, T. Cruse and W. Ebert (2015b). Fuel Matrix Degradation Model: Integration with Performance Assessment and Canister Corrosion Model Development. FCRD-UFD-2015- 000550. U.S. Department of Energy, Washington, DC.
- Mariner, P. E., W. P. Gardner, G. E. Hammond, S. D. Sevougian and E. R. Stein (2015). Application of Generic Disposal System Models. FCRD-UFD-2015-000126, SAND2015- 10037 R. Sandia National Laboratories, Albuquerque, New Mexico.
- Pedregosa, F., G. Varoquaux, A. Gramfort, V. Michel, B. Thirion, O. Grisel, M. Blondel, P. Prettenhofer, R. Weiss, V. Dubourg, J. Vanderplas, A. Passos, D. Cournapeau, M. Brucher, M. Perrot and E. Duchesnay (2011). "Scikit-learn: Machine Learning in Python," *Journal of Machine Learning Research*, **12**:2825-2830.
- Rasmussen, C. E. and C. K. I. Williams (2006). Gaussian Processes for Machine Learning, MIT Press.
- Santner, T., B. Williams and W. Notz (2003). The Design and Analysis of Computer Experiments. New York, New York, Springer.
- Seber, G. A. F. and C. J. Wild (2003). Nonlinear Regression. New York, New York, Wiley & Sons.
- Simpson, T. W., V. Toropov, V. Balabanov and V. F.A.C. (2008). "Design and analysis of computer experiments in multidisciplinary design optimization: A review of how far we have come or not," Proceedings of the 12th AIAA/ISSMO Multidisciplinary Analysis and Optimization Conference, Victoria, British Columbia, Canada. AIAA Paper 2008-5802.
- SNL. (2017). "GDSA Framework: A Geologic Disposal Safety Assessment Modeling Capability," pa.sandia.gov.
- Storlie, C. B., L. P. Swiler, J. C. Helton and C. J. Sallaberry (2009). "Implementation and evaluation of nonparametric regression procedures for sensitivity analysis of computationally demanding models," *Reliability Engineering & System Safety*, **94**(11):1735-1763.
- Viana, F. A. C., R. T. Haftka and V. Steffen (2009). "Multiple surrogates: how cross-validation errors can help us to obtain the best predictor," *Structural and Multidisciplinary Optimization*, **39**(4):439-457.
- Xiu, D. (2010). Numerical Methods for Stochastic Computations: A Spectral Method Approach, Princeton University Press.

Appendix B. PFLOTRAN QA TEST SUITE

PFLOTRAN QA TEST SUITE

QA Test Suite

Table B-1 shows the combinations of process models and physical requirements to be covered by the PFLOTRAN QA test suite.

Recent Additions to the Test Harness

Recent work on code verification has been focused on improving code coverage for transport and two-phase flow. Figure B-1 shows two new transport benchmark simulations for advection and dispersion of an inert tracer, while Figure B-2 and Figure B-3 show examples of two-phase flow as modelled by GENERAL mode, with and without thermal changes in the simulation.

Figure B-1 shows a transport benchmark against an analytical solution for advection and diffusion of a tracer. Two simulations have been benchmarked, a one-dimensional radial (left) and two-dimensional (right) simulation mesh. In both cases the analytical model represents constant rate injection of a tracer at a point source in an infinite radial porous medium (Bear, 1972). For the 2D model only $\frac{1}{4}$ of the domain is simulated. Both simulations converge to within 2% error after 3 levels of grid refinement. This test could be extended to benchmark flow from a line source three-dimensional porous medium of constant thickness.

A benchmark for two-phase flow in GENERAL mode is shown in Figure B-2. This 1D benchmark verifies purely advective flow of an injected fluid where both of the species present (air and water) can exist in either the vapor or liquid phase. Analytical solutions for this model and many similar models are available in Orr (2007) and Lake (1989). The benchmark solution in Figure B-3 is similar to that in Figure B-2, except that in this benchmark the injected fluid is colder than the porous medium. The analytical solution to this mode is in Sumnu-Dindoruk and Dindoruk (2008). This benchmark verifies the simulation of both the mass and energy conservation equations for purely-advective one-dimensional flow. Five similar models have also been added to the test suite (LaForce et al, 2019).

Table B-1. Process Models (columns) and Requirements (rows). Each ‘x’ in the table shows a combination that PFLOTRAN is currently capable of simulating and should be covered by the PFLOTRAN test suite.

TH = thermal-hydrologic, WF = WIPP_FLOW, RT = reactive transport, NW_RT = nuclear waste RT

	Richards	TH	General	WF	RT	NW_RT	WasteForm
Multiphase conditions	<i>Two fluids, compressible or incompressible</i>						
Miscible			X				
Immiscible				X			
Groundwater conditions	<i>The attributes encompass additional subcases including confined and/or unconfined conditions</i>						
Saturated	X	X	X	X			
Variably Saturated	X	X	X	X			
Heat Transfer	<i>The attributes encompass additional subcases including isothermal</i>						
Anisothermal			X		X		X
Thermal Convection			X				
Thermal Conduction			X				
Solute Transport	<i>The attributes encompass additional subcases including simple molecular diffusion</i>						
Advection					X	X	
Hydrodynamic Dispersion					X	X	
Reactions	<i>The attributes address irreversible radioactive and chemical reactions as well as reversible phenomena</i>						
Radioactive Decay					X	X	
Radioactive Decay in Precipitate Phase						X	
Sorption and desorption					X	X	
Mineral Precipitation/Dissolution					X	X	
Colloids	<i>The attributes address non electrokinetic colloid transport only</i>						
3D Discretization							
Structured Grids	X	X	X	X	X	X	
Unstructured Grids	X	X	X	X	X	X	
Equations of State							
Water	X	X	X	X			
Gas			X	X			
Characteristic Curves	<i>Non-linear look up tables for defining interrelated conditions of pressure, saturation and permeability.</i>						
Capillary Pressure/Saturation	X	X	X	X			
Relative Permeability	X	X	X	X			
Dryout and Resaturation			X				
Boundary Conditions	<i>Any subset of cells, including source term cells such as wells or waste packages.</i>						
Specified Value	X	X	X	X	X	X	

Specified Flux	X	X	X	X			
Zero Gradient					X	X	
Material Properties	<i>Uniformity, isotropy, heterogeneity and anisotropy options</i>						
Permeability	X	X	X	X			
Porosity	X	X	X	X	X	X	
Tortuosity			X	X	X	X	
Soil Particle Density	X	X	X	X			
Soil Compressibility	X	X	X	X			
Heat Capacity		X	X				
Thermal Conductivity		X	X				
Multi-Continuum							
External Datasets	X	X	X	X	X	X	
Nuclear Waste PM							X

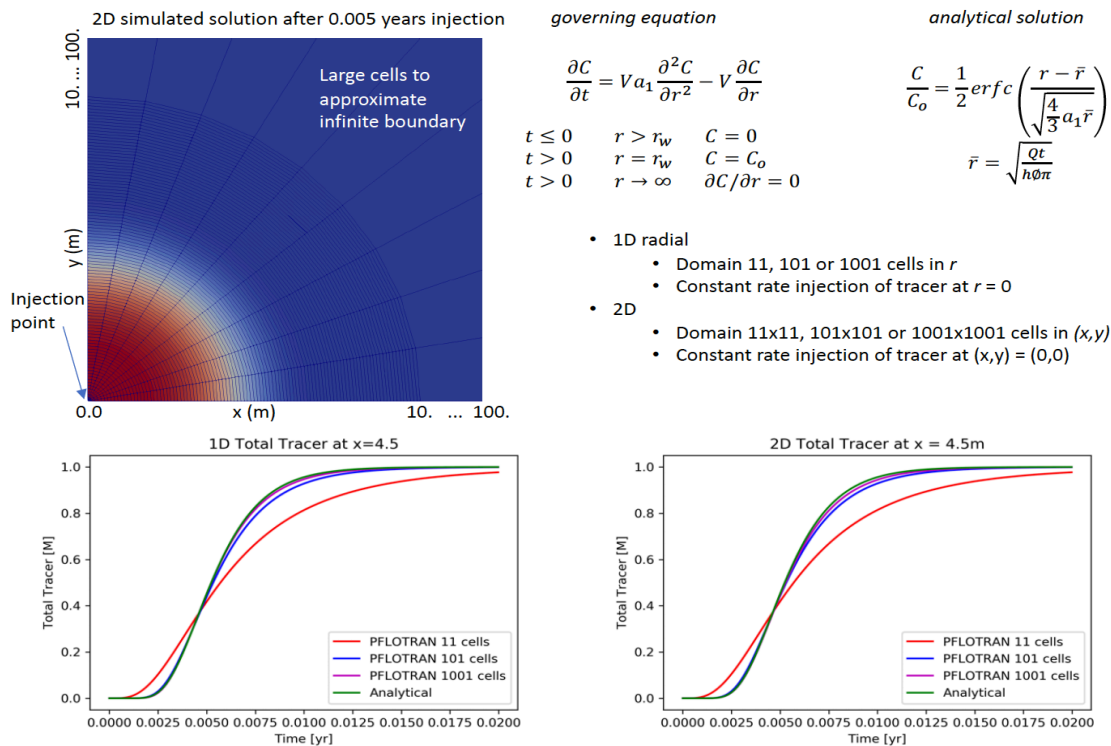


Figure B-1. Transport convergence test for advection and diffusion of a tracer from a point source on a 1D-radial domain (bottom left) and two-dimensional domain (bottom right). Plot shows tracer concentration at a monitoring point 4.5 m from the source as a function of time.

References

- Bear, J. (1972). Dynamics of fluids in porous media. New York, Dover Publications.
- LaForce, T., Frederick, J., Hammond, G., Stein, E., Mariner, P., (2019) “Benchmarking and QA testing in PFLOTRAN”, Proceedings of the 17th International High-Level Radioactive Waste Management Conference, Knoxville, Tennessee, April 14-18, American Nuclear Society.
- Lake, L. W. (1989). Enhanced oil recovery. Upper Saddle River, NJ. Prentice Hall
- Oberkampf, W. L., and T. G. Trucano (2007), Verification and Validation Benchmarks, SAND2007-0853, 67 pgs., Sandia National Laboratories, Albuquerque, NM.
- Orr, F. M. (2007). Theory of gas injection processes (Vol. 5). Copenhagen: Tie-Line Publications.
- Sumnu-Dindoruk, D. M., and Dindoruk, B. (2008). Analytical solution of nonisothermal Buckley-Leverett flow including tracers. SPE Reservoir Evaluation & Engineering, 11(03), 555-564